EVALUATION OF WATER PRODUCTION IN TIGHT GAS SANDS IN THE COTTON VALLEY FORMATION IN THE CASPIANA, ELM GROVE AND FRIERSON FIELDS

A Thesis

by

CHARLES CHINEDU OZOBEME

Submitted to the Office of Graduate Studies of
Texas A&M University
in partial fulfillment of the requirements for the degree of

MASTER OF SCIENCE

December 2006

Major Subject: Petroleum Engineering

EVALUATION OF WATER PRODUCTION IN TIGHT GAS SANDS IN THE COTTON VALLEY FORMATION IN THE CASPIANA, ELM GROVE AND FRIERSON FIELDS

A Thesis

by

CHARLES CHINEDU OZOBEME

Submitted to the Office of Graduate Studies of
Texas A&M University
in partial fulfillment of the requirements for the degree of

MASTER OF SCIENCE

Approved by:

Chair of Committee,	Stephen A. Holditch
Committee Members,	Duane McVay
	Brian Willis
Head of Department,	Stephen A. Holditch

December 2006

Major Subject: Petroleum Engineering

ABSTRACT

Evaluation of Water Production in Tight Gas Sands in the Cotton Valley Formation in the Caspiana, Elm Grove and Frierson Fields. (December 2006)

Charles Chinedu Ozobeme, B.Engr., University of Nigeria, Nsukka

Chair of Advisory Committee: Dr. Stephen A. Holditch

Normally in tight gas sands, water production is not a problem but in such low permeability reservoirs it is difficult to produce gas at commercial flow rates. Since water is more viscous than gas, very little water is normally produced in low permeability reservoirs. The production of large volumes of water from tight gas sands, say 50-100 bbls of water per MMcf of gas constitutes a cause for concern. High water production (>200 bbls of water per MMcf of gas) has been observed in the low permeability Cotton Valley sands in the Caspiana, Elm Grove and Frierson fields of North Louisiana.

This research evaluates water production in the above tight gas sands using field data provided by Matador Resource, a member of the Crisman Institute in Texas A&M University. The research is aimed at providing realistic reservoir scenarios of excess water production in tight gas sands. Log analysis, property trends and well production profiles have been used in establishing the different scenarios. The reservoir simulation results and the production trends show a possible water source from faults and fractures connecting the Travis Peak/Smackover sands to the Cotton Valley sands. An improved understanding of the reservoir would help in further field development.

DEDICATION

This thesis is dedicated to my loving wife, Oghenero, who has endured my absence and has continuously encouraged me even at difficult crossroads.

I also dedicate this work to my beautiful daughter, Serena, who reminds me continuously of how much she misses me.

ACKNOWLEDGMENTS

I would like to express my sincere gratitude and appreciation to the following people who greatly contributed in no small measure to this work:

Dr. Stephen Holditch, renowned Professor of Petroleum Engineering, who served as the chair of my graduate committee. His dedication, support, and enthusiasm guided me to the completion of this work. It has being a great pleasure to work under such supervision.

Dr Duane McVay and Dr Brian Willis for serving as members of my graduate committee. They walked with me all the way till the last day.

Thanks also to my colleagues, Sergio Jerez, Tarun Grover and Raj Malpani for their support. Additionally, the successful completion of my thesis would not have been possible without the blessing and support of my dear friend Efe Ejofodomi.

I, also, want to extend my gratitude to Matador Resource for sponsoring me throughout my Masters Program. I will always cherish the goodwill and will strive to keep the flag flying as a worthy ambassador of Texas A&M University.

Finally, thanks to all the department faculty and staff for making my time at Texas A&M University a great experience.

TABLE OF CONTENTS

Page

Page

LIST OF FIGURES

Page

Page

Page

LIST OF TABLES

Page

CHAPTER I

INTRODUCTION

1.1 Tight Gas Sands

Tight gas sands are unconventional formations with permeability generally less than 0.1mD. These formations are incapable of commercial gas production unless they are successfully stimulated by hydraulic fracturing. A significant percentage (25%) of the US natural gas resource base is produced from unconventional gas resources.

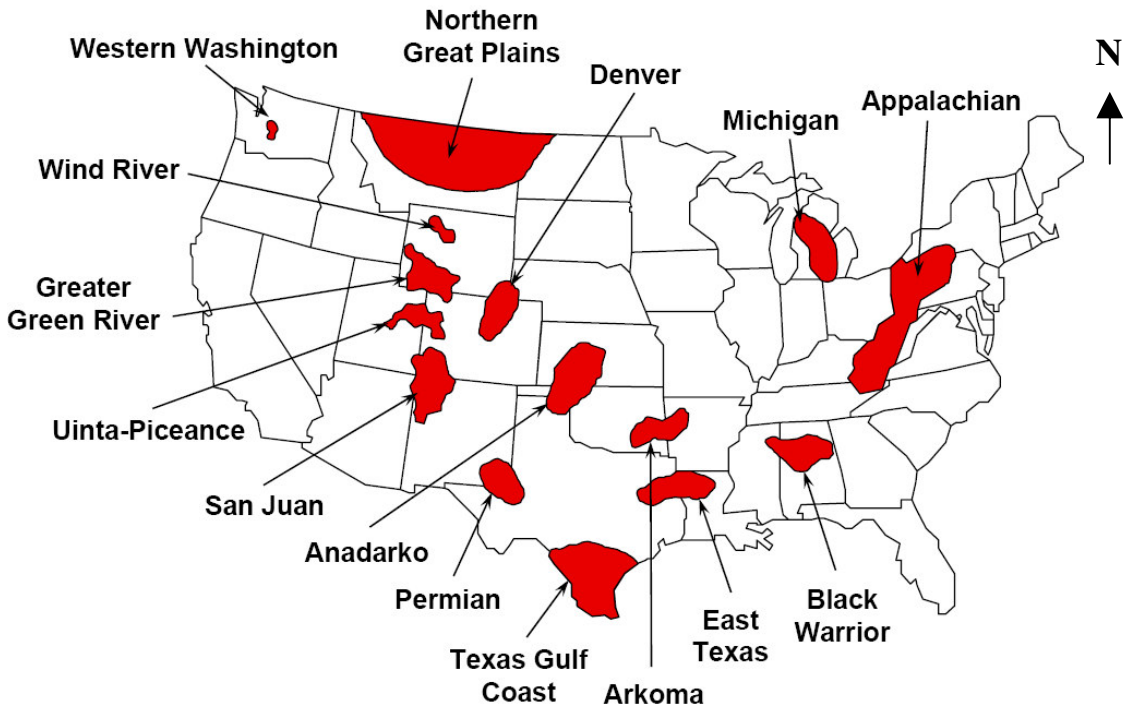

Fig. 1.1: Tight Gas Sand Basins in the United States.

This thesis follows the style of *SPE Production & Facilities.*

Tight gas sands constitute over 70% of the gas production from unconventional gas resources and 19% of the total gas production from both unconventional and conventional gas resources.[1] Tight gas formations are contained in many basins in the United States, from the Greater Green River Basin in the west to the East Texas-North Louisiana Basin in the central part of the United States to the Appalachian Basin in the east (**Fig. 1.1**).

One of the normal characteristics of tight gas sands is that they usually only produce dry gas with very little formation water. In general, water-gas ratios for wells drilled in a typical gas formation will be 10 bbls/MMcf or less. It is unusual for tight gas wells to produce large volumes of water from the same rock that has gas trapped in low permeability layers. However, in the Elm Grove and Caspiana fields in North Louisiana, the wells that are completed in the Cotton Valley formation producing gas from tight sands are also producing very large volumes of water, in the order of (100 – 1000) bbls/MMcf.

In this research, we have analyzed all the data available to us in the field area to determine feasible explanations of why these tight gas wells produce large volumes of water. We have analyzed open-hole logs, core data, geologic maps and production data from the Cotton Valley sands in the Elm Grove and Caspiana fields.

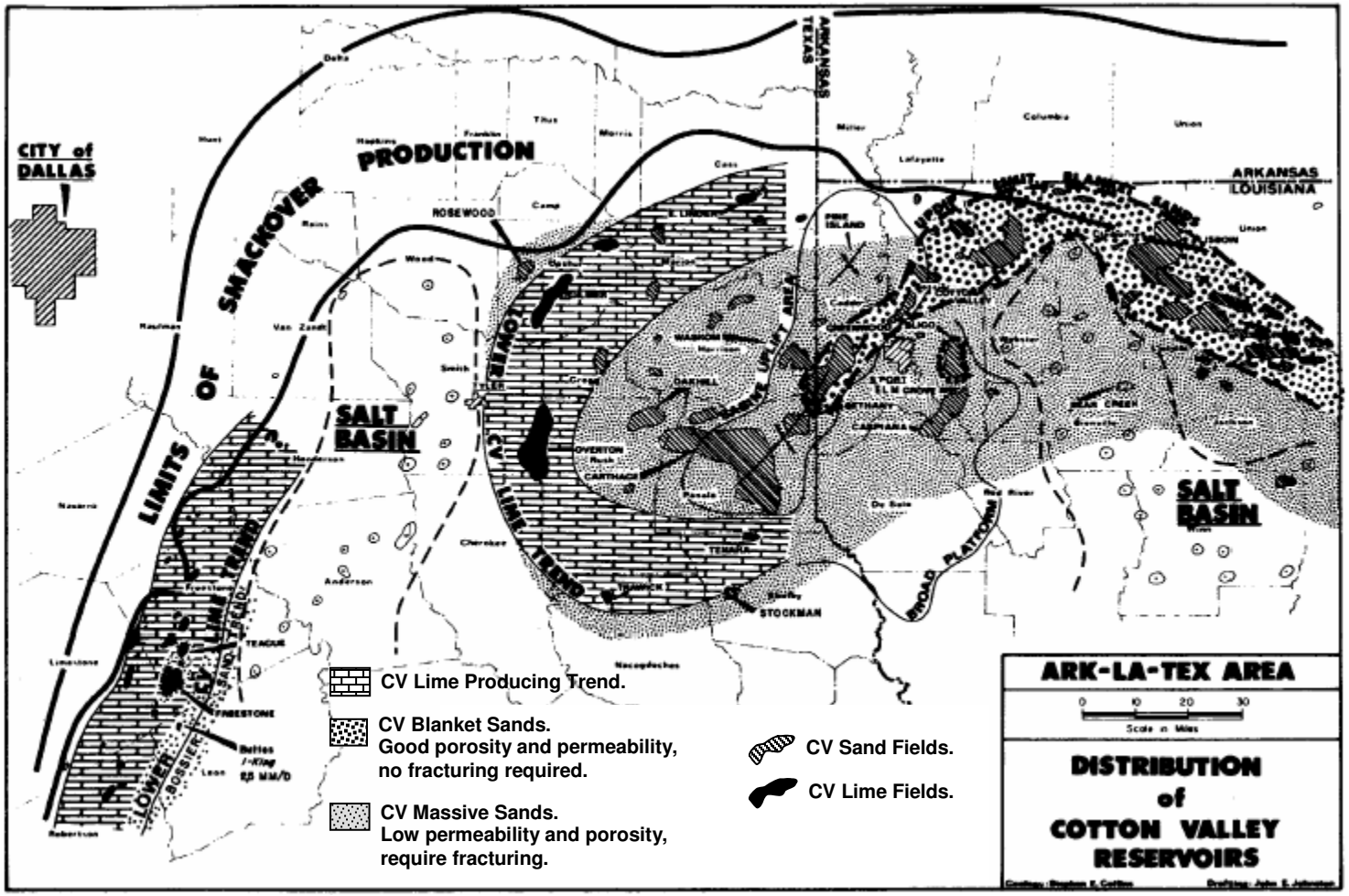

Fig. 1.2: Distribution of Cotton Valley Reservoirs across East Texas and North Louisiana. (Source - Collins[2])

1.2 The Cotton Valley Formation in Northwest Louisiana

The Cotton Valley formation is a tight gas sand play in the East Texas-North Louisiana Basin, and spans a large area covering portions of Texas and Louisiana (**Fig. 1.2**). The data used in this research came from the Cotton Valley formation in the Caspiana and the Elm Grove fields. These fields are located within the Sabine uplift that cuts across East Texas and North Louisiana (**Fig. 1.3**).

The Cotton Valley sandstones are generally of two types, the up dip porous and permeable blanket sandstones and the massive low permeability sandstones. The blanket sandstones are easily correlatable over many miles and readily produce oil and gas on open-flow drill stem tests. The down-dip low porosity, low permeability, fine-grained, massive, undifferentiated sandstones generally do not flow oil or gas on drill-stem tests but require hydraulic fracturing to produce at commercial flow rates.[2]

Production performance in the Elm Grove and Caspiana fields is typical of the Cotton Valley massive tight gas sands in the North Louisiana-East Texas Basin. The first well to encounter the Cotton Valley sands was drilled in 1927 in North Louisiana when most of the drilling activities were concentrated in the better quality Cotton Valley blanket sandstones. It was not until the 1970's that gas production from the low-permeability Cotton Valley massive sandstones became commercial as a result of increased gas prices and technical advances in hydraulic fracturing techniques. The first well through the Cotton Valley sands in the Elm Grove-Caspiana field area was drilled in 1973 in the northern part of the reservoir structure (**Fig. 1.4**). Further drilling continued but mainly within the central crestal region where higher gas productivity was

encountered. Today, over one thousand gas producing wells have been drilled in both the Caspiana and Elm Grove fields, and all of the wells have been hydraulically fractured to achieve commercial gas production rates. However, the field gas production has been affected by excessive water production, which has increased over the years.

The Cotton Valley Group is an Upper Jurassic to Lower Cretaceous deltaic sequence of sandstone, shale and limestone with a down-dip limit on gas production yet to be delineated by drilling. It is an entirely subsurface sequence of strata with top depth ranging from about 4,000 ft below sea level near the updip zero edge to more than 13,000 ft below sea level along the southern margins of the East Texas and Louisiana Salt Basins[3] (**Fig. 1.5**). The Sabine uplift (**Fig. 1.6**), where the Elm Grove and Caspiana fields are located is a broad, low relief basement-core arch, separating the East Texas and North Louisiana Salt Basins. It has a vertical relief of 2000 ft and a closed area of over 2500 square miles.[4]

The Cotton Valley lithofacies and associated stratigraphic nomenclature in northern Louisiana are presented in **Fig. 1.7**, **Fig. 1.8** and **Fig. 1.9**. The basal formation of the Cotton Valley Group is the Cotton Valley Limestone. The Bossier shale grades upwards into the Cotton Valley sandstones with inter-bedded shales. These Cotton Valley sandstones are referred to as the Terryville massive-sandstone complex in Northern Louisiana.[5,6,7] The Terryville or Cotton Valley sandstones averages about 1000-1400 ft in thickness.[8,9] The Bossier shale is underlain by the Smackover, Buckner, Haynesville, and Cotton Valley limestone formations. Overlying the Cotton Valley Group are the Travis Peak (Hosston) formation and Petit (Sligo) formation.

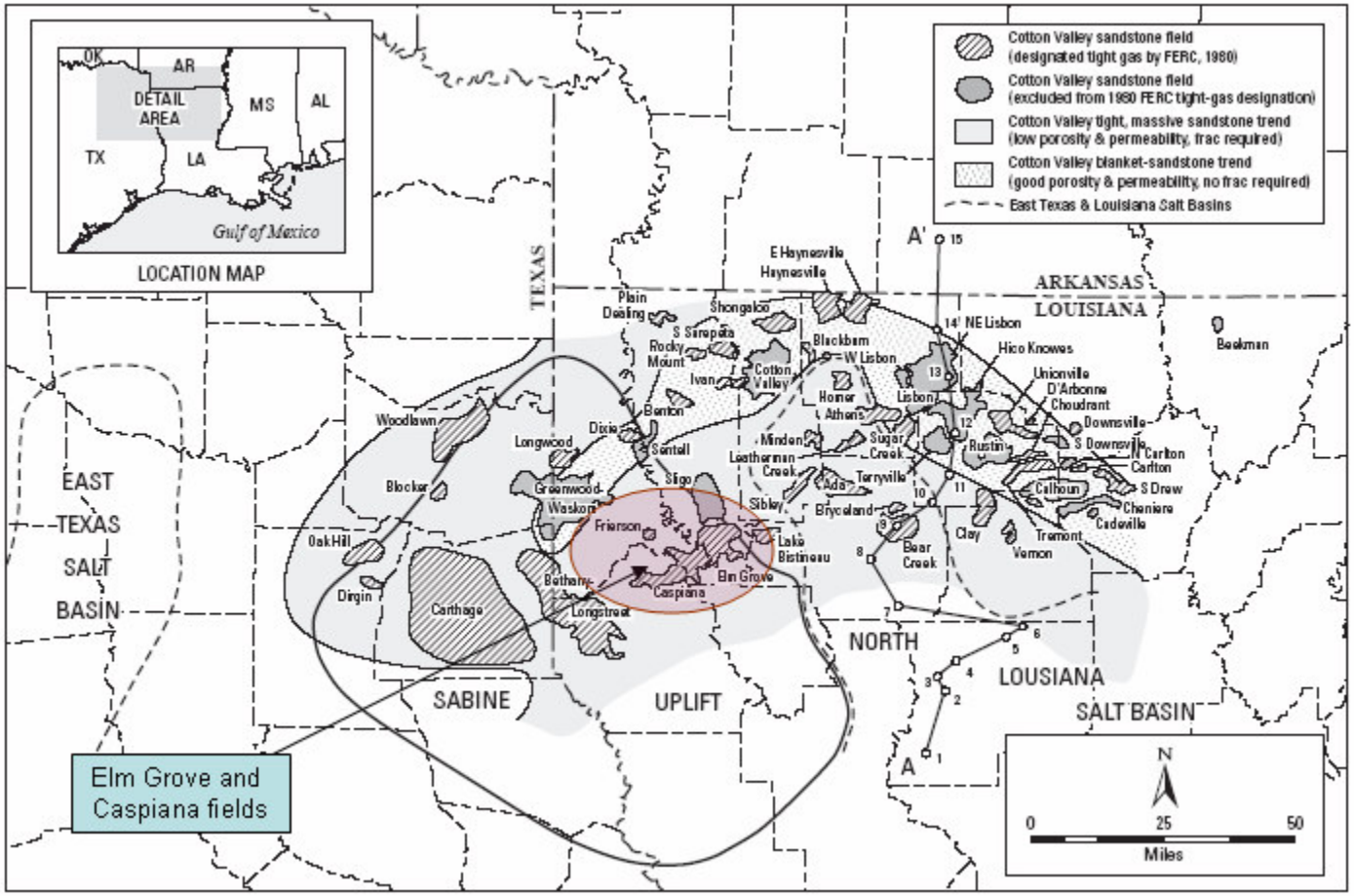

Fig. 1.3: Map of Northeastern Texas and Northwestern Louisiana. Map shows major fields that have produced hydrocarbon from the Cotton Valley Group sandstones. (Source - USGS Bulletin[3])

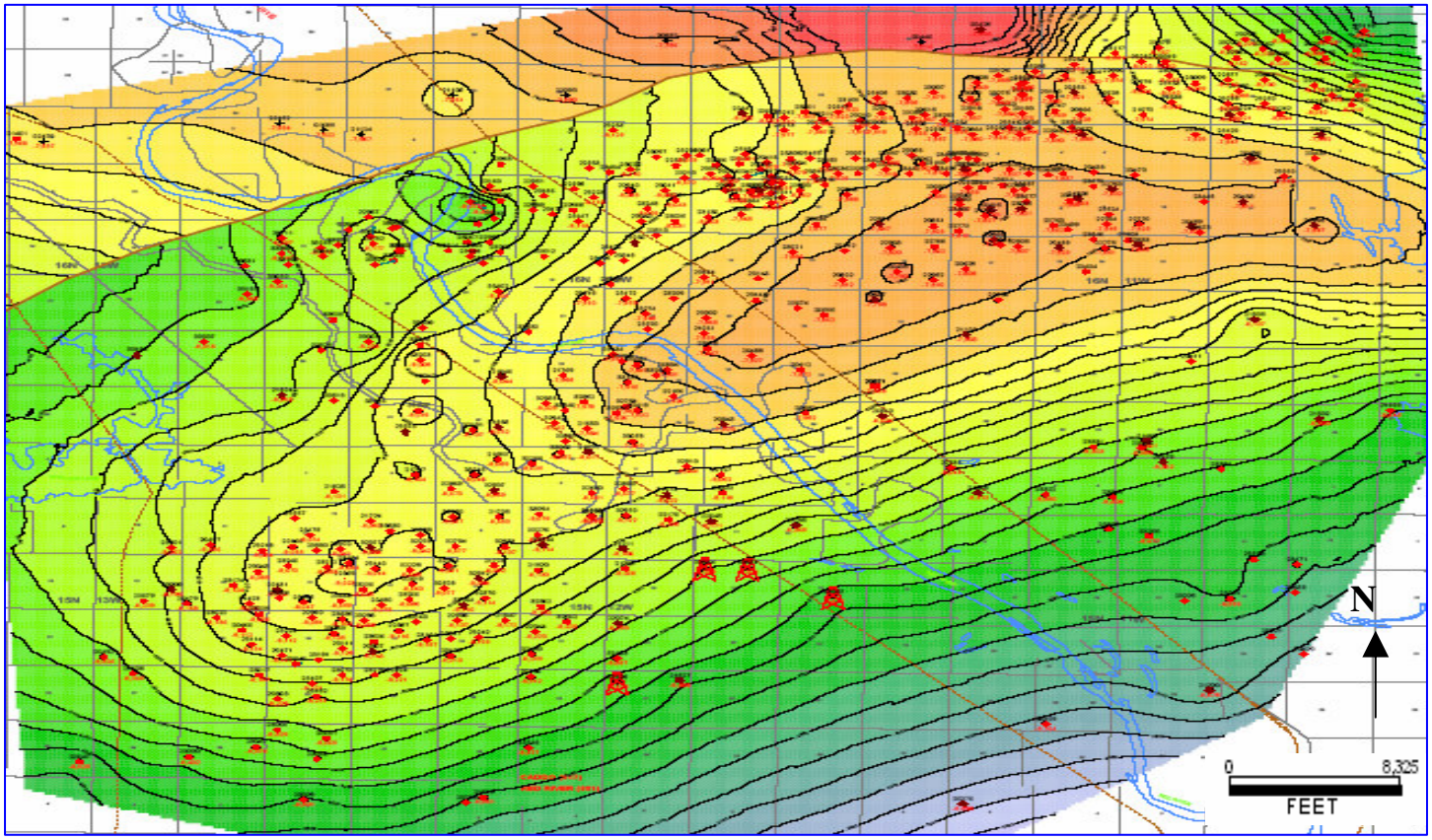

Fig. 1.4: Horizon Map of the Elm Grove and Caspiana Fields.
Map shows the structural configuration of the Cotton Valley sands in the Elm Grove and Caspiana fields.

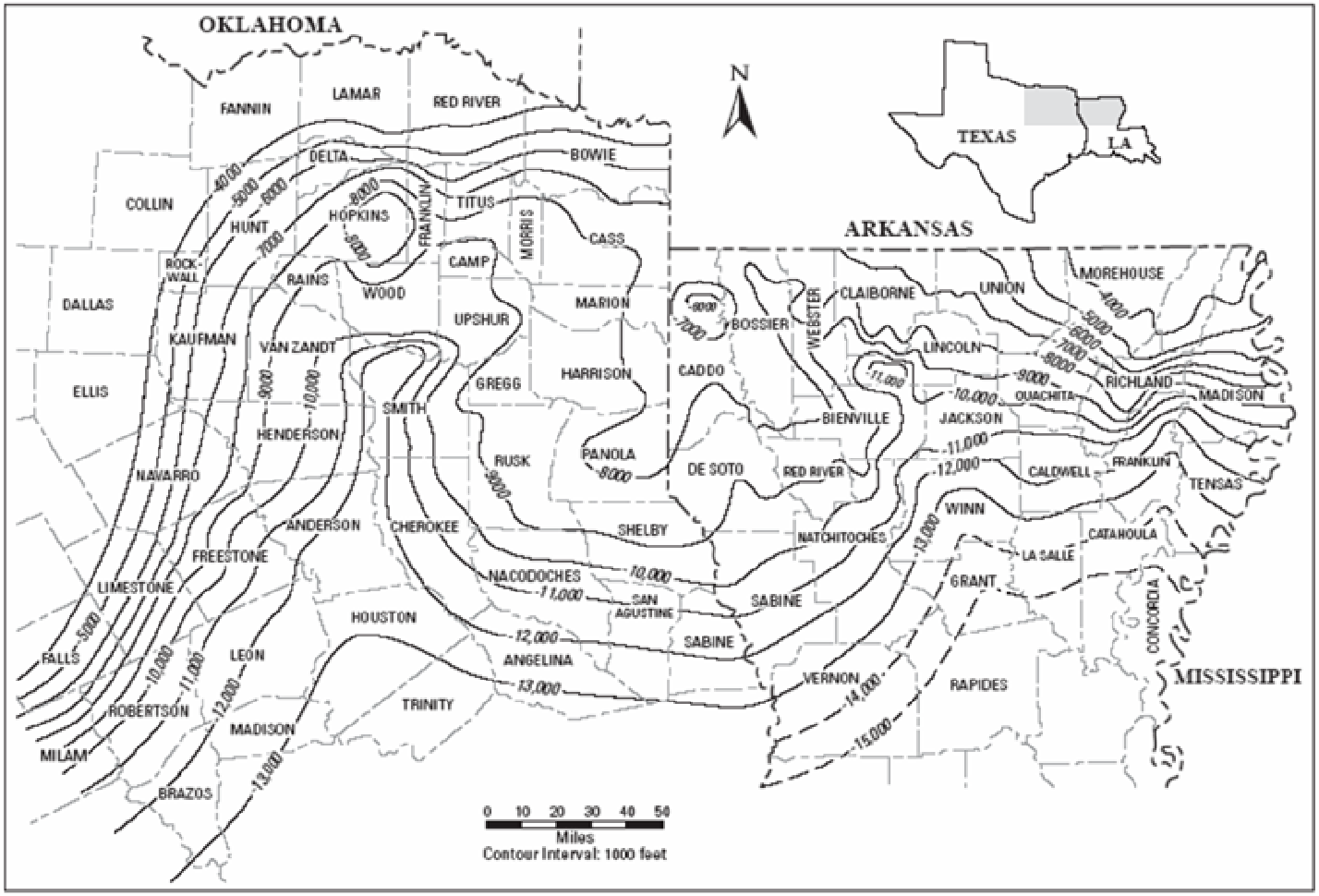

Fig. 1.5: Generalized Top Structure of the Cotton Valley Sandstones.
Map shows the structural configuration of the Cotton Valley sandstones across East Texas and North Louisiana. (Source – USGS Bulletin[3], modified from Finley[8])

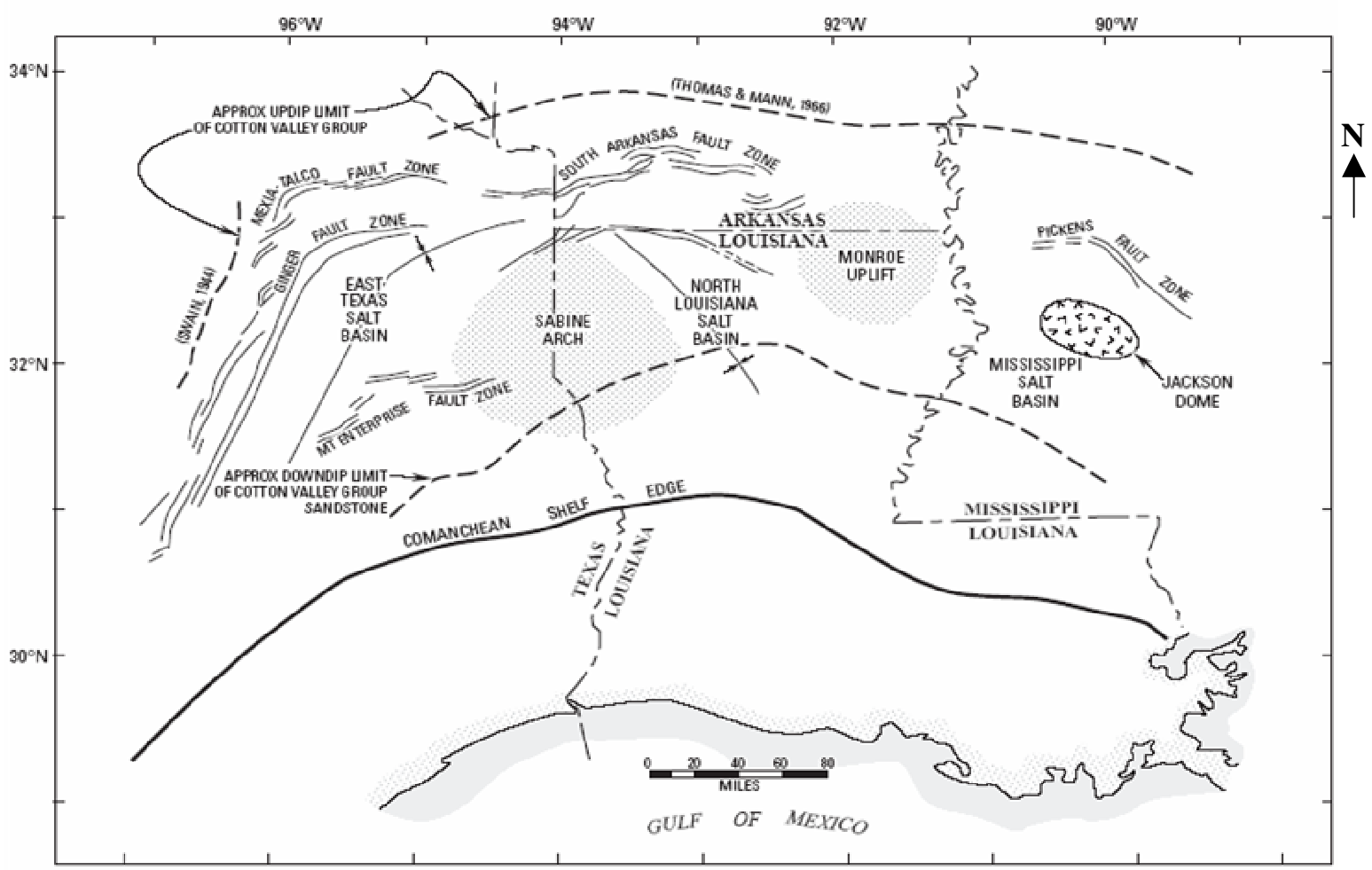

Fig. 1.6: Index Map of North-Central Gulf Coast Basin.
(Source - USGS Bulletin[3], modified from Dutton and others[10].)

The Knowles limestone appears in some regions between the Cotton Valley Sandstones and the Travis Peak.[11]

The Cotton Valley sandstones are products of complex diagenetic processes which include compaction, cementation, replacement and precipitation. The extensive compaction and cementation processes are primarily responsible for the low permeability and porosity exhibited by the formations. Carbonates do occur as secondary minerals and may account for over 50% of the rock matrix in some isolated intervals. The presence of carbonates in sandstone formations tends to increase the heterogeneity of the formation. Grain densities of the carbonates range from 2.71 g/cc to 3.96 g/cc, depending on the mineral forms of the carbonates.[12] Other minerals present include chert, pyrites and clay minerals. The effects of these minerals have a profound impact on the porosity computation in the log analysis especially with the grain densities which tends to vary with the corresponding relative proportions of the different minerals.

To properly account for the varied mineral composition, a probabilistic multi-mineral model is required to accurately determine the porosity profile of the formation. More often than not this model is not used. However, sophisticated logging solutions such as the nuclear magnetic resonance logs and the bore-hole image logs can be used to improve the formation evaluation.

The Cotton Valley sands are generally characterized by the presence of authogenic clays which coat the quartz grains and tend to affect the log interpretation process. Authogenic clay coatings can be comprised of conductive clay minerals which

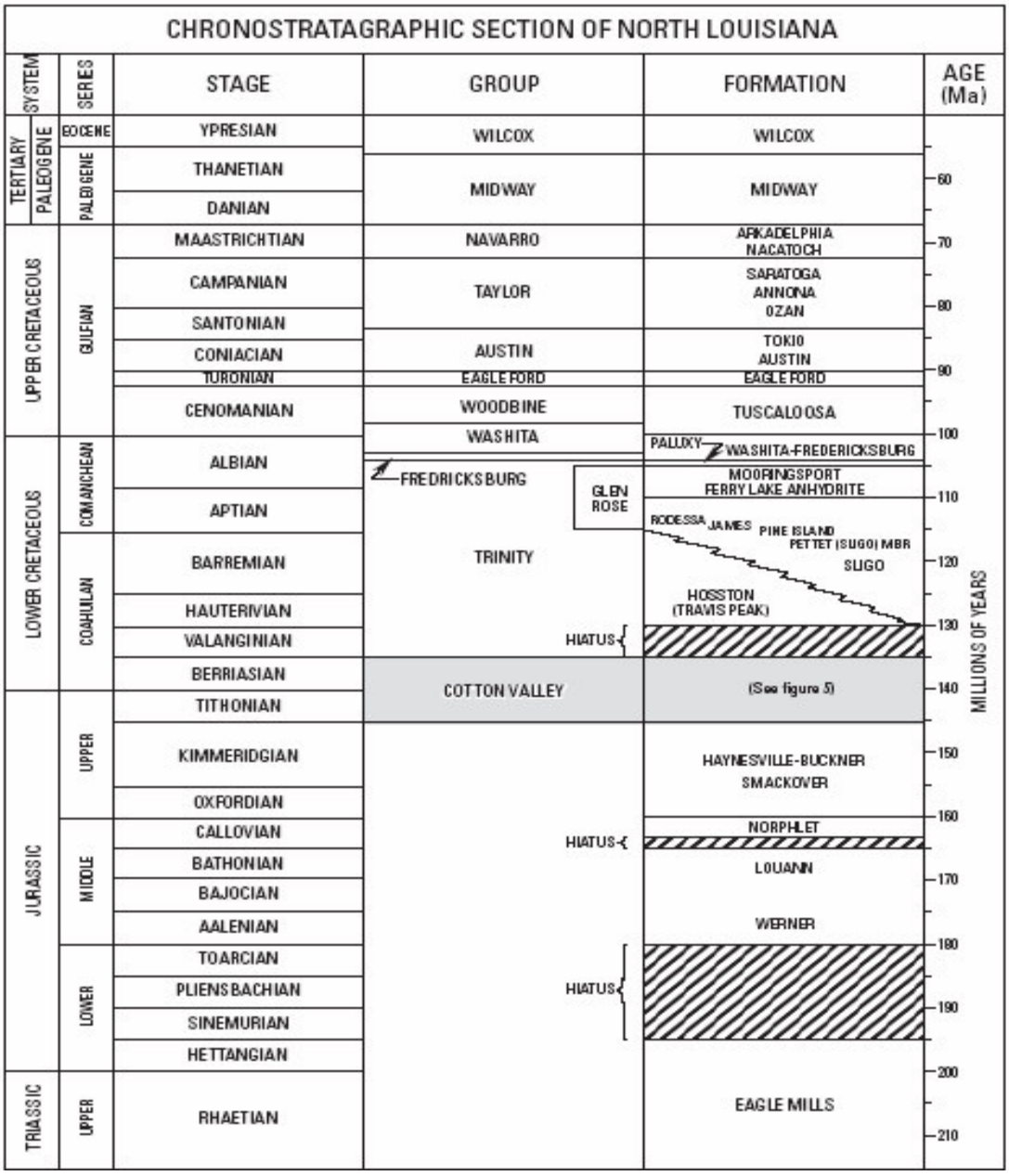

Fig. 1.7: Chronostratigraphic Section of Northern Louisiana. (Source – USGS Bulletin[13,3], modified from Shrevport Geological Society-1987.)

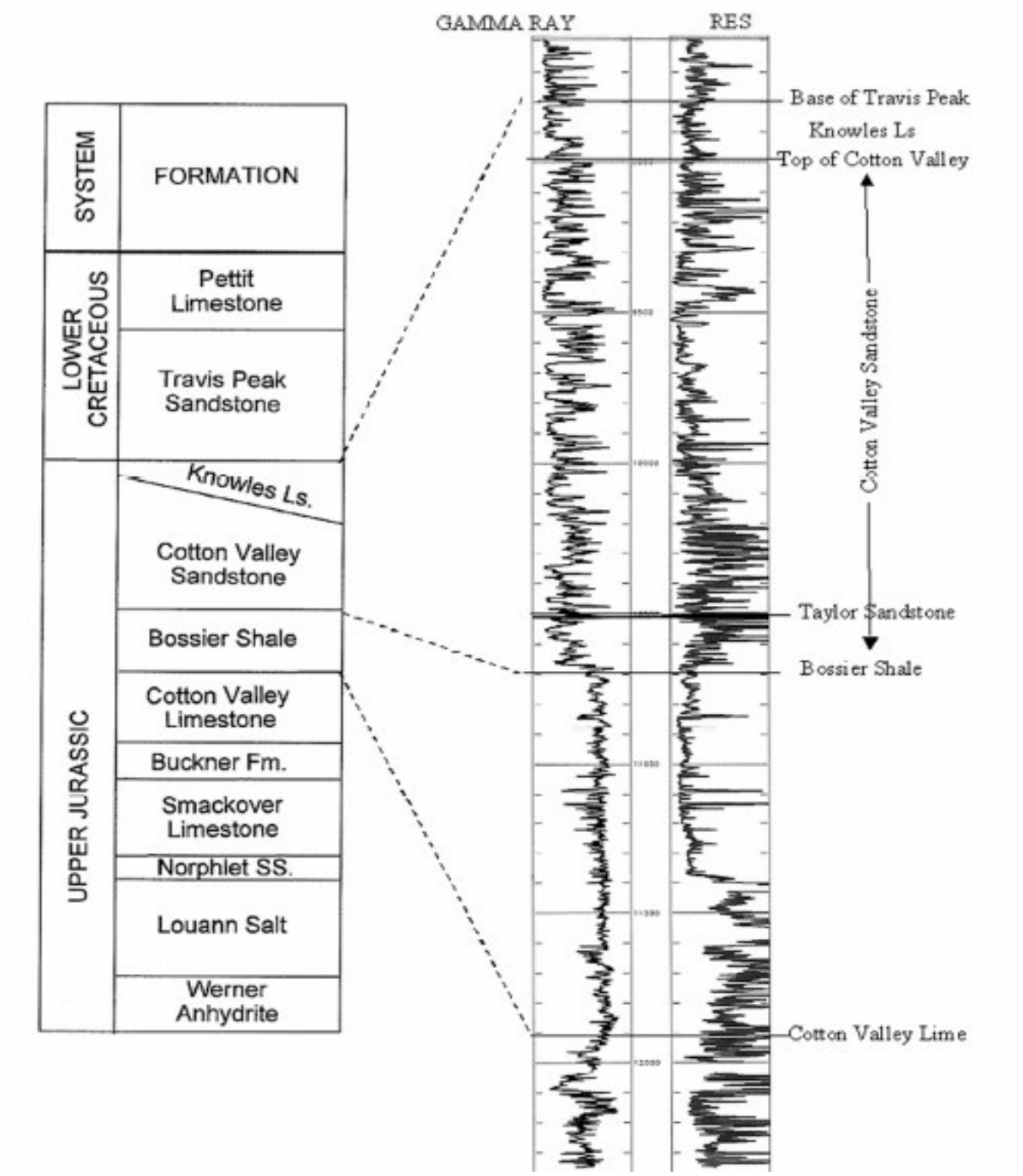

Fig. 1.8: Stratigraphic Column of the Upper Jurassic and Lower Cretaceous Units in the East Texas Basin.
(Source – Williams and others[11])

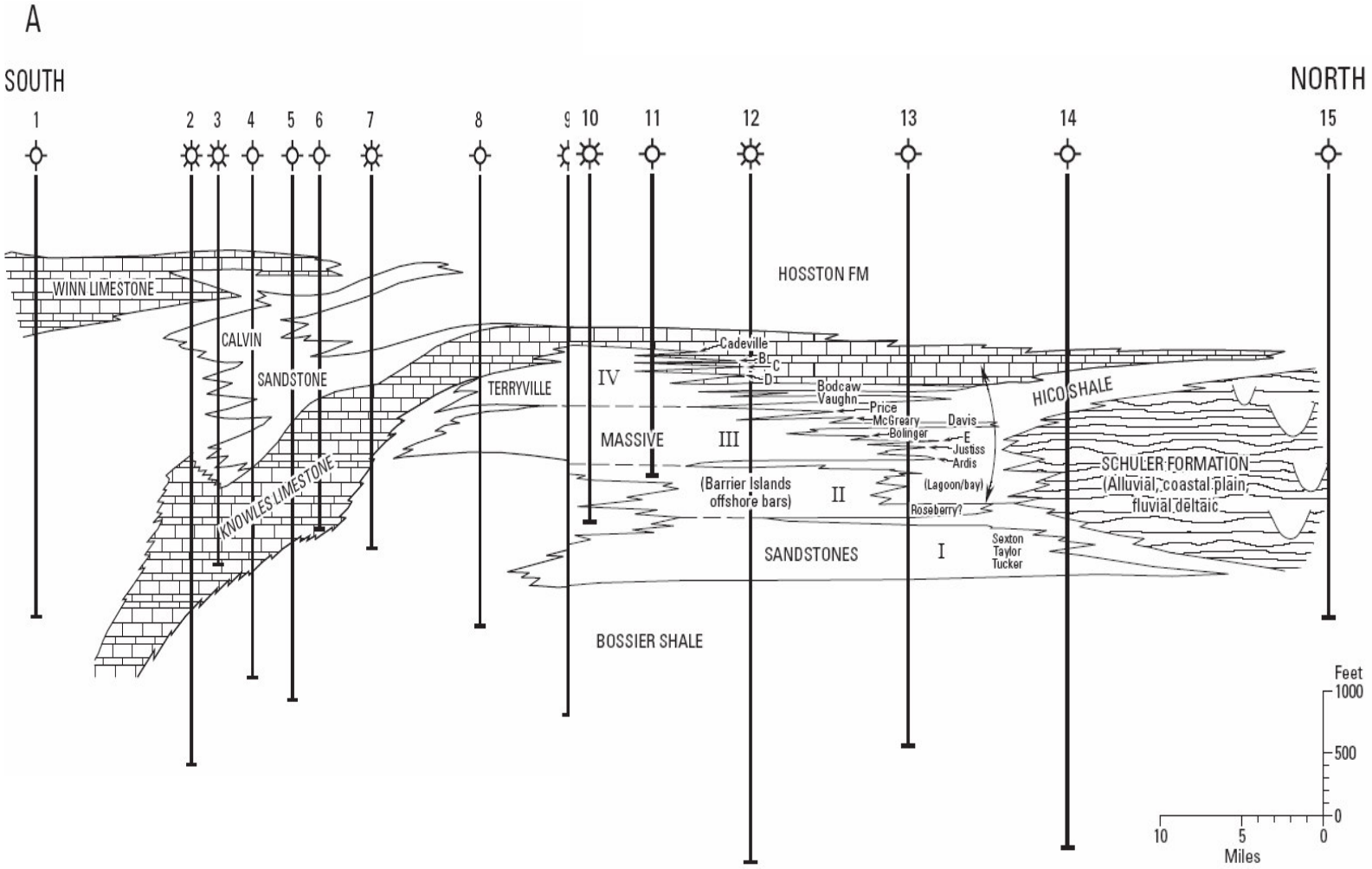

Fig. 1.9: North-South stratigraphic cross section of the Cotton Valley Group. Map shows typical stratigraphy of the Cotton Valley Group across northern Louisiana based on data from 15 Wells. (Source – USGS Bulletin[3], modified from Coleman and Coleman[7].)

tend to reduce resistivity measurements independently from other factors such as formation factor and pore fluid content. These minerals include kaolinite, illite, and chlorite. The most dominant are chlorites and illites, which can be observed with a scanning electron microscope if core samples are available.

The clay coatings tend to limit quartz growth and cementation, resulting in some porosity retention during diagenesis. The log responses in the Cotton Valley sandstones of the Elm Grove and Caspiana fields have been found to be affected by conductive clay minerals. The classic log interpretation procedure fails without due consideration of the effect of these clay minerals.

The geological map of the field was generated from the well tops data and shows an open anticline structure with a Northwest-Southeast trending boundary fault in the northern part of the field (Fig. 1.4). Since no seismic data are available for this study, uncertainties do exist in the structural profile of areas with limited well coverage.

The structural interpretation is crucial in evaluating the source of water production as possible fault leakages and water propagation paths are affected by the structural configuration. A close review of the production history of the field shows that most of the early water producing wells in the Cotton Valley sands tends to be located within the saddle region at the center of the structure. Because the structure can not be confirmed with 3-D seismic, it is possible that the “saddle region” where much of the water production occurs, could contain faults and fractures.

1.3 Production History

Although production commenced in some Cotton Valley Sands in 1927, production in the Elm Grove-Caspiana field did not commence until February, 1973 in the northern part of the field. Today, over 1,000 wells have been drilled with locations concentrated mainly in the center and crestal region of the field. Most of the production data were obtained from IHS Energy which had information on the monthly gas production flow rates, and results of periodic production well tests. Log data were provided for 39 wells located mainly in the saddle region of the field where most of the water production has been observed. Although completion depths are provided with the production data, the well log data are still required to tie the completions depth to the actual producing units.

The rate of production, timing and distribution of wells has a great impact on the water production in the fields. Sustained water production was first observed from a production test in October, 1974 in the Caspiana field from one of the earliest wells (CV RA SU 65; Cupples) drilled a month earlier in the central and crestal part of the field. The well produced with a water gas ratio of 66 bbls/MMcf, essentially upon initial completion. The timing of this water production barely a year after production commenced in the field, points to the existence of a water source in the field close to the well. There are no published data on the presence of a gas-water contact or production of water without gas on the flanks of the Elm Grove or Caspiana field or in any other tight gas Cotton Valley field in the massive-sandstone trend.[3]

In the low permeability massive Cotton Valley sandstone, gas-water contacts have been described as poorly defined with long transition zones when compared with the short well defined sharp gas-water contacts of the blanket-sandstone.[14,15] Dutton[10] also suggested the presence of long transition zones, when she indicated that water saturations should be less than 40 percent to achieve a successful gas completion when the producing zone is less than 200 vertical feet above the free water-level in the Cotton Valley sandstone.

Wescott[16, 17] reported that the Taylor sands located in the lower part of the Cotton Valley interval had the best reservoir potential in the Cotton Valley sandstones of the northeastern Texas area. Production logs from Oak Hill field, show that Taylor sandstones contributes about 80 percent of the total gas production, while sandstones in the middle and upper Cotton Valley section contribute most of the water production even though they also produce significant volumes of gas.[18] Presley and Reed[9] and Dutton and others[10] reported the presence of water bearing sandstones in the upper Cotton Valley interval. Since no gas-water contact has been identified in the Elm Grove and Caspiana field previously, the source of water has remained a great concern in the evaluation of the field production profile.

Some water production can be expected from tight gas sands, but the volume should only be a few barrels of water per million standard cubic feet of gas. Water condenses from the gas stream when it moves up the tubing from a region of high temperature to a cooler zone. However, water-gas ratios resulting from this water

condensation should be within the range of (0 - 20) bbls/MMcf. When the water gas ratio exceeds 20 bbls/MMcf, water is being produced from another source.

A close review of the water production data in the Elm Grove and Caspiana field wells producing from the Cotton Valley sands shows a progressive change in the water-gas ratios from values less than 30 bbls/MMcf to between 50bbls/MMcf and 200 bbls/MMcf, and then finally to values greater than 400 bbls/MMcf. This increase in water production can not be explained easily. A sustained water production rate greater than 100 bbls/MMcf is highly unusual in most tight gas reservoirs, and the source of the water is difficult to track, understand or prevent. One problem is that these tight gas wells must be fracture treated, which tends to break down any natural vertical barriers to fluid migration. Although gas production in the Elm Grove and Caspiana fields has been from the different units of the Cotton Valley formation, most of the production has been from the lower Cotton Valley unit which was the first to commence water production. However water production has been observed in all the units in different well locations and with varying rates of production. The selective water production in the different units tends to point to the possible existence of intercalating shale baffles or barriers.

1.4 Problems and Uncertainties

In this research, we have evaluated the excessive water production in the Cotton Valley sands of Elm Grove and Caspiana fields. While producing small volumes of water is normal in tight gas sands, excess water production from wells located at the center of a field, with no clearly defined gas-water contact is not normal. Excess water

production jeopardizes gas recovery and further development prospects of a field, and greatly increases operating costs.

The data used in this study came from public records and from Matador Resources. The varied ownership of concessions in the Caspiana and Elm Grove fields constitutes a problem for data access, quality control and integration. The ownership of leases varies from individuals, to both small and large independents, and a few major gas producers.

The production data were obtained from the IHS Energy data base, which is a recognized commercial oil and gas data depository. However, the water production data are suspect. Field operators in North Louisiana are not obligated to report and validate water production data. As a result, the water production trends have been evaluated using data from production tests.

There is uncertainty in the structural definition of the reservoir. The use of well tops for generating maps may result in a translation of errors from well tops to the structural profile. As such, contours are sometimes skewed in areas where there are large variations in the well tops. Similarly, in areas with little or no well coverage, the depth contours tend to be inaccurate and could substantially change the overall structural configuration of the field. Consistent discrepancies in the contouring of the map would normally indicate the possible existence of structural faults; however, due to possible errors from well tops, the existence of minor faults on the structure can not be readily ascertained. The faults and associated natural fractures could very well be the pathway that allows water to be produced from the Cotton Valley wells.

Data from 39 wells located mainly in the center of the field were digitized and analyzed (**Fig. 1.10**). The logs usually include resistivity, density, neutron and the gamma ray logs. Most of the logs were affected by bore-hole washouts, while others had either missing sections or sections with bad data. There was a need to model logs in sections were data where inaccurate or missing. While a modeled log is not a substitute for measured data, it can provide reasonable estimates of the general log profile in the absence of log measurements. The presence of clay minerals and carbonates in the Cotton Valley formation makes log interpretation and log evaluation more challenging. A multi-mineral model which corrects for the effects of clay minerals, pyrites and the presence of carbonates in the formation is required to properly evaluate the logs. Simple models used in this study introduced uncertainties in the results, especially those concerning the lithology and porosity evaluation.

Similar to log data analysis, both routine core analysis and special core analysis were carried out on cores cut from the field by a commercial laboratory. The special core analysis measurements included formation resistivity factor, resistivity index measurements, relative permeability measurements, and capillary pressure measurement. There were only a few measurements of relative permeability and capillary pressure because of the limited amount of core. Because of the large heterogeneity of the Cotton Valley formation, the measurements available were only of limited value. Additional data were obtained from published literature.

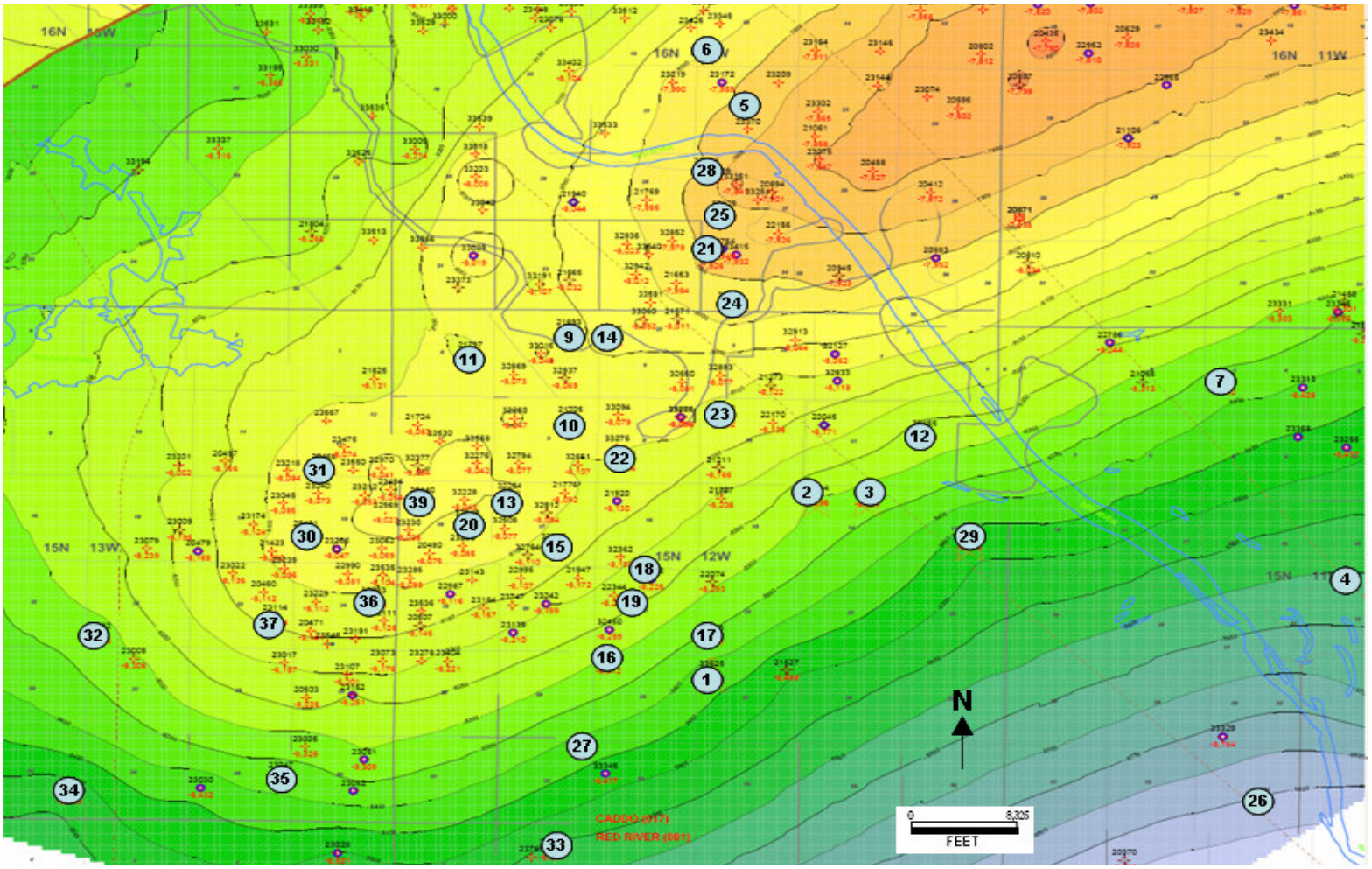

Fig. 1.10: Distribution of Wells across Elm Grove and Caspiana Fields.
Well number sequence for evaluation purpose.

1.5 Objectives

The objectives of this research project were as follows:

1. Analyze the logs and other data to obtain a reasonable reservoir description of the layered, Cotton Valley formation in Caspiana and Elm Grove fields;
2. Evaluate possible scenarios that would allow wells in tight gas sands such as the Cotton Valley formation in the Caspiana and Elm Grove fields to produce large volumes of water;
3. Review and outline the inconsistencies in the field data and the associated uncertainties; and
4. Provide results based recommendations on the source of water flow in the field, and how the field can be developed further to produce more gas and less formation water.

CHAPTER II

LITERATURE REVIEW

2.1 Definition of Tight Gas Sands

In 1970 tight gas sands was defined by the United States Government as reservoir sands with effective permeability to gas less than 0.1 mD. This was a political definition used to determine federal and/or state tax credits for producing gas from tight gas reservoirs.

Naik[19] refers to tight gas sands as a term coined for reservoirs of natural gas with an average permeability of less than 0.1mD. Naik[19] went further in his definition and referred to tight gas reservoirs as a gas bearing sandstone or carbonate matrix with possible existence of natural fractures, exhibiting in-situ permeability to gas of less than 0.1mD. The German Society of Petroleum and Coal Science Technology (DGMK) defined tight gas as reservoirs with average effective gas permeability less than 0.6 mD.

Holditch[20] in his distinguished author series article for SPE, defined a tight gas reservoir as a reservoir that cannot produce at economic rates nor recover economic volumes of natural gas unless wells in the reservoir are stimulated by a large hydraulic fracture treatment or produced by use of horizontal wellbore or multilateral wellbores.

2.2 Diagenetic History of Cotton Valley Tight Gas Sands

A lot of reasons have been adduced in the petroleum literature for the formation of tight gas sand. Almost all the reasons involve complex diagenetic processes such as compaction and cementation. Wescott[16] attributed the reduction in reservoir quality of

the Cotton Valley tight gas sands to the complex diagenetic process of compaction, cementation, and replacement. He made some exceptions for some cementation and replacement cases where relict primary porosity was preserved and micro-porosity created. The cementation process involves authogenic cements which include quartz, calcite, detrital clays, authogenic clays, feldspar and iron oxides.[16]

Wescott[16] gave a good description of the various types of cement observed in the Cotton Valley grain framework. Quartz cement occurs as syntaxial overgrowths which ultimately results in low permeability and porosity after the cementation process.[16] Calcite cements occurs probably very early in the burial history of the Cotton valley sands and are the most volumetrically significant authogenic constituent in the Cotton Valley formation.[16] Detrital clays occur as laminae or dispersed mineral complex within the sandstone lithology, mainly in bio-turbated zones. Much of these detrital clays occur as illites converted from smectites.[16] Authogenic clays occur as clay coats around the quartz grains and in some cases they may inhibit the formation of quartz overgrowths and help maintain porosity.[16,21,22,23] They also occur as pore fillings but mainly as growths into the pore space. Authogenic clays are mainly chlorites and illites, although kaolinite does occur as a result of the alteration of feldspars. Feldspar cements are rare in the Cotton Valley sands but occur as syntaxial overgrowths in K-spars (potassium feldspars). Iron oxide form minor amounts of cement in the Cotton Valley sandstone. They are generally associated with clayey or matrix-rich zones.

Wescott[16] also described the dissolution and replacement process. He defined replacement as the one-for-one change in solution of one mineral by precipitation of

another in its place. In the Cotton Valley sandstones the most common reactions involve the replacement of silicate minerals by carbonates, secondary porosity is formed by the direct dissolution of detrital grains or their replacement minerals, and the dissolution of authogenic cements. The most common observed type of secondary porosity in the cotton valley sandstone is the dissolution of feldspars.[16]

Wescott[16] concluded that Cotton Valley sandstones can be classified into three groups which can be related to porosity characteristics and can be used to predict potential reservoir rocks. Type-1 rocks are tightly cemented early in their diagenetic history by quartz overgrowths and calcites and make poor reservoirs. Type-II rocks are clay-rich sands with poor initial porosities and permeabilities but make better reservoir rocks because the clays prohibit nucleation of silica overgrowths. Type-II rocks do have micro-porosity that hold irreducible water and may produce gas. Type-III rocks are high in unstable grains and have good secondary porosity produced by the dissolution of grains and cements. Type-III rocks have the highest measured porosities in the Cotton Valley sand stones and are of relatively good reservoir quality. [16]

2.3 Basin Centered Gas Accumulation Systems

Another important factor in classification of tight gas sands is the gas accumulation system, which may be either conventional “stratigraphic/structural systems” or unconventional “basin centered gas accumulation systems” (BCGAs). The term tight gas sand has been widely used to describe a basin centered gas accumulation system (BCGAs). Other terms such as “Deep Basin Gas” by Masters[24] have been

ascribed to "continuous gas accumulations" which has also been referred to as pervasive BCGAs. All the definitions fall short of a general application to most low permeability reservoirs. Increased discovery and development of low permeability reservoirs have continued to shape the definition and classification of tight gas sands to accommodate evolving field cases. A petroleum system as defined by Magoon and Dow[25] includes all the elements and processes needed for an oil gas accumulation to exist. These elements include source rock, reservoir rock, seal rock and overburden rock. While the relevant processes include trap formation and generation, expulsion, migration and accumulation.

Law[26] defined BCGAs as regionally pervasive accumulations that are gas saturated, abnormally pressured (high or low), commonly lack a down-dip water contact and have low permeability reservoirs. According to Law[26] in the BCGAs, deep burial of gas and oil prone source rocks result in thermal heating and hydrocarbon generation. The gas generation results in migration of the gas and expulsion of water from pore spaces of low permeability reservoirs. Because the rate at which gas is generated and accumulated is greater then the rate at which gas is lost, the newly generated gas accumulates in the pore system until the capillary pressure of the water wet pores is exceeded and free mobile water is expelled. This results in the development of over-pressured gas-saturated reservoirs with little or no free water.[26] These gas-charged reservoirs are regionally pervasive and commonly encompass several thousand square miles. Wescott[27] linked hydrocarbon generation in the in the Jurassic intervals to the Bossier shales, while that of the Cretaceous intervals were linked to the Eagleford shale and shales in the Pearsal Group.

Seals in BCGAs range from lithological to relative permeability or water-block seals which can be referred to as capillary pressure seals. These capillary pressure seals generally occur in reservoirs that have very small pore throat sizes and two or more fluid phases, e.g. gas and water. The permeability of each phase is effectively reduced to block fluid flow.[26] Law[26] also categorized Basin Centered Gas Systems (BCGS) in the context of petroleum systems as direct and indirect type. He provided the attributes of direct and indirect BCGS given in **Table 2.1**. Naik[19] proposed that although tight gas sands are an important type of basin centered gas reservoir, not all of them are basin centered gas accumulation systems (BCGAs). He referred to Shanley[28] who provided field examples of low permeability reservoirs from the Greater Green River Basin (GGRB) of Southwest Wyoming. These low permeability reservoirs were not part of a continuous gas accumulation or a basin centered gas system, in which productivity is dependent on the development of enigmatic sweet spots, instead gas accumulations were found to occur in conventional traps. Shanley[40] contended that the GGRB is neither regionally gas saturated, nor is it near irreducible water saturation and that water production is both common and widespread. According to Shanley[40], natural gas is found in low permeability reservoirs in both conventional traps and as continuous-gas accumulation.

2.4 Natural Fractures

Shanley[40] and Tye[29] described the role of natural fractures in contributing to improved deliverability of natural gas in low permeability basin centered accumulations as poorly understood. Hyman and others[30] described the effects of microfractures on directional permeability. Spencer[31] and Ammer[1] suggested that gas-flow rates from some wells cannot be accounted for with the available permeability to gas at in-situ conditions, thereby pointing to the possible contribution of significant fracture permeability

Table 2.1: Attributes of Direct and Indirect Basin Centered Gas Systems (Source - Law[26])

Type	Direct	Indirect
Source Rocks	Gas-prone type-III kerogen	Liquid-prone types I/II Kerogen
Reservoir in-situ permeability	<0.1 mD	<0.1 mD
Hydrocarbon Migration distance	Short	Short/Long
Reservoir Pressure	Over-/underpressure	Over-/underpressure
Pressure Mechanism	Hydrocarbon generation	Thermal cracking of oil to gas
Seal	Capillary	Lithologic/Capillary
Seal quality	variable	good
Nature of upper boundary	Cuts across stratigraphy	Bedding parallel
Thermal Maturity top of BCGA	>0.7% Ro	Highly variable
Occurrence	Downdip from water	Downdip from water

. Shanley[40] stated that even though the contribution of natural fractures to improved gas production is sometimes unclear, they can contribute to increased rate of water flow and may impact the placement of hydraulic fractures via stimulation methods. He concluded that natural fractures may enhance gas production if encountered in a structurally high position within a trap. However, if fractures are encountered toward the base of a trap or outside a trap, they are unlikely to improve gas production and may account for high rates of water production.[40]

2.5 Capillary Pressure Measurements for Tight Gas Sands

Newsham and others[1] reported their laboratory and field observations of apparent sub capillary-equilibrium water saturation distribution in the Bossier tight gas sands. They concluded that water vaporization and dissolution in the hydrocarbon gas may be an effective mechanism for removing and transporting connate water up the vertical column.

Newsham, Rushing, Lasswell and Blasingame[33] did a comparative study of laboratory techniques for measuring drainage capillary pressures in tight gas sands. They used various techniques including, vapor desorption, high speed centrifuge, high pressure porous plate and high pressure mercury injection. Twenty-five core samples from the Lower Cotton Valley/Bossier sands in the East Texas and North Louisiana Salt Basin were used. The core porosities ranged from 2% to 14%, while permeabilities ranged from 0.0005 to 0.5 mD. The ranges of water saturation for the sands were from 5% to 60% representing both productive and non-productive zones.

Selection of core samples for the capillary pressure measurements were based on hydraulic rock types. Incremental mercury intrusion graphs and Pittman graphs of effective porosity and permeability (**Fig. B1** and **Fig. B2**) were used to classify the rock types. Type-1, 2A, 2B and 3A are considered as reservoir rock while Type 3B and 4A are considered as non-reservoir rocks having low permeability, high initial water saturation and significant heterogeneity. The poor reservoir quality makes them suitable to act as flow baffles, barriers and reservoir seals. Effective permeability and porosity of the twenty-five core samples are tabulated in **Table B1** to **Table B4**. The capillary pressure profile of the core samples are also given in **Fig. B3** to **Fig. B12**.

In **Fig. 2.1** and **Fig. 2.2** the capillary pressure profile of sample 2-39 clearly shows the need for additional measurements above 700 psi which is the maximum capillary pressure in the core data measurements available. The variation in the drainage capillary pressure profile is indicative of the high degree of heterogeneity prevalent in tight gas sands. It also highlights the need for additional capillary pressure data to account for rocks which ordinarily will act as seals.

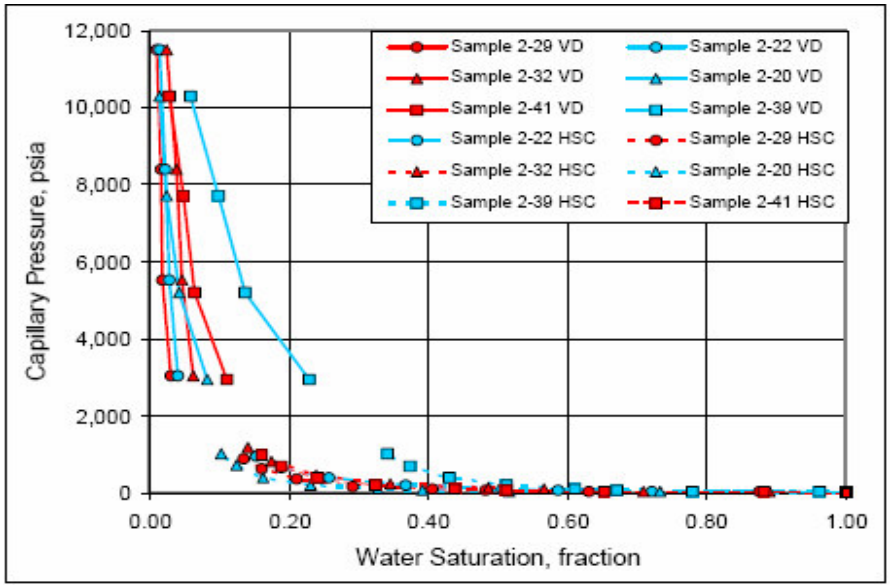

Fig. 2.1: Cartesian Plot of Capillary Pressures (VD, HSC).
Plot shows capillary pressure from vapor desorption (VD) and high speed centrifuge (HSC).
(Source – Newsham, Rushing, Lasswell and Blasingame[33])

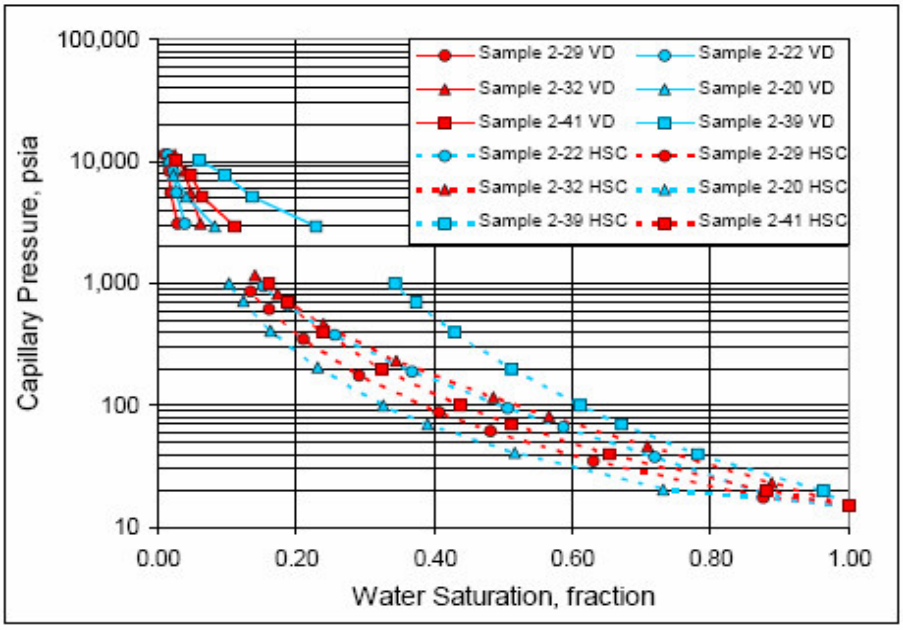

Fig. 2.2: Semi-log Plot of Capillary Pressures (VD, HSC).
(Source – Newsham, Rushing, Lasswell and Blasingame[33])

2.6 Relative Permeability Profile for Tight Gas Sands

While conventional traps are reasonably understood, continuous gas accumulation by contrast is relatively poorly understood. Shanley[40] using core data from the Lewis Sandstone taken from two different wells in the Greater Green River Basin showed that rock samples with similar porosity, base gas permeability (effective gas permeability at irreducible water saturation) and capillary pressure functions exhibit variable relative permeability to gas at overburden stress particularly at water saturations greater than 25% (**Fig. 2.3**).

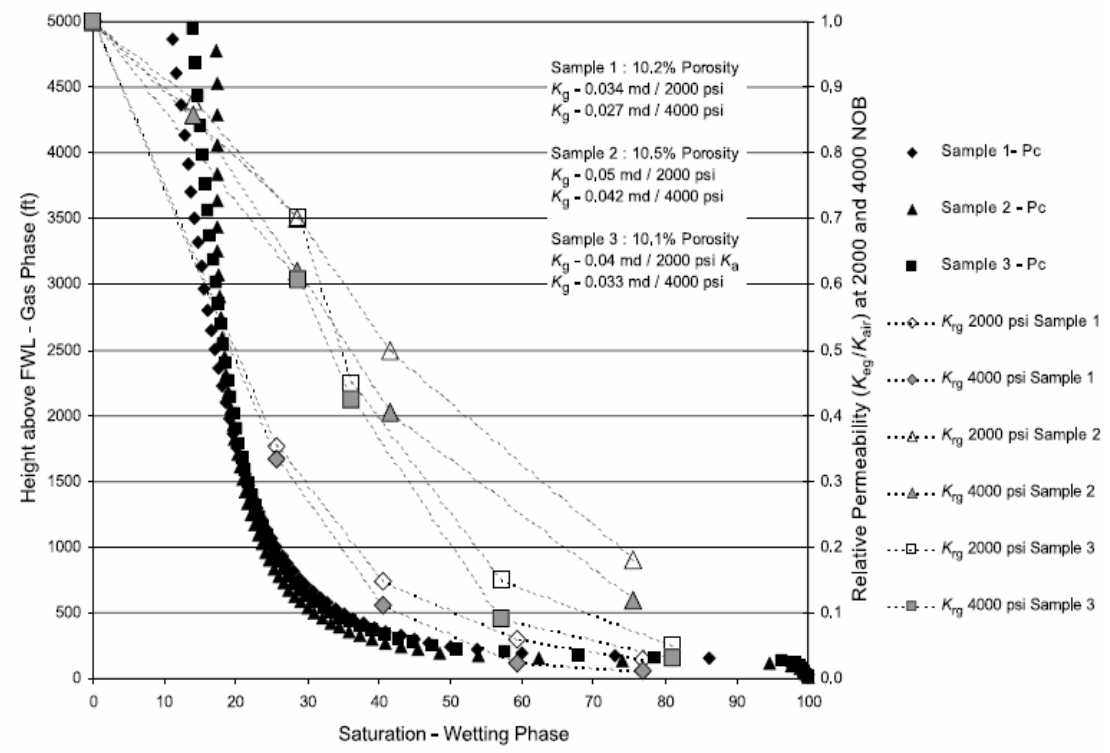

Fig. 2.3: Plot of Relative Permeability and Capillary Pressure Measurements. Plot shows core data measurements with similar capillary pressure profile and base gas effective permeability having different relative permeability profile with overburden stress and water saturation. (Source - Shanley[40])

One major difference between conventional reservoirs and low-permeability reservoirs is the response to overburden stress, and the impact that the low permeability structure has on effective permeability relationships under conditions of multiphase saturations.[34] Shanley[28] and Walls[35] provided illustrations of the relative permeability profile with changing water saturation for both conventional reservoir rock and low permeability reservoirs (**Fig. 2.4**). He discovered that some low permeability reservoirs today have been found to exhibit similar characteristics to conventional reservoirs. If we consider Shanley's findings and the fact that most low-permeability reservoirs are commonly comprised of a variety of rock types intercalated both horizontally and vertically, it is possible to have flow behaviors resulting from a combination of different relative water permeability profiles corresponding to both conventional and unconventional low permeability reservoir rock. Unconventional low permeability rocks are characterized by a water block phenomenon, in which the rock becomes impermeable to both gas and water flow over certain saturation ranges. These rocks tend to act as seals and constitute a dominant trapping mechanism in continuous gas accumulations or basin centered gas systems. The presence of both conventional and unconventional low permeability rocks tend to generate confusing fluid relationships such as the absence of clear water contacts associated with basin centered gas systems and excessive water production associated with conventional sands. This often times leads to misinterpretation of log data measurements especially in clay impacted or suppressed resistivity zones.

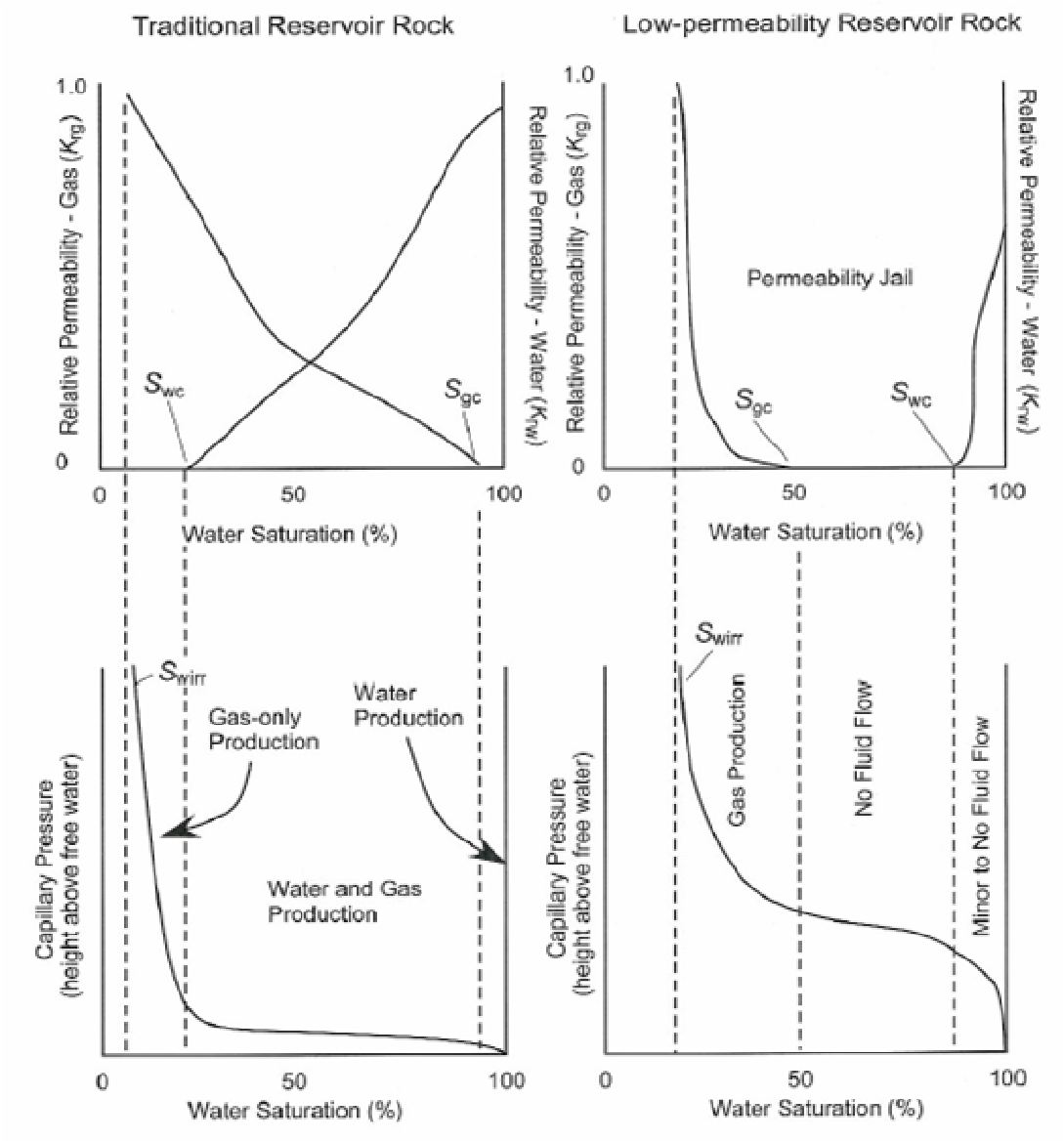

Fig. 2.4: Capillary Pressure and Relative Permeability Relationships in Conventional and Low-permeability Reservoirs.

(Source - Shanley[40])

2.7 Water Production in the Cotton Valley Sands of Elm Grove and Caspiana Fields

Water production can be associated with the initial gas production rate in the Elm Grove and Caspiana fields. High gas production rates may result in water coning or water cusping into drainage intervals. In the Elm Grove and Caspiana fields, initial gas production trends show that the wells located at the crest of the structure tend to have higher gas flow rates than wells located at the flanks. The initial gas production rates for wells in the Elm Grove and Caspiana fields are provided in **Fig. 2.5**.

Shanley[40] reported that a lack of water production or recovery from a test does not necessarily mean that the rocks are near irreducible water saturation or that the regions are water free. He explained that most transition zones are manifested by wells that fail to produce either water or gas in substantial quantities; as a result most drilling activities rarely extend sufficiently down-dip to encounter the free water level associated with the gas accumulations.

In the USGS Bulletin[3], an attempt was made to investigate the existence of a gas-water contact through analysis of DST and production test data. The objective was to determine if the Cotton Valley fields producing from the tight gas sandstones were flanked by dry holes that produced water with out any gas production. Such dry holes would then suggest the existence of a gas-water contact in the fields. Data from Carthage, Bethany, Oak Hill, Waskom and Woodlawn fields in northeastern Texas and from Bear Creek-Bryceland, Elm Grove and Caspiana field in north Louisiana were studied.

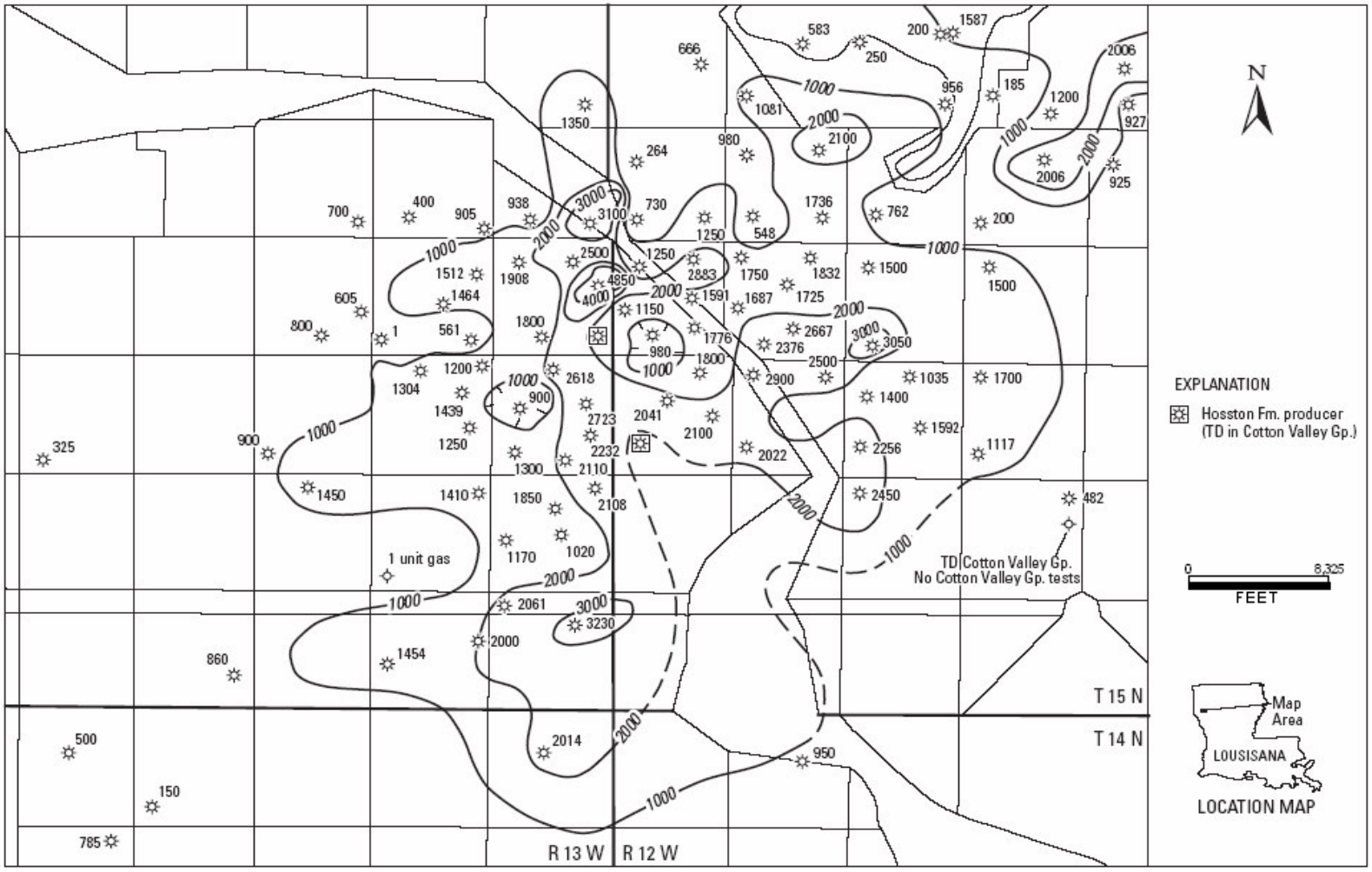

Fig. 2.5: Map of Initial Gas Production Rates in the Elm Grove – Caspiana Field. (Source-USGS Bulletin[3])

No flanking dry holes were found that tested only water. Some possible dry holes in the Cotton Valley field were not tested and were plugged-back based on evaluation from wireline logs. The test results from the Oak Hill and Elm Grove-Caspiana fields in Louisiana showed a similar general pattern with the crestal wells having higher initial gas production rates (1000-4000 Mcf/D) than the flank wells (less than 500 Mcf/D) in the field. However, some deviation to the trend was observed in the Oak Hill field where a large number of low rate wells occur in the structurally high, central part of the field. According to the USGS Bulletin[3], this variability in the trend could be attributed to a number of factors which includes reservoir variability, formation damage during drilling, and variable response to fracture-simulation treatments. On the western flank of the Oak Hill field, the initial gas production rates are high and show an abrupt change to dry holes rather than a gradual decline toward the flank of the field. A particular well producing initially over 4000 Mcf/D was reported as been flanked by four dry holes in the Cotton Valley sandstones.

An attempt was also made in the USGS Bulletin[3] to map initial water production rates (in barrels of water per day) in the Oak Hill and Elm Grove-Caspiana fields, but the results revealed a high variability in the initial rate of water production and an incomplete data set for the field. Some water production was observed to occur along with gas production in all the wells. Data was more complete in the Caspiana field and the trend in the water-gas ratios (in barrels of water per million cubic feet) were plotted (**Fig. 2.6**). Wells in the central part of the Caspiana field exhibit water-gas ratios less than 100 bbls of water/MMcf, but progressing outward toward the flanks of the field the

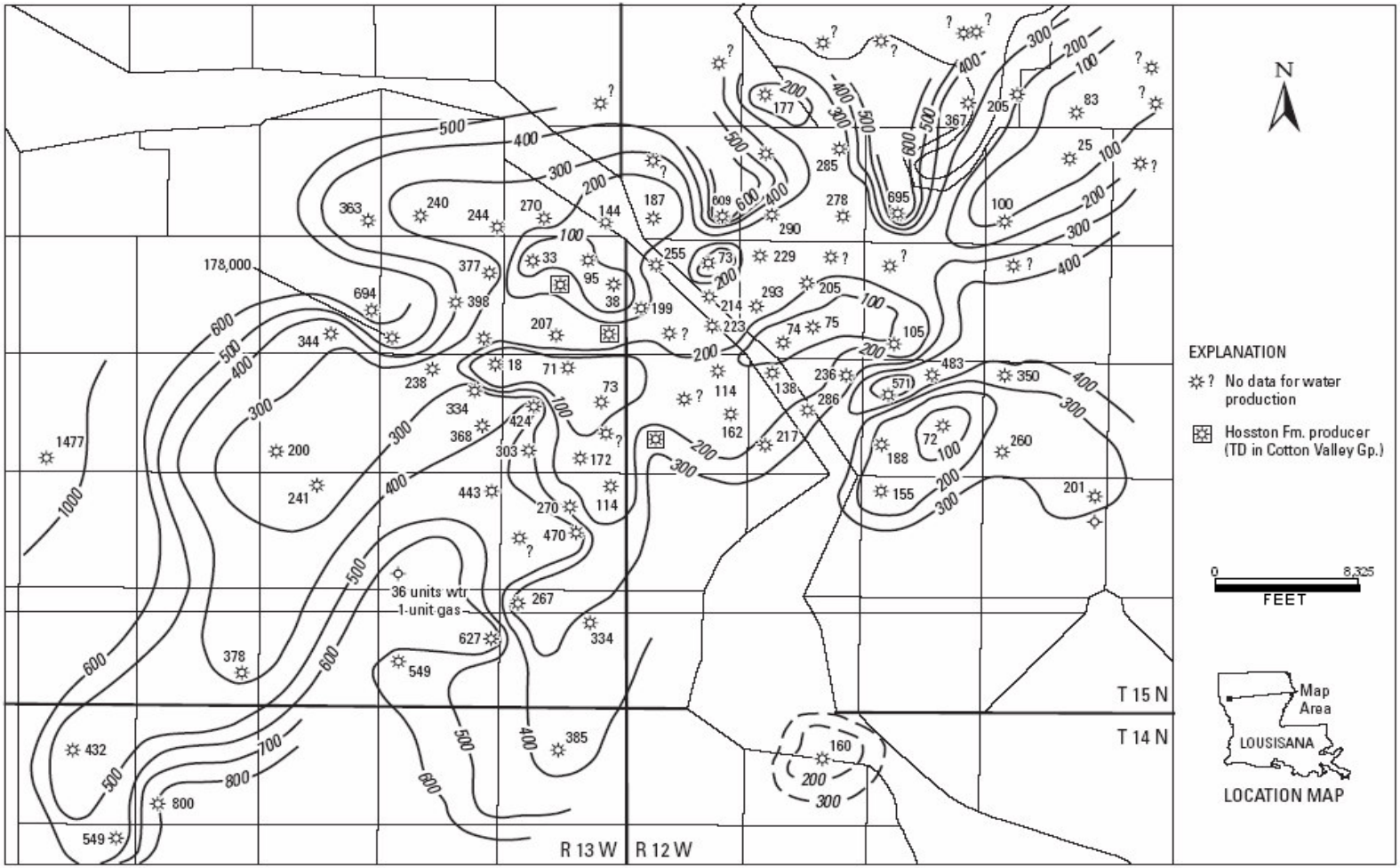

Fig. 2.6: Map of Initial Water Production Rates (bbls/MMcf) in the Elm Grove – Caspiana Fields. (Source- USGS Bulletin[3])

water-gas ratios increase to 300 bbls of water/MMcf and eventually to more than 600 bbls of water/MMcf. The highest initial water-gas ratio was observed in a well in the western flank of the field where production of 1477 bbls of water/MMcf was recorded. The well produced gas with an initial gas flow rate of 325 Mcf/D.

Above the Cotton Valley sands, in the Travis Peak formation, a similar analysis was made to investigate the presence of gas-water contacts. The analysis showed that water was recovered without gas from production tests or DST's in Travis Peak sandstone reservoirs in wells on one or more flanks of Bethany-Longstreet, Cheniere Creek, and Caspiana fields in northern Luisiana.[13] These data indicates the presence of gas-water contacts within Travis Peak sandstone reservoirs in those fields.[13]

CHAPTER III

METHODOLOGY

3.1 Data Gathering

Matador Resources provided log data, core data and some production data. Most of the production data was obtained from IHS Energy. The log data available for this project is tabulated in **Table A1**.

3.1.1 Previous Publications on Tight Gas Sands

Water production from tight gas sands have been previously reported in the Greater Green River Basin in field studies carried out in the Jonah field,[36,37] the Longwood field[38] and the Hay Reservoir field[39] all in the Greater Green River Basin. Geological and Petrophysical studies were done on the Almond Sandstone Formation[40,41] to help understand mineralogical effects, impact of fractures and general rock properties influencing production performance.

In the East Texas – North Louisiana Basin, field studies have been carried out in the Cotton Valley formation of the Kildare field[42] and Carthage field[43] in East Texas, and Frierson field[44] in North Louisiana. Most other publications discuss mainly the geology of the region. There are few published data on water production from the Cotton Valley formation in Louisiana because operators are not required to report water production. The only document on water production in the field was the USGS Bulletin[3] of 2002. A series of capillary pressure measurements were made using cores cut from the Cotton

Valley interval, but few relative permeability measurements were found in the public domain, except that from Shanley[40].

There were some published data on formation evaluation in tight gas sands which detailed various methods for evaluation of water saturation[45], permeability estimation[46] and reservoir characterization[43]. Data analysis methods were also available in published literature for general formation evaluation in Travis Peak formation and the Cotton Valley tight gas sands. [30,48,49, 50, 51,52]

3.1.2 Open-hole Logs

Open-hole logs were available from 39 wells (Fig. 1.9) for the petrophysical evaluation and included gamma ray and spontaneous potential logs for lithology identification, resistivity logs for hydrocarbon identification, photo-electric effect, density and neutron logs for porosity. Other logs available included sonic logs in 5 wells, and caliper logs in 27 wells. The logs were acquired through a period spanning over 3 decades (1973-2005), which means the logging tools used were not identical.

The log data were digitized from log prints by Matador Resources and provided in LAS format to us. The resistivity logs varied in vintage from the old short and long normal logs to the modern AIT logs. Most of the wells were reported as vertical wells and they were assumed as such. No sub-sea calculations were made in the log correlation, in the absence of deviation data.

3.1.3 Core Data

Cores were cut in the Cotton Valley sands in the Colbert-1 in the Caspiana field and the Dutton Family-1 in the Elm Grove field. Both routine and special core analysis were carried out on the cores. In the routine core analysis, grain density, porosity and permeability measurements were made on the cores, while capillary pressure measurements were carried out for the special core analysis. Gas relative permeability measurements were also made in the special core analysis, but with only two point measurements, the data hardly sufficed for the reservoir simulation. The capillary pressure measurements, the relative permeability measurements and the results of the core data analysis are given in **Table C1** to **Table C9** and **Fig. C1** to **Fig. C9**.

3.1.4 Geological Maps and Well Locations

Maps and well locations were provided by Matador Resources. Digital copies of maps of the Upper Davis and the Cotton Valley sands provided structural information for the Elm Grove and Caspiana field. Although digitized log data were provided for only 39 wells, the well locations of over 400 wells were included in the maps. The maps were generated from well tops in the absence of any seismic information.

3.1.5 Production Data

Production data were obtained mainly from IHS Energy and spanned from 1973 to 2004. While statutory requirements demand that gas production be reported in Louisiana, it is not required for companies to report water production. As such, the

validity of most of the water production data obtained from IHS Energy data resource could not be ascertained. However, production test results were provided by IHS energy data resource, and those tests do provide useful information on the water production from the tested wells. The most recent water production data were obtained from Matador Resource from the wells they drilled in the Elm Grove field.

3.2 Log Data Preparation and Quality Assurance

Although log data were provided for the 39 wells, some of the wells lacked log measurements across the entire Cotton Valley sands. Pseudo density logs were generated for 18 wells using both correlations and data from nearby wells. Bore hole wash-outs were encountered in most of the wells. Log data measurements are affected by wash-outs, which adds uncertainty to the petrophysical evaluation. Environmental corrections had been carried out on the logs previously, so there was no need for further environmental corrections.

3.2.1 Log Normalization

As a result of the varying vintages of logs, log normalization was required for some of the logs. Log normalization was carried out for the Gamma Ray logs by re-scaling the sand and shale modal peaks to 24 API units for clean sands and 90 API units for clean shale (**Fig. D2** and **Fig. D3**). Most of the density and neutron log data were affected by wash-outs. An overlay of the resistivity log data from wells located in similar geographical locations was used to normalize the logs on the basis of the resistivity in

the clean shales. Overlays in the shale zones let us determine if the resistivity log data needed to be shifted because of difference in the characteristics of the logging tools. For regions were log measurements were either absent or very poor, modeled resistivity data from nearby wells was spliced with the existing data (**Fig. D1**).

3.3 Formation Evaluation

Many of the Cotton Valley sandstones contain various minerals which affect the evaluation of reservoir properties from logs. The presence of clay minerals which include chlorites, illites and kaolinites will suppress the resistivity response in potential hydrocarbon zones. Low resistivity measurements may result in erroneous water saturation computations if the wrong water saturation model is used. Conductive minerals such as pyrite exhibit similar effects on the resistivity logs, and may also have to be considered in the analysis. Carbonates in the sandstone matrix will alter the grain density, and can result in pessimistic porosity computations if no corrections are made to the matrix density values. There is a high degree of heterogeneity in the sand quality as the rock cementation, and composition can vary both laterally and vertically. Parameters used in the evaluation are tabulated in **Table 3.1**

3.3.1 Volume of Shale

Shale volume was determined from the gamma ray log and was used in the water saturation computation. The shale volume was also used in delineating pay and non-pay sands. Shaliness indicator is determined from the gamma ray using **Eq. 1**.

$$Vsh = \frac{GR - GR_{clean}}{GR_{sh} - GR_{clean}} \quad \text{.....Eq. 1}$$

Table 3.1: Parameters Used in the Evaluations

	Matrix Density (g/cc)	Shale Porosity (Frac)	Water Resistivity (Rw) ohmm	Shale Resistivity (Rt) ohmm	Cementation Exponent (m*)	Saturation Index (n*)	BQv
Sandstone (Layer_SS)	2.65		0.026	2	2.02	1.53	1.28[1/ϕ-10)
Carbonate Layer (Layer_LS)	2.76		0.026	2	2.02	1.53	3.76[1/ϕ-10)
Heterolithic Layer (Layer_HT)	2.74		0.026	2	2.02	1.53	1.28[1/ϕ-10)
Shale layer (Layer_SH)	2.68	0.005	-	-	-	-	-

3.3.2 Porosity

Stressed measurements of porosity were made on the cores from Colbert-1 and Dutton Family-1 wells (Table C7 to Table C9). These porosity measurements were used to validate the porosity calculations from log data. Evaluation of porosity from log data has mainly been by deterministic methods in the absence of probabilistic tools for evaluating multi-mineral models. Varying grain densities have been used for different intervals in the Cotton Valley sandstone to account for the multi-mineral content of the sand formation. In zones with high carbonate content an average grain density of 2.76 g/cc has been used while in sandstone regions without substantial carbonate content

a grain density of 2.65 g/cc has been used. The grain density of carbonates range from 2.71 g/cc to 3.96 g/cc depending on the form of carbonate present in the formation matrix. Porosity was also computed with the neutron- density porosity computation module and results compared well with the average density computation. However, significant differences were observed in washed-out zones. Porosity was obtained from the density logs using **Eq. 2**.

$$\phi_d = \left(\frac{Rho_{ma} - Rho_b}{Rho_{ma} - Rho_{fl}} \right) \text{.....Eq. 2}$$

The various matrix densities used in the evaluation is given in Table 3.1.

3.3.3 Water Saturation

Water saturation was calculated using the dual-water model. The modified Simandoux equation was used to compute water saturation. The input parameters required for the water saturation computation are cementation factor, saturation index, formation water resistivity, and shale resistivity. A value of 0.026 ohm-meter obtained from produced water analysis (**Table A2**) was used for the water resistivity. Cementation factor of 2.02 and saturation index of 1.53 were obtained from results of the special core analysis measurements (Fig. C1 and Fig. C2). Shale resistivity was read from the logs and a value of 2 ohmm was used. The modified Simandoux equation is given in **Eq. 3**.

$$Sw = \left[\left(\frac{FR_w}{R_t}\right) + V_{sh}\left(\frac{FR_w}{2R_{sh}}\right)\right]^{1/2} - Vsh\left(\frac{FR_w}{2R_{sh}}\right) \quad \text{.....Eq. 3}$$

Water saturation was also computed with the Waxman Smit method (**Eq. 4**) to compare and validate the saturation values determined from the dual water model (**Fig. D6**).

$$Sw = \left[\frac{aR_w}{R_t\phi_t{}^m\left(1 + R_w\frac{BQ_v}{Sw}\right)}\right]^{1/n} \quad \text{.....Eq. 4}$$

A plot of water conductivity against inverse porosity was used to estimate the BQv parameters in the absence of core measurements. The results (**Fig. D4** and **Fig. D5**) show some agreement in clean sands but tend to deviate in shaly zones where excess shaliness correction occurred.

3.3.4 Permeability

Stressed permeability measurements were made on cores cut from Colbert-1 and Dutton Family-1 wells (Table C1 to Table C9). Oriented permeability measurements were also carried out to evaluate permeability anisotropy in two azimuthal directions. A cross plot of porosity and permeability was developed to evaluate the permeability-porosity relationship. However, due to the large heterogeneity of the Cotton Valley

sands, a permeability-porosity relationship from two cored wells can not be expected to describe the entire reservoir. Yao and Holditch[53] developed an empirical method for estimating permeability from logs using core data to calibrate the correlation. They made permeability a function of porosity, deep and shallow resistivity, volume of shale and water resistivity. This permeability relationship is given in **Eq. 5**. They also gave ranges for the constants to be applied in the equation.

$$K = U \frac{\phi^{e1} (1 - V_{sh})^{e2} R_{ild}{}^{e3}}{(R_{ild} / R_{sfl})^{e4}} \quad \text{.....Eq. 5}$$

Where U = factor that varies for different reservoirs and mud systems;

The ranges for the parameters are;

e1 (5.87 – 6.89), e2 (0.2 – 0.3), e3 (1.18 – 2.54), e4 (1.08 – 1.65), U (2800 – 20160)

Permeability measurements derived from Eq-5 failed to match permeability derived from core and gave significantly higher values (>2mD) when applied to other wells. The equation fails in sand regions with low formation resistivity such as low resistivity zones. The permeability prediction in this zones tends to be exceedingly low (<0.0002 mD). The empirical relationship was most probably derived using data from tight gas sand wells that had little or no water influx. A modification has been carried out on equation-5 to accommodate wet zones. The modified equation is given in **Eq. 6**.

$$K = 600 * \phi^{6.23} * (1 - V_{sh})^{0.2} * R_{ild}{}^{1.13} * (R_{ild} / R_{sfl}) \quad \text{.....Eq. 6}$$

Although Eq. 6 did not match with measured values of permeability from cores, it appears to give realistic estimates in the low resistivity zones.

3.4 Fluid Interpretation and Fluid Distribution

In the absence of more sophisticated logging tools, like the NMR and geochemical tools, fluid interpretation was based mainly on the resistivity logs since there are only two types of fluid in the reservoir, gas and water. However, the impact of conductive minerals on the resistivity profile introduces some uncertainty on the fluid interpretation. The water saturation in the low resistivity zones can not be accurately computed without knowing more about the clay content and distribution. We used resistivity logs also to see if global saturation changes occurred versus time in certain sands that are producing formation water today. The wells used for the overlay are shown in **Fig. 3.1**.

3.5 Reservoir Simulation

Having evaluated the petrophysical properties of the field and possible fluid distribution in the field, a dynamic reservoir simulator (Eclipse) was used to investigate different scenarios of possible water production in a tight gas sand model. The input data for the ECLIPSE simulation are presented in **Table E1** to **Table E4** and **Fig. E1** to **Fig. E10** and include, the simulation grid, rock properties, fluid properties, the initial pressure conditions, fluid distribution and production constraints.

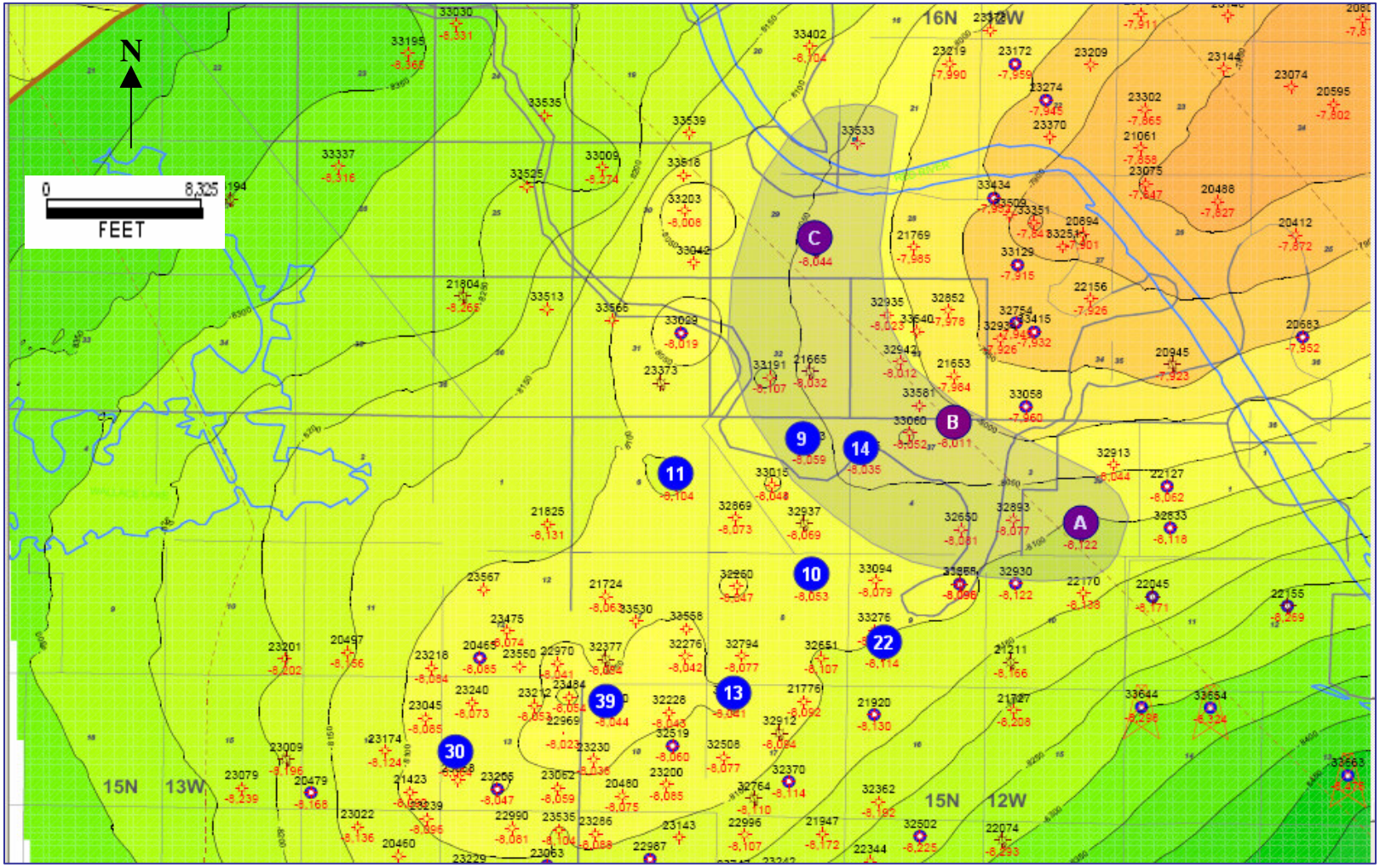

Fig. 3.1: The Wells Used in the Resistivity Log Overlay; (Wells 9, 11 and 14), (10 and 22), (30, 39 and 13). Sustained high production was first observed in 1974 in Well A. Well B and Well C started production in 1975 and 1977 respectively, and produced high water-gas ratios.

3.5.1 Simulation Grid

Cox and others[53] in their simulation model determined that an effective drainage area for permeabilities of 0.01, 0.1 and 1 mD ranged from 5 to over 600 acres. This formed the basis for the grid configuration of the single well simulation. An inclined grid with corner point geometry and a total of 5400 cells (45 x 8 x 15) was used in the simulation. A hydraulic fracture 1 ft in width and 500 ft fracture half length was used in the model. The simulation grid is shown in **Fig. 3.2**. To account for near well bore effects and high pressure gradients around the fracture, smaller grid sizes were used at the edge of the fractures and close to the well bore.

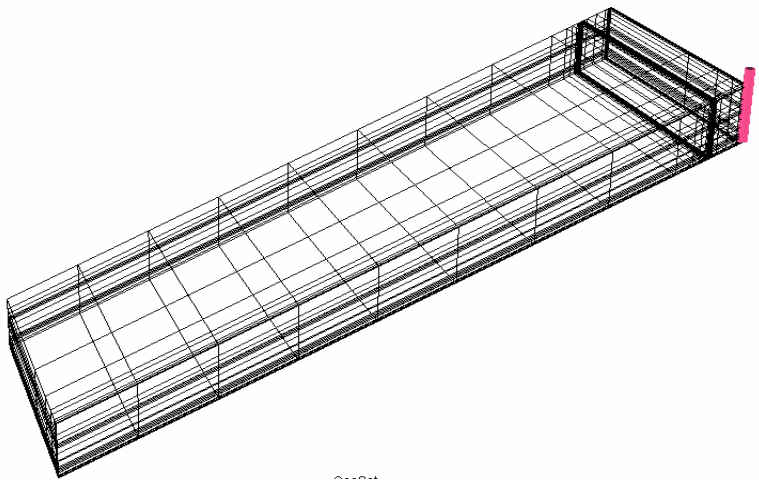

Fig. 3.2: Inclined Grid, (45 x 8 x 15) cells.
Grid dimensions are 10000 ft (length) x 1000 ft (height) x 500 ft (width).
Fracture dimensions are (500 x 1) ft.

3.5.2 Capillary Pressure

Gas-Water drainage capillary pressure measurements were made on the cores cut from Colbert-1 well in the Elm Grove field. A total of seven core plugs were used for the measurements. The results are given in Fig. C7. To incorporate a wide range of capillary pressure measurements for tight gas sands, both the capillary pressure measurements from the core data and the comparative study[33] were used in the study. The capillary pressure measurements from sample 3 and 21 from the core analysis measurement in Cobert-1 were selected for the study. The capillary pressure profiles are given in **Fig. 3.3**.

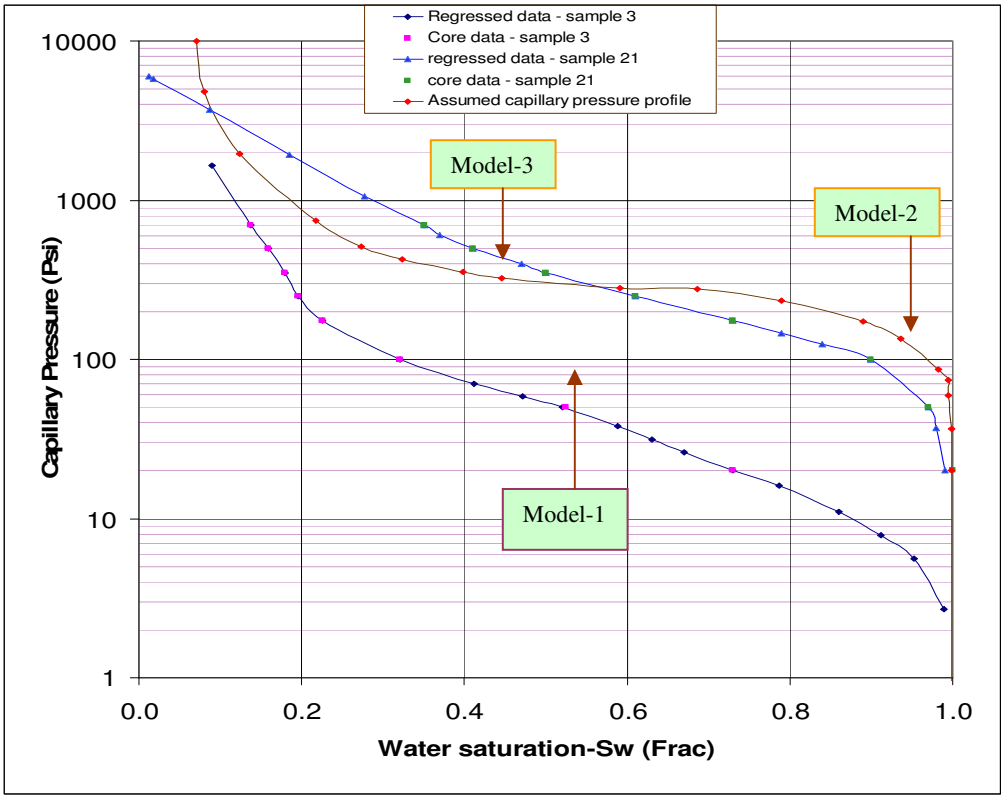

Fig. 3.3: Capillary Pressure Used in the Simulations for Different Scenarios.

3.5.3 Relative Permeability

Relative permeability measurements were made with cores cut from the Colbert-1 well in the Caspiana field. Both imbibition and drainage relative permeability values were measured on four core samples. The relative permeability graphs are given in Fig. C3 and Fig. C6. The plot contains very few data points that are insufficient to generate a complete relative permeability curve for the gas flow simulation. A typical graph is shown in **Fig. 3.4**. No water relative permeability measurements were made. The relative permeability measurements used in the study were extrapolated from the few data points in the core data. Approximate profiles for conventional sands based on the theory put forward by Shanley[28] were also used.

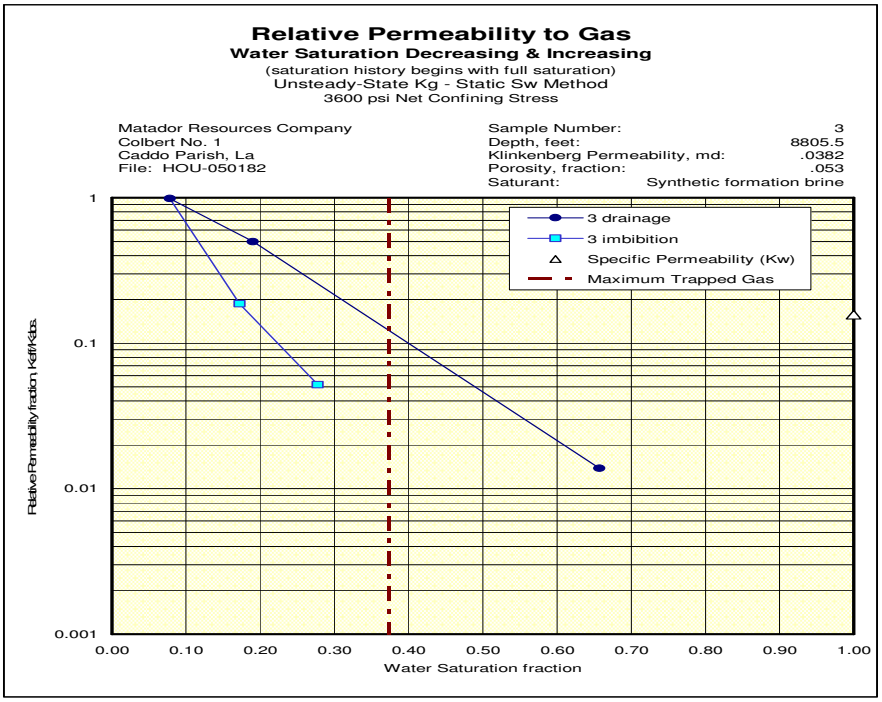

Fig. 3.4: Relative Permeability Measurements for Core Sample-3. Note the few number of data points.

Since the relative permeability profile of the reservoir rock is central and essential to understanding the water production in the field, different scenarios of relative permeabilities were simulated. Three models based on the area enclosed under both the water and gas relative permeability curves, were used in the simulation (**Fig. 3.5**, **Fig. 3.6** and **Fig. 3.7**).

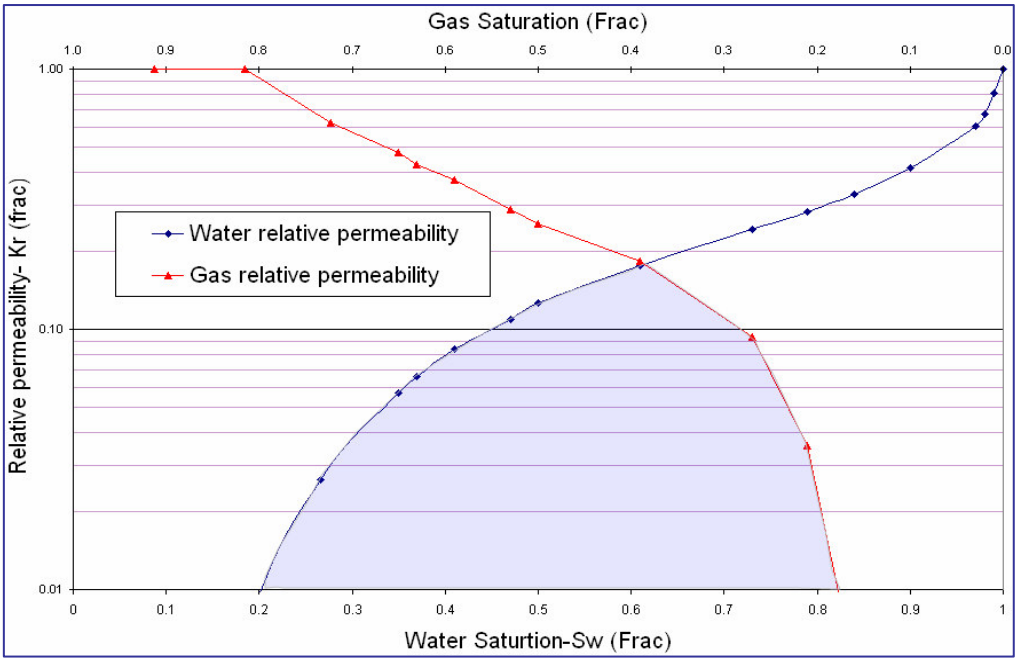

Fig. 3.5: Model-1, Conventional Relative Permeability Profile.
Significant area enclosed beneath the relative permeability curves.

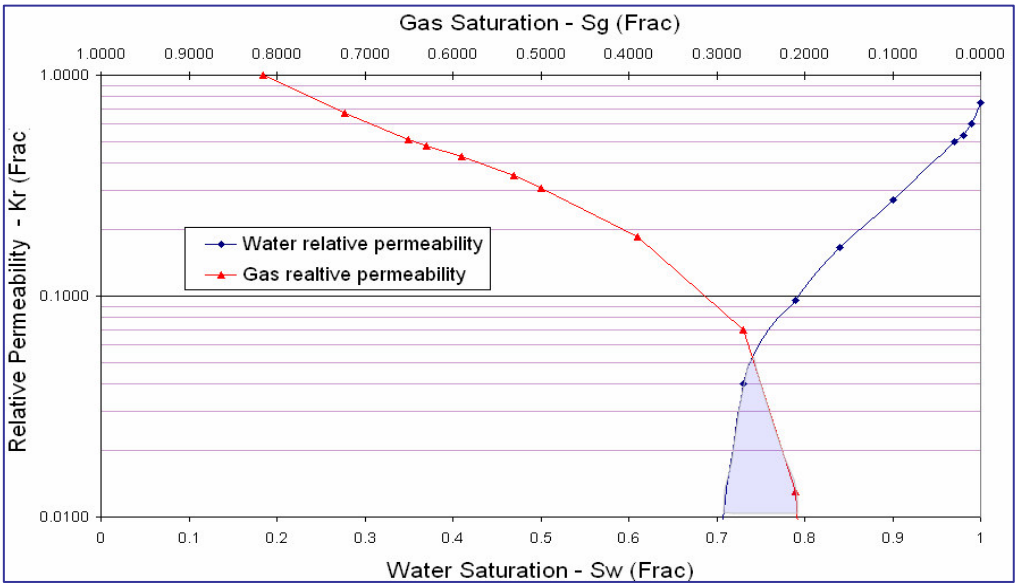

Fig. 3.6: Model-2, Unconventional Relative Permeability Profile.
Limited area enclosed beneath the relative permeability curves.

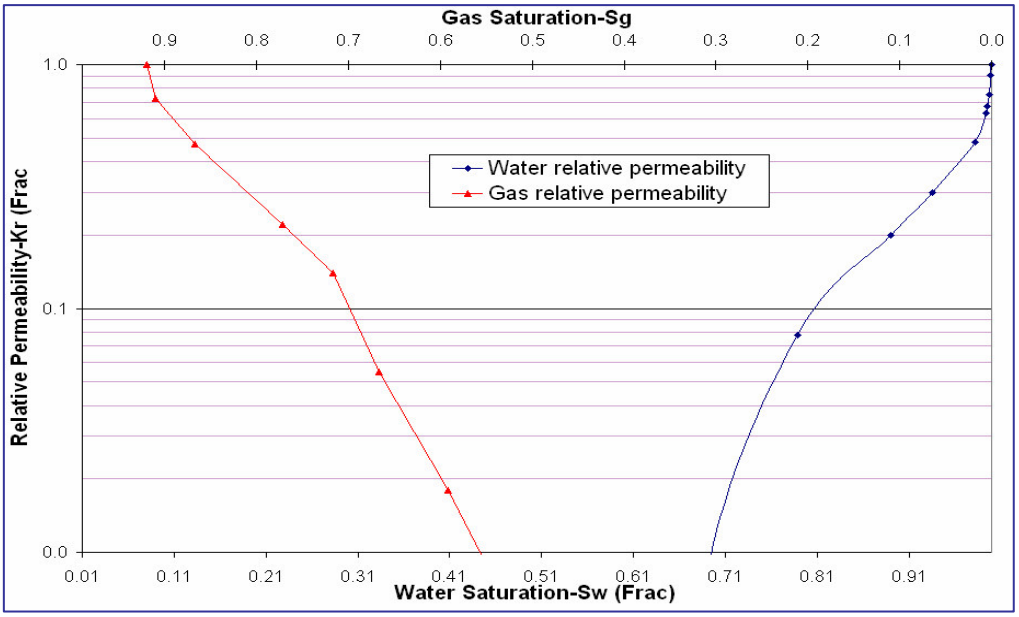

Fig. 3.7: Relative Permeability Profile Associated with Rock Seals.
No area enclosed beneath the relative permeability curves.
No fluid flow occurs within water saturation ranges of (0.45 – 0.68) resulting in a permeability jail or water block.

3.6 Water Production Trend Analysis

Water production test data were obtained from IHS Energy Resource. Since oil and gas companies are not required to report water production in Louisiana, the validity of the IHS monthly water production data may not always be reliable. In conventional multi-layered reservoirs, production can usually be attributed to distinctive perforated units. However, in tight gas sands, production is usually through a hydraulic fracture which tends to commingle multiple units in a multi-layered reservoir. This commingling makes it difficult to determine patterns in water-gas ratio trends in the field. Water production in the Caspiana and Elm Grove field were analyzed however, for possible trends that might exist. The available production data spanned from 1973 to 2004 and was mainly restricted to the mapped area in the Petra data base provided by Matador Resources. This region does not include the area around the fault in the northern part of the field. Trends were analyzed in categories on the basis of water-gas ratios.

The importance of the sampling rate can be seen with the bubble map of water gas ratios (**Fig. 3.8** and **Fig. 3.9**). The coarser the sampling rate used, the more likely it is to obtain a trend. Variations in hydraulic fracture efficiency and mixed flow from multiple layers tend to distort trends made with fine sample classifications (increments of 25 bbls/MMcf). Improved trends are obtained from coarser sampling (increments of 50 bbls/MMcf) of the water gas ratios. The resulting trends for individual years are given in **Fig. H1** to **Fig. H4**.

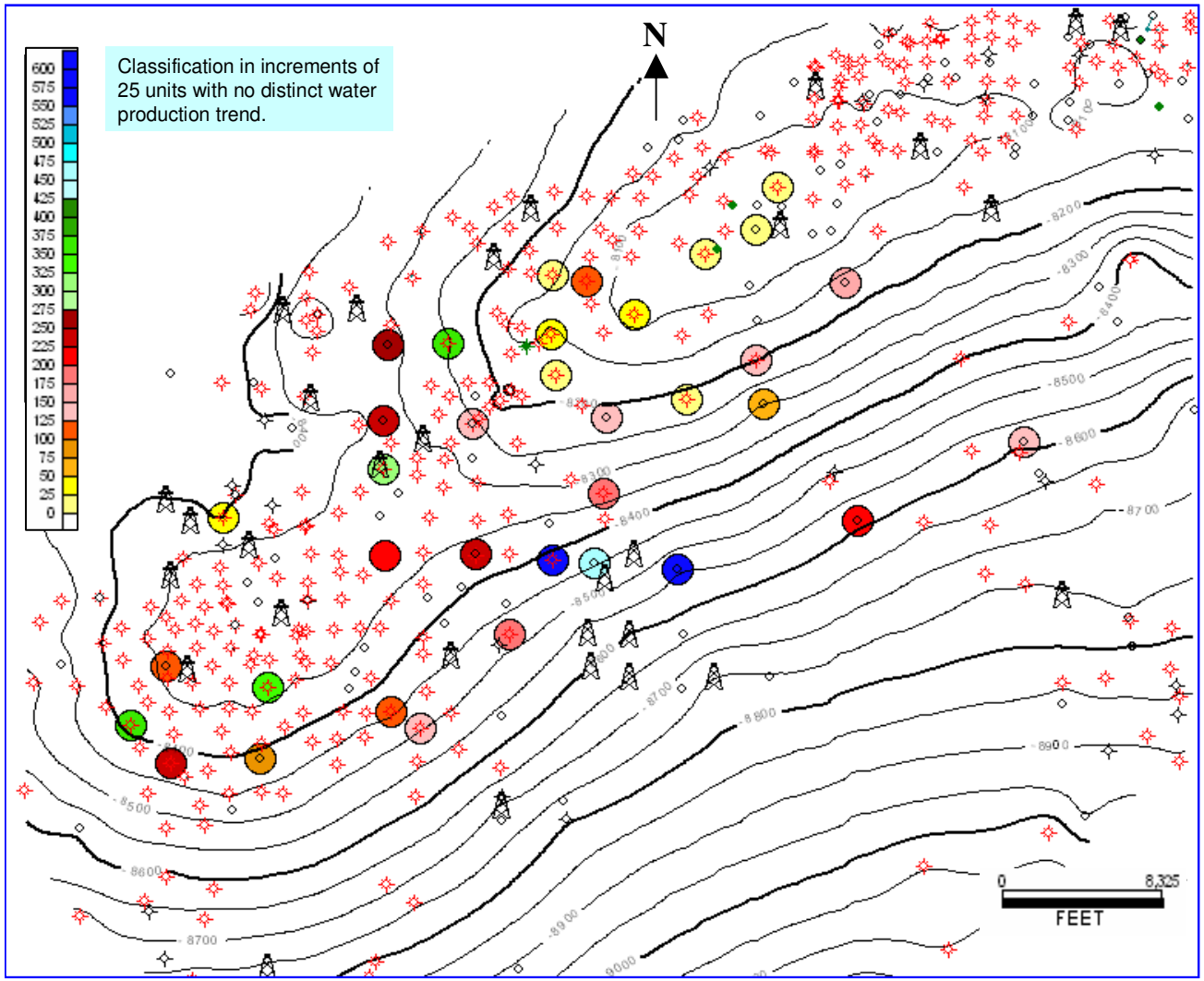

Fig. 3.8: Distribution of Water-Gas Ratios with Sampling Rate of 25 bbls/MMcf from 1976 Production Data.

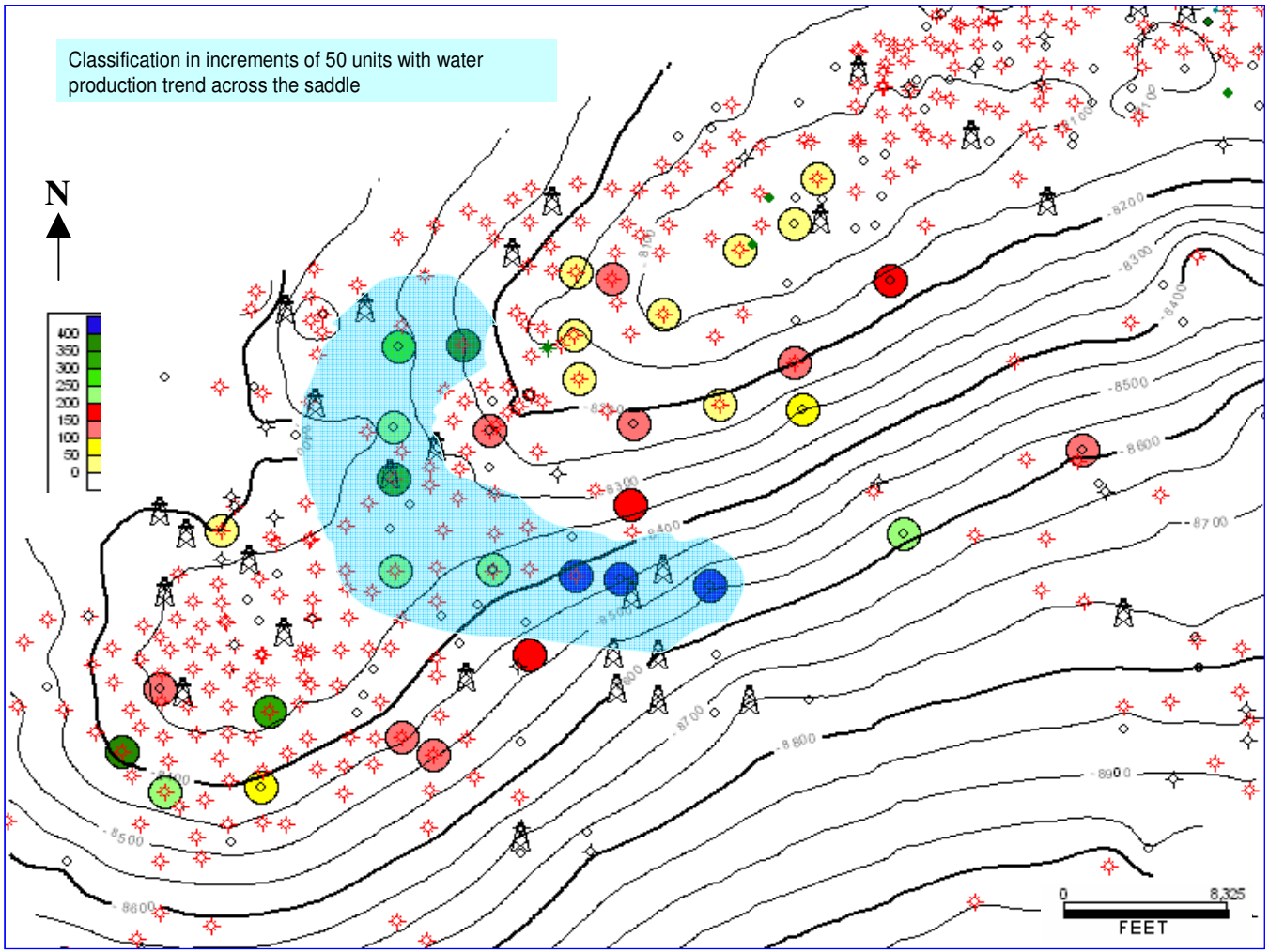

Fig. 3.9: Distribution of Water-Gas Ratios with Sampling Rate of 50 bbls/MMcf from 1976 Production Data. Water production trend emerging within the saddle region.

3.7 Scenario Analysis for Reservoir Simulation

To properly evaluate the flow behavior in tight gas sands, different scenarios were generated for the relative permeability, capillary pressure, production rate and distance of the water source from the drainage point. The different scenarios have been chosen based on the geological structure, the reservoir stratigraphy, the petrophysical property variation, possible fluid distribution and the recorded production characteristics in the Cotton Valley sandstones of the Elm Grove and Caspiana fields.

A multi-layered grid, inclined at 30° with corner point geometry was used in the simulation model for the sensitivity runs in ECLIPSE. Although this is a far departure from the 2.3° dip of the reservoir structure, the need to accommodate vertical depths of about 2000 ft in the single well simulation model makes it imperative to exaggerate the grid inclination. The model was constructed with 15 layers to represent the complex stratigraphy of the Cotton Valley interval. All the 15 layers were assigned different reservoir properties with porosities ranging from 2-14% and permeabilities ranging from 2-100 μD. In some cases layers with permeabilities of 6 and 10 mD were introduced to account for the existence of high permeability streaks in the field as seen from the stressed core data measurements. The relative permeability was defined based on the relative permeability profile of the rock and its capacity to flow water and gas simultaneously. Three scenarios, model-1, model-2 and model-3 were used in the simulation. Model-1 has relative permeability curves similar to conventional rocks with a substantial area definition enclosed under both relative permeability curves as shown in Fig. 3.5. This case serves to investigate possible upside in the gas-water flow capacity

of the Cotton Valley tight gas sands. Model-2 has limited gas-water flow capacity based on the area definition enclosed under the relative permeability curves in Fig. 3.6. It serves to investigate the downside in the water flow capacity of the Cotton Valley tight gas sands, where the reservoir rocks cannot be totally classified as seals. The different scenarios are presented in **Table 3.2**.

Table 3.2: Different Scenarios of Reservoir Properties Simulated to Evaluate Water Flow.

Scenarios	Transmissibility Z-direction (Tz)	Gas Permeability (Kg)	Capillary Pressure (Pc)	Relative Permeability (Kr)	Vertical Distance (Depth)	Flow Rate (Qg)
1	>0	<0.1 mD	Model-1	Model-1	600ft	20 MMcf
2					200ft	20 MMcf
3					20ft	20 MMcf
4					200ft	14 MMcf
5					200ft	8 MMcf
6				Model-2	200ft	20 MMcf
7					20ft	14 MMcf
8	>0	<0.1 mD	Model-2	Model-1	2000ft	20 MMcf
9					600ft	20 MMcf
10					200ft	20 MMcf
11					2000ft	14 MMcf
12					2000ft	8 MMcf
13				Model-2	2000ft	20 MMcf
14					200ft	14 MMcf
15	0	<0.1mD	Model-1,2,3	Model-1,2,3	Variable	20 MMcf
16						14 MMcf
17						8 MMcf
18	>0	<0.1mD	Model-3	Model-3	3450ft	20 MMcf
19	0	>0.1 mD	Model-1,2,3	Model-1,2,3	200ft	20 MMcf
20					200ft	14 MMcF
21					200ft	8 MMcf
22					2000ft	20 MMcf
23					2000ft	14 MMcf
24					2000ft	8 MMcf

Model-3 investigates a production scenario where the reservoir rocks act as seals and are impermeable to fluid flow at some saturation range.

Three capillary pressure curves used in the different scenarios were based on the capillary pressure measurements from core data. Sample-3 and 21 (see Fig. C7) were used to represent the downside and upside in water saturation distribution, which apparently relates to the coning capacity and break through timing of the water influx. Sample-1 has been used in model-1 while sample-21 has been used in model-2. A third scenario related to rock seals was also investigated. In this third scenario, capillary pressure profiles tend to take the shape of an inflexion curve with no saturation ranges for simultaneous water and gas flow (see model-3 in Fig. 3.3). Different production rates of 8, 14 and 20 MMcf/D were also investigated with the different scenarios. These rates were selected to investigate the effect of gas flow rates on water production in the field as they affect coning/cusping and water breakthrough timing in the well.

Different distances of the point of water influx to the drainage points were simulated to investigate the location of the water source. An infinite acting aquifer was used to represent the water source. Vertical distances of 20, 200, 600 and 2000 ft were simulated. The maximum distance of 2000 vertical feet (4000 feet from the well based on the 30° dip of the grid) was selected to investigate possible limits of the water source location on the reservoir structure.

3.7.1 Selected Model (Field Scenario with 2.3° Dip)

The previous field scenarios were based on the sensitivities previously run for different effects on water gas ratios with a 30° inclined grid. An inclined Grid of 2.3° dip was used to represent the actual dip in the field (**Fig. 3.10**). A six-layered reservoir model based on the log analysis, with no vertical transmissibility across layers was used in the model. The model-1 capillary pressure and relative permeability were selected for the simulation. Layer-1 and Layer-3 were flooded with water while an aquifer vertical distance of 1000 ft from the well was applied for other layers. An absolute permeability of 2 mD was used for layer-3 to account for high permeability streaks. The reservoir model was produced at a gas flow rate of 1200 Mcf/D.

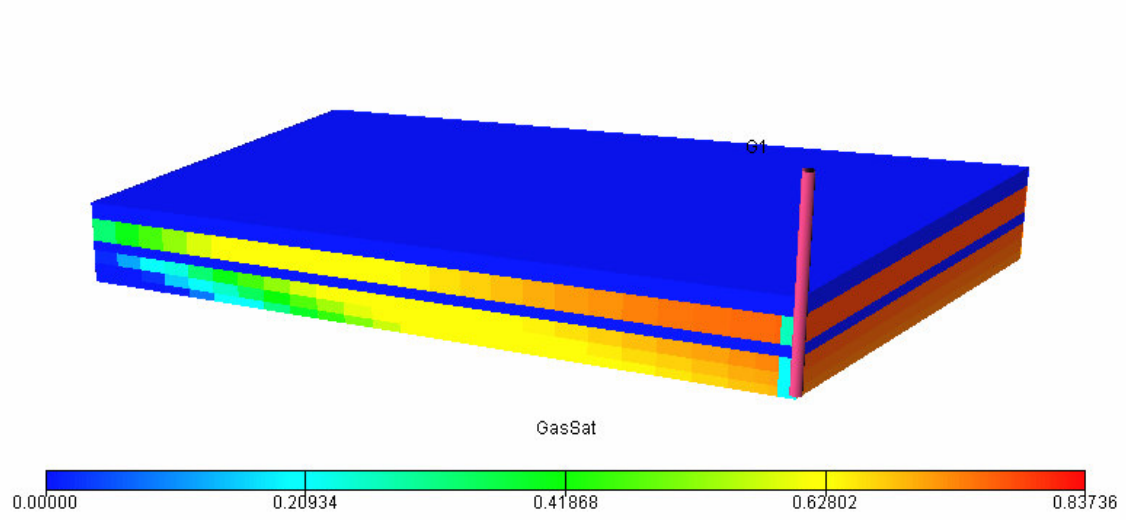

Fig. 3.10: Field Reservoir Model with 2.3° Dip and Two of Six Layers Flooded. Model with high permeability streak and no vertical transmissibility.

CHAPTER IV

RESULTS

4.1 Log Data Evaluation Results

Reservoir properties evaluated include porosity, permeability, water saturation and shale volume. These results have been presented graphically in a composite log plot (**Fig. 4.1**). Log to core data comparisons and log saturation trends are also included in the results (**Fig. 4.2**).

4.1.1 Petrophysical Property Evaluation Results

Petrophysical evaluation results are presented in **Table I1** to **Table I9**. A composite log containing gamma ray, resistivity and rock and fluid volume is shown in Fig. 4.1. In the log presentation, the gamma ray log is on track-1 on a scale of (0 – 150) API units, the resistivity logs are in track -2 with a scale of (0.2 – 200) ohmm. The deep and shallow resistivity curves are represented in blue and red respectively. The color shading in track-1 and 2 serves to emphasize the sand regions as opposed to the shale regions.

The density and neutron curves are represented in blue and green respectively in track-3, with the density on a scale of (1.8 – 2.8) g/cc and the neutron log on a scale of (0.51- (-0.09)) neutron porosity units. The color shading in track-3 emphasizes reservoir sandstone regions with red for the neutron cross-over to the right and hatched-grey for cross-over to the left representing a different lithology.

The shale and fluid volume is presented on track-4 with different color codes. Gas volume is in red while water volume is in blue. The sand volume is in yellow and the shale volume is in hatched-grey. The log presentation gives a graphic presentation of the evaluation results for the well. The individual results for 38-wells are provided in **Fig. F1** to **Fig. F38**.

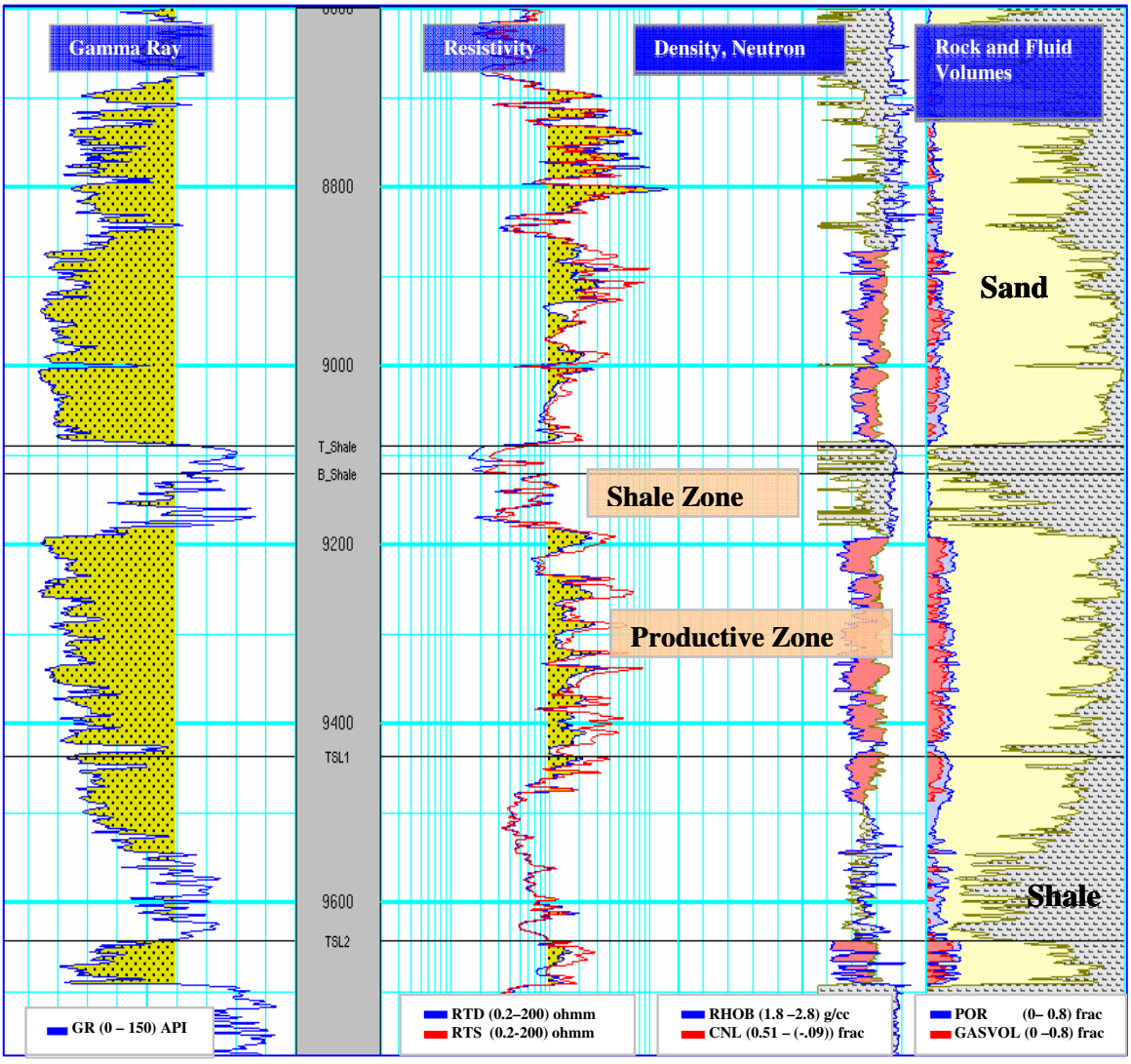

Fig. 4.1: Composite Log Plot Showing Evaluated Rock and Fluid Volumes.

4.1.2 Log and Core Data Comparison

The presentation in tracks 1, 2, 3 and 4 (Fig. 4.2) are essentially the same as in Fig. 4.1. Tracks 4 and 5 are porosity, and permeability curves. In tracks 4 and 5 the log computed data are plotted in red while the core data are plotted in blue.

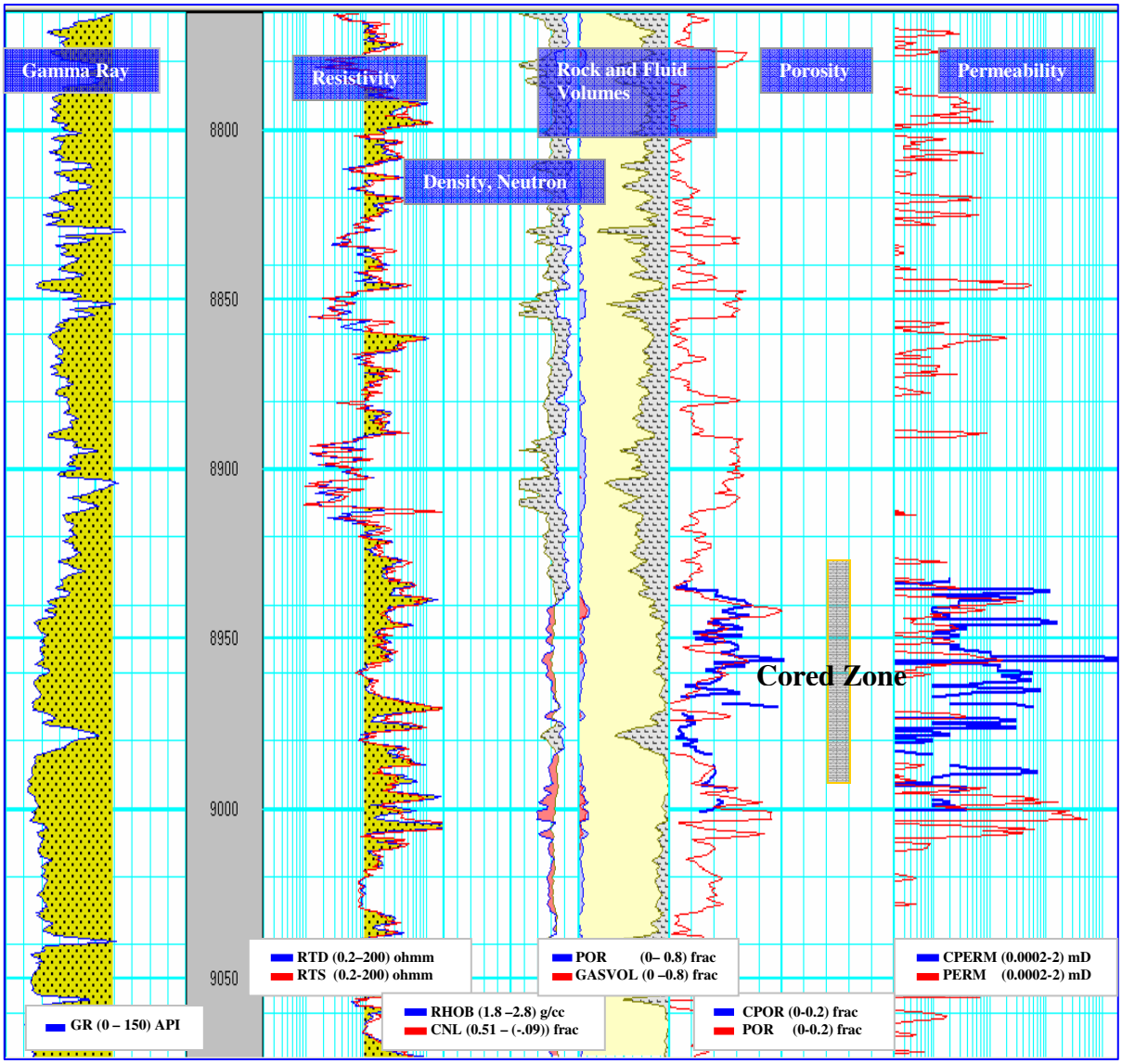

Fig. 4.2: Log and Core Data Comparison for Porosity and Permeability (Colbert-1).

The stressed core data measurements were obtained from Dutton Family-1 which has been evaluated as Well-29 in the log analysis. The overlay shows a reasonable match between the core and log derived porosities. The match of log permeability against core permeability was not very good. The difference in measured permeability and calculated permeability are not unusual for the low porosity tight gas sands especially.

4.1.3 Fluid Interpretation and Fluid Distribution

An overlay of the resistivity logs from Wells 9, 11 and 14 is presented in **Fig. 4.3a** and **Fig. 4.3b**. Wells 9 and 11 were logged in 1975, while Well 14 was logged in June 1995, some 20 years later. The resistivity curve for Well 14 is presented in dark blue while the resistivity curves for Wells 11 and 9 are presented in red and cyan respectively. The red and cyan shading represents the saturation changes related to location and gas production. The gamma ray logs for the three wells are plotted in track-1. The well locations are presented in **Fig. 4.4.**

An overlay of the resistivity logs from Wells 30, 39 and 13 is presented in **Fig. 4.5a** and **Fig. 4.5b**. Well 30 was logged in 1975, while Well 13 and Well 39 were logged over 20 years later. The resistivity curve for Well 13 is presented in dark blue while the resistivity curves for Wells 30 and 39 are presented in red and cyan respectively. The red and cyan shading represents the saturation changes related to location and gas production. The saturation changes shown are in the lower Cotton Valley sands. The gamma ray logs for the three wells are plotted in track-1. The location of wells 30, 39 and 13 can be seen on the structural map (Fig. 4.4).

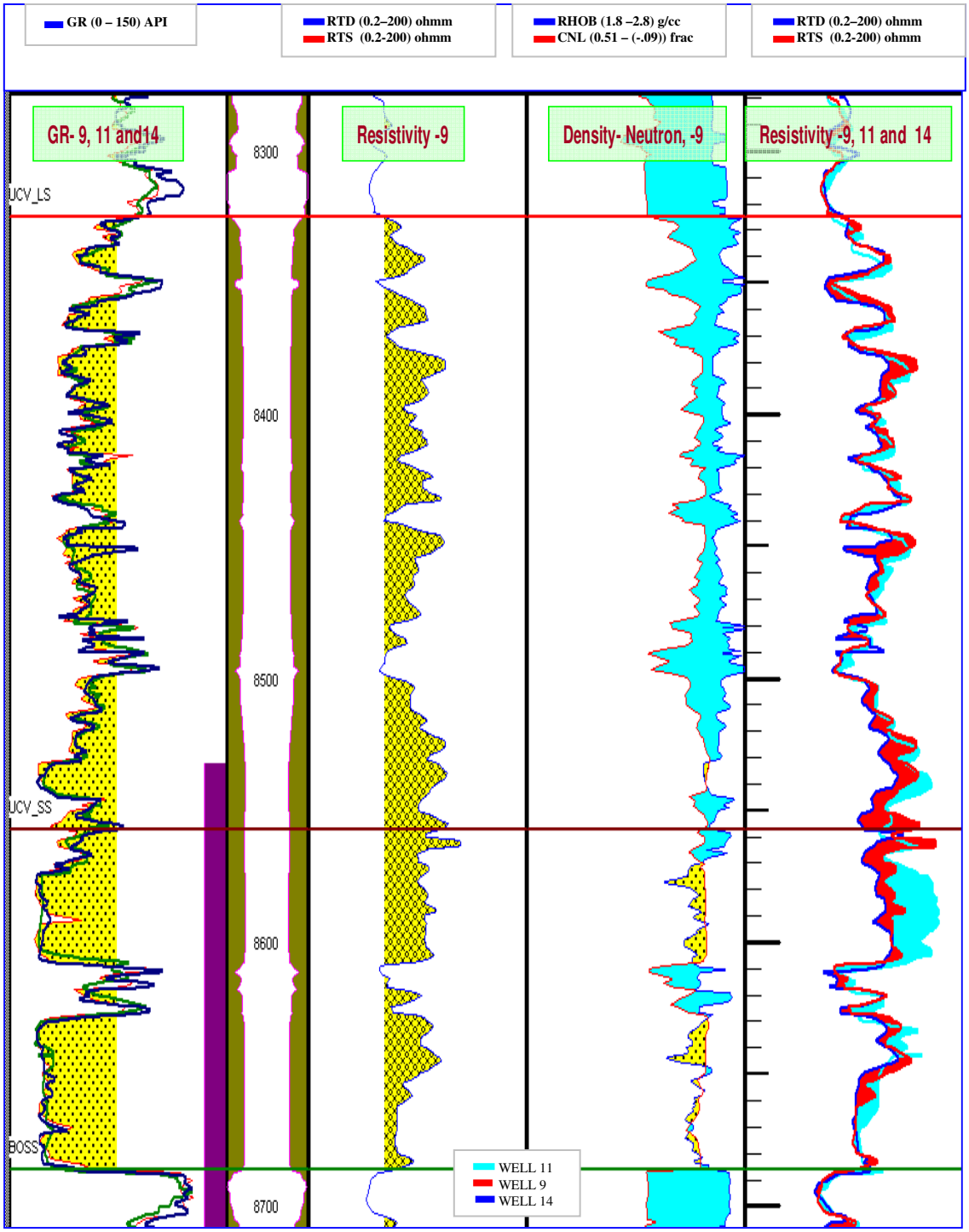

Fig. 4.3a: Saturation Changes from Resistivity Overlay in Wells 9, 11 and 14. Well 11, 9 and 14 represented in cyan, red and blue respectively.

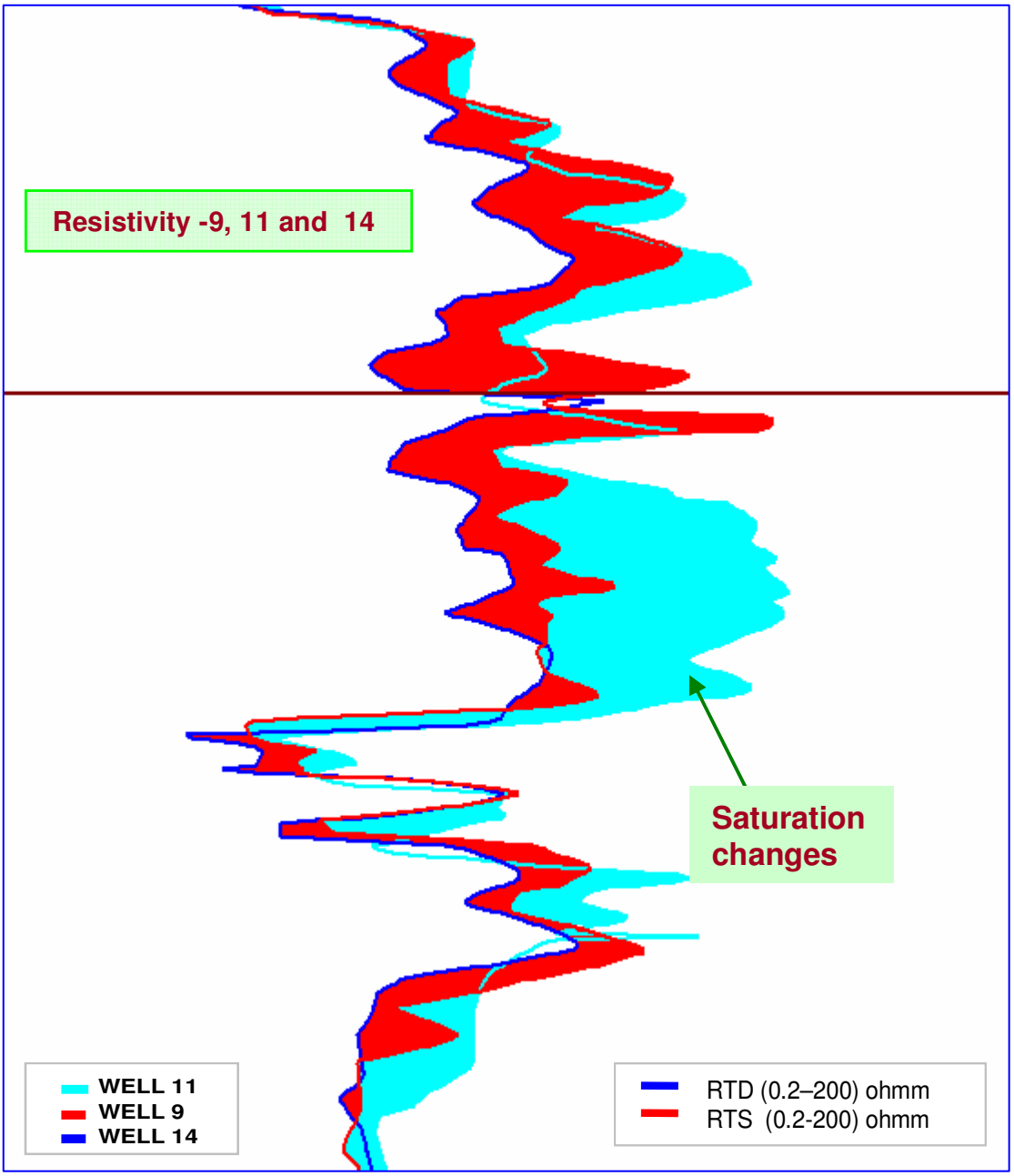

Fig. 4.3b: Enlarged Presentation of Saturation Changes from Resistivity Overlay in Wells 9, 11 and 14.

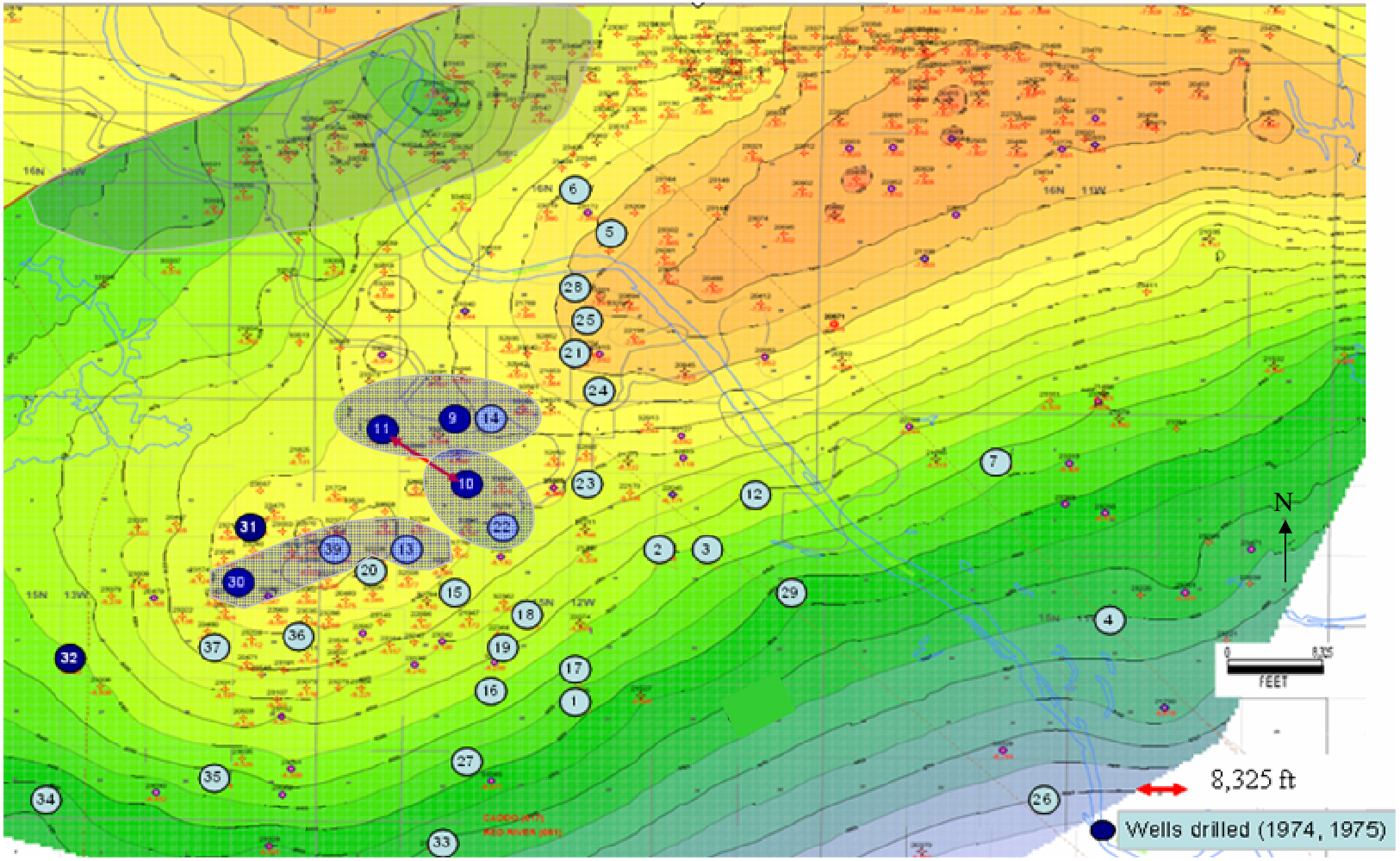

Fig. 4.4: Selection of Wells for Resistivity Overlay: (Wells 11, 9, 14), (30, 39, 13) and (10, 22).

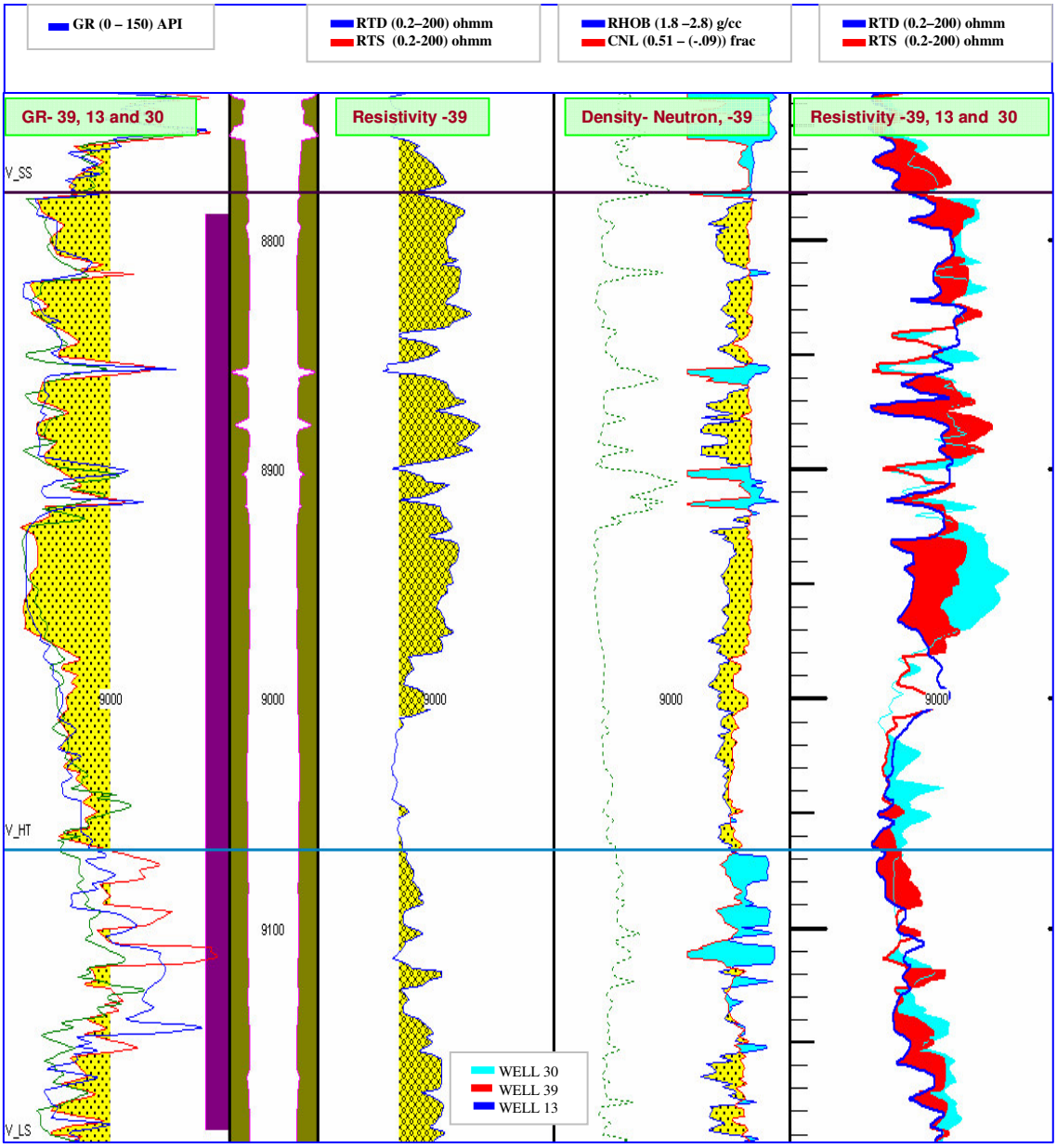

Fig. 4.5a: Saturation Changes from Resistivity Overlay in Wells 39, 13 and 30. Well 39, 13 and 30 are in red, blue and cyan, respectively.

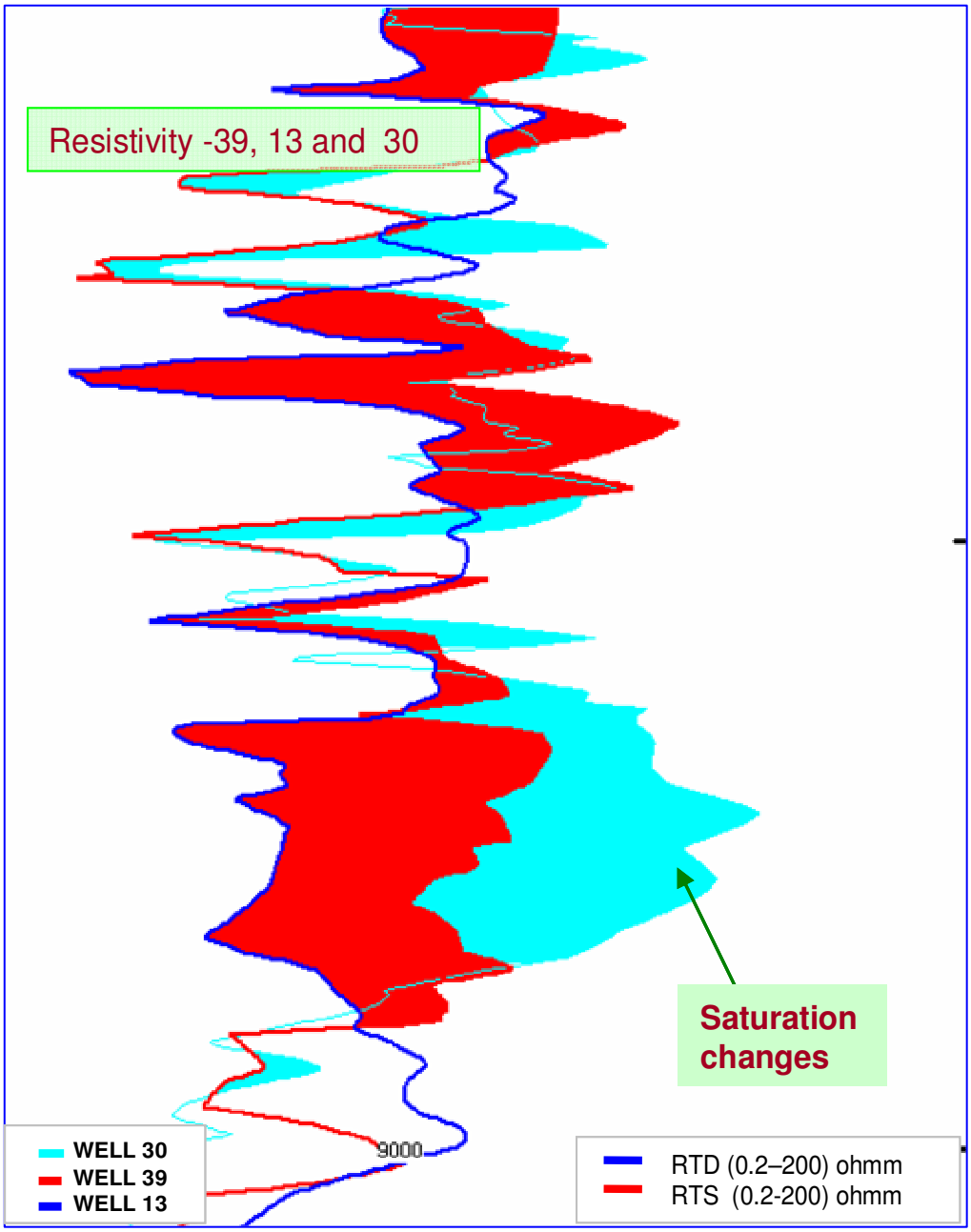

Fig. 4.5b: Enlarged Presentation of Saturation Changes from Resistivity Overlay in Wells 39, 30 and 13.

In **Fig. 4.6a** and **Fig. 4.6b**, an overlay of Well 10 and Well 22 is presented. Well 10 was logged in 1975 while Well 22 was logged over 20 years after. The resistivity curve for Well 22 is presented in dark blue while the resistivity curve for Well 10 is presented in red. The red shading represents the saturation changes related to gas production. These saturation changes may indicate water encroachment in the field. The resistivity overlay was made with early wells to investigate the effect of production. However, there is still the effect of location as the wells are drilled in different locations in the field. Resistivity overlay with wells far apart introduce some uncertainties because of lateral variation in facies. A close examination of the logs in Fig. F1 to Fig. F38, shows that resistivity trends in some of the wells do not follow a simple north–south or east-west pattern. Well 7 and Well 38 tend to show limited water saturation changes.

In general, the fluid distribution in the field can be said to vary both with location and time of drilling and do not conform to any simple directional pattern. Factors related to the geology and rock properties may be responsible for the complex water encroachment pattern.

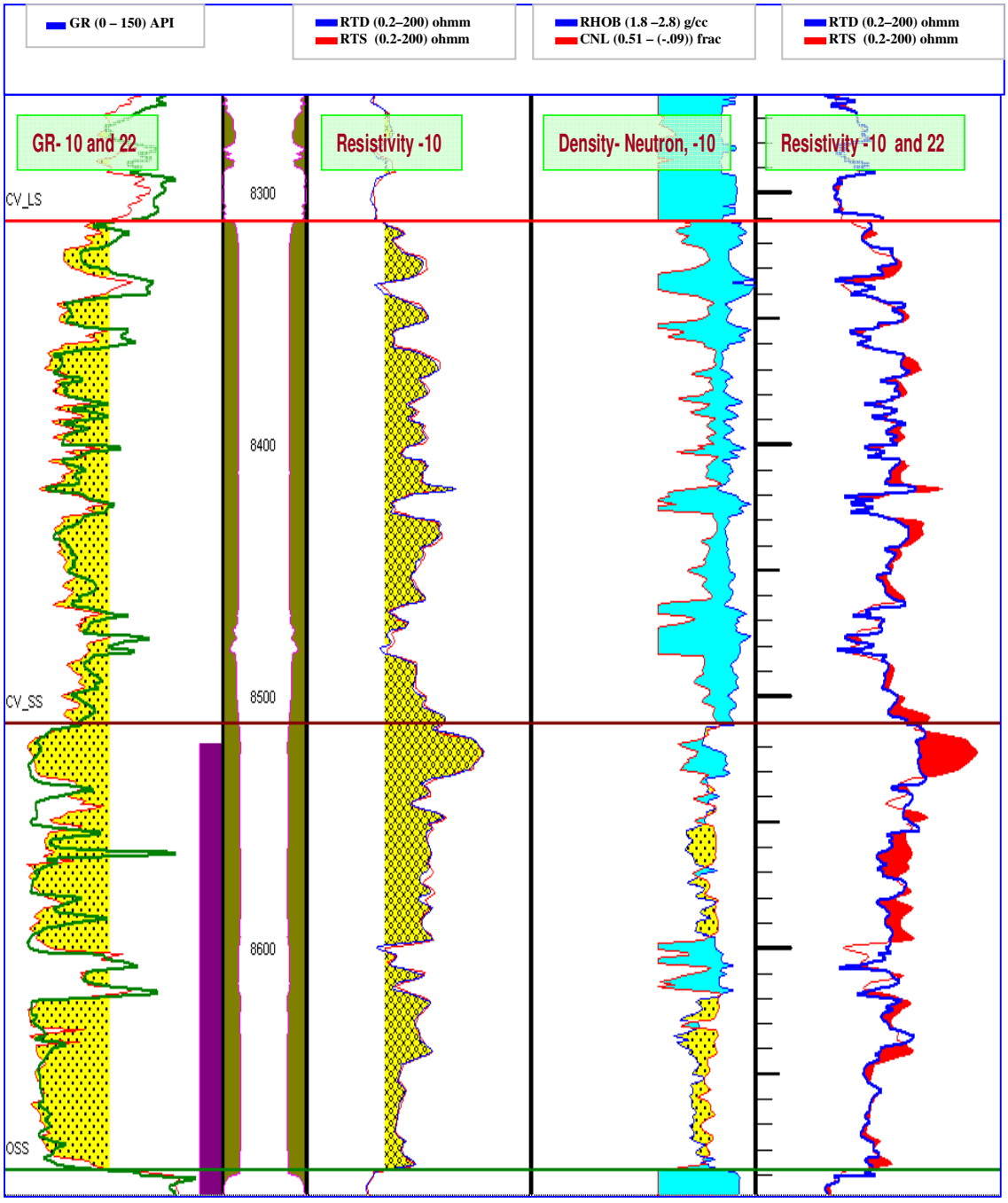

Fig. 4.6a: Saturation Changes from Resistivity Overlay in Wells 22 and 10. Wells 22 and 10 are in blue and red, respectively.

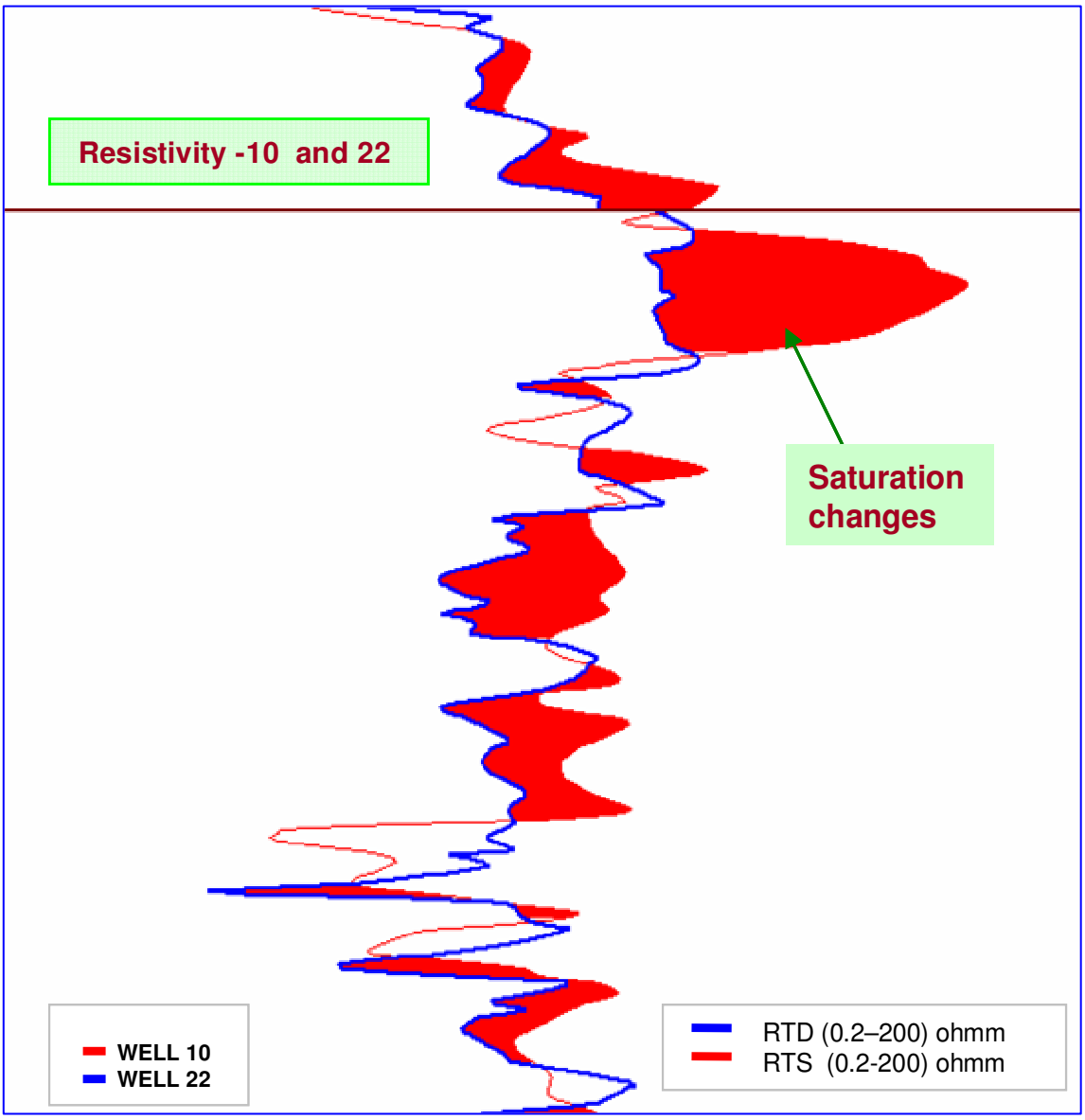

Fig. 4.6b: Enlarged Presentation of Saturation Changes from Resistivity Overlay in Wells 22 and 10.

4.2 Water Production Trend Analysis

Water production trends from the Cotton Valley sands were evaluated using data from IHS Energy. Periodic production tests data were available in Elm Grove and Caspiana fields from 1974 to 2004. However, only the first 4 years of production are presented in the text. The rest of the water production data are presented in the Fig. H1 to Fig. H4. The water production trend becomes more confusing in later years with the inclusion of more wells. Distortions from changes in production rates and local well effects results in a scattered combination of high and low water-gas ratios with no definite trend.

4.2.1 Water-Gas Ratio Trend in 1974

Table 4.1 provides the water-gas ratios from production tests in wells drilled in 1974. High water production commenced in 1974 with the Well, CV RA SU 65; Cupples, located at the central and crestal region of the field (**Fig. 4.7**) with a water-gas ratio of 66 bbls/MMcf. This well is some 30,000 ft from the both the south and north down dip currently known limits of the Elm Grove and Caspiana fields. Other wells drilled in 1974 were drilled structurally higher than the Cupples well and produced with lower water-gas ratios with the exception of the very first well CV RA SU 11. H.L. Tompkins drilled and completed this well in 1973. The CV RA SU 11 well produced with a water gas ratio of 100 bbls/MMcf, but was unable to sustain the high water production in subsequent years. This high water production can be attributed to fracture fluids pumped into the formation.

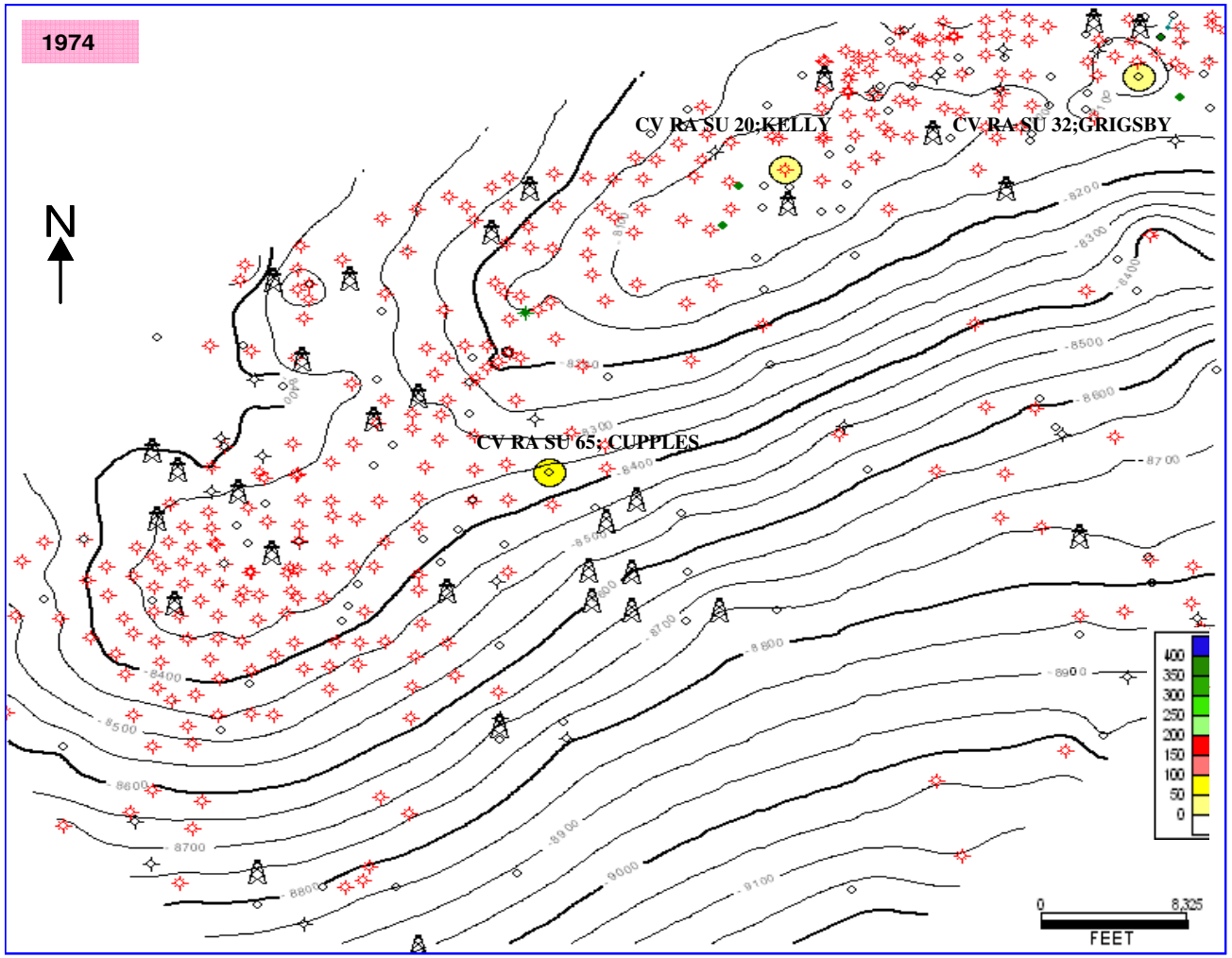

Fig. 4.7: Water Production Trend (1974).

Table 4.1: Production Test Data for 1974

Well Name	Well (API)	Date	Cum Test Gas (Mcf)	Flow Gas (Mcf/d)	Flow Water (bbls/d)	WGR (bbls/MMcf)
CV RA SU 65; CUPPLES	17017212730000	1974/10/07	39740	1400	93	66
CV RA SU 20;KELLY	17015204530000	1974/11/01	133055	550	19	35
CV RA SU 32;GRIGSBY	17015204350000	1974/11/21	27400	2000	55	28
CV RA SU11;H L TOMPKINS	17015204160000	1974/11/21	151566	550	55	100

4.2.2 Water-Gas Ratio Trend in 1975

Table 4.2 provides the water-gas ratios from production tests in wells drilled in 1975, located mainly at the central region of the field. A reversal in water-gas ratio trend is seen in the first well, CV RA SU 11; H.L. Tompkins. The water-gas ratio decreases to 33 bbls/MMcf, an indication that the initial water-gas ratio was due to a local well effect. An increase in water-gas ratio from 66 bbls/MMcf to 210 bbls/MMcf is seen in the well, CV RA SU 65; Cupples. The well, CV RA SU 66; A. Hutchinson, drilled north of the Cupples well (**Fig. 4.8**) produced excess water almost immediately. Water-gas ratios from production test in the Hutchinson well taken 8 months later had a value of 705 bbls/MMcf. Two wells (CV RA SU 19; Muslow and Day) and (CV RA SU 20; Kelly) drilled at the crest produced with water gas-ratios in excess of 90 bbls/MMcf. While the high water production in the Kelly well can be attributed to local well effect as the high water–gas ratio decreased in subsequent years, the Muslow and Day well located at the eastern part of the crest produced with increasing water-gas ratio. This was the only well located within the crestal region that was found to produce at high water-gas ratios.

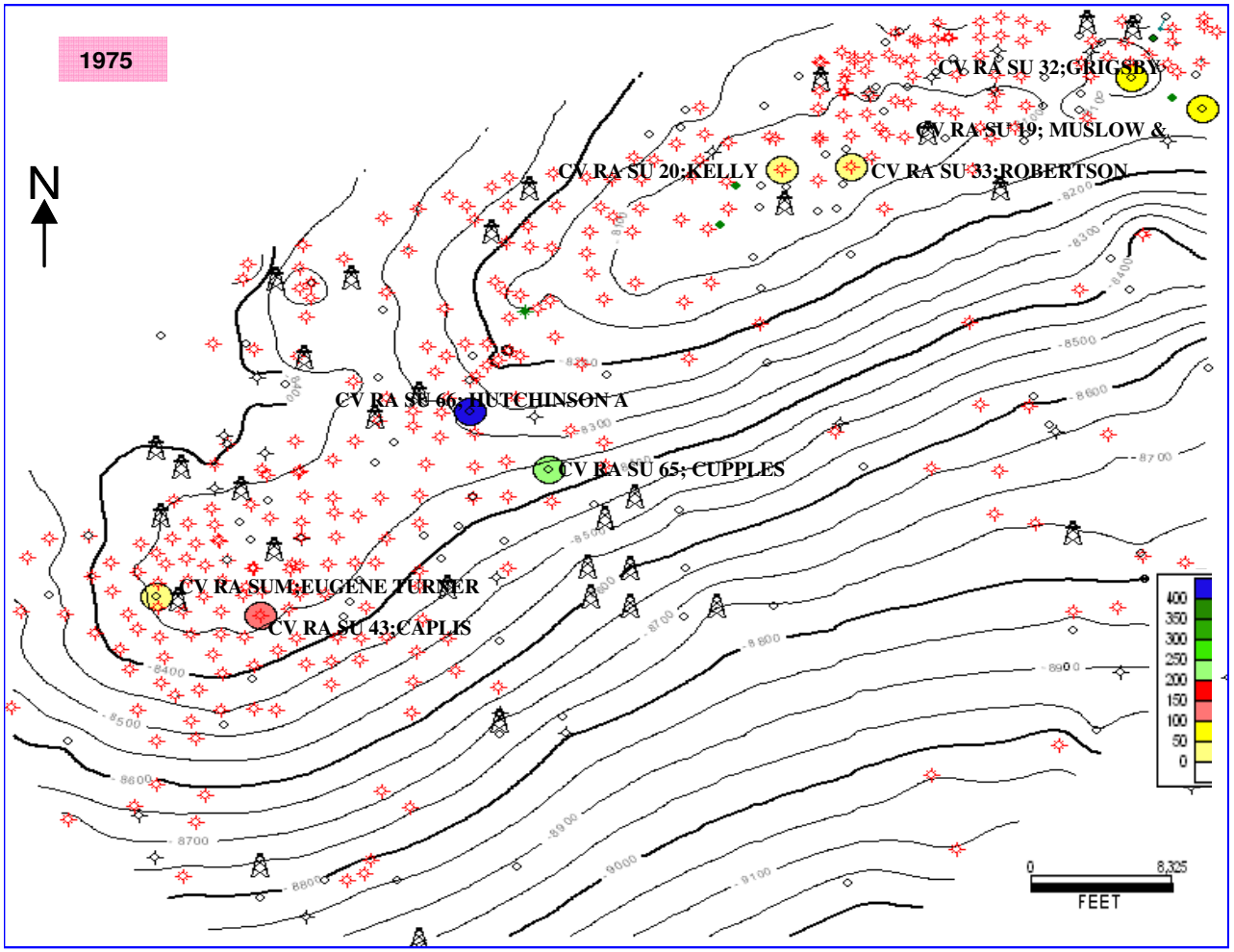

Fig. 4.8: Water Production Trend (1975).

The actual producing layer could not be confirmed as log data was not available for this well. Two more wells were drilled in the western central part of the crest, but while the well, CV RA SU 19; Eugene Turner produced gas with out high water production, the other well, CV RA SU 19; T.J. Smith Etal had a water-gas ratio of about 125 bbls/MMcf. This high water production was not sustained in subsequent years indicating local well effect rather than field water production.

Table 4.2: Production Test Data for 1975

Well Name	Well (API)	Date	Cum Test Gas (Mcf)	Flow Gas (Mcf/d)	Flow Water (bbls/d)	WGR (bbls/MMcf)
CV RA SU11;H L TOMPKINS	17015204160000	1975/01/09	172360	600	20	33
CV RA SU 32;GRIGSBY	17015204350000	1975/01/09	105842	1900	30	16
CV RA SU 20;KELLY	17015204530000	1975/05/01	198829	410	37	90
CV RA SU 19; MUSLOW & DAY	17015204950000	1975/11/03	50595	210	20	95
CV RA SU 33;ROBERTSON	17015206290000	1975/11/09	72417	1100	16	15
CV RA SU 65; CUPPLES	17017212730000	1975/11/03	398329	700	145	207
CV RA SU 66; HUTCHINSON A	17017215710000	1975/11/05	44041	200	141	705
CV RA SUM;EUGENE TURNER JR ET	17031204310000	1975/10/03	7458	1065	1	1
CV RA SU 43;CAPLIS	17031204800000	1975/09/26	7572	1000	126	126

4.2.3 Water-Gas Ratio Trend in 1976

Table 4.3 provides the water-gas ratios from production tests in wells drilled in 1976. In 1976 two additional wells (CV RA SU 62; Frierson) and (CV RA SU 67; Caplis) completed in the central region of the field (**Fig. 4.9**) some 10,000 – 11,000 ft north west of the Cupples well in the central region produced with dramatic increases in water-gas ratios to values of 516 bbls/MMcf and 324 bbls/MMcf respectively.

Table 4.3: Production Test Data for 1976

Well Name	Well (API)	Date	Cum Test Gas (Mcf)	Flow Gas (Mcf/d)	Flow Water (bbls/d)	WGR (bbls/MMcf)
CV RA SU11;H L TOMPKINS	17015204160000	1976/05/20	181067	550	15	27
CV RA SU 32;GRIGSBY	17015204350000	1976/05/17	277108	1500	10	7
CV RA SU 20;KELLY	17015204530000	1976/05/16	299416	400	1	3
CV RA SU 43;CAPLIS	17015204880000	1976/05/10		300	10	33
CV RA SU 19; MUSLOW & DAY	17015204950000	1976/11/27	102298	115	50	435
CV RA SU 39;ELM GROVE PLANTATION	17015205950000	1976/05/24	135317	1950	10	5
CV RA SU 33;ROBERTSON	17015206290000	1976/05/16	217800	1050	3	3
CV RA SU 49;SNYDER	17015206830000	1976/05/22	155288	2700	5	2
CV RA SU 38;ROBERTS	17015206970000	1976/05/24	138616	1950	10	5
CV RA SU 65; CUPPLES	17017212730000	1976/05/04	458876	400	132	330
CV RA SU 66; HUTCHINSON A	17017215710000	1976/04/27	57675	200	127	635
CV RA SU 63;HUTCHINSON	17017216530000	1976/10/30	112344	1521	161	106
CV RA SU 62;FRIERSON	17017216650000	1976/10/30	36183	490	253	516
CV RA SU 69;HUTCHINSON	17017216680000	1976/10/29	133359	1187	275	232
CV RA SU 67;CAPLIS	17017216930000	1976/03/21	20042	568	184	324
CV RA SU 68;HUTCHINSON	17017217050000	1976/10/23	105644	1657	98	59
CV RA SUB; G A FRIERSON	17017217240000	1976/11/23	27922	350	150	429
CV RA SU 73;CASPIANA PLANTATION	17017217270000	1976/04/07		955	257	269
CV RA SUM;EUGENE TURNER JR ET	17031204310000	1976/11/22	690452	1010	56	55
CV RA SUQ;JACK M WHITED	17031204600000	1976/10/19	123659	835	128	153
CV RA SUL; G A FRIERSON	17031204650000	1976/10/21	145976	350	24	69
CV RA SUR;PACE	17031204710000	1976/10/09	166641	430	119	277
CV RA SUD;T J SMITH ETAL	17031204800000	1976/11/22	331334	230	20	87
CV RA SUE;J W GRIGSBY	17031205070000	1976/11/23	402480	1300	85	65

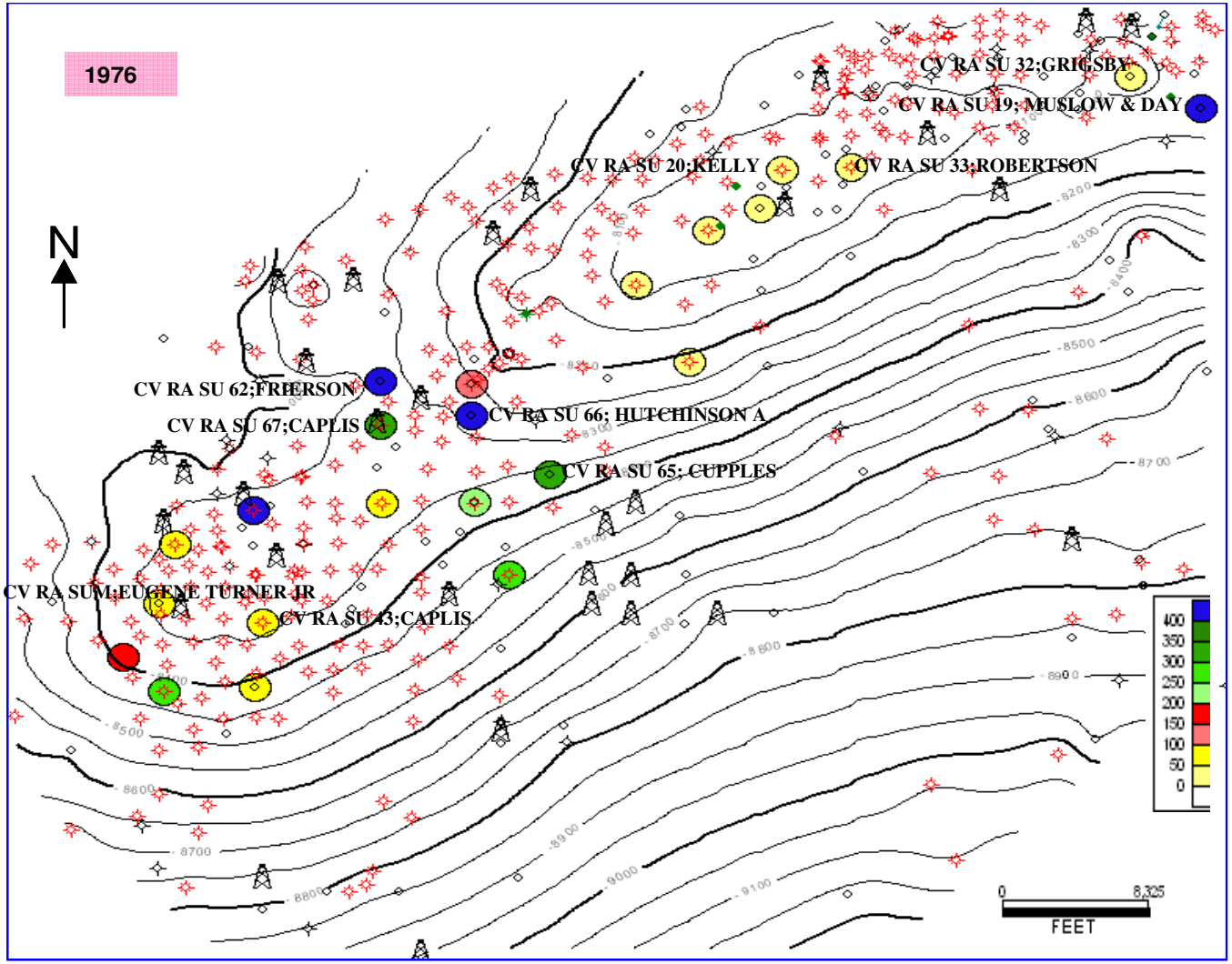

Fig. 4.9: Water Production Trend (1976).

This trend is not replicated in the south as the two additional wells (CV RA SU 69; Hutchinson) and (CV RA SU 73; Caspiana Plantation) although produced at high water-gas ratios of 232 bbls/MMcf and 269 bbls/MMcf respectively, did not exhibit such a dramatic increase and may have been due to the combined effect of water encroachment and local well effect from the hydraulic fracture.

The two wells (CV RA SUQ; Jack M. Whited) and (CV RA SUR; Pace) both drilled in the western part of the crestal region produced with water-gas ratios of 153 bbls/MMcf and 277 bbls/MMcf which progressively increased in the subsequent years. The well, CV RA SUB; G.A. Frierson produced at very high water-gas ratio (429 bbls/MMcf) but had no data recorded in the subsequent years.

4.2.4 Water-Gas Ratio Trend in 1977

Table 4.4 provides the water-gas ratios from production tests in wells drilled in 1977. In 1977, most of the wells were producing with very high water production and a general trend could be mapped around the saddle region. An additional well CV RA SU 61; Whitting Ton, drilled some 5,000 ft north of Well CV. RA SU 67; Caplis, which commenced production with high water-gas ratio in 1976. The well CV RA SU 61; Whitting Ton (**Fig. 4.9**) produced gas with a water-gas ratio of 421 bbls/MMcf. This high water-gas ratio produced at start of production points to the presence of water close to the well. The sequence of high water-gas ratios at start of production, which trends towards the north points to possibility of water encroachment from the northern flank.

Table 4.4: Production Test Data for 1977

Well Name	Well (API)	Date	Cum Test Gas (Mcf)	Flow Gas (Mcf/d)	Flow Water (bbls/d)	WGR (bbls/MMcf)
CV RA SU11;H L TOMPKINS	17015204160000	1977/06/01	306038	280	10	36
CV RA SU 32;GRIGSBY	17015204350000	1977/06/01	492990	440	10	23
CV RA SU 43;CAPLIS	17015204880000	1977/06/01	58240	150	10	67
CV RA SU 19; MUSLOW & DAY	17015204950000	1977/05/13	115457	90	50	556
CV RA SU 39;ELM GROVE PLANTATION	17015205950000	1977/06/01	499284	1000	10	10
CV RA SU 33;ROBERTSON	17015206290000	1977/04/24	451631	700	3	4
CV RA SU 49;SNYDER	17015206830000	1977/06/01	886167	2600	5	2
CV RA SU 38;ROBERTS	17015206970000	1977/06/01	541943	1210	10	8
CV RA SU 48;SNYDER	17015208100000	1977/06/01	281007	900	40	44
CV RA SU24;ROBERTSON	17015208610000	1977/03/29	12041	130	20	154
CV RA SU 41; SNYDER	17015208790000	1977/10/07	68188	300	6	20
CV RA SU 42;HUTCHINSON	17015208940000	1977/11/08	24676	400	3	8
CV RA SU 65; CUPPLES	17017212730000	1977/05/05	506405	250	122	488
CV RA SU 66; HUTCHINSON A	17017215710000	1977/09/26	73198	92	98	1065
CV RA SU 63;HUTCHINSON	17017216530000	1977/04/18	249025	613	99	162
CV RA SU 62;FRIERSON	17017216650000	1977/09/30	98464	260	126	485
CV RA SU 69;HUTCHINSON	17017216680000	1977/09/30	358587	980	302	308
CV RA SU 67;CAPLIS	17017216930000	1977/09/20	75377	240	81	338
CV RA SU 68;HUTCHINSON	17017217050000	1977/04/18	287469	714	99	139
CV RA SU 73;CASPIANA PLANTATION	17017217270000	1977/09/27	84883	260	28	108
CV RA SUC;L C HUTCHINSON JR	17017217760000	1977/04/06	303879	895	86	96
CV RA SUI;E J CRAWFORD	17017218250000	1977/04/26	23179	290	32	110
CV RA SU 61;WHITTINGTON	17017219400000	1977/09/30	61211	425	179	421
CV RA SUF;EGAN-WEBB	17017219470000	1977/04/13	125040	1225	159	130
CV RA SU 71;CUPPLES	17017220450000	1977/10/20		1878	1028	547
CV RA SU 64;CUPPLES	17017221270000	1977/11/15	665	1695	339	200
CV RA SU 72;CUPPLES	17017221550000	1977/11/10		2397	931	388
CV RA SU70;CUPPLES	17017221700000	1977/11/03	125	1950	538	276
CV RA SUM;EUGENE TURNER JR ET	17031204310000	1977/04/15	815448	945	47	50
CV RA SUQ;JACK M WHITED	17031204600000	1977/04/04	223868	580	99	171
CV RA SUL; G A FRIERSON	17031204650000	1977/04/10	191776	260	16	62
CV RA SUR;PACE	17031204710000	1977/04/21	233545	430	118	274
CV RA SUE;J W GRIGSBY	17031205070000	1977/05/24	573429	1100	75	68

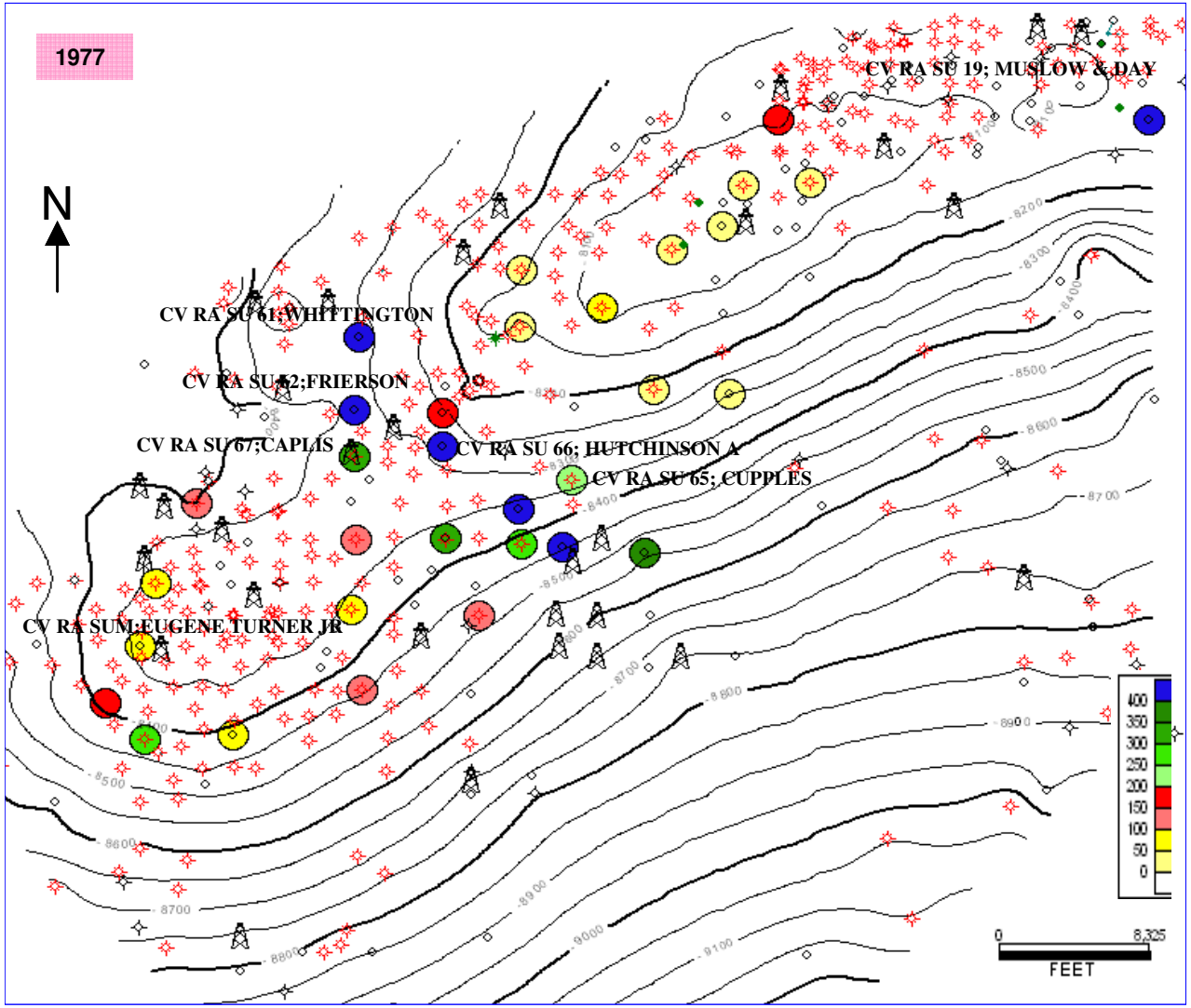

Fig. 4.10: Water Production Trend (1977).

4.2.5 Water-Gas Ratio Trend 1978 – 2004

As the years progress more wells were put on production and the recorded water-gas ratios from production test becomes more erratic without a definite pattern. Water encroachment is driven by the effective permeability of the rock to both gas and water. This is influenced by the presence of natural fractures which provides an easy path for the water to get to the well. A high water-gas ratio greater than 300 bbls/MMcf would clearly confirm a water breakthrough at the well location. Since such high values of water-gas ratios are spread almost across the entire field, high water production should have been encountered by all the wells. However, this has not been the case as some wells still produce at relatively lower water-gas ratios even down dip the reservoir structure. This variation in water-gas ratio points to a complex pattern of water encroachment which can be attributed to the reservoir geology and the distribution of rock properties in the field.

The water gas ratio trend from 1978 to 1980 (**Fig. 4.11**, **Fig. 4.12** and **Fig. 4.13**), consistently show high water production at the central crestal region in the Elm Grove and Caspiana field which confirms the recorded water-gas ratios as being due to formation water encroachment as opposed to hydraulic fracture fluids which in most cases lasts for not more than a year or two, depending on the amount of fluid pumped into the formation.

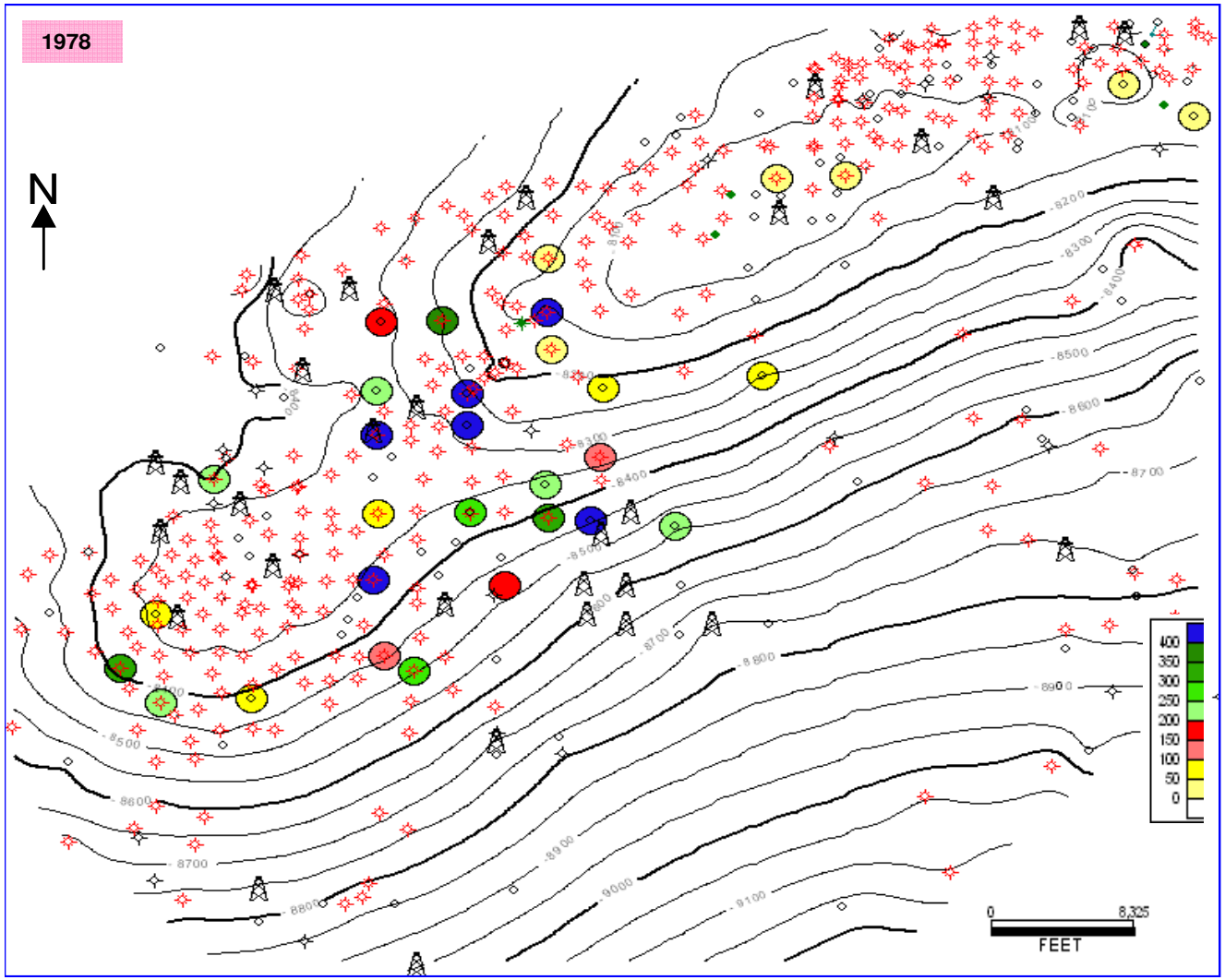

Fig. 4.11: Water Production Trend (1978).

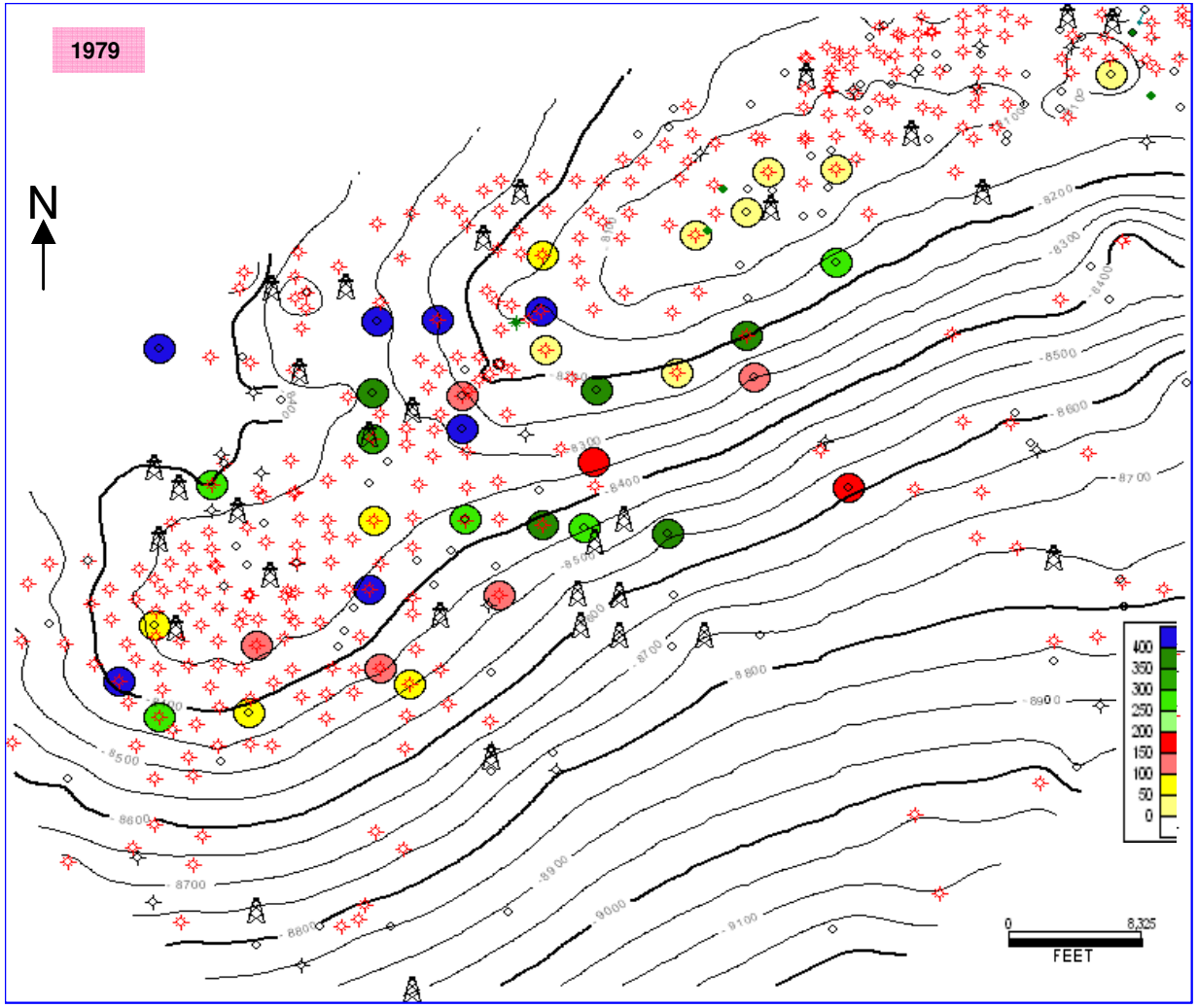

Fig. 4.12: Water Production Trend (1979).

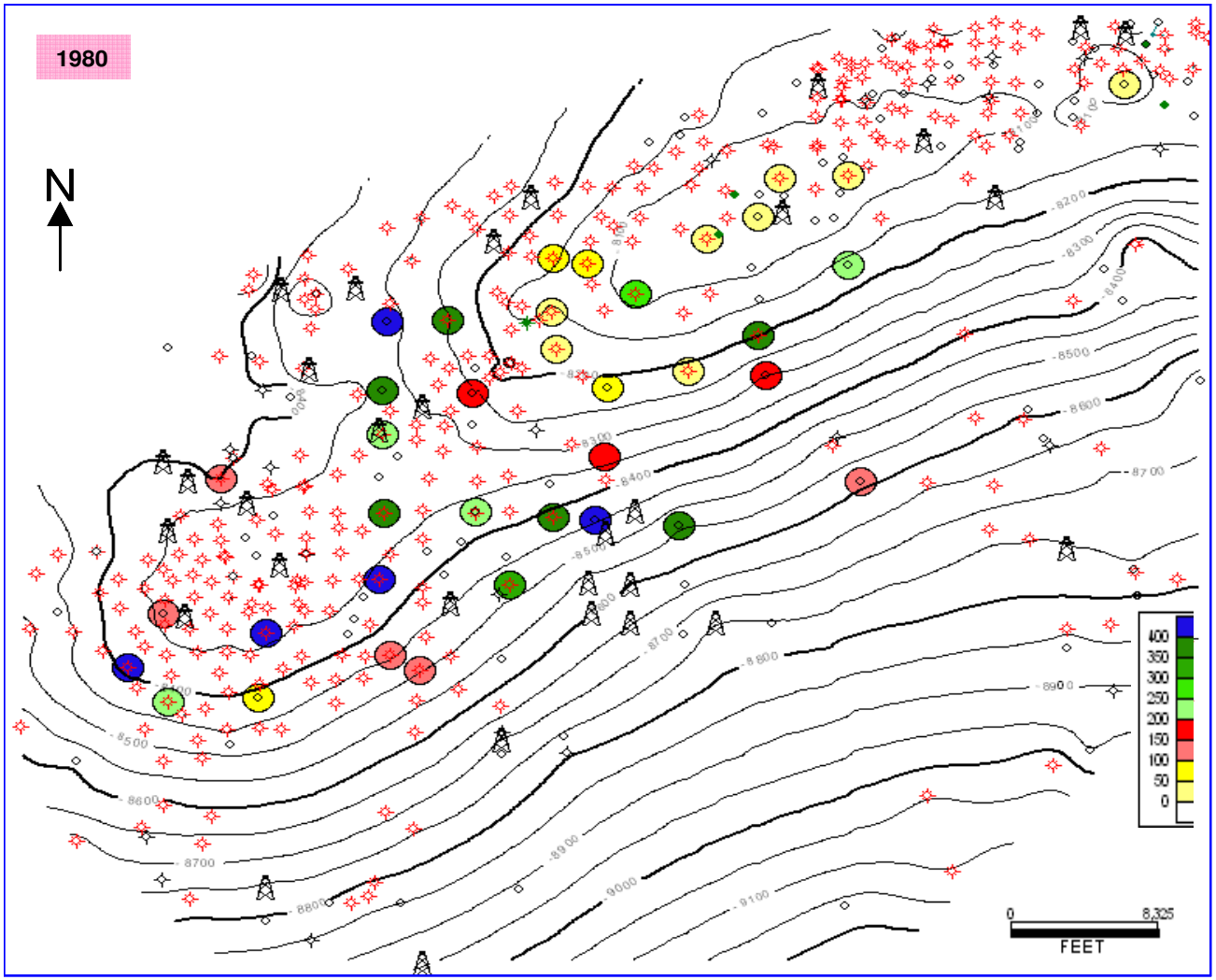

Fig. 4.13: Water Production Trend (1980).

4.3 Reservoir Simulation Results

I have used Eclipse to make over 20 simulation runs. The data file, BHP profile, water production and water gas ratios for all the cases are presented in **Fig. G1** to **Fig. G7**. A minimum BHP of 400psi was applied in all cases.

4.3.1 Effect of Water Relative Permeability Variations

The different relative permeability models presented in Table 3.2 (p.60) were used in these runs. The water-gas ratio for the different relative permeability profiles are given in **Fig. 4.14** and **Fig. 4.15**.

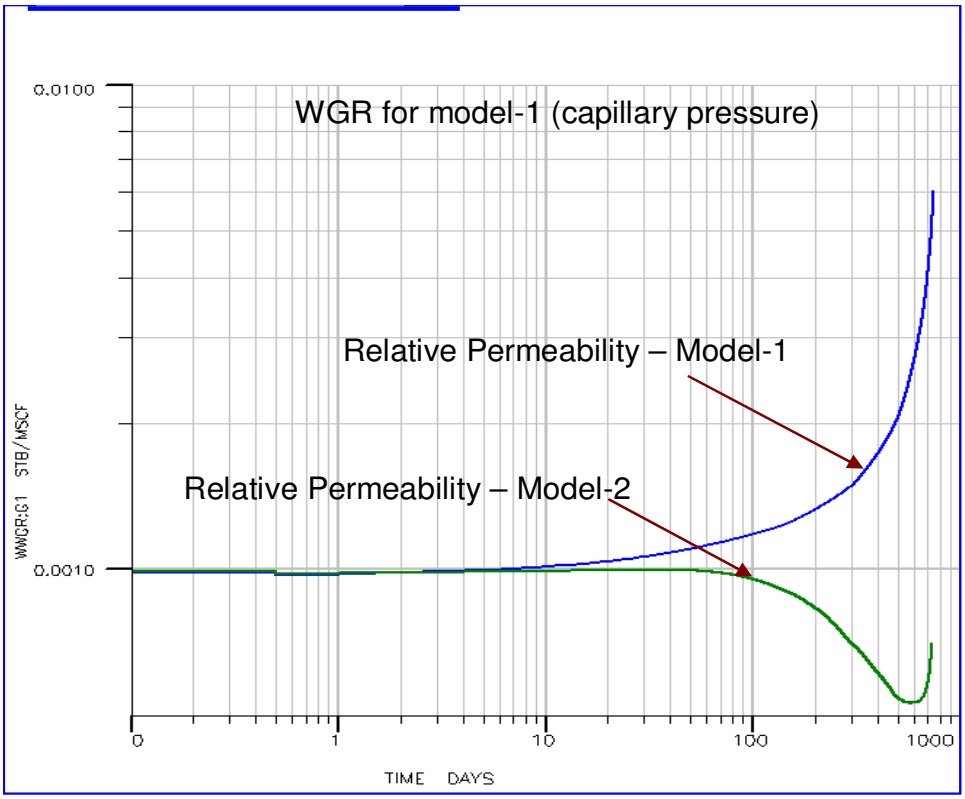

Fig. 4.14: Water Relative Permeability (Scenario 2 and 6). [Refer to Table 3.2]

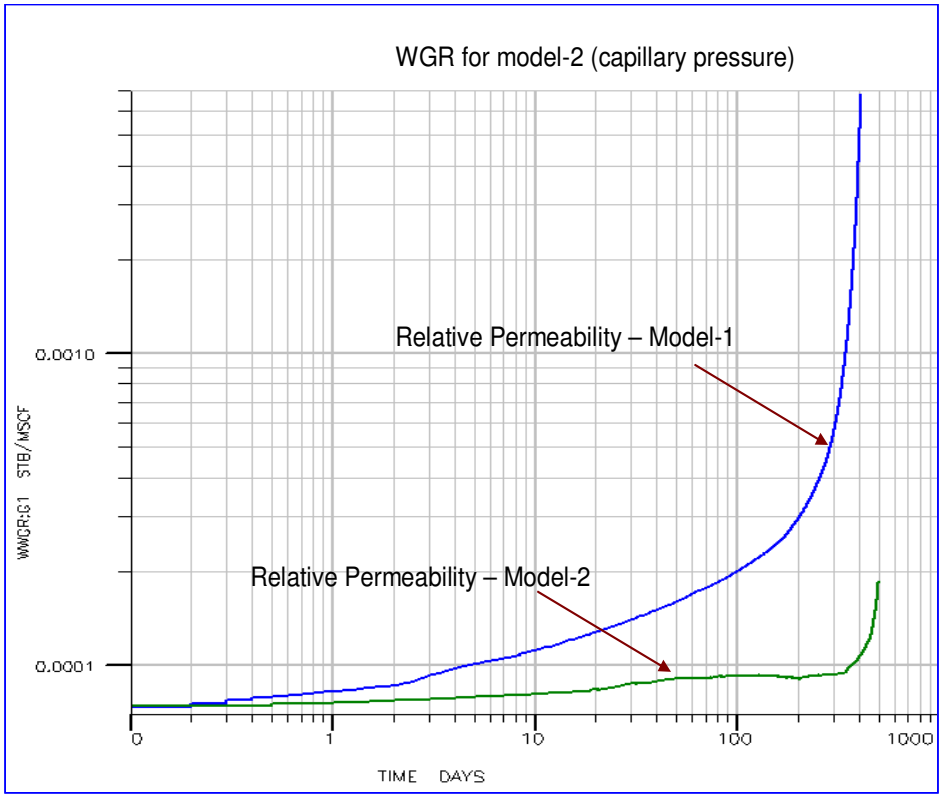

Fig. 4.15: Water Relative Permeability (Scenario 8 and 13). [Refer to Table 3.2]

Fig. 4.14 provides results from scenarios 2 (blue) and 6 (green) while Fig. 4.15 provides results from scenario 8 (blue) and 13 (green). No water production was recorded for Scenario-18 and as such does not appear on the plots.

4.3.2 Effect of Varying Vertical Distance of Water Source from Well Location

Simulation results of water gas ratios for scenarios 1 (red), 2 (green) and 3 (blue) are presented in **Fig. 4.16** while the corresponding results for scenarios 8 (red), 9 (green) and 10 (blue) are presented in **Fig. 4.17**. The various vertical distances to the water source are also shown on the graph.

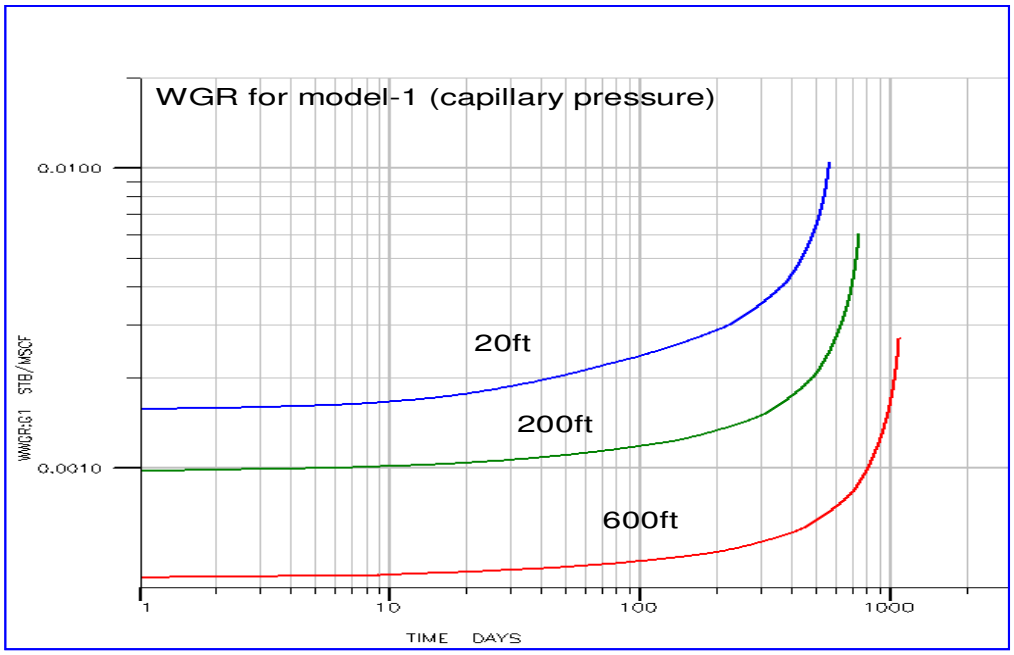

Fig. 4.16: Water-Gas Permeability Profiles (Scenario 1, 2 and 3) [Refer to Table 3.2]

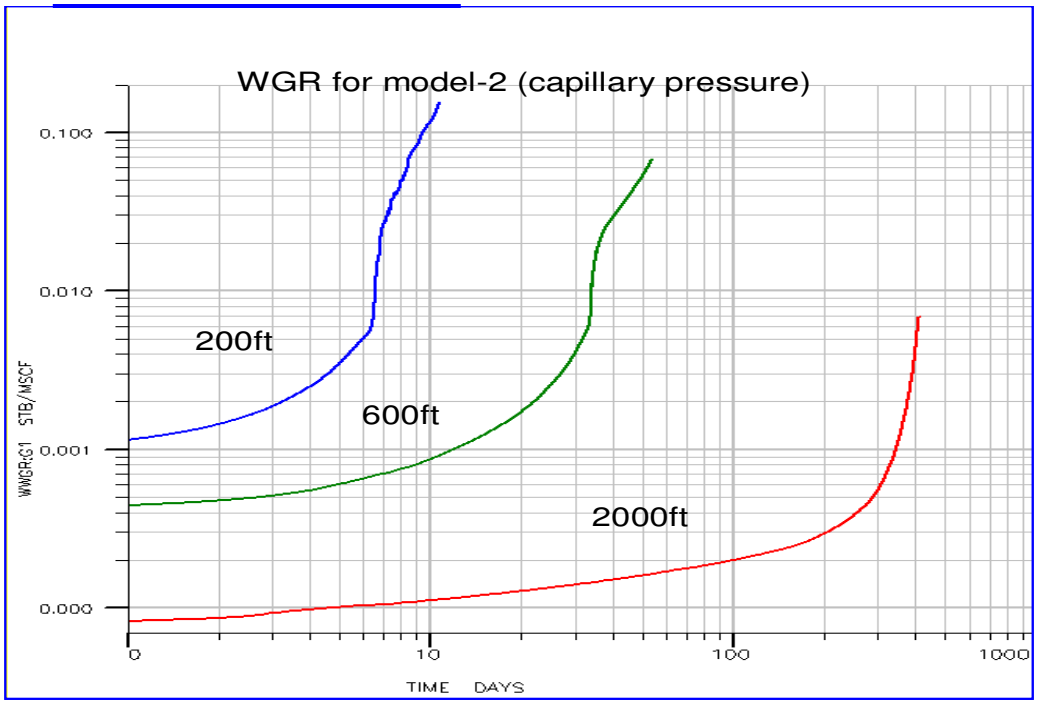

Fig. 4.17: Water-Gas Permeability Profiles (Scenario 8, 9 and 10). [Refer to Table 3.2]

4.3.3 Effect of Gas Production Rate

Increasing gas production rate results in faster breakthrough time. The water gas ratios resulting from gas rates of 20 MMcf, 14 MMcf and 8 MMcf have been provided below. Scenarios-2 (blue), 4 (green) and 5 (red) are presented in **Fig. 4.18** while scenarios -8 (blue), 11 (green) and 12 (red) are presented in **Fig. 4.19**.

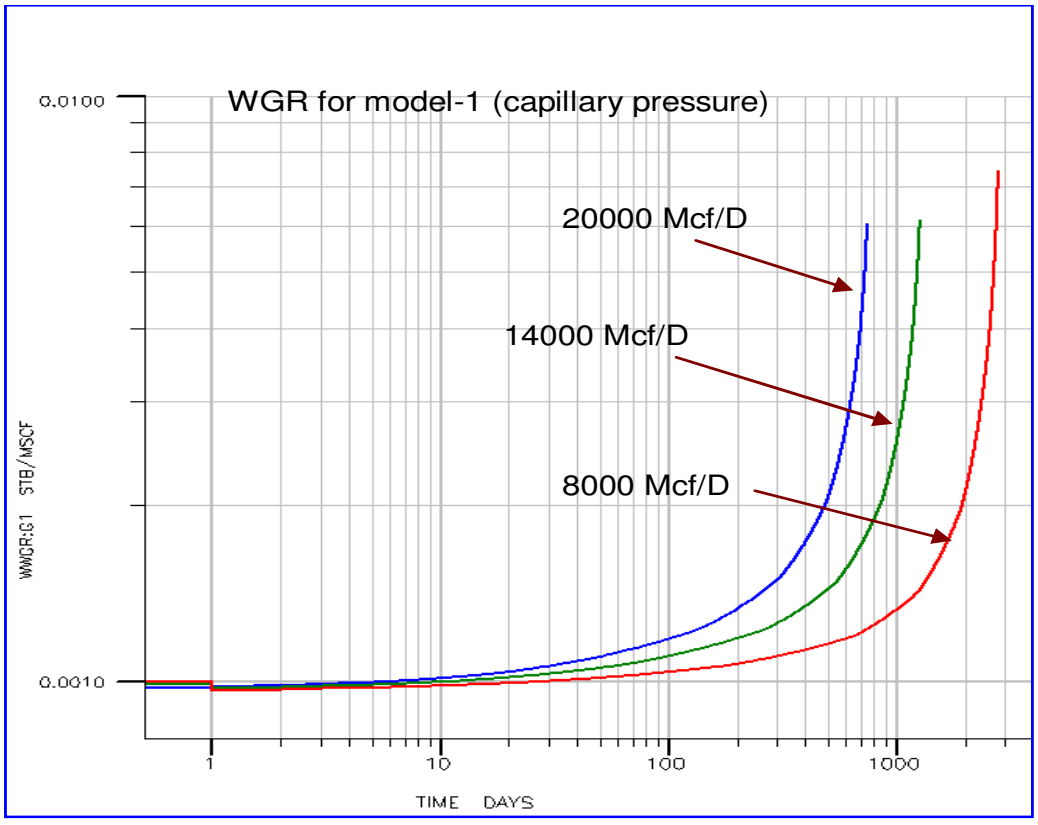

Fig. 4.18: Water-Gas Permeability Profiles (Scenario 2, 4 and 5). [Refer to Table 3.2]

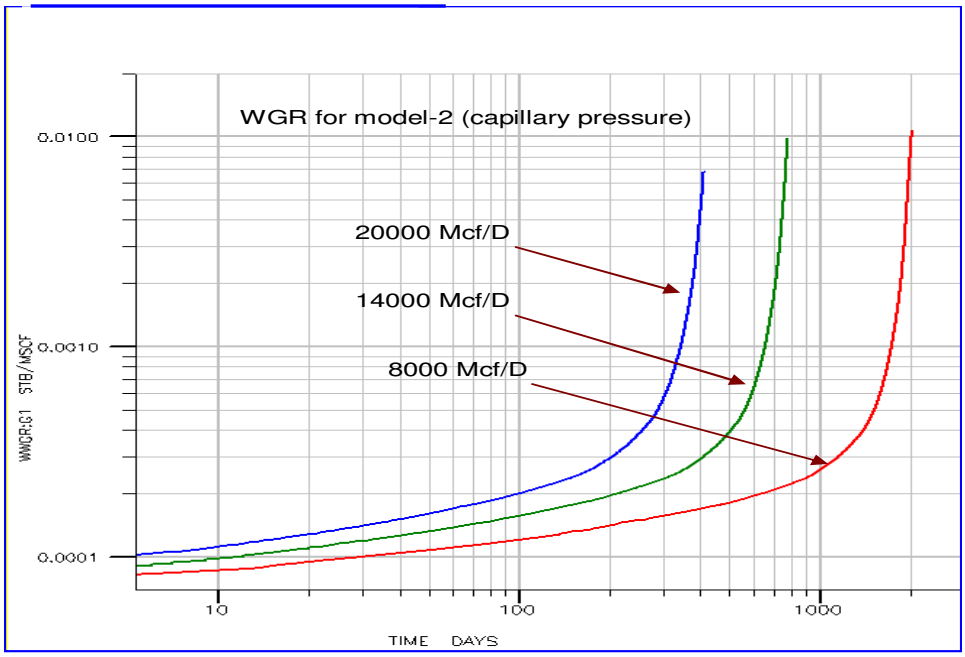

Fig. 4.19: Water Gas Permeability Profiles (Scenario 8, 11 and 12). [Refer to Table 3.2]

4.3.4 Layering Effect

The multi-layer effect on water production as opposed to that of a single layer was investigated with the simulation model. To achieve a multi-layer configuration, transmissibilities across cells in the vertical direction was set to zero, such that flow was only horizontally across cells. Two multi-layer cases were simulated, one case involved layers with absolute permeabilities as high as 6 mD to 10 mD, to act as high permeability streaks, while the second case had permeabilities in the range of (0.002-0.1) mD. A single layer model having cell transmissibilities defined for all directions, and having vertically varying permeabilities and porosities, was also simulated. The resulting gas water ratios are presented Fig. 4.20 and Fig. 4.21.

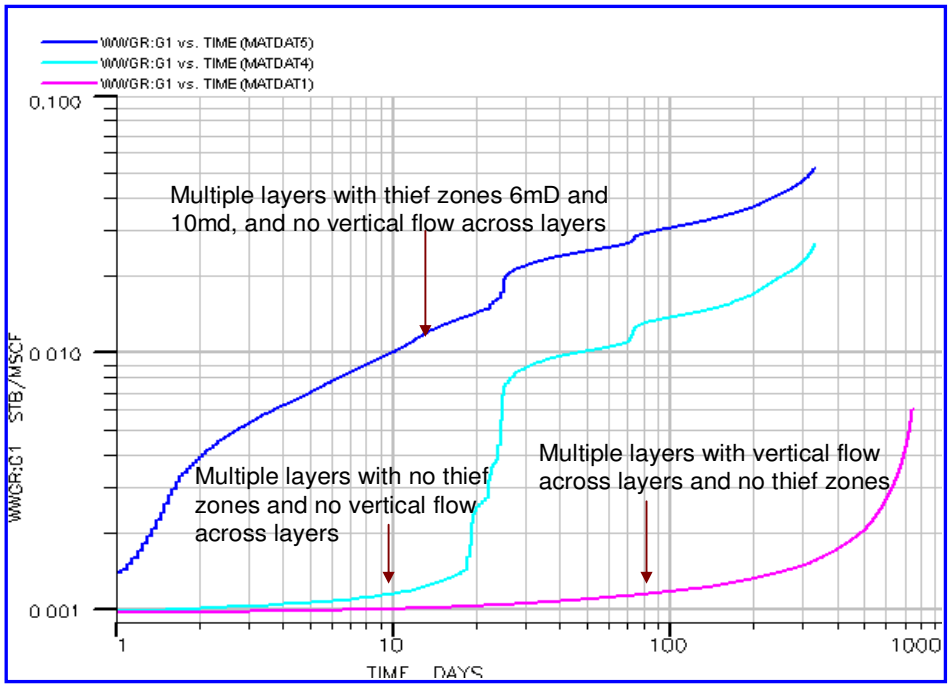

Fig. 4.20: Water-Gas Permeability Profiles (Scenario 2, 15 and 16). [Refer to Table 3.2]

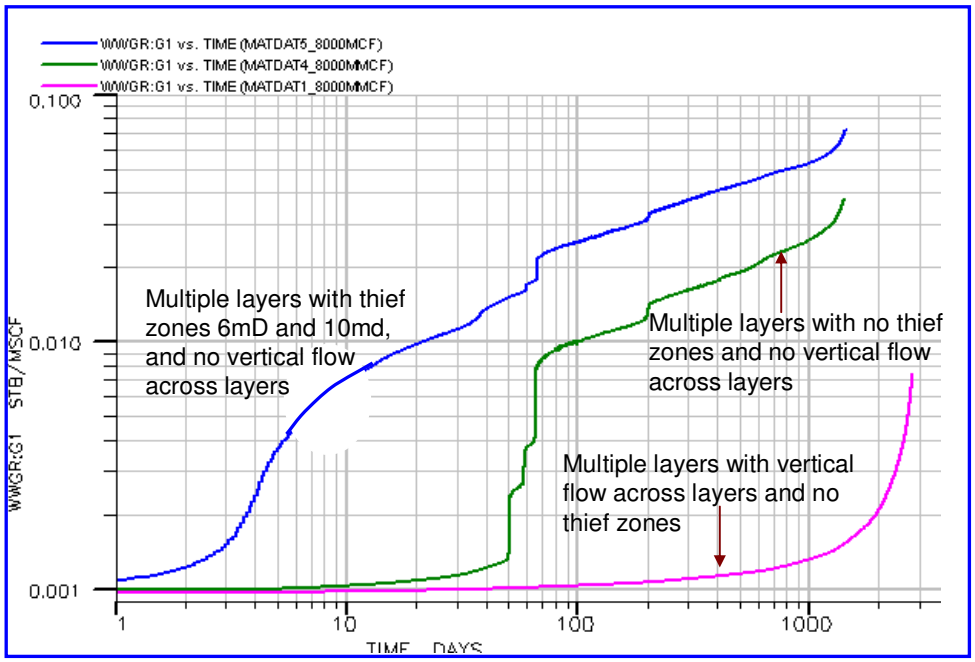

Fig. 4.21: Water-Gas Permeability Profiles (Scenario 5, 17 and 21). [Refer to Table 3.2]

Scenarios-2 (purple), 15 (cyan) and 19 (dark blue) are presented in Fig. 4.20 while Scenarios -5 (purple), 17 (green) and 21(dark blue) are presented in Fig. 4.21.

4.3.5 Effect of Water Source Distance in the Multi-layered Scenarios

In the previous section, the simulation results for the multi layer effect were presented. In these runs, we investigated the effect of the distance of the water source from the well drainage point in the multi-layer scenarios. Vertical distances of 200 ft and 2000 ft were simulated. The resulting water gas ratios are presented below. Scenarios 19 (blue) and 22 (green) are presented in **Fig. 4.22** while scenarios 21 (green) and 24 (blue) are presented in **Fig. 4.23**.

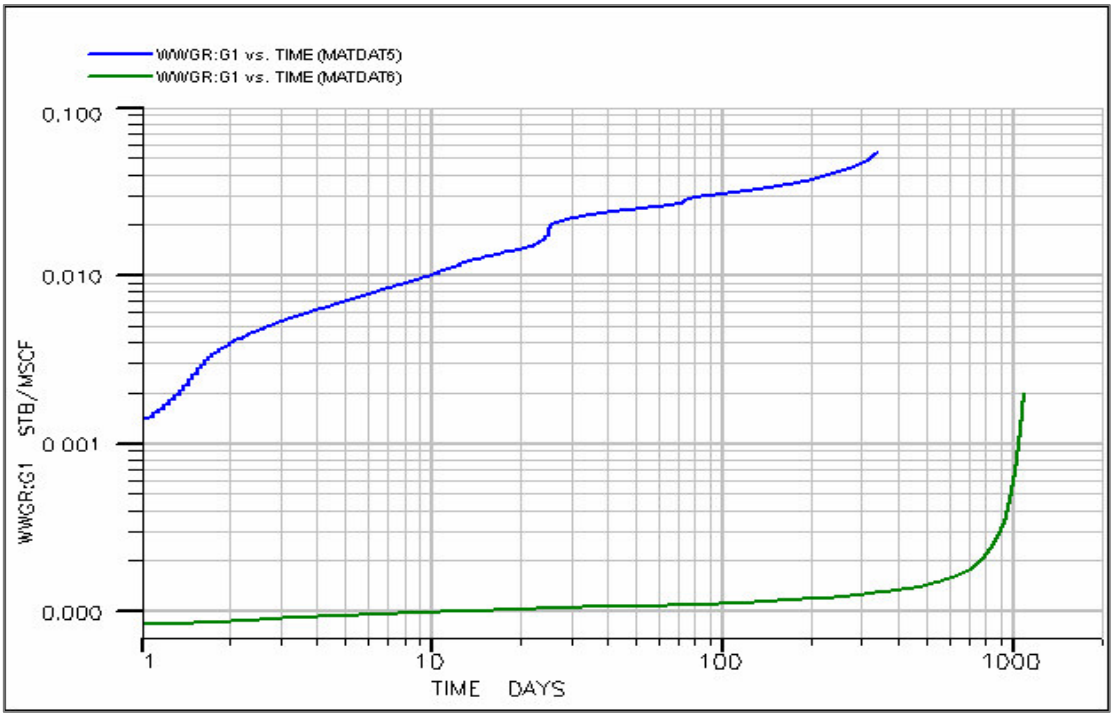

Fig. 4.22: Water-Gas Permeability Profiles (Scenario 19 and 22). [Refer to Table 3.2]

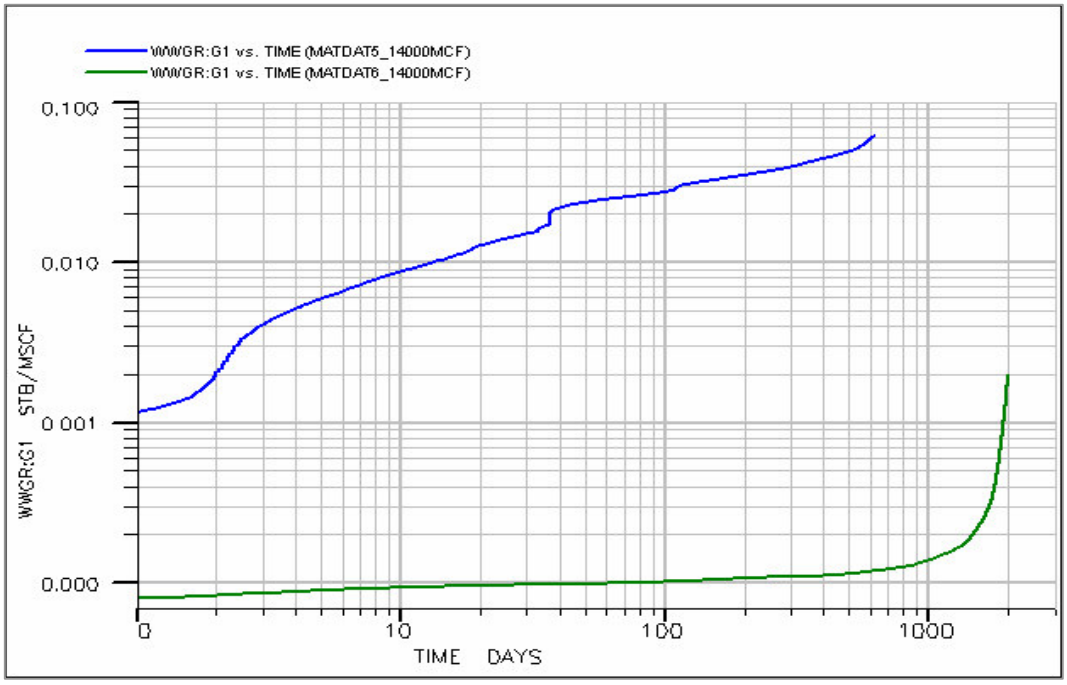

Fig. 4.23: Water-Gas Permeability Profiles (Scenario 21 and 24). [Refer to Table 3.2]

4.4 Selected Reservoir Model

The simulation result of the selected reservoir model is shown in **Fig. 4.24**. The flat water-gas ration output on a log scale matches the actual trend obtained in the field. The graph presentation has been made similar to the production data provided from Matador resource.

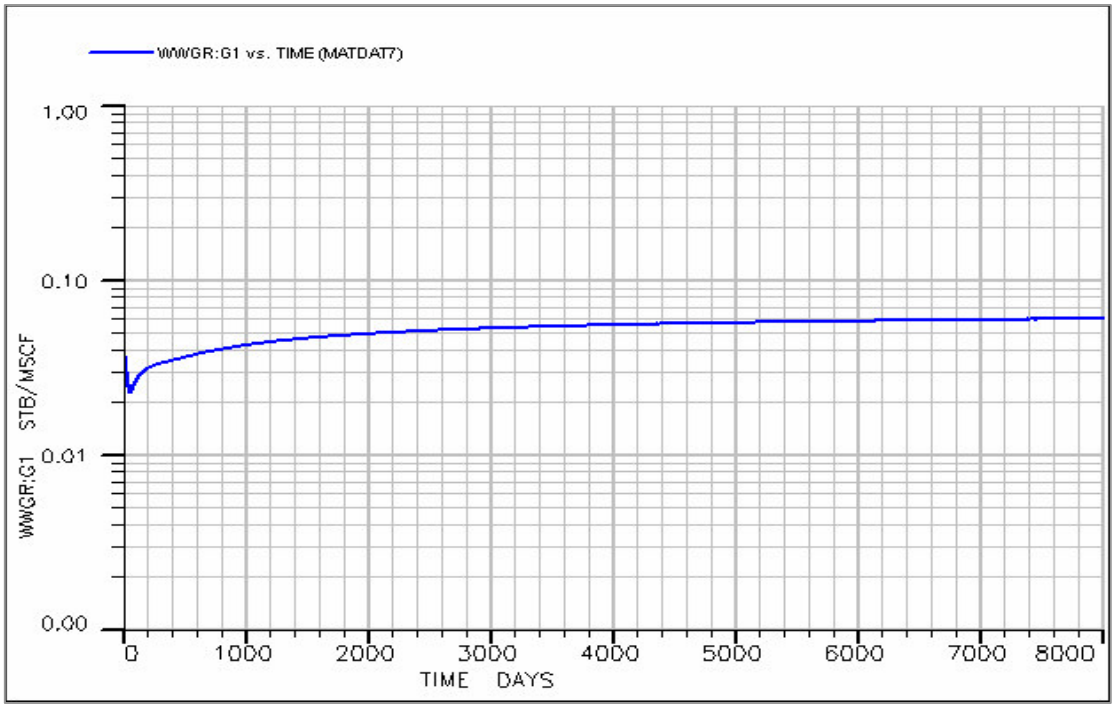

Fig. 4.24: Water-Gas Ratios Result from the Field Reservoir Model.

CHAPTER V

DISCUSSION OF RESULTS

5.1 Fluid Distribution and Fluid Interpretation

Unlike conventional sands (permeability greater than 0.1 mD) that have distinctive hydrocarbon water contacts, tight gas sands often do not have discernible hydrocarbon water contacts. In the Cotton Valley sands of Elm Grove and Caspiana fields, no distinct gas-water contact has been identified in the field. However, a time lapse review of the resistivity log data in areas where there has been significant production shows some reduction in the resistivity response in some sections, which indicates possible water encroachment. For water encroachment to occur, the reservoir rock should have significant effective permeability to water on the order of several millidarcies. If the formation effective permeability to water is in the microDarcy range, the water could not move through the formation fast enough to produce high gas-water ratios, as we have observed in this field. Some sections in the field with little changes in water saturation have also been observed in sand regions of the Cotton Valley interval, in spite of the large gas production. This lack of saturation change points to a lack of water encroachment in those sections, and can be most likely attributed to low effective permeability to water. The effect of the relative permeability to the fluid distribution points to a post hydrocarbon accumulation water encroachment. This is supported by the absence of a distinct gas-water contact located within the proximity of the early water producing wells.

5.2 Log Data Evaluation Results

The properties derived from the log evaluation include porosity, permeability, water saturation, and shale volume. The presence of multiple minerals affects the porosity evaluation such that some sections may be pessimistic due to the error in grain density. However, the core-log porosity match indicates a reasonable matrix density assumption.

The presence of conductive clay minerals affects the calculated values of water saturation evaluation. Both the Waxman-Smit's and the dual water model gave similar results except for some low resistivity regions where the Waxman-Smit's equation resulted in excessive shaliness corrections on the saturations.

The results of the permeability evaluation failed to match the core measured permeability; however, the results of the calculation falls within the range of the core-measured data. One significant outcome in the permeability evaluation is the existence of high permeability streaks with permeability values greater that 2 mD. Zones with high permeability were also observed in the stressed core data measurements.

5.3 Reservoir Simulation Results

The reservoir simulation results show the corresponding reservoir effects of varying fluid and rock properties. The major properties that affect water production are formation permeability, water relative permeability, water capillary pressure, gas production rate, and the distance of the well to the water source. Understanding the effects of these properties on reservoir flow on a small scale simulation grid helps to

understand the reservoir flow behavior and production performance of a large scale tight gas sand field. In this case it is the Cotton Valley sands of the Elm Grove and Caspiana fields.

5.3.1 Effects of Water Relative Permeability

Section 4.2.1 shows the effect of water relative permeability on water production. Model-1 represents cases with significant relative permeability for simultaneous flow of both water and gas, while model-2 represents cases with poor relative permeability for the simultaneous flow of both fluids. To account for the large heterogeneity in the rock, both relative permeability profiles were used in the simulation model with different capillary pressure profiles obtained from the core measurements. The results show an increase in water-gas ratio as relative permeability for simultaneous water and gas flow increases. The results for relative permeability Model-2 in **Fig. 4.14** shows the initial effects of the hydraulic fracture on the water gas ratios. The results here clearly shows that for substantial water flow to occur, the rock must have significant relative permeability for simultaneous gas and water flow.

5.3.2 Effects of Varying Distance of Water Source to Drainage Point

Section 4.2.2 shows the resultant effect of varying distances of water source from the well. An infinite acting aquifer has been used to define the water source and placed at varying distances from the edge of the well bore and hydraulic fracture. Simulation results are provided for different capillary pressure profiles to account for the

heterogeneity of the rock formation. The results show that for capillary pressure profiles with large transition zones, early water break-through should be expected at wells approximately 600 ft vertical distance from the water source, provided there is enough permeability to both water and gas to permit simultaneous flow of both fluids. However, for vertical distances 2000 ft away, no significant water production was encountered during the first year of simulation. This is a critical result and relates very well to the Elm Grove and Caspiana field where the north and south boundaries to the earliest water producing well is over 30,000 horizontal feet away. It is highly unlikely that water is pulled-in from some 30,000 ft away from the well because Cotton Valley sand bodies would not be expected to be continuous over that distance. The most likely scenario would be a water source located some 200 to 600 ft vertical distance from the well.

5.3.3 Effects of Gas Production Rates

Section 4.2.3 shows the resultant effect of varying gas production rates, or really the pressure drawdown in the reservoir upon water encroachment. The results show little sensitivity at early production time but show different water break-through times. The water will breakthrough more rapidly when the reservoir pressure decreases more rapidly. The simulation assumes sufficient effective permeability to both water and gas for simultaneous flow. Due to the varying capillary pressure profiles, **Fig. 4.15** is based on a vertical distance of 200 ft from the water source while Fig. 4.16 is based on a vertical distance of 2000 ft from the water source.

5.3.4 Effects of Layering on Water Production

A multi-layer effect was modeled by setting vertical transmissibility between the layers equal to zero. Normally, this would have been achieved by setting vertical permeability to zero but because the simulation was carried out on an inclined grid, vertical permeability does not necessarily translate to vertical permeability between cells. Three cases were investigated and include:

(i) multiple layers with high permeability layers of 6-10 mD and vertical transmissibility of zero,

(ii) multiple layers with permeability less than or equal to 0.1 mD, and vertical transmissibility of zero,

(iii) multiple layers with permeability less than 0.1 mD and vertical transmissibility not equal to zero.

Section 4.2.5 provides the water production for different gas flow rates. The results show early water production and an increase in water-gas ratio with increased layer effect. The presence of high permeability layers results in a significant increase in the water gas ratio especially at the early time production. Core measurements from cores cut from the Cotton Valley formation revealed some permeability values greater than 2 mD, which points to the existence of high permeability which form easy paths for water flow and has the potential to greatly increase water production. In addition to the high permeability streaks included in the multi-layer model, varied distances of the well drainage point to the water source was also simulated (section 4.2.5). The results show that in spite of the existence of high permeability zones, excessive water production is

highly unlikely from a water source at a distance 2000 vertical feet away from the well drainage point.

5.3.5 Simulation Result from Final Reservoir Model

In the final model, two out of the six layers were flooded with water to represent current field status in the well regions. The multi-layered model with high permeability streaks was selected because the WGR profile from the simulation was closest to the profiles in the Matador Wells. The result of the simulation with the 2.3° dip, inclined grid shows a flat WGR ratio with time and matches the production data from Caspiana Int. Well. The flat profile would most probably be due to the relatively constant flow from the flooded zone while other layers continue to produce gas. This result further goes to support the presence of two possible types of gas sand formation, one impermeable to water flow and the other, permeable to flow of water.

5.4 Water Production Trend Analysis

Fig. 5.1 shows a structural map of the Elm Grove-Caspiana field and the location of the first 10 wells initially producing from the Cotton Valley sands. The wells are numbered to signify the sequence in which the wells were drilled. Well 1 was spudded in March, 1973 and was completed in July 1973 (**Table 5.1**). The first production test reported was in August 1973 with a water-gas ratio of approximately 30 bbls/MMcf. Wells 2, 3, and 4 were also drilled in 1973 but did not commence production until early in the year in 1974. In 1974, the highest WGR recorded was from Well 1 at 100

bbls/MMcf, followed by Well 4 with 66 bbls/MMcf. In 1975, the other 6 wells commenced production with the highest WGR recorded from Well 9 at 705 bbls/MMcf followed by Well 4 with 207 bbls/MMcf. The initial high WGR from Well 1 was observed to sharply reduce to about 33 bbls/MMcf and continued to remain low for subsequent years. The high WGR recorded in Wells 4 and 9 was sustained until the

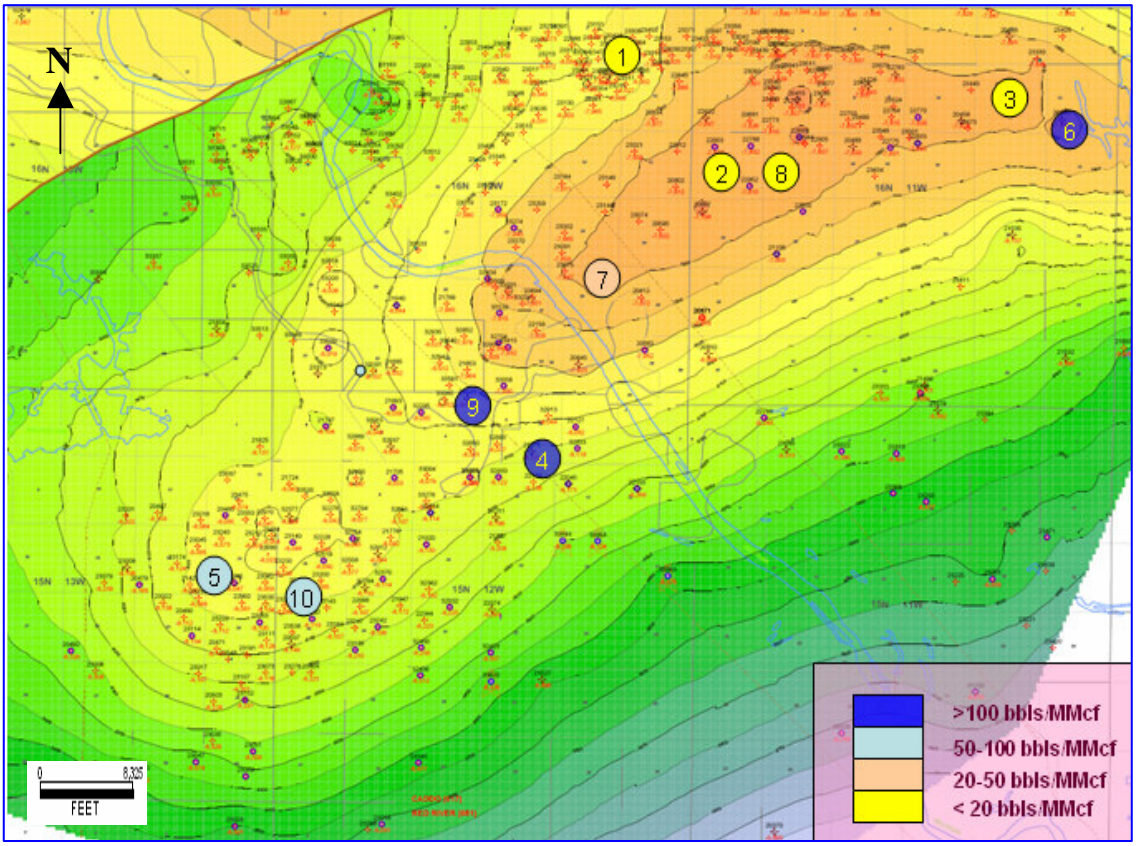

Fig. 5.1: Structural Map of the Elm Grove and Caspiana Fields with the Locations of the First Ten Wells Drilled and Produced from the Cotton Valley Sands. The water-gas ratios from production tests carried out after two years of production from the field, are presented with color codes and range from less than 20bbls/MMcf to over 100 bbls/MMcf.

wells were finally shut down. Thus, Well 4 provides the first consistent indication of sustained water production with a WGR of 66 bbls/MMcf from production tests carried out in October 1974.

Table 5.1: Water-Gas Ratios for Early Wells in Elm Grove and Caspiana Fields

Drill Seq.	Well API Number	Spud Date (mm-dd-yyyy)	Compl. Date (mm-dd-yyyy)	WGR (1973) bbls/MMcf	WGR (1974) bbls/MMcf	WGR (1975) bbls/MMcf	WGR (1976) bbls/MMcf	WGR (1977) bbls/MMcf
1	17015204160000	3/29/1973	7/23/1973	31	100	33	27	36
2	17015204350000	6/19/1973	12/28/1973		28	16	7	23
3	17015204530000	11/6/1973	2/28/1974		35	90	3	-
4	17017212730000	9/19/1973	4/16/1974		66	207	330	488
5	17031204310000	5/16/1974	12/17/1974			1	55	50
6	17015204950000	9/11/1974	12/20/1974			95	435	556
7	17015204880000	3/3/1974	1/9/1975			-	33	67
8	17015206290000	11/27/1974	1/9/1975			15	3	4
9	17017215710000	1/15/1974	3/7/1975			705	635	1065
10	17031204800000	1/17/1975	7/29/1975			126	80	-
Well	Well API Number	Spud Date (mm-dd-yyyy)	Completion Date (mm-dd-yyyy)	WGR (2000) bbls/MMcf	WGR (2001) bbls/MMcf	WGR (2002) bbls/MMcf	WGR (2003) bbls/MMcf	
1F	17015229500000	12/11/1998	2/20/1999	94	151	152	166	
2F	17015229510000	3/19/1999	5/7/1999	180	146	137	140	
3F	17015229530000	3/4/1999	5/10/1999	755	333	2016	-	
4F	17015229540000	2/17/1999	4/2/1999	113	141	88	96	
5F	17015229650000	3/4/2000	4/24/2000		6000	3813	33	

The location and timing of water production from Well 4 just above a year after production commenced in the field, points to the following scenarios:

(i) The water source is an unconventional water accumulation, most probably from a post hydrocarbon accumulation water charge (since a conventional aquifer with water contact at a crestal location would result in little or no gas in place for production);

(ii) The water source should be at some depth not greater than approximately 500 ft from the edge of the hydraulic fracture of Well-4. (This has been shown in section 4.2.2);

(iii) Water production is selective with targeted flow paths in a multi-layered and laterally heterogeneous reservoir sand play. (This can be seen from the log data and the WGR distribution from production tests recorded in the field.

(iv) The water source is largely infinite acting as water production has progressively increased continuously in the reservoir for over 30 years and may most likely result from large natural fractures, or a poor fault sealing at the north of the field.

(v) The high WGR indicates conventional relative permeability profile and a significant capacity for simultaneous gas and water flow.

Most of the early drilling activity was concentrated at the central and crestal region of the field and areas close to the fault and the down dip portion of the field were avoided. But as field development progressed, more wells were drilled and between 1999 and 2000 over 10 wells had been drilled close to the fault on the Northwest side of the field. Production tests in some of this wells yielded exceedingly high water gas ratios which point to the existence of water migration up the fault. The highest water gas ratios were recorded in 2000 was 755 bbls/MMcf from Well 3F. In 2001 and 2002, WGR's of 6,000 and 3,813 bbls/MMcf have been recorded for Well-5F. **Fig. 5.2** shows the wells

drilled close to the fault. It is evident thus, that water accumulation could emerge from the fault. Unfortunately data within the fault regions were not provided. A well log cross section of the field is presented in **Fig. J1** to **Fig. J8.**

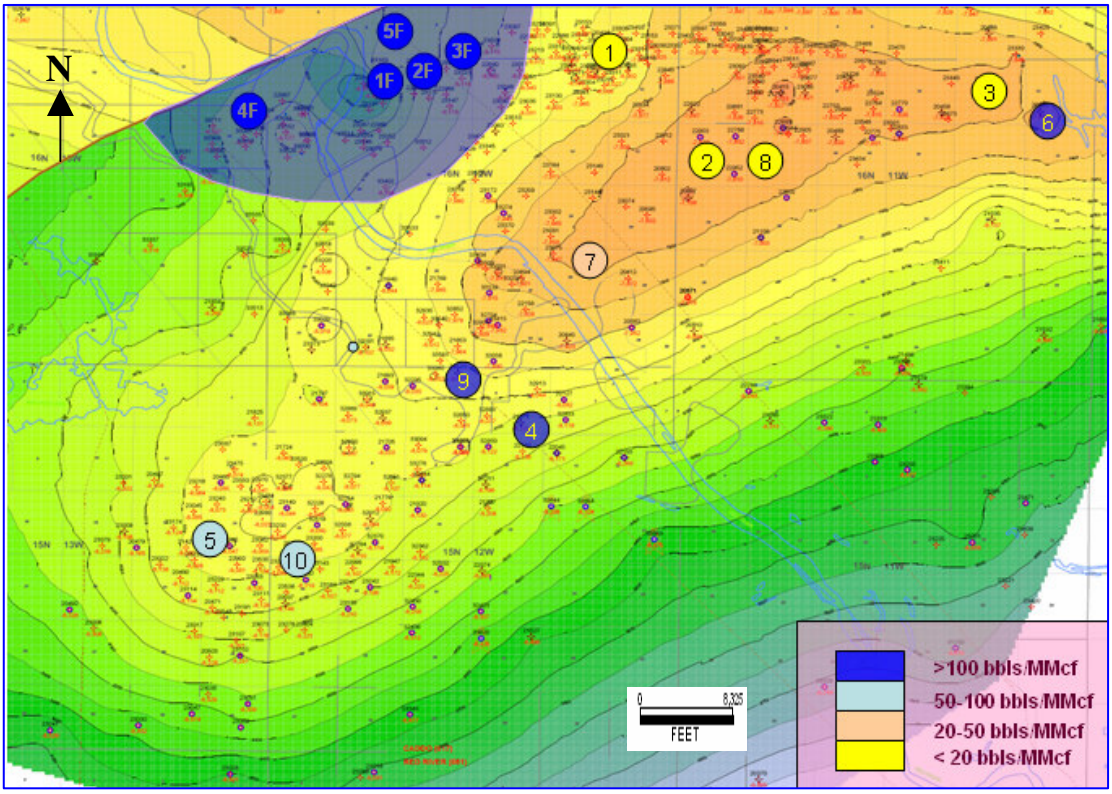

Fig. 5.2: Structural Map Showing Wells Drilled Close to the Fault Producing with High Water-Gas Ratios.

5.5 Possible Water Source and Flow Path

The distribution of zones with high water saturation and the water-gas ratio trend in the field clearly points to a complex and irregular water encroachment pattern in the field. The source of the water is yet to be precisely defined even though over a thousand wells have been drilled in the field. The USGS Bulletin reported the absence of a down dip limit for gas production in the Cotton Valley sands of the Elm Grove-Caspiana field. There are three possible paths for water encroachment in to the field and these include:

- Water moving in from the fault that is north and west of the field.
- Water could be moving up from the South and East of the field through a long transition zone; or
- Water could be moving up from above or below the Cotton Valley sandstones through fractures resulting from major faulting.

Water movement from down dip in the south is highly unlikely due to the central and crestal location of the first high water producing well in the field which is some 30,000 ft from the deepest producing well in the South. With water production commencing within the first 1-2 years of production in the field, the well has to be near the water source as shown by the simulation run (Fig. 4.16 and Fig. 4.17).

Water encroachment from the fault is supported by the dramatic high water production encountered with wells drilled near to the fault. However, there is no well established evidence that the water comes from the fault. The fault is some 20,000 - 30,000 horizontal feet and 300 – 400 vertical feet, from the earliest high water producing well at the central and crestal region of the field. Thus for water production to occur so

soon in the field, water must be coming from a source close to the well. While flushed zones have been seen in isolated layers in the reservoir interval, the existence of gas zones below the water flushed zones can not be easily explained.

Another possible source of the water production is water encroachment from possible natural fractures or secondary faults occurring as a result of salt tectonics such as the Sabine uplift and associated with the major fault to the North and West of the field. The existence of natural fractures has been known to contribute to improved gas production in the field, especially when they occur at the crest of the structure, however, their contribution to water production is not well documented in literature. This is probably due to limited well data as most water producing zones have very little gas production and are not very attractive for development drilling. To better understand the contribution of natural fractures and/or secondary faults in the Elm Grove and Caspiana fields, a 3-dimensional seismic data survey would be required. A schematic cross section of the main fault and possible secondary faults or natural fracture scenarios has been drawn in **Fig. 5.3**.

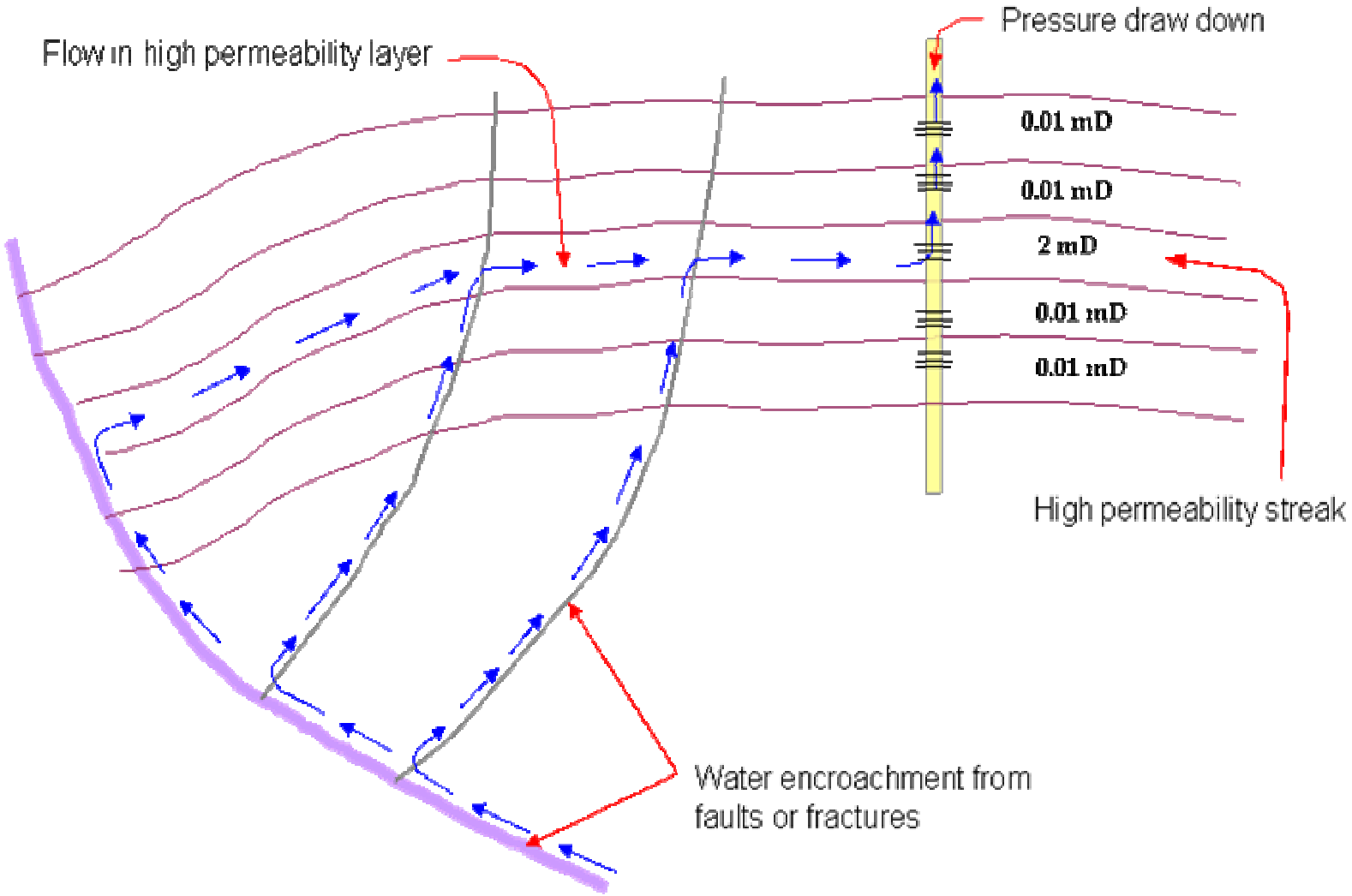

Fig. 5.3: Structural Cross-Section Showing Possible Water Source.

5.6 Water Production from the Matador Wells

Most of the Matador wells are located at the southern flank of the reservoir structure. The production data from the field shows that most of the wells are producing with water-gas ratios of between (100 – 800) bbls/MMcf and gas production averages about 300 Mcf/D.

One outcome of this research is the identification of flushed zones or high water saturation zoned from log analysis. Flushed zones have been identified in both the upper and lower Cotton Valleys sands and could possibly impact the design and placement of hydraulic fractures. The high activity on the gamma ray logs and the results of the sensitivities carried out (Fig. 4.22) points to the existence of some isolated layers with some high permeability streaks conducting water to the well. These layers need to be identified with sophisticated logs as the NMR, FMI and Geochemical tools. Although these logs are expensive to run, they may prove to be worth the cost if the wet zones can be identified.

The possible location of the faults or fractures at the northern flank of the field should make the Matador wells in the southern flank better located to avoid high water production, relative to wells on the saddle or the north of the field. However, due to the complex pattern of the water encroachment in the field, the lateral distribution of the water flow path cannot be easily established. Wells not very far from each other could produce at significantly different water-gas ratios. Any development activity at the north or saddle area should include water handling facilities to accommodate the water production.

CHAPTER VI

SUMMARY AND CONCLUSIONS

6.1 Summary

Normally tight gas sands produce at water-gas ratios of 10 – 20 bbls/MMcf or less. However, in the Elm Grove and Caspiana Fields, many of the wells produce with water-gas ratios on the order of 100 bbls/MMcf. The high water production increases operating costs and can reduce ultimate gas recovery. Source of the water being produced in the Elm Grove and Caspiana fields has not been fully explained to date. There has been no gas-water contact identified in the field, even as gas development and production extends progressively down-dip. The problem is further complicated as early water production was recorded at the central and crestal regions in the field. Water production can not easily be attributed to a nearby, down-dip, gas-water contact. Gas production has been recorded some 700 vertical feet down dip from the earliest producing well.

The USGS Bulletin[3] clearly states that a solely water producing well is yet to be encountered in the field. However, another USGS Bulletin[13] reports gas-water contacts in the Travis Peak formation located above the Cotton Valley sands in the Caspiana field. From our investigation, the most logical source of the water is from the major fault to the North, and possibly, from secondary faults and fractures caused by the fault movements and tectonics. The extremely high water gas ratios encountered by wells drilled close to the fault during the past few years is evidence of a possible leaking fault. Alternating high and low resistivity zones on logs tend to show selective water

encroachment in the field as reservoir pressure decreases. Resistivity overlays from wells in the same region, but logged at different times show possible water encroachment in some of the layers.

The sensitivity analysis from the simulated scenarios shows that the water flow zones in the reservoir sands must have conventional relative permeability profiles to flow substantial amount of water. Although the required distance of the drainage point from the water source is dependent on many factors, the sensitivity analysis shows that water production from a water source 4000 vertical feet away from the drainage point is highly unlikely.

In addition to layering in the reservoir, the high degree of heterogeneity in sand quality both vertically and laterally provides for a complex water encroachment pattern in the reservoir that cannot be explained by a simple down-dip aquifer movement. Water encroachment is driven primarily by the relative permeability profile of the rock post hydrocarbon accumulation and thus the water distribution would not be governed solely by simple gravity segregation or capillary pressure effects.

6.2 Conclusions

1. The Cotton Valley sands of the Elm Grove and Caspiana fields cannot be classified as a basin-centered system because high water production rates have been found to commonly occur in the field with hydrocarbons trapped in conventional structural traps.
2. Early wells drilled near the crest of the structure produced initially at high water-gas ratios, which indicates there was a source of formation water nearby.
3. The evaluation of water-gas ratio data from wells versus time does not present a clear pattern. In fact the data appears to be random. Such behavior leads to the conclusion that the water may be associated with faults or natural fractures below the Cotton Valley.
4. The existence of relatively high permeability layers (> 2mD) which can act as high permeability zones help in accelerating the water production but hardly accounts for water production from a far down-dip aquifer located possible at depths greater than 2000 vertical ft away from the drainage point. However, as these high permeability layers are pressure depleted, water could flow up faults or fractures from below causing the water saturation in these zones to increase.

NOMENCLATURE

API = Unit for the Gamma Ray log

a = Saturation constant

BQ_v = Shale conductivity

CV = Cotton Valley formation

F =Formation resistivity factor

GR = Gamma Ray logs.

GR_{clean} = Clean sands Gamma Ray value (API)

GR_{shale} = Pure shale Gamma Ray value (API)

GWC = Gas Water Contact (ft)

K = Absolute permeability (milliDarcy -mD)

K_r = Relative permeability

K_{rg} = Relative permeability to gas

K_{rw} = Relative permeability to water

Layer_HT = Heterolithic layer

Layer_LS = Limestone layer

Layer_SH = Shale layer

Layer_SS = Sandstone layer

m, m^* = Cementation exponent

n, n^* = Saturation exponent

p_c = Capillary pressure (psi)

p_i = initial reservoir pressure, psi

Q_g = Gas flow rate (MMcf)

Rho_{fl} = Fluid density (g/cc)

Rho_{ma} = Matrix density (g/cc)

R_{ild} = Deep resistivity measurements (Ohmm)

R_w = Formation water resistivity (Ohmm)

R_{sfl} = Shallow resistivity measurements (Ohmm)

R_{sh} = Shale resistivity (Ohmm)

R_t = Formation resistivity (Ohmm)

Sw = Water Saturation

Temp. = Temperature (degF)

V_{sh} = Shale volume

WGR = Water-Gas ratio (bbls/MMcf)

Φ = porosity (Fraction)

Φ_d = Porosity from density log (Fraction)

Φ_t = Total porosity from density log (Fraction)

REFERENCES

1. Newsham K.E., Rushing J.A.: "Laboratory and Field Observations of an Apparent Sub Capillary-Equilibrium Water Saturation Distribution in a Tight Gas Sand Reservoir," paper SPE 75710 presented at the 2002 SPE Gas Technology Symposium, Calgary, April 30 –May.
2. Collins, S.E.: "Jurassic Cotton Valley and Smackover Reservoir Trends, East Texas, North Louisiana, and South Arkansas." *AAPG* (1980) **64**, 1004 -1013.
3. Bartbeger, C.E., Dyman, T.S., Condon, M.S.: "Is there a Basin Centered Gas Accumulation in Cotton Valley Group Sandstones, Gulf Coast Basin, USA?" US Geological Survey Bulletin 2184-D (2002). [http://geology.cr.usgs.gov/pub/bulletins/b2184-d/]
4. Kosters, E.C., Bebout, D.G., Seni, S.J., Garret, C.M., Brown, L.F., Hamlin, H.S., Dutton, S.P., Ruppel, S.C., Finley, R.J., Tyler, N.: "Atlas of Major Texas Gas Reservoirs," *BEG*, (1989) 161.
5. Eversull, G.L.: "Depositional Systems and Distribution of Cotton Valley Blanket Sandstones in Northern Louisiana." *Trans. GCAGS* (1985) **35**, 49 – 58.
6. Pate, B.F.: "Significant North Louisiana Cotton Valley Stratigraphic Traps" *Trans. GCAGS*, (1963) **13**, 177-183.
7. Coleman, J.L, Jr., Coleman, C.J.: "Stratigraphic Sedimentologic and Diagenetic Framework for the Jurassic Cotton Valley Terryville Massive Sandstone Complex, Northern Louisiana," *Trans. GCAGS,* (1981) **31**, 71-79.

8. Finley, R.J.: "Geology and Engineering Characteristics of Selected Low-Permeability Gas Sandstones: A National Survey" *BEG, Report of Investigations* (1984) **138**, 220.
9. Presley, M.W., Reed, C.H.: "Jurassic Exploration Trends of East Texas" *Trans GCAGS,* (1984) **34**, 443.
10. Dutton, S.P., Clift, S.J., Hamilton, D.S., Hamlin, H.S., Hentz, T.F., Howard, W.E., Akhter, M.S., Laubach, S.E.: "Major Low Permeability Sandstone Gas Reservoirs in the Continental United States," *BEG Report of Investigation* (1993) **211**, 221.
11. Williams, R.A., Robinson, M.C., Fernandez, E.G., Mitchum, R.M.: "Cotton Valley/Bossier of East Texas: Sequence Stratigraphy Recreates the Depositional History" *Trans. GCAGS*, (2001) **51**, 379-388.
12. Ganer, B.L.: "Case History of Cotton Valley Sand Log Interpretation for a North Louisiana Field," paper SPE 12182 presented at the 1983 SPE Annual Technical Conference and Exhibition, San Francisco, California, Oct. 5-8.
13. Bartbeger, C.E., Dyman, T.S., Condon, M.S.: "Potential for Basin Centered Gas Accumulation in Travis Peak (Hosston) Formation, Gulf Coast Basin, USA." US Geological Survey Bulletin 2184-E (2003). [http://geology.cr.usgs.gov/pub/bulletins/b2184-e/]
14. Dyman, T.S., Bartberger, C.E., Nuccio, V.F., Schenk, C.J.: "Re-evaluation of Cotton Valley Gas Plays in Gulf Coast Region for Petroleum Resource Assessment." 2001 Abstract, AAPG Annual Meeting, Denver, June 3 – 6.

15. Nangle, P., Fertl, W.H., and Frost, E., Jr.: "What to Expect when Logging the Cotton Valley Trend" *World Oil* (1982) **195**, 175-195.

16. Wescott, W.A.: "Diagenesis of Cotton Valley Sandstone (Upper Jurassic) East Texas: Implication for Tight Gas Formation Pay Recognition," *AAPG* (1983) **67**, 1002-1013.

17. Wescott, W.A.: "Diagenesis of Cotton Valley Sandstone (Upper Jurassic) East Texas: Implication for Tight Gas Formation Pay Recognition: Reply," *AAPG* (1985) **69**, 816-818.

18. Tindell, W.A., Neal, J.K., Hunter, J.C.: "Evolution of Fracturing in the Cotton Valley Sands in Oak Hill Field." Paper SPE 9067 presented at the 1980 SPE Cotton Valley Symposium, Tyler, Texas, May 21.

19. Naik, G.C.: "Tight Gas Reservoirs – An Unconventional Natural Energy Source for the Future," (2005). [www.apgindia.org/tight_gas.pdf]

20. Holditch, S. A.: "Tight Gas Sands" paper SPE 103356, Distinguished Author Series, (2006) 86 – 93, available from SPE, Richardson, TX.

21. Coleman, J.L., Jr.: "Diagenesis of Cotton Valley Sandstone (Upper Jurassic), East Texas: Implications for Tight Gas Formation Pay Recognition: Discussion," *AAPG* (1985) **69**, 813–815.

22. Trojan, M.: "Effects of Diagenesis on Reservoir Properties and Log Response, Upper Jurassic Taylor Sandstone, Cotton Valley Group, Lincoln Parish, Louisiana." *Trans, GCAGS* (1985) **35**, 515 -524.

23. Turner, J.R.: "Recognition of Low Resistivity, High Permeability Reservoir Beds in the Travis Peak and Cotton Valley of East Texas" *Trans. Gulf Coast Association of Geological Societies* (1997) **47**, 585-593.

24. Masters, J.A.: "Deep Basin Gas Trap, Western Canada" *AAPG* (1979) **63** 152-181.

25. Magoon and L.B., Dow, W.G.: "The Petroleum Systems from Source to Trap" *AAPG Memoir* (1994) **60**, 655

26. Law B.E.: "Basin Centered Gas Systems," *AAPG* (2002) **86**, 1891 – 1919.

27. Wescott, W.A., Hood, W.C.: "Hydrocarbon Generation and Migration Routes in the East Texas Basin" *Trans GCAGS*, (1991) **41**, 675.

28. Shanley, K.W., Cluff, R.M., Ronbinson, W.J.: "Factors Controlling Prolific Gas Production from Low Permeability Sandstone Reservoirs: Implications for Resource Assessment, Prospect Development, and Risk Analysis" *AAPG* (2004) **88**, 1083 – 1121.

29. Tye, R.S., Laubach, S.E., Dutton, S.P., Herrington, K.L.: "The Role of Geology in Characterizing Low-Permeability Sandstones, North Appleby Field, East Texas Basin," paper SPE 18964 presented at the 1989 SPE Joint Rocky Mountains Regional/Low Permeability Reservoirs Symposiums and Exhibition, Denver, March 6-8.

30. Hyman, L.A., Malek, D.J., Admire, C.A., Walls, J.D.: "The effects of Microfractures on Directional Permeability in Tight Gas Sands." paper SPE

21878 presented at the 1991 SPE Rocky Mountain Regional/Low Permeability Reservoirs Symposium and Exhibition, Denver, Colorado, April. 15-17.

31. Spencer, C.W.: "Review of Characteristics of Low-Permeability Gas Reservoirs in Western United States," *AAPG* (1989) **73**, 613-629.
32. Ammer, J.R., Covatch, G.L., Sames, G.P., Mroz, T.H., Gwilliam, W.J.: "Technology for Increased Gas Production from Low Permeability Gas Reservoirs: An Overview of US DOE's Gas Program-Success and Future Plans" Paper SPE 60310 presented at the 2000 SPE Rocky Mountain Regional/Low-Permeability Reservoirs Symposium and Exhibition, Denver, March 12-15.
33. Newsham K.E., Rushing J.A., Lasswell, P.M., Cox, J.C., Blasingame, T.A.: "A Comparative Study of Laboratory Techniques for Measuring Capillary Pressures in Tight Gas Sands," paper SPE 89866 presented at the 2004 SPE Annual Technical Conference and Exhibition, Houston, Texas, April 30 -May 2.
34. Cluff, S.G., Cluff, R.M.: "Jonah Field-Case Study of a Tight Gas Fluvial Reservoir: AAPG Studies in Geology 52 and Rocky Mountain Association of Geologists 2004 Guidebook: Chapter 12: Petrophysics of Lance Stone Reservoirs in Jonah Field, Sublette County, Wyoming," *AAPG Special Volumes* (2004).
35. Walls J.D.: "Tight Gas Sands-Permeability, Pore Structure, and Clay," *JPT* (1982) 2708-2714.
36. Law, B.E., Spencer, C.W.: "Jonah Field: Case Study of a Tight-Gas Fluvial Reservoir: AAPG Studies in Geology 52 and Rocky Mountain Association of

Geologists 2004 Guidebook: Chapter 9: Basin Centered Gas Systems and the Jonah Field," *AAPG Special Volumes* (2004).

37. Robinson, J.W., Shanley, K.W.: "Jonah Field, Case Study of a Tight Gas Fluvial Reservoir: AAPG Studies in Geology 52 and Rocky Mountain Association of Geologists 2004 Guidebook: Chapter 1: Introduction," *AAPG Special Volumes* (2004).
38. Russel, B.J., Sartin, A.A., and Ledger, E.B.: "Depositional and Diagenetic History of the Bodcaw Sand, Cotton Valley Group (Upper Jurassic), Longwood Field, Caddo Parish. Louisiana" *Trans*. *GCAGS* (1984) **34**, 217-228.
39. Van Horn, M.D., Shannon, L.T.: "Hay Reservoir Field: A submarine Fan Gas Reservoir within the Lewis Shale, Sweetwater County, Wyoming," *WGA Annual Field Conference Guide Book* (1989) 155 – 180.
40. Dunn, T.L., Bernabe, A., Humphreys, J., Surdam, R.C.: "Cements and In-situ Widths of Natural Fractures, Almond Formation, Green River Basin, Wyoming." *WGA Field Conference Guide Book,* (1995) 255-269.
41. Yin, P., Liu, J., Surdam, R.C.: "Petrographic and Petrophysical Properties of the Almond Sandstone in the Washakie Basin" *WGA Annual Field Conference Guide Book*, (1992) 191 – 205.
42. Black, C.E., Robert, R.R.: "Fan-Delta Reservoirs in the Lower Cotton Valley Group (Jurassic) Kildare Field, Northeast Texas," *Trans. GCAGS* (1987) **37**, 35 – 42.

43. McCain, W.D., Voneiff, G.W., Hunt, Semmelbeck, M.E.: "A Tight Gas Field Study: Carthage (Cotton Valley) Field," paper SPE 26141 presented at the 1983 SPE Gas Technology Symposium, Calgary, June 28-30.

44. Sonnenberg, S.A.: "Interpretation of Cotton Valley Depositional Environment from Core Study, Frierson Field, Louisiana." *Trans. GCAGS* (1967) **26**, 320 – 325.

45. Rosepiler, M.J.: "Calculation and Significance of Water Saturations in Low Porosity Shaly Gas Sands," paper SPE 10910 presented at the 1982 SPE Cotton Valley Symposium, Tyler, Texas, May 20.

46. Kukal, G.C., Simmons, K.E.: "Log Analysis Techniques for Quantifying the Permeability of Submillidarcy Sandstone Reservoirs," paper SPE 13880 presented at the 1985 SPE/DOE/GRI Low Permeability Gas Reservoir Symposium, Denver, Colorado, May 19-22.

47. Davies, D.K., Vessel, R.K., Auman, J.B.: "Improved Prediction of Reservoir Behavior Through Integration of Quantitative Geological and Petrophysical Data," *SPEREE* (1999) **2**, 149-159.

48. Dutton S.P., Diggs, T.N.: "Evolution of Porosity and Permeability in the Lower Cretaceous Travis Peak Formation, East Texas," *AAPG* (1992) **76**, 252-269.

49. Everett, R.V., Johnston, D.J., Quirein, M.C.: "A Comparison of Log Interpretation to Core Results Using a Full Element Model and a Reduced Element Model in the East Texas Cotton Valley Sandstone of GRI Well No. 3,"

paper SPE 24727 presented at the 1992 SPE Annual Technical Conference and Exhibition, Washington DC, October 4-7.

50. Forgotson, J.M.: "Porosity Pod": Concept for Successful Stratigraphic Exploration of Fine Grained Sandstones," *AAPG* (1975) **59**, 1113 – 1125.
51. Hunt, R.E., Raymond D.H., Hasket C.E., Pirie, G.R.: "Application of New Well Logs and Geology to Fracturing and Producibility in Tight Gas Sands, Cotton Valley Group," paper SPE/DOE 9832 presented at the 1981 SPE/DOE/GRI Low Permeability Symposium, Denver, Colorado, May 27-29.
52. Kukal, G.C.: "A Systematic Approach for the Effective Log Analysis of Tight Gas Sands," paper SPE 121851 presented at the 1984 SPE/DOE/GRI Unconventional Gas Recovery Symposium, Pittsburgh, PA. May 13-15.
53. Yao, C.Y., Holditch, S.A.: "Estimating Permeability Profiles Using Core and Log Data," paper SPE 26921 presented at the 1993 Eastern Regional Conference and Exhibition, Pittsburgh, PA, Nov 2-4.
54. Cox, S.A., Sutton, R.P., Stoltz, R.P., Knobloch, T.: "Determination of Effective Drainage Area for Tight Gas Wells," paper SPE 98035 presented at the 2005 SPE Eastern Region Meeting, Morgantown, West Virginia, Sept. 14-16.

APPENDIX A

DATA AVAILABILITY

Table A1: Log Availability in the Field

No.	Well Name	API Number	Log Dates	Completion Date	Start Production	Top (Ft)	Bot (Ft)	GR (GAPI)	SP (mV)	CALI (in)	ILD (OHMM)	ILM (OHMM)	SFLU	RHOB (gr/cm3)	NPHI	DT	PE B/E
1	SMITH HEIRS #1	17017336250000	30-Dec-04			1639.5	9825	Yes	Yes	Yes	Yes	Yes	Yes	Yes	Yes	No	No
2	COLBERT #1	17017336440000	26-Jan-05			1837	9646.5	Yes	Yes	Yes	Yes	Yes	Yes	Yes	Yes	No	No
3	CASPIANA INT #1 ALT	17017336540000	21-Feb-05			1851	9604	Yes	Yes	Yes	Yes	Yes	Yes	Yes	Yes	No	No
4	LOTT 14	17015232010000	24-Sep-01			8000	9803.5	Yes	Yes	No	Yes	Yes	Yes	No	Yes	No	Yes
5	LCV RA SU72;CAPLIS 22	17015232740000	8-May-03	1-Jun-03	1-Jun-03	7999	10099	Yes	Yes	No	Yes	Yes	Yes	No	Yes	Yes	Yes
6	LCV RA SU71;CAPLIS 15	17015232780000	13-Apr-03	1-May-03	1-May-03	7999	10107	Yes	Yes	Yes	Yes	Yes	Yes	No	Yes	No	Yes
7	CV RA SU107;BROWN 4	17015233220000	7-Apr-03	1-May-03	1-May-03	7052	9588	Yes	Yes	Yes	Yes	Yes	Yes	Yes	Yes	No	Yes
8	NINOCK LAND CO 35	17015234310000	6-Feb-04			7998.5	9948	Yes	Yes	No	Yes	Yes	Yes	No	Yes	No	No
9	CV RA SU 67;CAPLIS	17017216930000	2-Jul-75	1-Aug-75	1-Nov-75	7999.5	9355.5	Yes	Yes	Yes	Yes	Yes	Yes	Yes	Yes	No	No
10	HOSS RA SU62;HUTCHINSON	17017217050000	29-Jul-75	19-Sep-75	1-Jan-97	7999	9299	Yes	Yes	Yes	Yes	Yes	Yes	No	Yes	No	No
11	FRIERSON TRUST	17017217970000	20-Oct-75	1-Mar-76		7950	9370	Yes	Yes	Yes	Yes	Yes	Yes	Yes	Yes	No	No
12	CV RA SU 72;CUPPLES	17017221550000	2-Mar-77	1-Apr-77	1-Jan-78	6300	9526	Yes	Yes	Yes	Yes	Yes	Yes	Yes	Yes	No	No
13	CV RA SUC;DENNY-WEBB	17017322540000	28-Nov-94	1-Dec-94	1-Dec-94	7999	9342	Yes	Yes	Yes	Yes	Yes	Yes	Yes	Yes	No	No
14	CV RA SU66;HUTCHINSON 4	17017322950000	19-Jun-95	1-Sep-95	1-Sep-95	8000	9298	Yes	Yes	Yes	Yes	Yes	Yes	No	Yes	No	No
15	CV RA SUC;DENNEY WEBB	17017323700000	29-May-96	1-Jun-96	1-Jul-96	7999	9443	Yes	Yes	Yes	Yes	Yes	Yes	Yes	Yes	No	Yes
16	CV RA SU16;SAM W SMITH 28	17017324060000	2-Aug-96	1-Aug-96	1-Aug-96	8700	9660	Yes	Yes	No	Yes	Yes	Yes	Yes	Yes	No	No
17	CV RA SU55;LEVEE BOARD 22	17017324230000	9-Aug-96	1-Sep-96	1-Oct-96	7000	9688	Yes	Yes	No	Yes	Yes	Yes	Yes	Yes	No	No
18	CV RA SU54;ELLERBE HEIRS 21	17017325020000	2-Mar-97	1-Mar-97	1-Jul-97	7999.5	9549	yes	Yes	Yes	Yes	Yes	Yes	Yes	Yes	No	No
19	CV RA SU54;ELLERBE HEIRS 21	17017325070000	4-Apr-97	1-May-97	1-Jul-97	7999	9449	Yes	Yes	Yes	Yes	Yes	Yes	Yes	Yes	No	No
20	CV RA SUD;D A RICHLEN LAND 18	17017325190000	9-Jul-97	1-Aug-97	1-Oct-97	7999	9320	Yes	Yes	Yes	Yes	Yes	Yes	Yes	Yes	No	Yes

Table A1 (continued): Log Availability in the Field

No.	Well Name	API Number	Log Dates	Completion Date	Start Production	Top (Ft)	Bot (Ft)	GR (GAPI)	SP (mV)	CALI (in)	ILD (OHMM)	ILM (OHMM)	SFLU (OHMM)	RHOB (gr/cm3)	NPHI	DT	PE B/E
21	CV RA SU51;HUTCHINSON	17017327540000	30-Jun-98	1-Sep-98	1-Sep-98	7999	9176	Yes	Yes	Yes	Yes	Yes	Yes	No	Yes	No	Yes
22	CV RA SU69;HUTCHINSON 9	17017328140000	17-Nov-98	1-Feb-99	1-Feb-99	8000	10000	Yes	Yes	No	Yes	Yes	Yes	No	Yes	No	No
23	CV RA SU70;HUTCHINSON 10	17017329300000	10-Sep-00	1-Sep-99	1-Oct-99	7999	9314	Yes	Yes	No	Yes	Yes	Yes	No	Yes	No	No
24	CV RA SU51;HUTCHINSON	17017330580000	14-Sep-00	1-Oct-00	1-Mar-02	7701	9234	Yes	Yes	No	Yes	Yes	Yes	No	Yes	No	Yes
25	CV RA SU42;HUTCHINSON	17017331290000	14-Nov-00	1-Dec-00	1-Mar-02	7999	9171	Yes	Yes	Yes	Yes	Yes	Yes	No	Yes	No	Yes
26	ALLEN, CV RA SUI	17017333160000	20-Aug-01			8000	10192	Yes	Yes	No	Yes	Yes	Yes	No	Yes	No	No
27	CV RA SU63;SAM W SMITH ETAL 32	17017333330000	4-Sep-01	1-Oct-01	1-Oct-01	8000	9893	Yes	Yes	No	Yes	Yes	Yes	No	Yes	No	Yes
28	CV RA SU42;FRIERSON 30	17017334340000	9-Oct-02	1-Nov-02	1-Mar-03	7950	9216	Yes	Yes	No	Yes	Yes	Yes	No	Yes	Yes	Yes
29	DUTTON FAMILY LLC #1	17017335630000	20-Mar-05	17-May-74	13-Oct-04	1175	10472	Yes	Yes	Yes	Yes	Yes	Yes	Yes	Yes	No	No
30	CV RA SUM;EUGENE TURNER JR ET	17031204310000	7-May-74	1-Nov-74	1-Sep-75	8000	9558	Yes	Yes	Yes	Yes	Yes	Yes	No	Yes	Yes	No
31	CV RA SUL; G A FRIERSON	17031204650000	24-Nov-74	22-May-75	1-Oct-75	7999	9399	Yes	Yes	Yes	Yes	Yes	Yes	No	Yes	No	No
32	HOSS RA SUP; J R CALDWELL	17031204920000	14-Jul-75	1-Sep-75	1-Nov-75	7999	9718	Yes	Yes	Yes	Yes	Yes	Yes	Yes	Yes	Yes	No
33	CV RA SU68;GUY	17031215180000	14-Jun-97	1-Dec-82	1-Sep-82	8000	9930	Yes	Yes	Yes	Yes	Yes	Yes	Yes	Yes	Yes	No
34	HOSS RA SULL;GRIFFIN 33	17031230410000	30-Apr-96	1-May-96	1-Jan-00	7999	9999	yes	Yes	Yes	Yes	Yes	Yes	Yes	Yes	No	Yes
35	CV RA SUU; HUNT PLYWOOD C	17031230470000	8-Jun-96	1-Jun-96	1-Jul-96	7999	9840	Yes	Yes	Yes	Yes	Yes	Yes	No	Yes	No	No
36	CV RA SUR;WILKINSON 24	17031230630000	7-Oct-96	1-Nov-96	1-Oct-96	7949.5	9460	Yes	Yes	Yes	Yes	Yes	Yes	No	Yes	No	No
37	CV RA SUQ;AARON WASHINGTON 23	17031231140000	14-Jun-97	1-Jul-97	1-Oct-97	7965	9471	Yes	Yes	Yes	Yes	Yes	Yes	Yes	Yes	No	No
38	CV RA SUM;RAYMOND GATLIN 13	17031231230000	11-Jul-97	1-Aug-97	1-Oct-97	7999	9319	Yes	Yes	Yes	Yes	Yes	Yes	Yes	Yes	No	Yes
39	CV RA SUD;D A RICHLEN LAND 18	17031231400000	4-Sep-97	1-Oct-97	1-Oct-97	7900	9289	Yes	Yes	No	Yes	Yes	Yes	Yes	Yes	No	No

Table A2: Water Analysis Data

WATER ANALYSIS			
	Dutton Family-1	Colbert-1	Caspiana Int-1
Date	5/10/2005	5/10/2005	5/10/2005
Specific Gravity	1.093	1.11	1.09
Density (LB/GAL)	9.105	9.25	9.08
pH (SU)	5.53	5.48	5.75
Chlorides (Mg/l)	84000	92500	90000
Chlorides (PPM)	76853	83258	82569
Bacteria (Microbes/ml)	1.00E+04	1.00E+04	1.00E+04
Calcium (Mg/l)	8801	10000	8600
T.D.S (Mg/l)	134850	159500	130500
Resistivity (Ohms/Metrer2/Meter)	0.077	0.079	0.082
Temperature (°F)	68	68	68

APPENDIX B

COMPARATIVE LABORATORY STUDY OF CAPILLARY PRESSURES

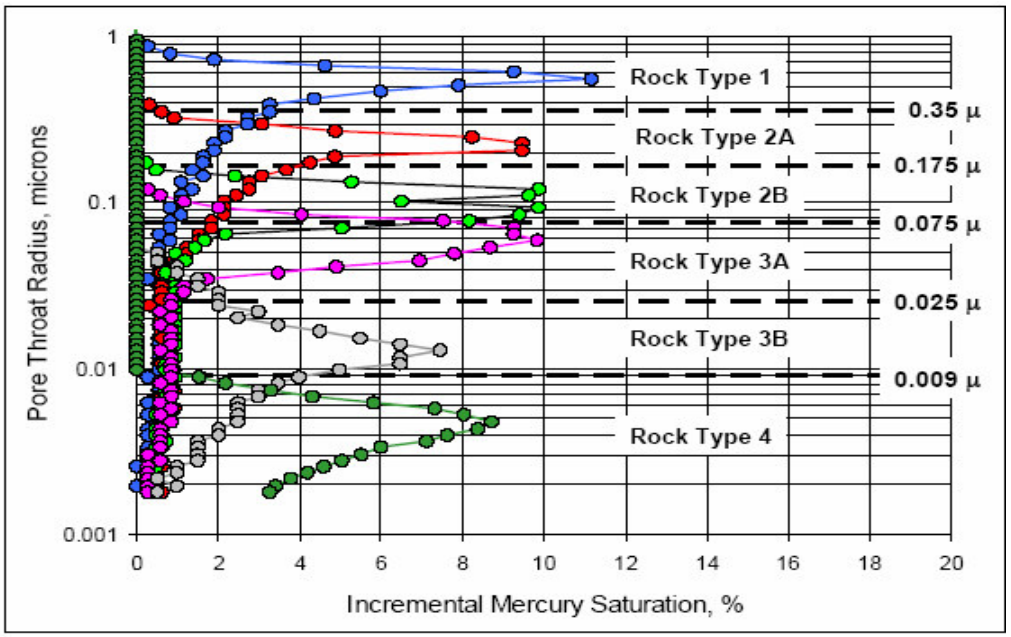

Fig. B1: Increment Mercury Intrusion Plot to Identify Hydraulic Types for the Core Study.

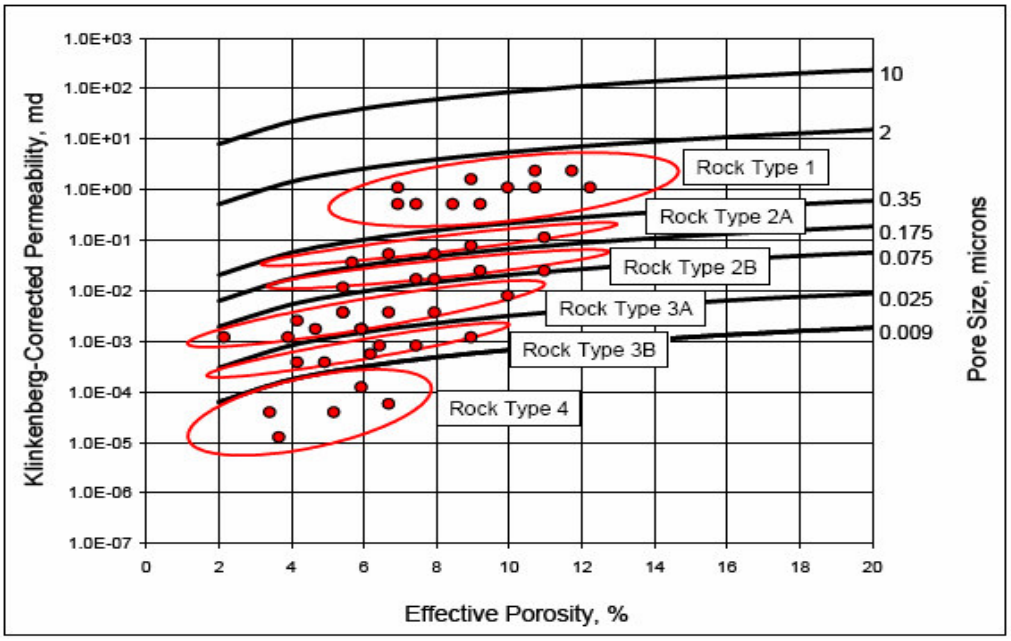

Fig. B2: Pittman Plot Showing Range of Porosity and Permeability for Hydraulic Rock Types Used in the Study.

Table B1: Summary of Intrinsic Rock Properties for East Texas Field-1, Well 1

Sample No.	Effective Porosity (%)	Klinkenberg-Corrected Permeability (md)	Capillary Pressure Measurement Technique
2-20A	11.9	0.0870	HSC, VD, MICP
2-22A	11.2	0.0770	HSC, VD, MICP
2-29A	8.4	0.0300	HSC, VD, MICP
2-32B	7.5	0.0130	HSC, VD, MICP
2-39A	1.9	0.0055	HSC, VD, MICP
2-41A	8.7	0.0480	HSC, VD, MICP

Table B2: Summary of Intrinsic Rock Properties for East Texas Field-2, Well 1

Sample No.	Effective Porosity (%)	Klinkenberg-Corrected Permeability (md)	Capillary Pressure Measurement Technique
36	4.3	0.0027	HPPP, VD
49	10.3	0.0210	HPPP, VD, MICP
70	12.0	0.0073	HPPP, VD, MICP
211	11.8	0.0117	HPPP, VD
212	12.3	0.0221	HPPP, VD
218	6.7	0.0268	HPPP, VD

Table B3: Summary of Intrinsic Rock Properties for North Louisiana Field-1, Well 1

Sample No.	Effective Porosity (%)	Klinkenberg-Corrected Permeability (md)	Capillary Pressure Measurement Technique
1-26	5.3	0.0040	HPPP, HSC, VD, MICP
2-28	4.9	0.0006	HPPP, HSC, VD, MICP
2-32	8.4	0.0850	HPPP, HSC, VD, MICP
2-50	7.6	0.0009	HPPP, VD
3-17	13.8	0.1430	HSC, , VD
3-42	13.0	0.0410	HPPP, HSC, VD, MICP
4-18	8.7	0.0066	HSC, VD
4-44	9.8	0.027	HPPP, VD, MICP

Table B4: Summary of Intrinsic Rock Properties for North Louisiana Field-2, Well 1

Sample No.	Effective Porosity (%)	Klinkenberg-Corrected Permeability (md)	Capillary Pressure Measurement Technique
3-22	6.2	0.0120	HPPP, VD, MICP
3-40	11.2	0.0550	HPPP, VD
5-16	2.4	0.0015	VD, MICP
6-21	6.7	0.0007	HPPP, VD
8-21	10.6	0.0140	HPPP, VD, MICP

HPPP: high-pressure porous plate
HSC high-speed centrifuge
MICP: high-pressure mercury injection
VD: vapor desorption

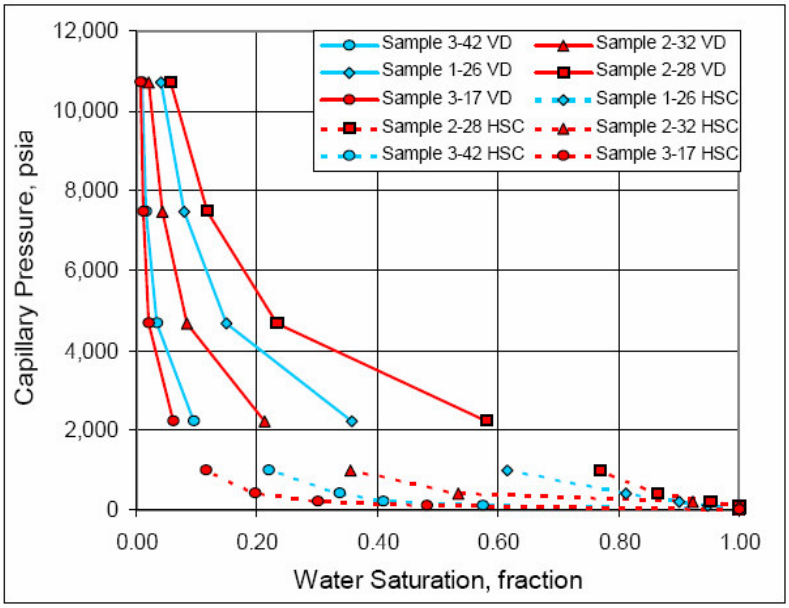

Fig. B3: Cartesian Plot Comparing Pressures from Vapor Desorption (VD) and High Speed Centrifuge (HSC) Techniques, North Louisiana Field, Well 1.

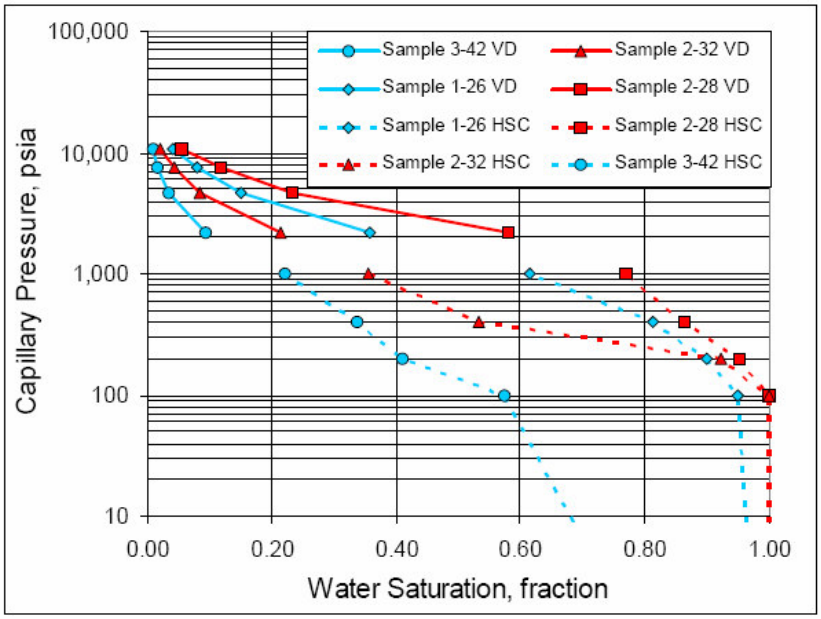

Fig. B4: Semi-log Plot Comparing Pressures from Vapor Desorption (VD) and High Speed Centrifuge (HSC) Techniques, North Louisiana Field, Well 1.

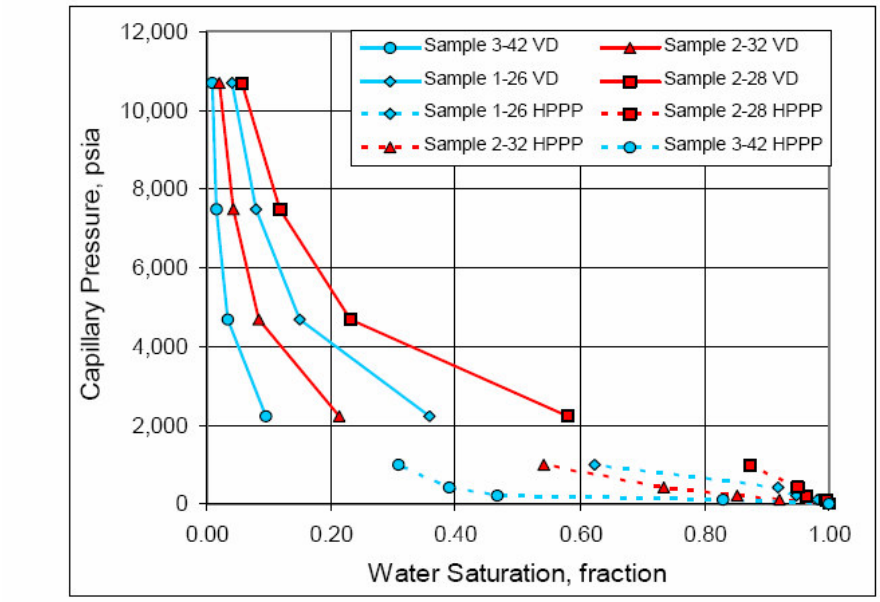

Fig. B5: Cartesian Plot Comparing Pressures from Vapor Desorption (VD) and High Pressure Porous Plate (HPP) Techniques, North Louisiana Field, Well 1.

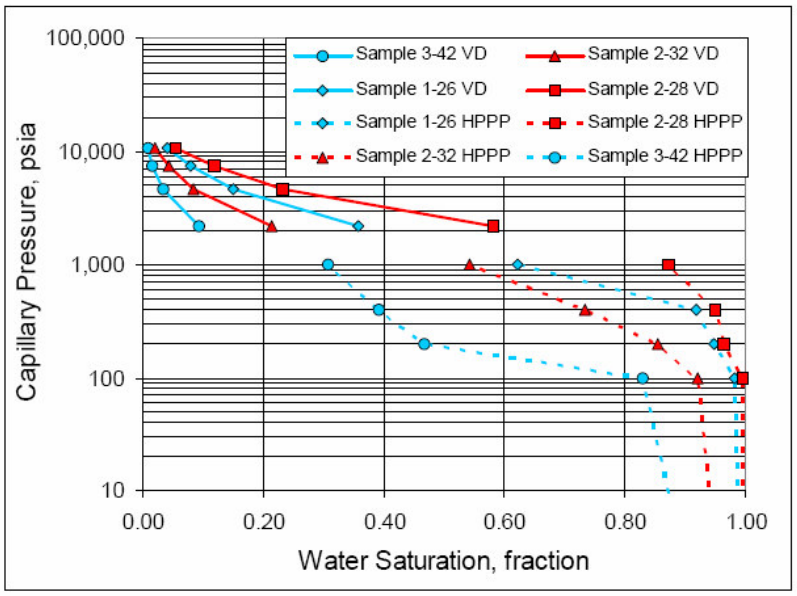

Fig. B6: Semi-log Plot Comparing Pressures from Vapor Desorption (VD) and High Pressure Porous Plate (HPP) Techniques, North Louisiana Field, Well 1.

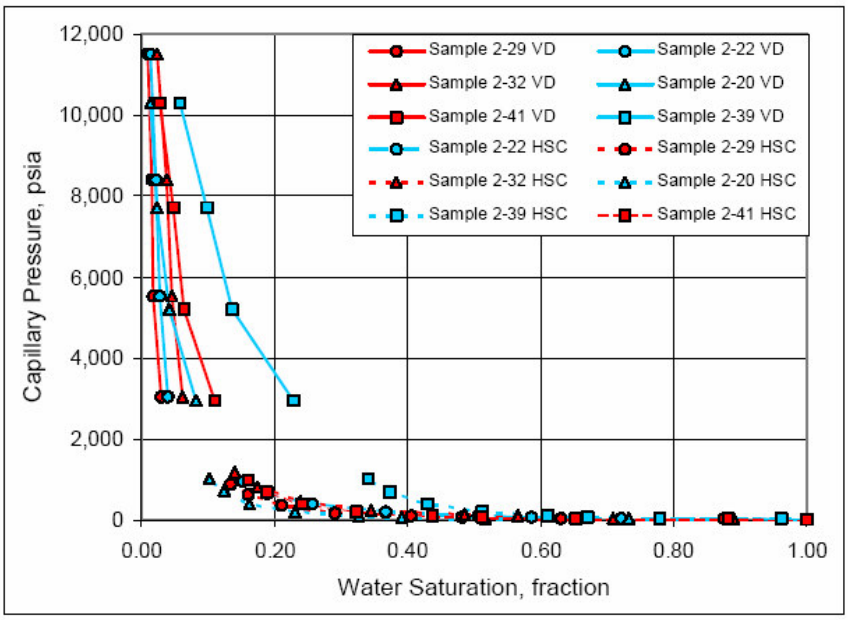

Fig. B7: Cartesian Plot Comparing Pressures from Vapor Desorption (VD) and High Speed Centrifuge (HSC) Techniques East Texas Field 1, Well 1.

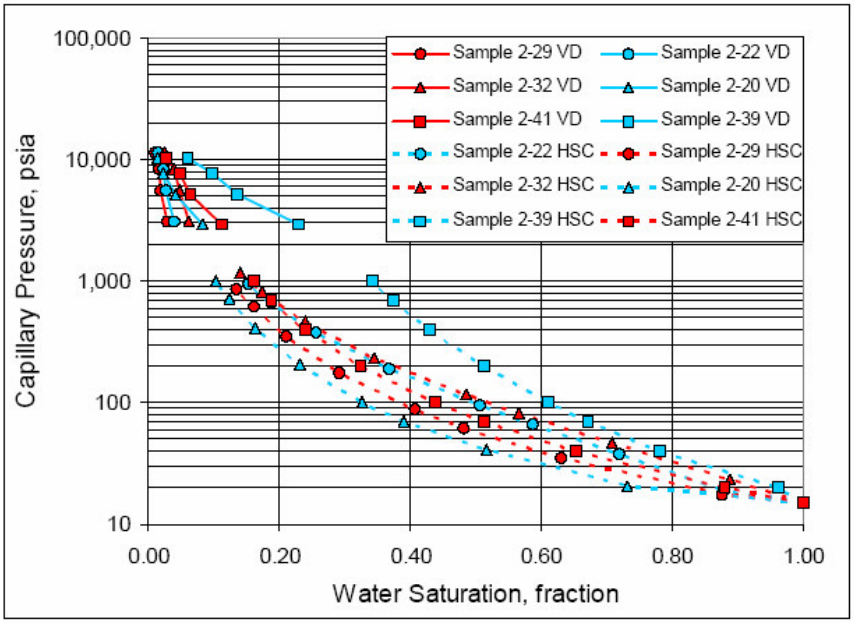

Fig. B8: Semi-log Plot Comparing Pressures from Vapor Desorption (VD) and High Speed Centrifuge (HSC) Techniques East Texas Field 1, Well 1.

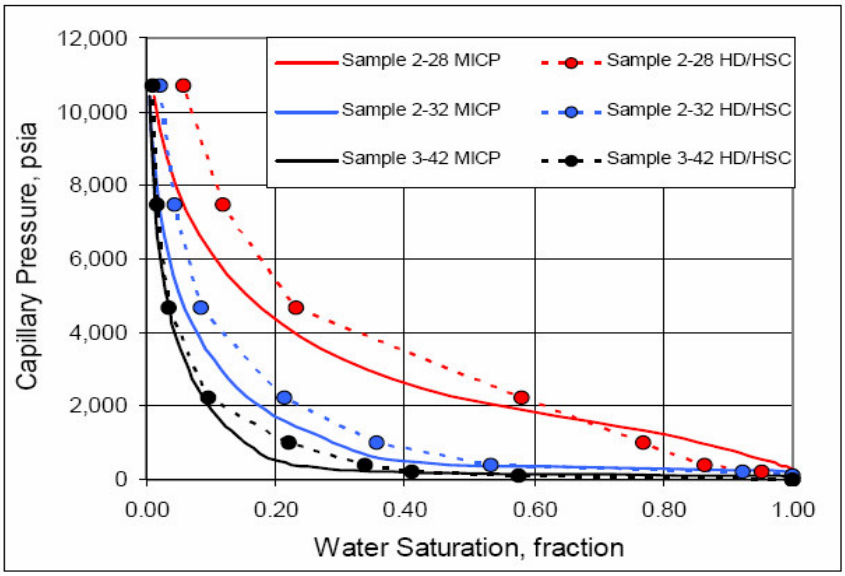

Fig. B9: Cartesian Plot Comparing Pressures Mercury Injection Capillary Pressure (MICP) to Composite Vapor Desorption/High Speed Centrifuge Data (HD/HSC), North Louisiana Field, Well 1.

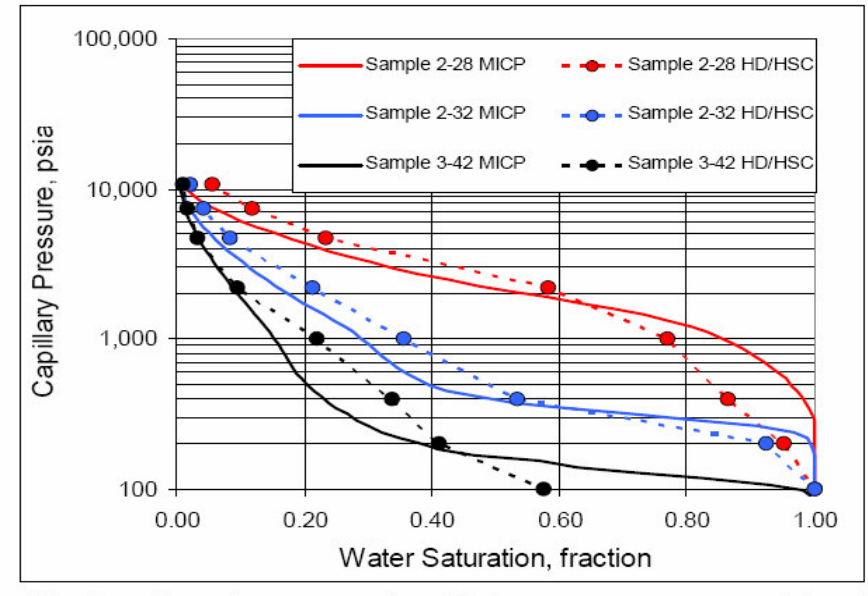

Fig. B10: Semi-log Plot Comparing Pressures Mercury Injection Capillary Pressure(MICP) to Composite Vapor Desorption/High Speed Centrifuge Data (HD/HSC), North Louisiana Field, Well 1.

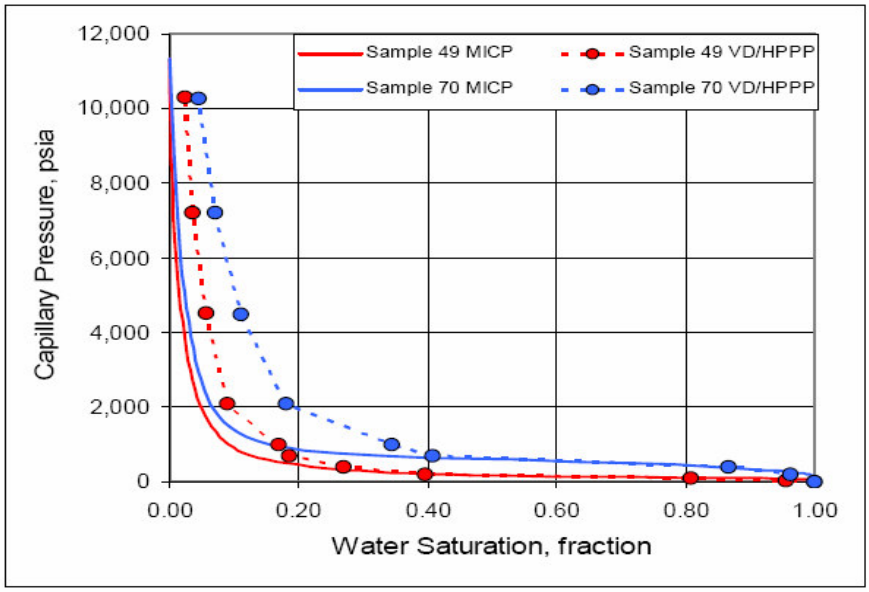

Fig. B11: Cartesian Plot Comparing Pressures from Mercury Injection Capillary Pressure (MICP) to Composite Vapor Desorption/High Pressure Porous Plate Data (HD/HPP), East Texas Field 2, Well 1.

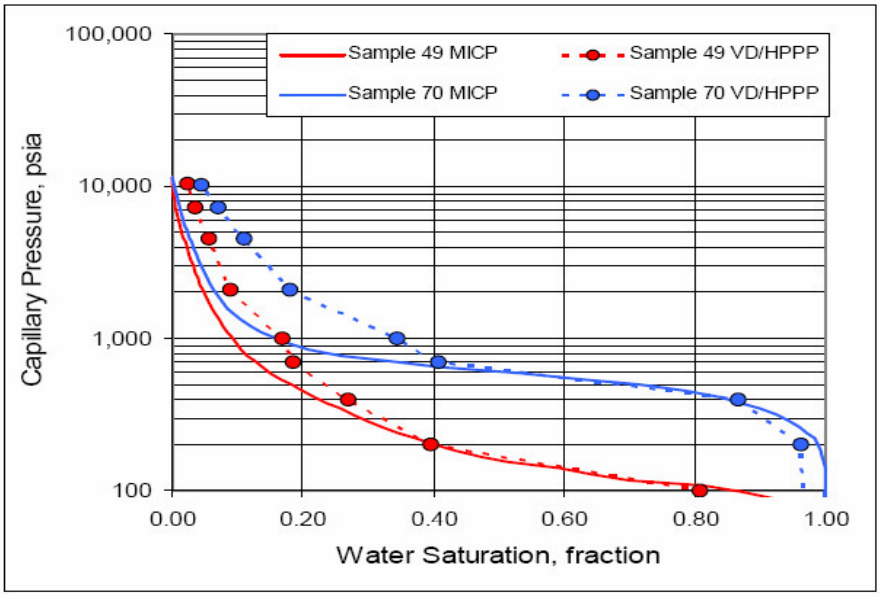

Fig. B12: Semi-log Plot Comparing Pressures from Mercury Injection Capillary Pressure (MICP) to Composite Vapor Desorption/High Pressure Porous Plate Data (HD/HPP), East Texas Field 2, Well 1.

APPENDIX C

CORE DATA ANALYSIS

Table C1: Formation Resistivity Factor Measurements (Colbert-1)

Company:	Matador Resources Co.	Saturant, ppm:	165,000
Well:	Colbert #1(Cotton Valley)	Confining Stress, psi:	3,600
Field:	Caspiana	Brine Resistivity, ohm-m @25°C:	0.0486
Location:	Caddo Parish, La.	Porosity Exponent (m) [Composite]:	2.02
File:	HOU-050182	Intercept (a):	1.00

Sample Number	Depth, feet	Grain Density gm/cc	Klinkenberg Permeability md	Porosity, fraction	Formation Factor, (Apparent)		
					Fa	Ro, ohm-m	m
2	8,776.00	2.66	0.003	0.059	305.41	14.83	2.02
3	8,805.00	2.65	0.038	0.053	310.71	15.09	1.95
6	8,876.00	2.66	0.061	0.070	208.17	10.11	2.01
8	8,892.00	2.65	0.005	0.069	254.97	12.38	2.07
14	9,130.00	2.67	0.005	0.064	234.18	11.38	1.98
20	9,312.00	2.66	0.002	0.094	134.86	6.55	2.07
21	9,320.00	2.67	0.005	0.106	101.30	4.92	2.06

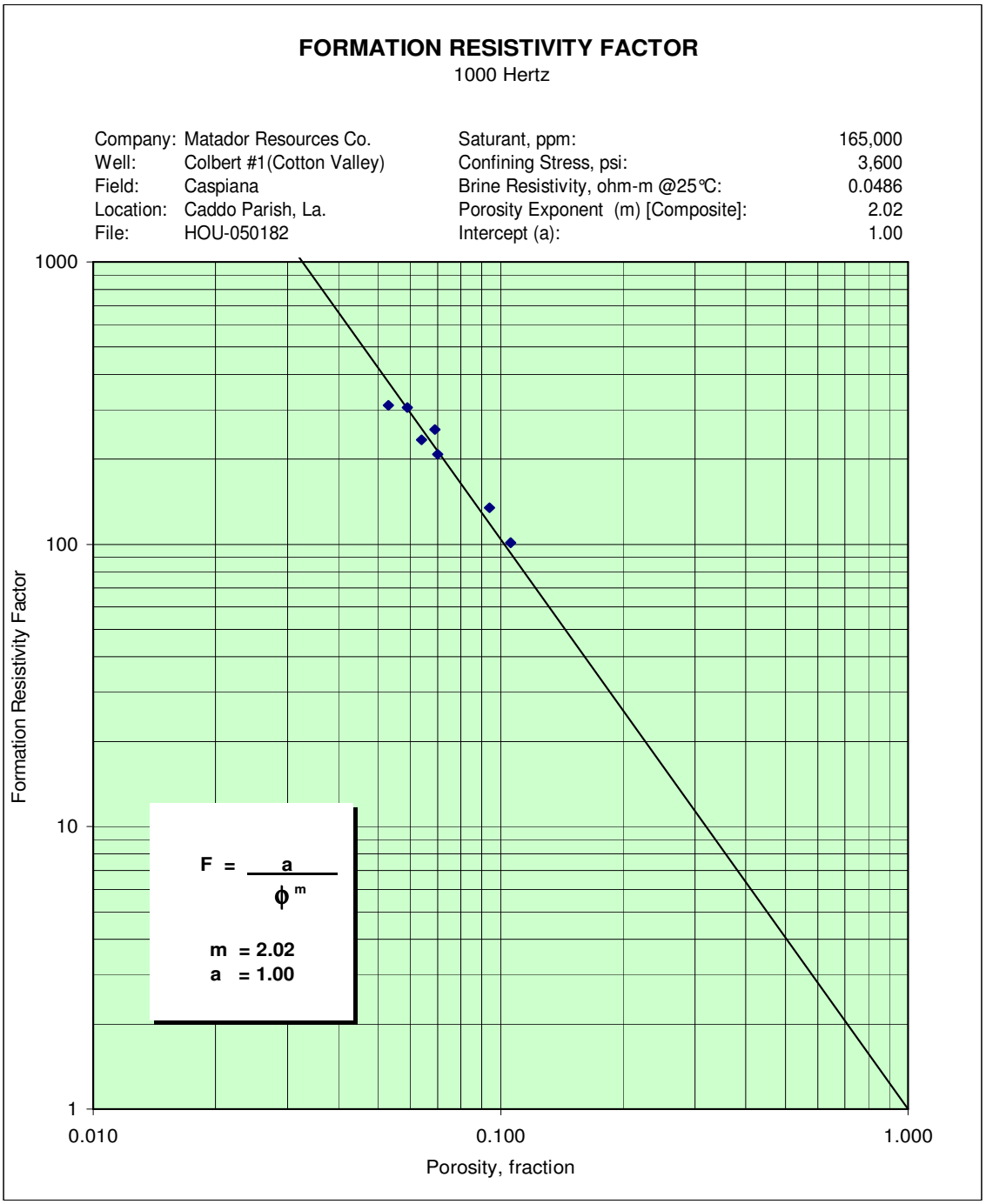

Fig. C1: Formation Resistivity Factor vs Porosity (Colbert-1).

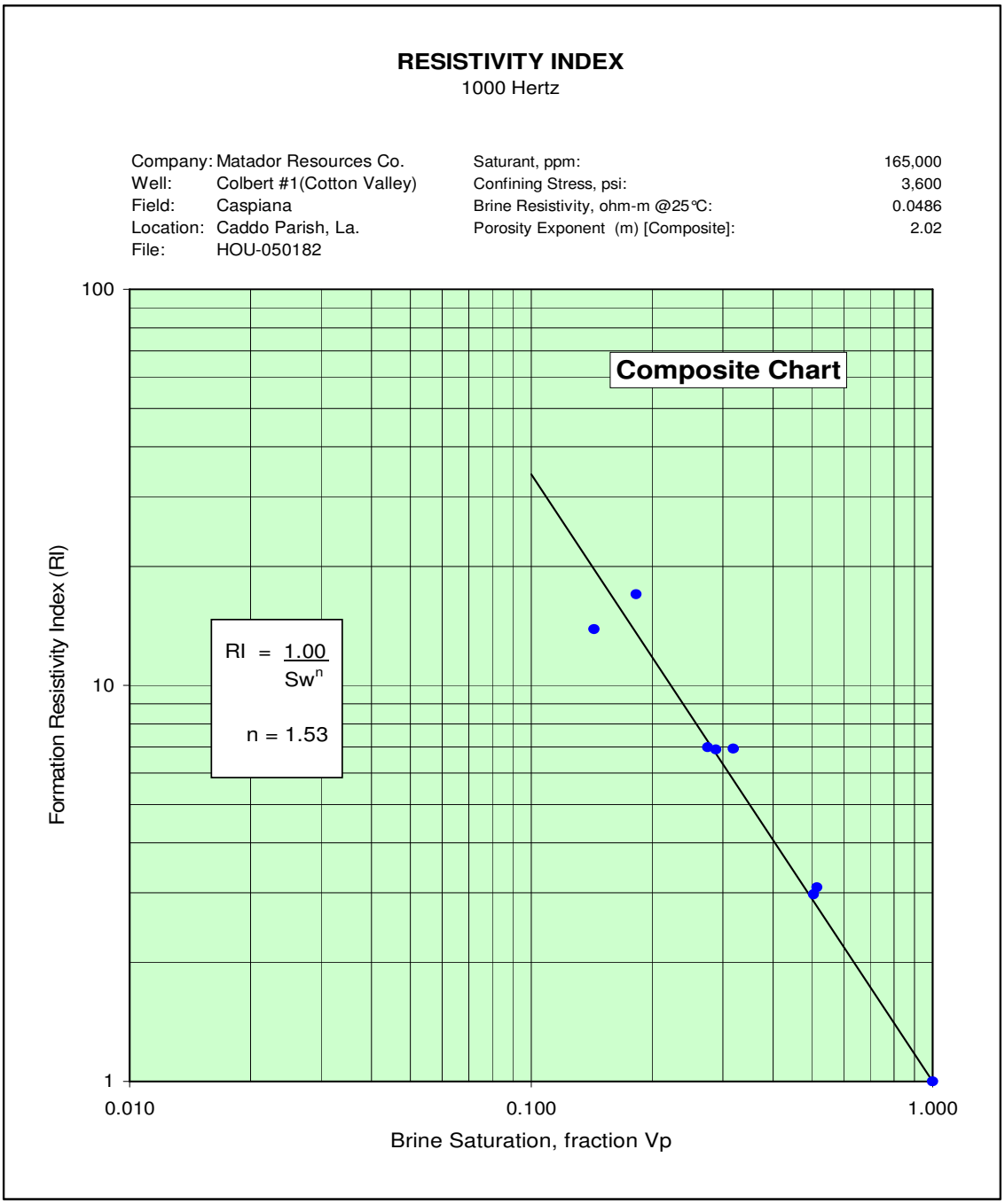

Fig. C2: Resistivity Index vs Water Saturation (Colbert-1).

Table C2: Absolute Permeability Measurements (Colbert-1)

Matador Resources Company
Colbert No. 1
File: HOU-050182

Date: 7-Mar-2005
Sleeving: None
Analyst(s): CM, MK

Sample Number	Sample Depth feet	Confining Pressure psi	Permeability millidarcys		Porosity fraction	Grain Density gm/cc
			Klinkenberg	to Air		
1	8766.0	3600	0.002	0.004	0.029	2.68
2	8776.0	3600	0.003	0.007	0.059	2.66
3	8805.0	3600	0.038	0.056	0.053	2.65
5	8836.0	3600	0.0002	0.001	0.009	2.70
6	8876.0	3600	0.061	0.080	0.070	2.66
7	8885.0	3600	0.006	0.010	0.058	2.66
8	8892.0	3600	0.005	0.008	0.069	2.65
9	8910.0	3600	0.002	0.006	0.056	2.66
10	8930.0	3600	0.002	0.005	0.062	2.67
12	9092.0	3600	0.0003	0.001	0.046	2.74
14	9130.0	3600	0.005	0.009	0.064	2.67
15	9206.0	3600	0.0002	0.0007	0.018	2.65
16	9231.0	3600	0.013	0.017	0.047	2.65
17	9272.0	3600	0.004	0.006	0.030	2.66
18	9284.0	3600	0.002	0.005	0.053	2.68
19	9287.0	3600	0.003	0.006	0.072	2.67
20	9312.0	3600	0.002	0.006	0.094	2.66
21	9320.0	3600	0.005	0.010	0.106	2.67
22	9460.0	3600	0.0004	0.001	0.034	2.69
23	9463.0	3600	0.0004	0.001	0.042	2.67

Table C3: Stressed Measurements of Permeability and Porosity

SUMMARY OF CORE ANALYSES RESULTS

Samples selected for gas/water Pc

Company: Matador Resources Company
Well: Colbert No. 1
Job No.: Hou-050182

Date: 7-Mar-2005
Sleeving: None
Analyst(s): CM, MK

Sample Number	Sample Depth feet	Confining Pressure psi	Permeability millidarcys		Porosity fraction	Pore Volume cc	Dry Weight grams	Grain Volume cc	Grain Density gm/cc	Length cm	Diameter cm
			Klinkenberg	to Air							
3	8805.0	800	0.074	0.124	0.066	0.557	20.978	7.929	2.646	1.970	2.340
		1200	0.057	0.089	0.062	0.522					
		3600	0.038	0.056	0.053	0.446					
8	8892.0	800	0.012	0.019	0.082	0.759	22.420	8.449	2.654	2.144	2.328
		1200	0.010	0.015	0.078	0.715					
		3600	0.005	0.008	0.069	0.624					
14	9130.0	800	0.015	0.023	0.078	0.756	23.806	8.928	2.666	2.260	2.339
		1200	0.011	0.018	0.074	0.712					
		3600	0.005	0.009	0.064	0.612					
20	9312.0	800	0.006	0.012	0.107	1.260	27.977	10.508	2.662	2.727	2.343
		1200	0.005	0.010	0.103	1.206					
		3600	0.002	0.006	0.094	1.084					

Table C4: Absolute Permeability Measurements and Water Saturation

Company: Matador Resources Company
Well: Colbert No. 1
Field: Caspiana
Formation: Cotton Valley

Location: Caddo Parish, La.
File: Hou-050182

Sample Number	Sample Depth, feet	Confining Pressure psi	Porosity, fraction	Klinkenberg Permeability millidarcys absolute	Klinkenberg Permeability millidarcys effective	Permeability Specific millidarcys	Water Saturation, fraction	Krg, K(eff)/K(abs)	Displacement Direction
3	8805.00	3600	0.053	0.03820	-	0.00600	1.000	0.157	Saturated
					0.000527		0.657	0.014	Drainage
					0.019070		0.190	0.499	Drainage
					0.037700		0.078	0.987	Drainage
					0.007140		0.172	0.187	Imbibition
					0.001980		0.278	0.052	Imbibition
8	8892.00	3600	0.069	0.00462	-	0.00200	1.000	0.433	Saturated
					0.000070		0.580	0.015	Drainage
					0.000418		0.430	0.090	Drainage
					0.004340		0.089	0.939	Drainage
					0.001560		0.209	0.338	Imbibition
					0.000758		0.286	0.164	Imbibition
14	9130.00	3600	0.064	0.00489	-	0.00200	1.000	0.409	Saturated
					0.000071		0.649	0.014	Drainage
					0.002410		0.232	0.493	Drainage
					0.004690		0.078	0.959	Drainage
					0.001200		0.247	0.245	Imbibition
					0.000480		0.319	0.098	Imbibition
20	9312.00	3600	0.094	0.00241	-	0.00100	1.000	0.415	Saturated
					0.000016		0.808	0.007	Drainage
					0.000326		0.427	0.135	Drainage
					0.001860		0.107	0.772	Drainage
					0.000380		0.266	0.158	Imbibition
					0.000213		0.327	0.088	Imbibition

Table C5: Liquid Permeability Measurements for the Relative Permeability Experiment

Core Lab
RESERVOIR OPTIMIZATION

PETROLEUM SERVICES

SUMMARY OF LIQUID PERMEABILITY MEASUREMENTS

Net Confining Stress: 3600 psi Temperature: 70°F
Fluid: 165,000 ppm NaCl Brine

Company:	Matador Resources Co.
Well:	Colbert #1(Cotton Valley)
Field:	Caspiana
Location:	Caddo Parish, La.
File:	HOU-050182

Sample Number	Depth feet	Length, cm	Area, cm^2	Viscosity, cp	Permeability to Fluid, millidarcys
3	8805.00	1.97	4.30	1.37	0.006
8	8892.00	2.14	4.26	1.37	0.002
14	9130.00	2.26	4.30	1.37	0.002
20	9312.00	2.73	4.31	1.37	0.001

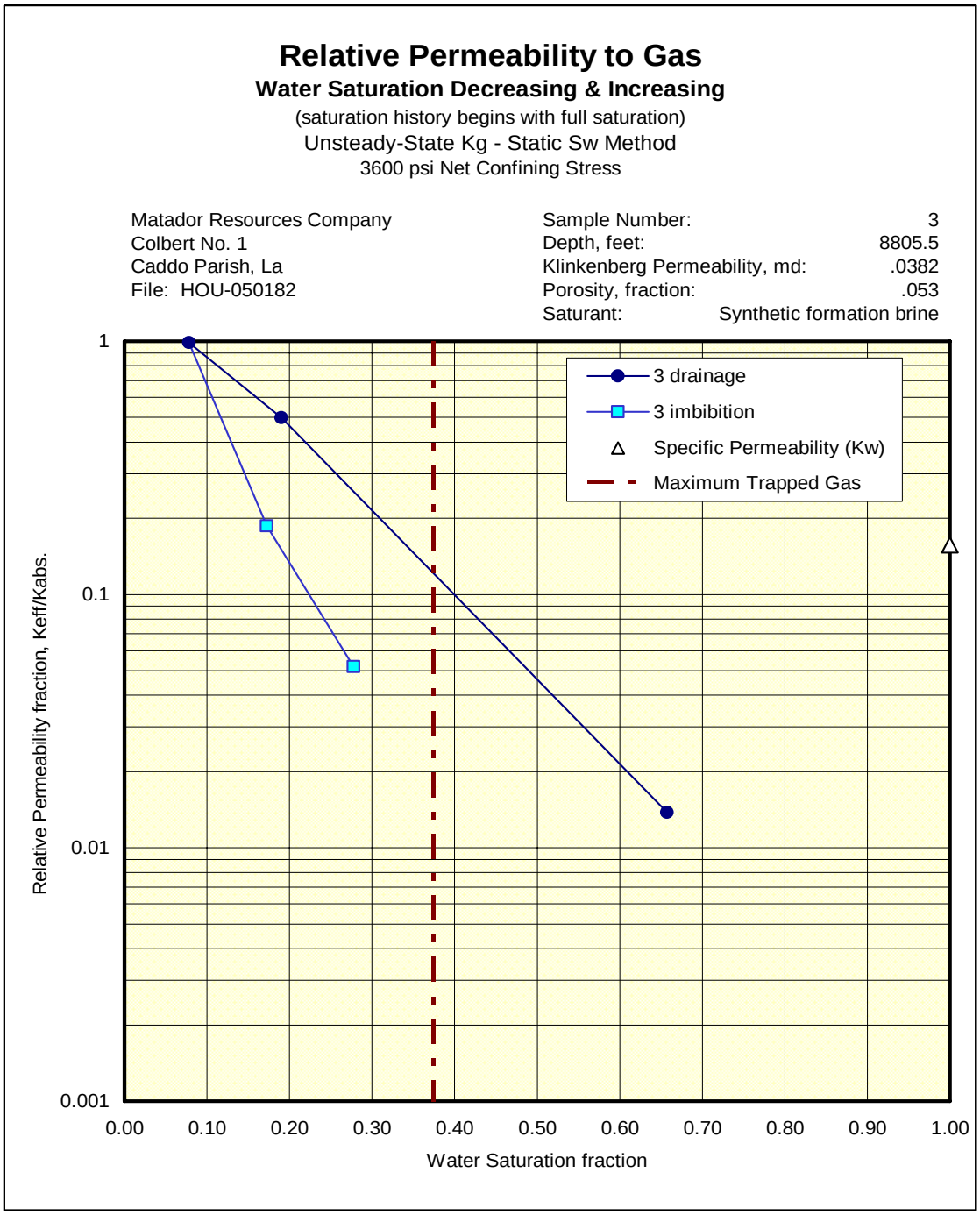

Fig. C3: Relative Permeability Plot for Sample 3.

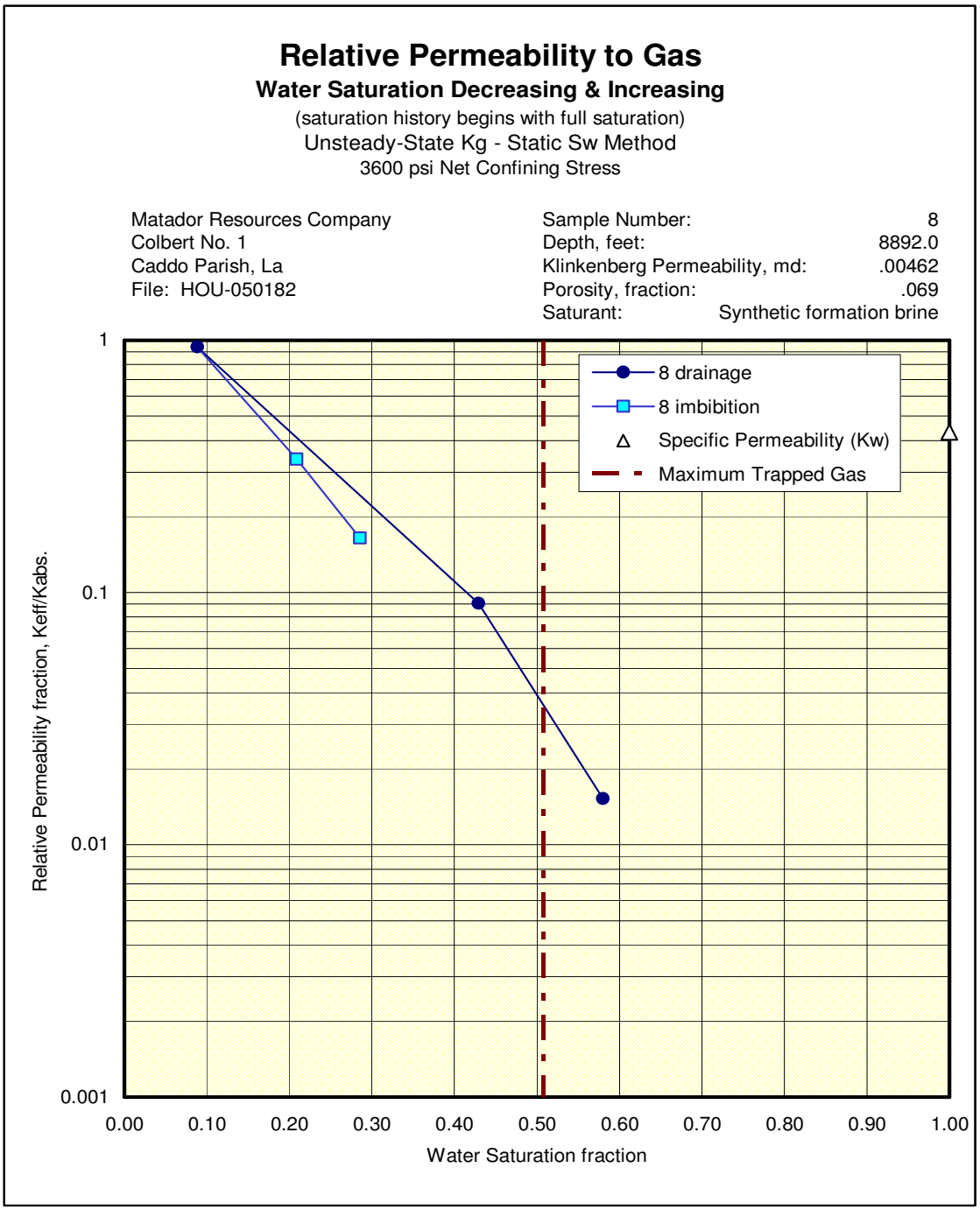

Fig. C4: Relative Permeability Plot for Sample 8.

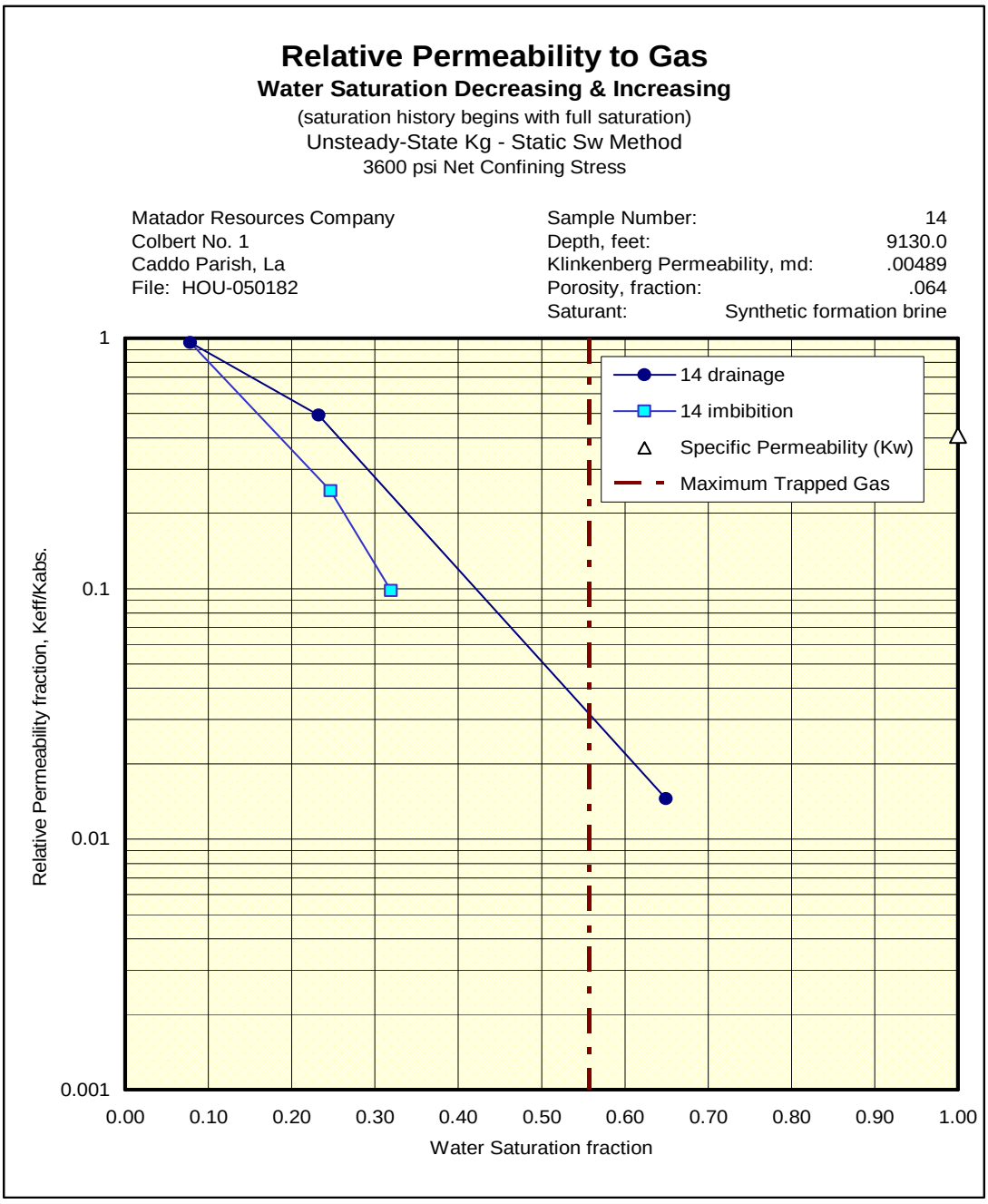

Fig. C5: Relative Permeability Plot for Sample 14.

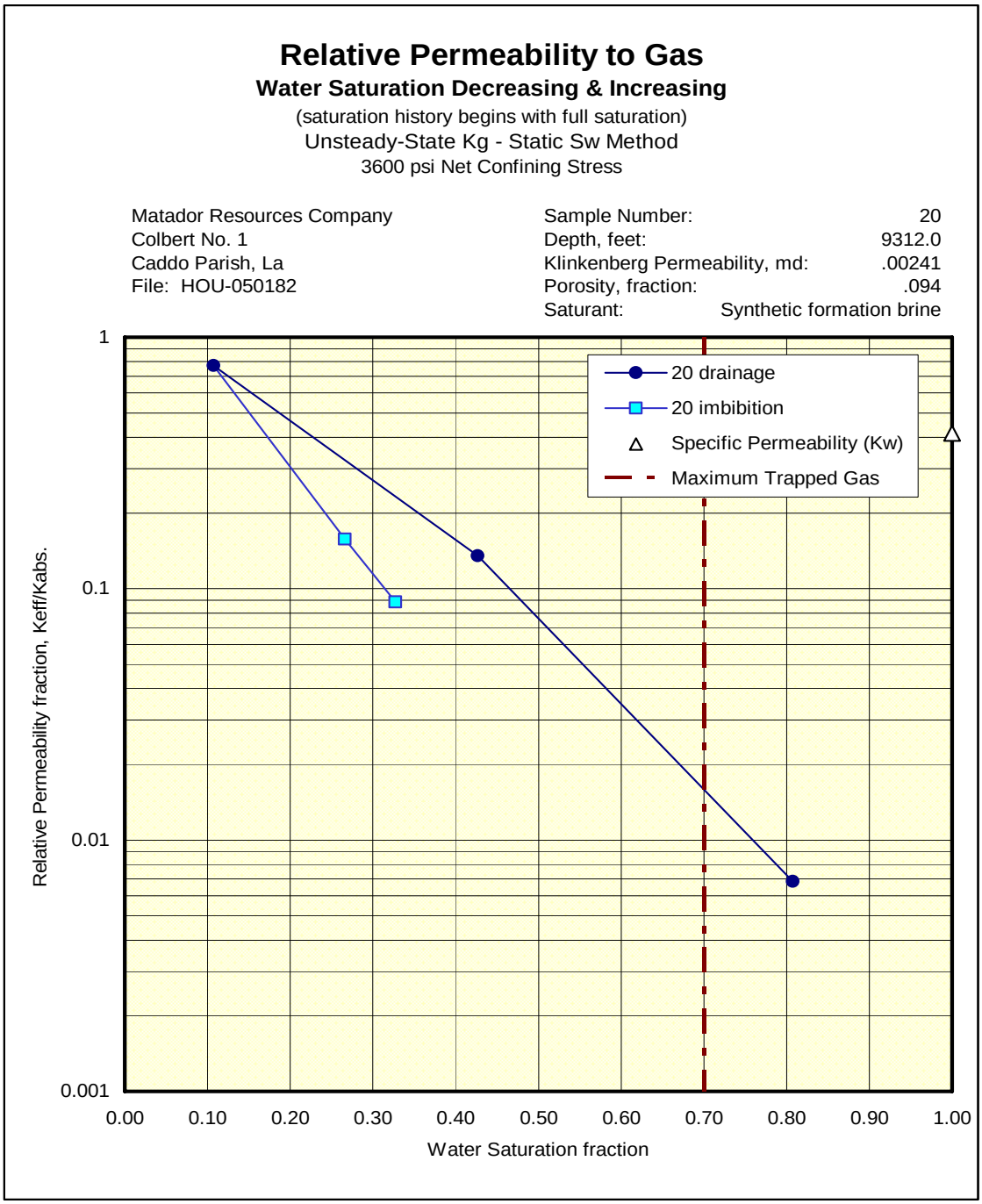

Fig. C6: Relative Permeability Plot for Sample 20.

Table C6: Capillary Pressure Measurements

Core Lab
PETROLEUM SERVICES

CAPILLARY PRESSURE
High Speed Centrifuge Method
Gas-Water System

Matador Resources Company		Displaced Phase:	Water
Colbert No. 1 Well		Displacing Phase:	Gas (air)
Caspiana Field		Confining Stress, psi:	ambient
Caddo Parish, LA		Temperature, ° F:	ambient
File: HOU-050182		Saturant:	100,000 ppm NaCl Brine

	Capillary Pressure, psi:	0	20	50	100	175	250	350	500	700

Sample Number	Depth, feet	Klinkenberg Permeability millidarcys	Porosity, fraction	Initial Saturation fraction	Inlet-Face Water Saturation, fraction pore volume							
2	8776.0	0.014	0.071	1.000	0.930	0.770	0.500	0.380	0.318	0.266	0.212	0.169
3	8805.0	0.074	0.066	1.000	0.730	0.525	0.320	0.225	0.195	0.179	0.159	0.137
6	8876.0	0.091	0.086	1.000	0.835	0.615	0.427	0.351	0.317	0.302	0.291	0.283
8	8892.0	0.012	0.082	1.000	1.000	0.756	0.568	0.408	0.331	0.307	0.292	0.278
14	9130.0	0.015	0.078	1.000	1.000	1.000	0.849	0.622	0.472	0.377	0.295	0.231
20	9312.0	0.006	0.107	1.000	1.000	0.985	0.920	0.780	0.675	0.560	0.430	0.320
21	9320.0	0.012	0.121	1.000	1.000	0.970	0.900	0.730	0.610	0.500	0.410	0.350

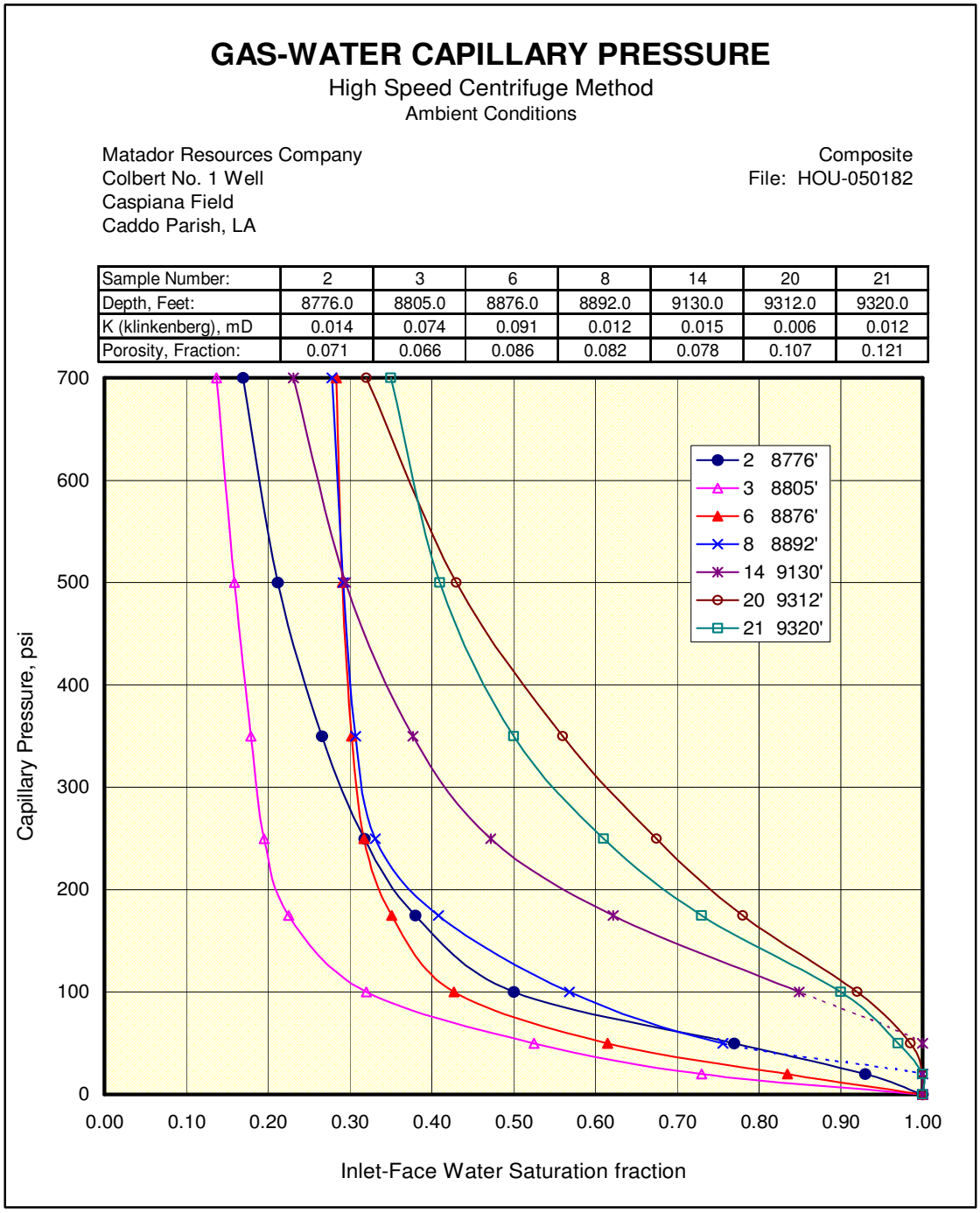

Fig. C7: Capillary Pressure Plots with Seven Samples.

Table C7: Rotary Sidewall Core Analysis Measurements of Porosity and Permeability (Dutton Family-1)

Matador Resources
Dutton Family #1
Elm Grove Field
Caddo Parish, Louisiana

CL File No.: HOU-050277
Date: April 14, 2005
Analyst(s): RP, LA, JH

CMS-300 ROTARY SIDEWALL CORE ANALYSIS DATA

Sample Number	Depth (ft)	Net Confining Stress (psig)	Porosity (%)	Permeability Klinkenberg (mD)	Permeability Kair (mD)	Beta ft(-1)	Alpha microns	Saturation Oil % Pore Volume	Saturation Water % Pore Volume	Grain Density g/cm3	Footnote
18	9027.00	3600	6.68	0.016	0.023	2.36E+14	2.65E+04	0.0	46.7	2.665	(3)
17	9100.00	3600	4.87	0.001	0.003	1.99E+16	2.70E+05	3.8	34.2	2.663	
16	9110.00	3600	6.32	0.006	0.012	8.41E+14	6.83E+04	0.0	47.6	2.653	(3)
15	9130.00	3600	6.93	0.005	0.011	9.81E+14	6.31E+04	2.9	36.1	2.655	(3)
14	9426.00	3600	5.65	0.003	0.006	4.24E+15	1.03E+05	0.0	36.1	2.649	
13	9465.00	3600	6.10	0.005	0.009	9.74E+14	3.49E+04	0.0	19.2	2.656	(3)
12	9523.00	Ambient	7.15	0.027	0.073	N/A	N/A	0.0	36.0	2.669	(2)
11	9531.00	3600	6.20	0.002	0.004	1.68E+16	3.63E+05	3.8	43.8	2.668	
10	9541.00	3600	6.84	0.002	0.005	8.12E+15	2.02E+05	1.1	38.1	2.674	
9	9575.00	3600	6.24	0.001	0.002	2.48E+15	1.50E+04	1.7	43.9	2.669	
8	9585.00	Ambient	5.10	0.017	0.051	N/A	N/A	0.0	27.2	2.662	(2)
7	9614.00	3600	2.50	0.0001	0.0003	2.42E+18	6.92E+05	2.4	70.3	2.743	
6	9635.00	3600	2.88	0.0003	0.001	2.13E+17	1.86E+05	1.6	19.5	2.662	
5	9639.00	Ambient	4.85	0.005	0.020	N/A	N/A	3.7	10.3	2.660	(2)
4	9651.00	3600	9.20	0.096	0.120	3.45E+12	1.70E+03	2.4	7.6	2.660	(3)
3	9657.00	Ambient	9.57	0.015	0.018	N/A	N/A	0.0	21.4	2.721	(2)
2	9659.00	3600	7.54	0.003	0.006	3.51E+15	1.41E+05	0.0	26.9	2.658	
1	9667.00	3600	6.41	0.001	0.003	2.55E+16	2.68E+05	0.0	19.0	2.658	

Footnotes :

(1) : Denotes fractured or chipped sample. Permeability and/or porosity may be optimistic.

(2) : Denotes sample unsuitable for measurement at stress. Porosity detemined using Archimedes bulk volume at ambient conditions. Permeability determined using unsteady-state profile permeameter.

(3) : Denotes very short sample, porosity may be optimistic due to lack of conformation of boot material to plug surface.

Table C8: North Oriented Core Analysis Data (Dutton Family-1)

Matador Resources
Dutton Family No. 1
Elm Grove Field
Caddo Parish, Louisiana

CL File No.: HOU-050235
Date: June 6, 2005
Analyst(s): RP, LA, JH

CMS-300 CORE ANALYSIS DATA

Sample Number	Depth (ft)	Net Confining Stress (psig)	Porosity (%)	Permeability Klinkenberg (mD)	Permeability Kair (mD)	Beta ft(-1)	Alpha microns	Grain Density g/cm3	Saturation Oil % Pore Volume	Saturation Water % Pore Volume	Footnote
2N	8932.85	3600	1.36	0.010	0.021	1.09E+14	3.52E+03	2.683	2.3	76.9	
3N	8934.15	3600	1.59	0.002	0.004	3.44E+15	1.92E+04	2.833	2.6	37.4	
4N	8935.15	3600	0.57	0.0002	0.001	2.85E+17	1.79E+05	2.679	2.6	43.4	
5N	8936.05	3600	4.37	0.124	0.134	2.01E+12	7.96E+02	2.665	1.6	70.9	
6N	8936.95	3600	4.14	0.002	0.005	2.05E+15	1.50E+04	2.690	3.3	47.0	
7N	8937.95	3600	5.34	0.001	0.003	5.79E+15	2.50E+04	2.659	1.8	22.6	
8N	8939.00	3600	6.78	0.003	0.007	1.02E+15	1.06E+04	2.663	4.6	34.1	
9N	8940.10	3600	7.32	0.003	0.008	9.84E+14	1.04E+04	2.655	2.2	36.4	
10N	8941.00	3600	5.80	0.003	0.005	7.95E+13	6.78E+02	2.656	0.3	39.6	
11N	8942.05	3600	4.71	0.002	0.004	4.32E+15	2.16E+04	2.657	1.7	38.1	
12N	8943.40	3600	7.18	0.002	0.006	1.94E+15	1.45E+04	2.658	6.6	41.4	
13N	8944.05	3600	5.35	0.002	0.004	3.45E+15	1.94E+04	2.658	1.5	51.2	
14N	8945.05	3600	3.50	0.169	0.192	3.60E+12	1.95E+03	2.676	5.3	50.9	(1)
15N	8946.20	3600	5.76	0.002	0.006	1.79E+15	1.40E+04	2.660	3.4	39.1	
16N	8947.05	3600	6.59	0.004	0.009	2.87E+14	3.66E+03	2.658	2.4	36.2	
17N	8948.05	3600	2.17	0.001	0.002	1.46E+16	4.02E+04	2.683	2.0	54.6	
18N	8949.10	3600	6.48	0.021	0.027	1.38E+12	9.55E+01	2.659	1.4	42.4	
19N	8950.10	3600	2.38	0.001	0.001	3.77E+16	6.38E+04	2.673	2.6	52.1	
20N	8951.05	3600	5.57	0.001	0.002	1.58E+16	4.10E+04	2.652	2.0	20.9	

Footnotes :

(1) : Denotes fractured or chipped sample. Permeability and/or porosity may be optimistic.

(2) : Sample permeability below the measurement range of CMS-300 equipment at requested net confining stress (NCS). Data unavailable.

(3) : Denotes very short sample, porosity may be optimistic due to lack of conformation of boot material to plug surface.

(4) : Denotes sample unsuitable for measurement at stress. Porosity detemined using Archimedes bulk volume at ambient conditions. Permeability unavailable.

Table C8 (Continued): North Oriented Core Analysis Data (Dutton Family-1)

Matador Resources
Dutton Family No. 1
Elm Grove Field
Caddo Parish, Louisiana

CL File No.: HOU-050235
Date: June 6, 2005
Analyst(s): RP, LA, JH

CMS-300 CORE ANALYSIS DATA

Sample Number	Depth (ft)	Net Confining Stress (psig)	Porosity (%)	Permeability Klinkenberg (mD)	Permeability Kair (mD)	Beta ft(-1)	Alpha microns	Grain Density g/cm3	Saturation Oil % Pore Volume	Saturation Water % Pore Volume	Footnote
20N	8951.05	3600	5.57	0.001	0.002	1.58E+16	4.10E+04	2.652	2.0	20.9	
21N	8952.10	3600	6.17	0.002	0.004	3.61E+15	1.97E+04	2.655	1.6	44.8	
22N	8953.05	3600	6.20	0.003	0.005	1.17E+14	1.06E+03	2.653	1.0	32.1	
23N	8954.25	3600	4.69	0.011	0.017	8.64E+12	3.22E+02	2.651	1.0	34.2	(1)
24N	8955.10	3600	5.89	0.010	0.015	2.89E+13	9.40E+02	2.653	1.8	45.2	
25N	8956.05	3600	10.24	2.36	2.50	2.50E+10	1.92E+02	2.653	1.2	42.0	
26N	8957.10	3600	3.97	0.0003	0.001	8.30E+16	9.46E+04	2.648	1.3	28.9	
27N	8958.05	3600	6.73	0.060	0.075	1.50E+12	2.93E+02	2.649	1.4	58.4	
28N	8959.10	3600	3.24	0.002	0.006	1.57E+15	1.30E+04	2.693	2.3	58.3	
29N	8960.15	3600	4.68	0.017	0.022	1.57E+13	8.55E+02	2.675	2.4	26.1	
30N	8961.25	3600	4.73	0.016	0.022	1.55E+13	8.27E+02	2.655	3.3	36.0	
31N	8962.10	3600	4.31	0.023	0.029	4.33E+12	3.28E+02	2.697	6.2	54.8	
32N	8963.10	3600	3.72	0.002	0.004	3.33E+15	1.90E+04	2.653	4.0	48.0	
33N	8964.00	3600	1.44	0.001	0.003	5.61E+15	2.45E+04	2.681	2.4	80.8	
34N	8965.10	3600	5.25	0.075	0.088	1.64E+12	3.99E+02	2.654	5.8	16.7	
35N	8966.25	3600	6.32	0.005	0.008	2.93E+13	4.69E+02	2.666	3.0	38.5	
36N	8967.20	3600	1.04	0.001	0.002	1.22E+16	3.63E+04	2.677	6.8	82.4	
37N	8968.85	3600	4.76	0.001	0.003	7.05E+15	2.77E+04	2.660	2.1	38.7	
38N	8970.05	3600	9.69	0.014	0.021	5.67E+12	2.53E+02	2.666	2.9	47.4	
39N	8972.10	3600	1.15	0.001	0.001	3.81E+16	6.58E+04	2.682	7.8	41.6	
40N	8973.10	3600	2.13	0.0001	0.0005	1.02E+18	5.06E+05	2.716	7.3	65.0	(3)

Footnotes :

(1) : Denotes fractured or chipped sample. Permeability and/or porosity may be optimistic.
(2) : Sample permeability below the measurement range of CMS-300 equipment at requested net confining stress (NCS). Data unavailable.
(3) : Denotes very short sample, porosity may be optimistic due to lack of conformation of boot material to plug surface.
(4) : Denotes sample unsuitable for measurement at stress. Porosity detemined using Archimedes bulk volume at ambient conditions. Permeability unavailable.

Table C8 (Continued): North Oriented Core Analysis Data (Dutton Family-1)

Matador Resources
Dutton Family No. 1
Elm Grove Field
Caddo Parish, Louisiana

CL File No.: HOU-050235
Date: June 6, 2005
Analyst(s): RP, LA, JH

CMS-300 CORE ANALYSIS DATA

Sample Number	Depth (ft)	Net Confining Stress (psig)	Porosity (%)	Permeability Klinkenberg (mD)	Permeability Kair (mD)	Beta ft(-1)	Alpha microns	Grain Density g/cm3	Saturation Oil % Pore Volume	Saturation Water % Pore Volume	Footnote
41N	8974.10	3600	1.48	0.031	0.035	1.55E+13	1.53E+03	2.690	1.6	90.1	(1)
42N	8975.10	3600	2.34	0.001	0.003	5.65E+15	2.48E+04	2.715	2.4	90.9	
43N	8976.10	3600	0.95	0.031	0.031	1.14E+11	1.14E+01	2.712	4.5	91.8	(1)
44N	8977.15	3600	0.88	N/A	N/A	N/A	N/A	2.693	7.7	85.5	(2)
45N	8978.10	3600	1.31	0.003	0.006	1.35E+15	1.21E+04	2.711	4.0	88.9	
46N	8979.10	3600	0.59	0.0001	0.0003	1.70E+18	4.49E+05	2.693	4.1	88.6	
47N	8980.10	3600	2.54	0.001	0.003	6.29E+15	2.62E+04	2.661	4.8	34.8	
48N	8981.05	3600	1.29	0.0002	0.001	2.29E+17	1.61E+05	2.651	4.5	38.8	
49N	8982.10	3600	2.41	0.0004	0.001	5.30E+16	7.64E+04	2.644	4.3	12.9	
50N	8982.95	3600	2.35	0.0004	0.001	4.92E+16	7.35E+04	2.650	2.0	57.3	
51N	8984.10	3600	3.84	0.002	0.005	2.15E+15	1.53E+04	2.649	9.9	84.7	
52N	8987.20	3600	3.97	0.002	0.006	1.95E+15	1.46E+04	2.649	7.2	23.1	
53N	8988.25	3600	4.09	0.005	0.011	4.53E+14	7.10E+03	2.646	5.4	41.0	
54N	8989.10	3600	4.16	0.073	0.092	3.05E+12	7.13E+02	2.646	3.2	32.7	(1)
55N	8990.15	3600	4.02	0.003	0.007	1.26E+15	1.17E+04	2.646	6.7	17.9	
56N	8991.25	3600	3.77	0.002	0.004	3.83E+15	2.05E+04	2.648	3.8	27.3	
57N	8992.10	3600	3.45	0.001	0.003	6.22E+15	2.62E+04	2.646	7.4	9.6	
58N	8993.10	3600	2.91	0.0005	0.001	4.96E+16	7.39E+04	2.645	2.3	35.6	
59N	8994.10	3600	5.15	0.002	0.006	1.83E+15	1.45E+04	2.646	0.9	44.1	
60N	8995.20	3600	5.34	0.002	0.005	2.01E+15	1.48E+04	2.649	1.0	51.6	(1)
61N	8996.50	3600	4.35	0.001	0.002	3.21E+16	5.96E+04	2.647	0.2	44.3	
62N	8997.05	3600	4.31	0.001	0.002	1.78E+16	4.44E+04	2.646	0.1	47.2	
63N	8998.05	3600	4.84	0.002	0.005	2.45E+15	1.65E+04	2.647	2.7	49.9	
64N	8999.10	3600	4.35	0.004	0.009	7.61E+14	9.17E+03	2.647	2.4	47.5	
65N	9000.10	3600	3.96	0.001	0.002	1.18E+16	3.61E+04	2.646	5.0	49.1	
66N	9001.05	3600	2.74	0.0003	0.001	1.33E+17	1.23E+05	2.648	3.3	51.5	

Footnotes :

(1) : Denotes fractured or chipped sample. Permeability and/or porosity may be optimistic.
(2) : Sample permeability below the measurement range of CMS-300 equipment at requested net confining stress (NCS). Data unavailable.
(3) : Denotes very short sample, porosity may be optimistic due to lack of conformation of boot material to plug surface.
(4) : Denotes sample unsuitable for measurement at stress. Porosity detemined using Archimedes bulk volume at ambient conditions. Permeability unavailable.

Table C9: East Oriented Core Analysis Data (Dutton Family-1)

Matador Resources
Dutton Family No. 1
Elm Grove Field
Caddo Parish, Louisiana

CL File No.: HOU-050235
Date: June 6, 2005
Analyst(s): RP, LA, JH

CMS-300 CORE ANALYSIS DATA

	Sample Number	Depth (ft)	Net Confining Stress (psig)	Porosity (%)	Permeability Klinkenberg (mD)	Permeability Kair (mD)	Beta ft(-1)	Alpha microns	Grain Density g/cm3	Saturation Oil % Pore Volume	Saturation Water % Pore Volume	Footnote		Sample Number	Depth (ft)	Net Confining Stress (psig)
1	1E	8932.45	3600	1.61	0.002	0.004	3.72E+15	2.02E+04	2.716			(1)				
2	2E	8932.95	3600	1.54	0.002	0.004	3.34E+15	1.90E+04	2.684				5.731947	2N	8932.85	3600
3	3E	8934.25	3600	0.71	0.0004	0.001	5.92E+16	7.99E+04	2.686				4.204068	3N	8934.15	3600
4	4E	8935.30	3600	0.83	0.0003	0.001	1.29E+17	1.20E+05	2.675				0.682927	4N	8935.15	3600
6	6E	8937.05	3600	6.02	0.001	0.004	4.75E+15	2.28E+04	2.658				1.53444	6N	8936.95	3600
7	7E	8938.05	3600	5.80	0.030	0.036	1.80E+12	1.74E+02	2.653				0.044492	7N	8937.95	3600
9	9E	8940.20	3600	6.30	0.003	0.005	4.35E+13	3.68E+02	2.655				1.259105	9N	8940.10	3600
10	10E	8941.10	3600	5.28	0.001	0.004	4.63E+15	2.23E+04	2.652				1.784491	10N	8941.00	3600
11	11E	8942.15	3600	4.52	0.001	0.002	1.47E+16	3.96E+04	2.651				1.869394	11N	8942.05	3600
12	12E	8943.50	3600	7.19	0.002	0.004	4.06E+15	2.10E+04	2.655				1.462796	12N	8943.40	3600
13	13E	8944.15	3600	5.18	0.001	0.003	7.79E+15	2.91E+04	2.650				1.519799	13N	8944.05	3600
15	15E	8946.30	3600	6.28	0.002	0.004	4.24E+15	2.14E+04	2.654				1.555637	15N	8946.20	3600
16	16E	8947.15	3600	6.89	0.004	0.007	6.91E+13	8.32E+02	2.655				1.06652	16N	8947.05	3600
17	17E	8948.15	3600	5.73	0.001	0.002	3.13E+16	5.98E+04	2.667				1.459176	17N	8948.05	3600
18	18E	8949.20	3600	6.16	0.003	0.005	9.43E+13	1.04E+03	2.658				6.391954	18N	8949.10	3600
20	20E	8951.15	3600	5.23	0.001	0.001	3.57E+16	6.09E+04	2.655				1.527619	20N	8951.05	3600
21	21E	8952.20	3600	6.80	0.003	0.006	1.33E+15	1.20E+04	2.655				0.600044	21N	8952.10	3600
22	22E	8953.15	3600	7.10	0.002	0.004	3.95E+15	2.07E+04	2.655				1.72158	22N	8953.05	3600
24	24E	8955.15	3600	6.22	0.011	0.016	1.99E+13	6.87E+02	2.657				0.937886	24N	8955.10	3600
26	26E	8957.20	3600	3.26	0.0003	0.001	1.14E+17	1.11E+05	2.649				1.154411	26N	8957.10	3600
27	27E	8958.30	3600	4.19	0.016	0.020	2.17E+13	1.16E+03	2.656				3.672986	27N	8958.05	3600
28	28E	8959.20	3600	4.30	0.014	0.019	2.29E+13	1.04E+03	2.658				0.180919	28N	8959.10	3600
29	29E	8960.25	3600	5.04	0.06	0.07	2.26E+12	4.46E+02	2.655				0.27414	29N	8960.15	3600
30	30E	8961.35	3600	5.38	0.017	0.023	1.14E+13	6.25E+02	2.661				0.977213	30N	8961.25	3600
31	31E	8962.00	3600	4.04	0.057	0.067	1.89E+12	3.54E+02	2.690				0.402734	31N	8962.10	3600
32	32E	8963.35	3600	3.39	0.008	0.011	2.01E+13	5.41E+02	2.675				0.208721	32N	8963.10	3600
33	33E	8964.10	3600	1.18	0.001	0.003	9.34E+15	3.15E+04	2.676				1.293755	33N	8964.00	3600
34	34E	8965.20	3600	4.64	0.083	0.096	2.29E+12	6.16E+02	2.659				0.90274	34N	8965.10	3600
35	35E	8966.40	3600	4.36	0.005	0.011	3.74E+14	6.42E+03	2.676				0.939512	35N	8966.25	3600

Footnotes :

(1) : Denotes fractured or chipped sample. Permeability and/or porosity may be optimistic.
(2) : Sample permeability below the measurement range of CMS-300 equipment at requested net confining stress (NCS). Data unavailable.
(3) : Denotes very short sample, porosity may be optimistic due to lack of conformation of boot material to plug surface.

Table C10 (Continued): East Oriented Core Analysis Data (Dutton Family-1)

Matador Resources
Dutton Family No. 1
Elm Grove Field
Caddo Parish, Louisiana

CL File No.: HOU-050235
Date: June 6, 2005
Analyst(s): RP, LA, JH

CMS-300 CORE ANALYSIS DATA

Sample Number	Depth (ft)	Net Confining Stress (psig)	Porosity (%)	Permeability Klinkenberg (mD)	Permeability Kair (mD)	Beta ft(-1)	Alpha microns	Grain Density g/cm3	Saturation Oil % Pore Volume	Saturation Water % Pore Volume	Footnote		Sample Number	Depth (ft)	Net Confining Stress (psig)
36	36E	8967.30	3600	1.87	0.001	0.003	7.80E+15	2.88E+04	2.679			0.808811	36N	8967.20	3600
37	37E	8968.70	3600	4.95	0.002	0.004	3.74E+15	2.00E+04	2.663			0.73628	37N	8968.85	3600
38	38E	8970.15	3600	7.25	0.062	0.073	7.08E+11	1.42E+02	2.662			0.222016	38N	8970.05	3600
39	39E	8972.20	3600	1.20	0.0004	0.001	6.17E+16	8.20E+04	2.684			1.302393	39N	8972.10	3600
45	45E	8978.20	3600	1.27	0.002	0.005	2.49E+15	1.63E+04	2.708			1.391822	45N	8978.10	3600
47	47E	8980.20	3600	2.73	0.001	0.002	1.89E+16	4.52E+04	2.658			1.764363	47N	8980.10	3600
48	48E	8981.15	3600	1.23	0.0001	0.0004	6.39E+17	2.71E+05	2.651			1.669505	48N	8981.05	3600
49	49E	8982.20	3600	2.05	0.0002	0.001	2.39E+17	1.67E+05	2.646			2.073221	49N	8982.10	3600
51	51E	8984.20	3600	3.76	0.001	0.004	4.94E+15	2.30E+04	2.649			1.54683	51N	8984.10	3600
52	52E	8987.30	3600	3.81	0.002	0.005	1.91E+15	1.43E+04	2.645			1.046142	52N	8987.20	3600
53	53E	8988.35	3600	4.01	0.004	0.009	5.91E+14	8.06E+03	2.645			1.188352	53N	8988.25	3600
55	55E	8990.25	3600	3.58	0.002	0.005	2.67E+15	1.69E+04	2.645			1.519787	55N	8990.15	3600
56	56E	8991.35	3600	3.80	0.001	0.003	5.66E+15	2.54E+04	2.645			1.232383	56N	8991.25	3600
57	57E	8992.25	3600	2.90	0.001	0.002	2.96E+16	5.63E+04	2.645			2.312944	57N	8992.10	3600
58	58E	8993.20	3600	3.00	0.0004	0.001	6.39E+16	8.45E+04	2.646			1.162595	58N	8993.10	3600
59	59E	8994.20	3600	4.85	0.004	0.007	6.06E+13	8.28E+02	2.646			0.593635	59N	8994.10	3600
61	61E	8996.60	3600	3.02	0.0004	0.001	7.58E+16	9.15E+04	2.645			1.596452	61N	8996.50	3600
62	62E	8997.15	3600	4.51	0.001	0.002	1.29E+16	3.75E+04	2.645			0.884079	62N	8997.05	3600
63	63E	8998.15	3600	3.79	0.002	0.004	3.56E+15	1.97E+04	2.644			1.249959	63N	8998.05	3600
64	64E	8999.25	3600	3.92	0.001	0.002	3.23E+16	5.90E+04	2.645			6.889073	64N	8999.10	3600
65	65E	9000.20	3600	5.30	0.004	0.009	5.67E+14	7.89E+03	2.648			0.219636	65N	9000.10	3600

Footnotes :

(1) : Denotes fractured or chipped sample. Permeability and/or porosity may be optimistic.

(2) : Sample permeability below the measurement range of CMS-300 equipment at requested net confining stress (NCS). Data unavailable.

(3) : Denotes very short sample, porosity may be optimistic due to lack of conformation of boot material to plug surface.

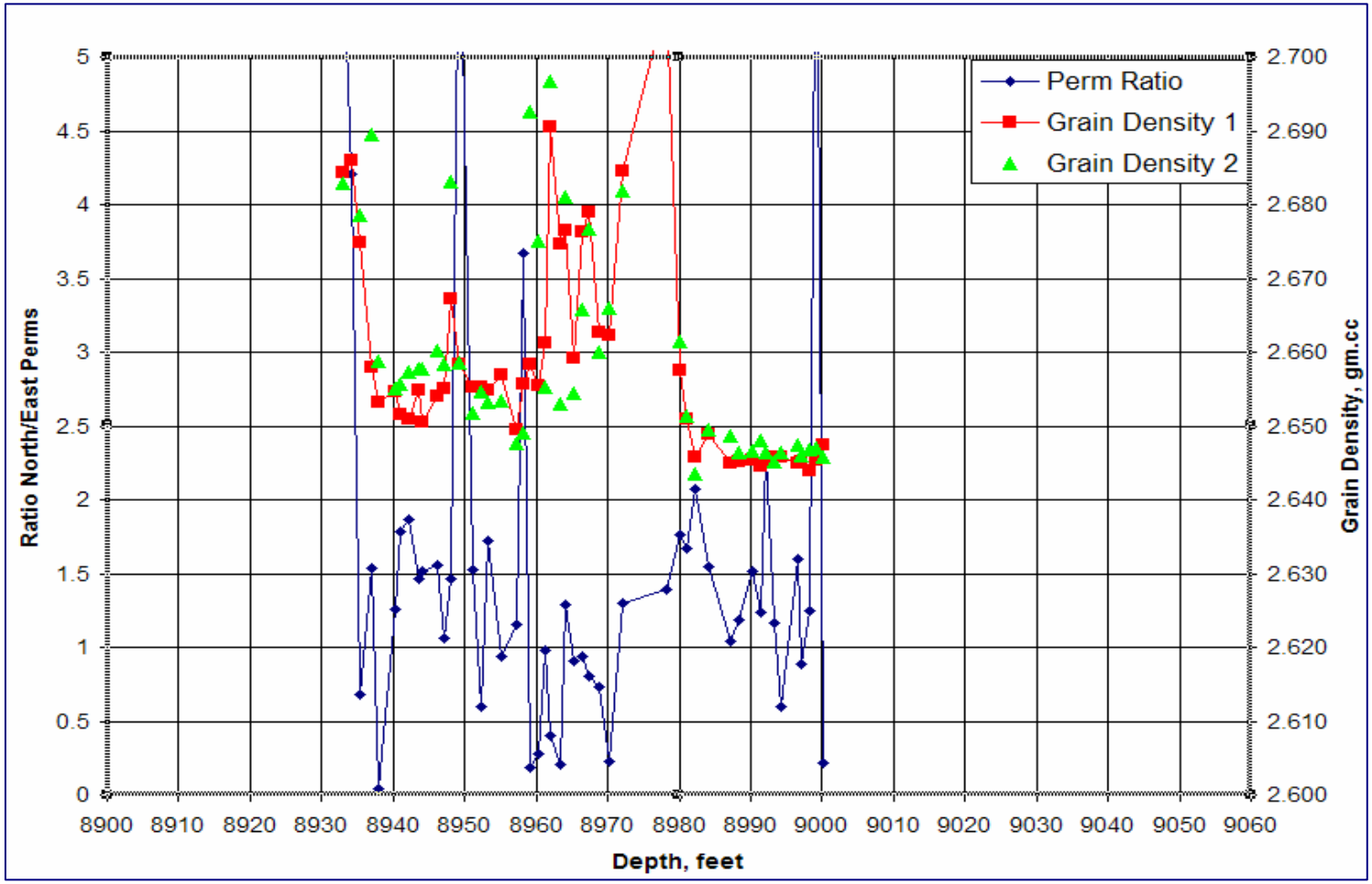

Fig. C8: North/East Permeability Ratio.

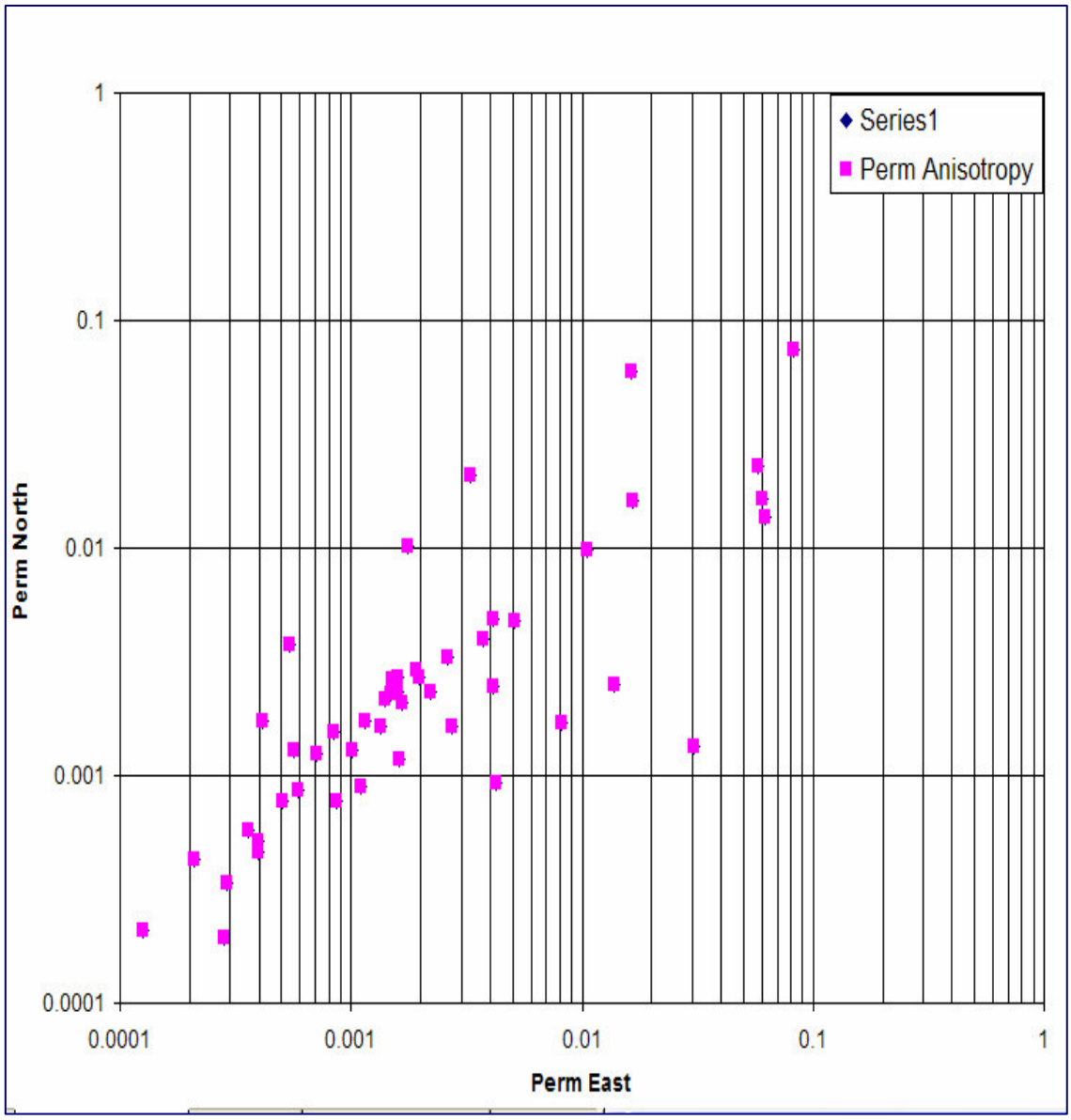

Fig. C9: North Permeability vs East Permeability.

APPENDIX D

DATA QUALITY CONTROL AND PARAMETER DETERMINATION

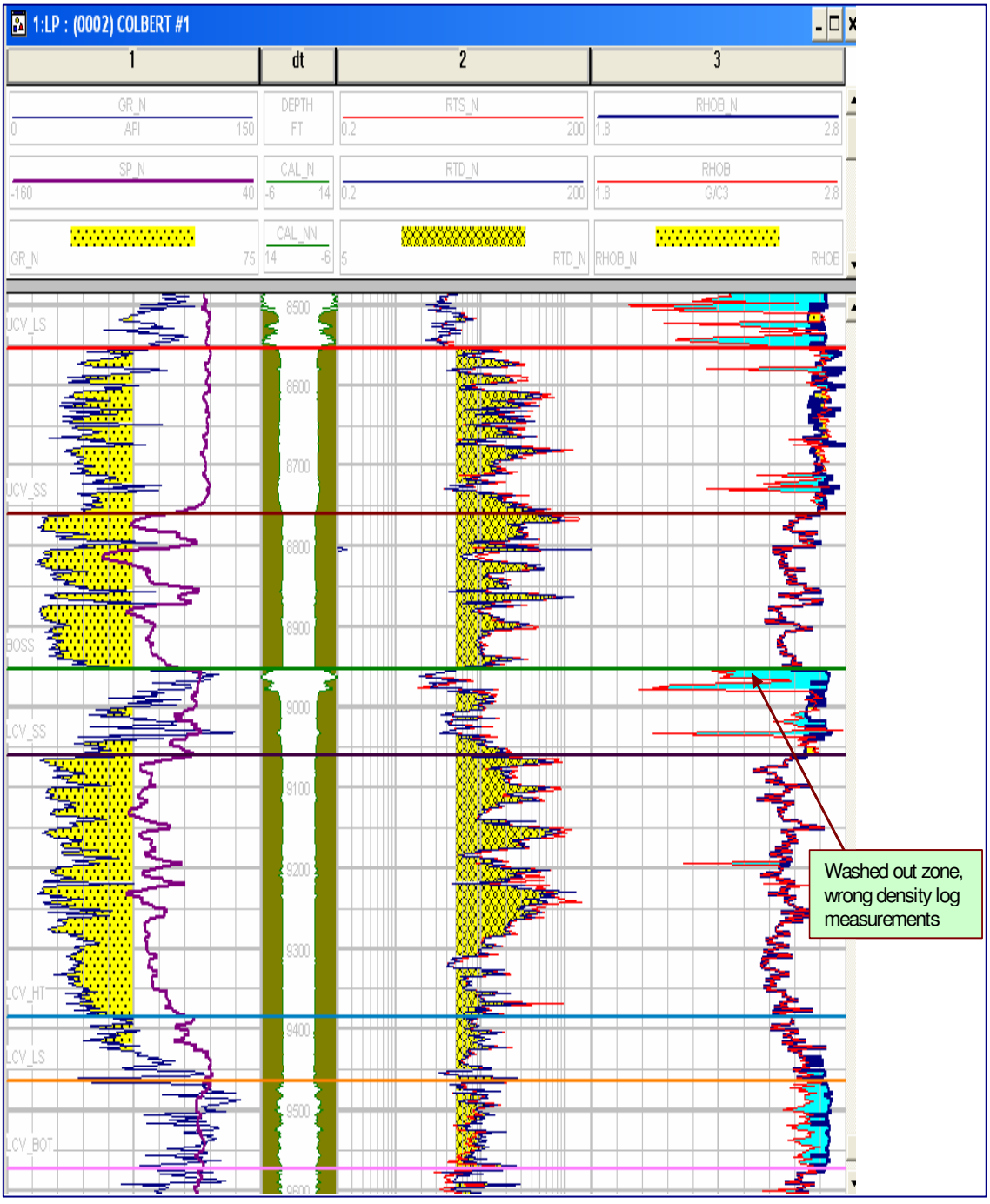

Fig. D1: Modeled Log Spliced into Bad Log Section.

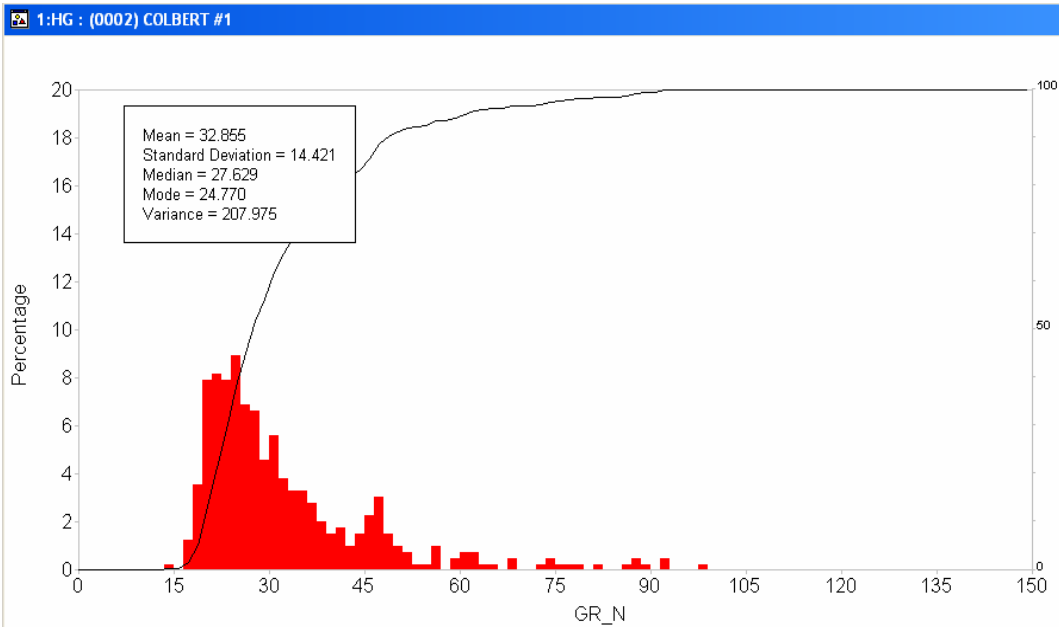

Fig. D2: Gamma Ray Normalization (Sand peak).

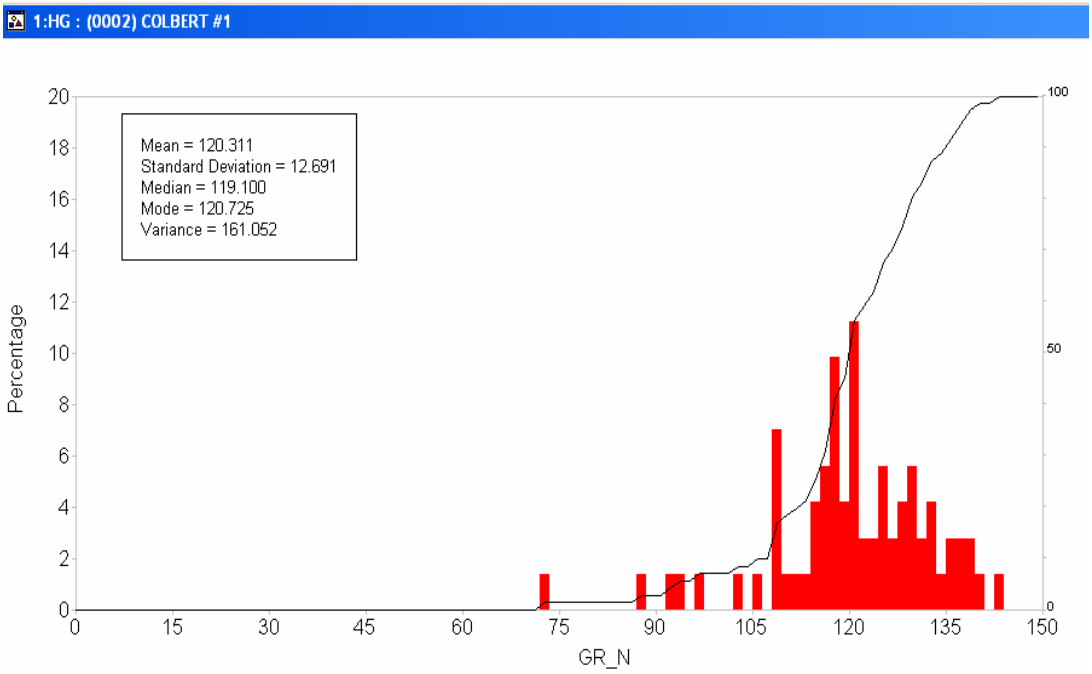

Fig. D3: Gamma Ray Normalization (Shale peak).

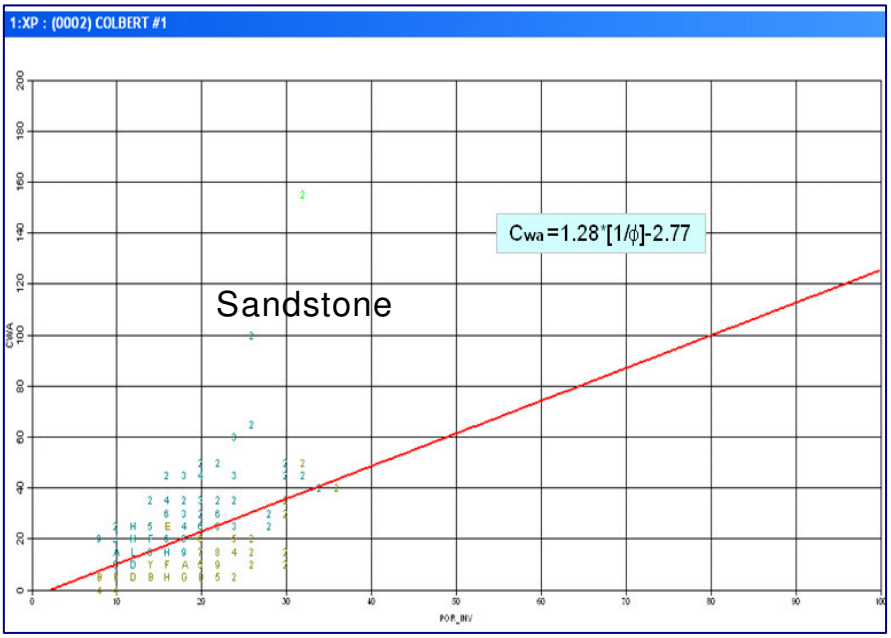

Fig. D4: BQv Analysis (Sand Zone) - Cwa vs 1//ϕ.

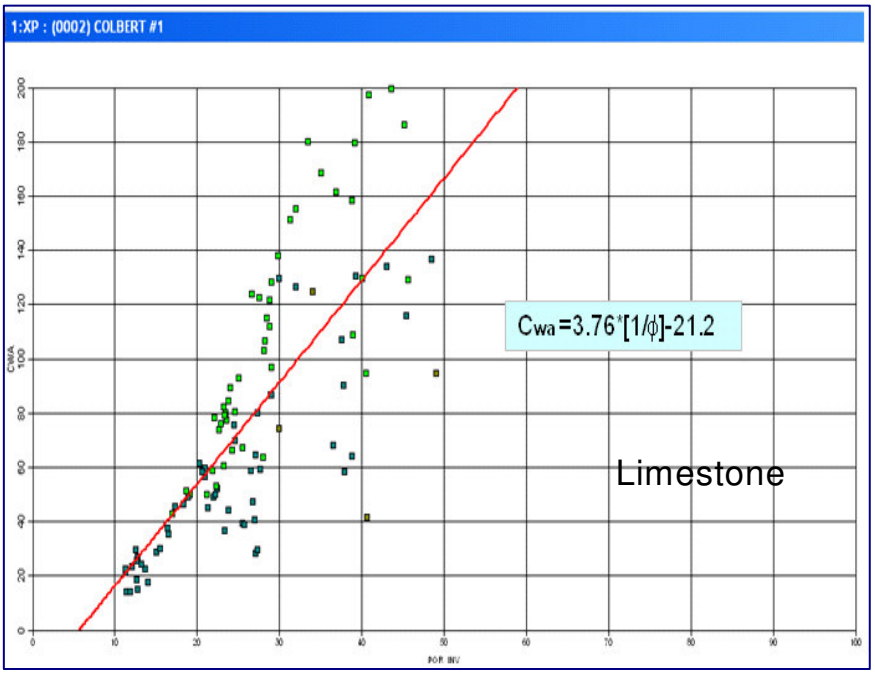

Fig. D5: BQv Analysis (Carbonate Zone) - Cwa vs 1//ϕ.

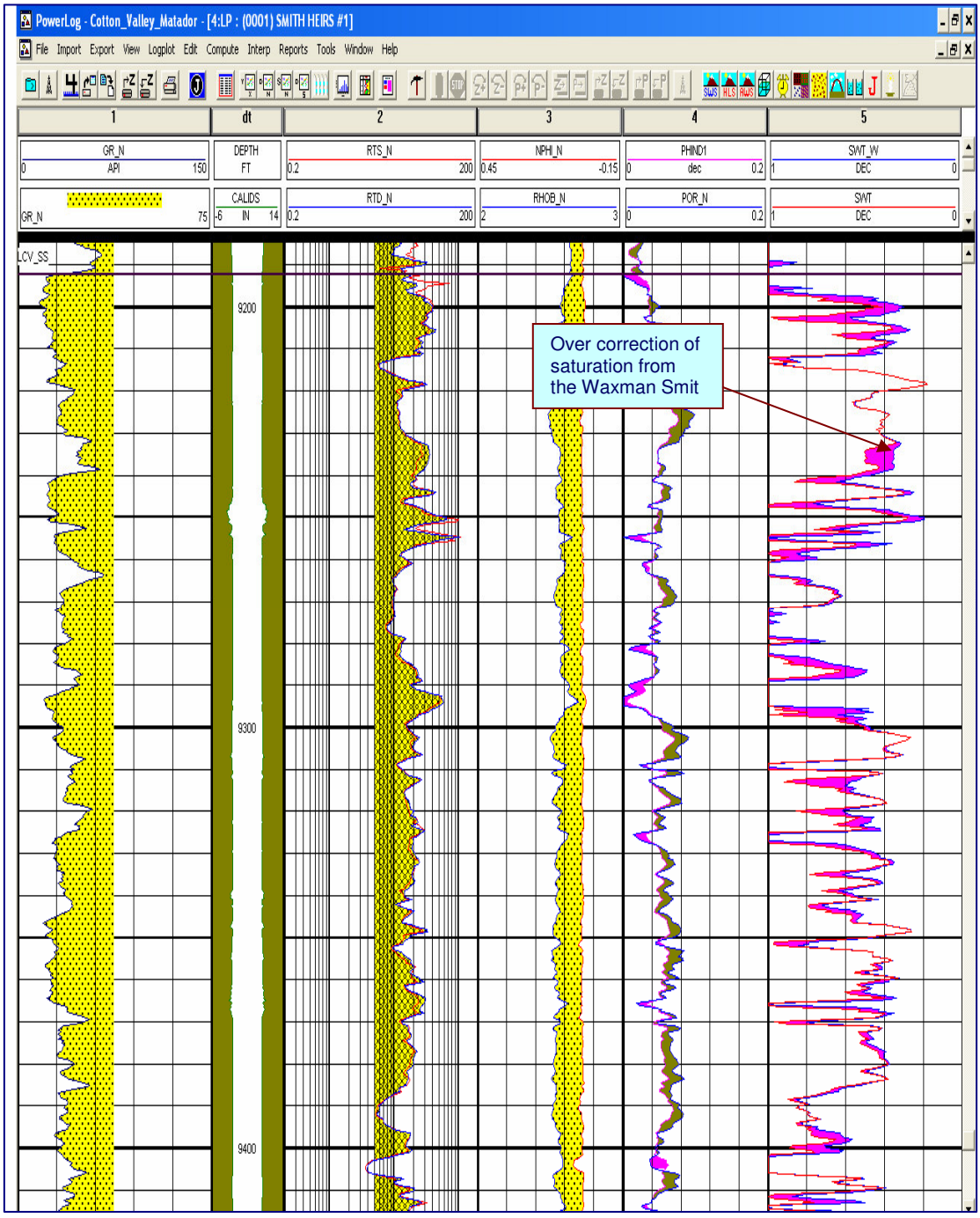

Fig. D6: Comparison of the Waxman Smit and the Dual Water Model.

APPENDIX E

RESERVOIR SIMULATION DATA INPUT

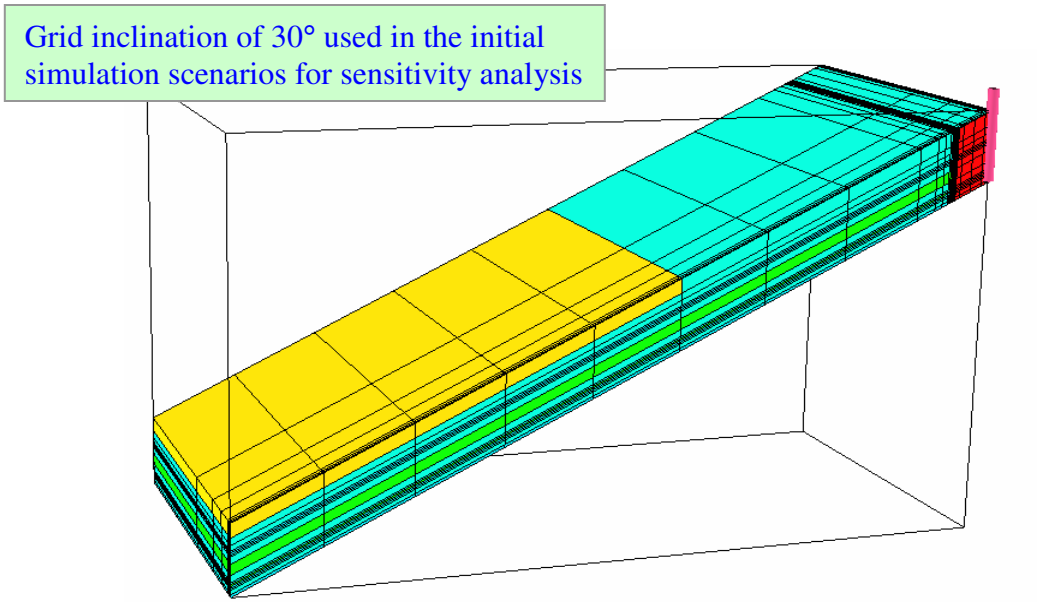

Fig. E1: Grid Configuration for Sensitivity Analysis (30° dip).

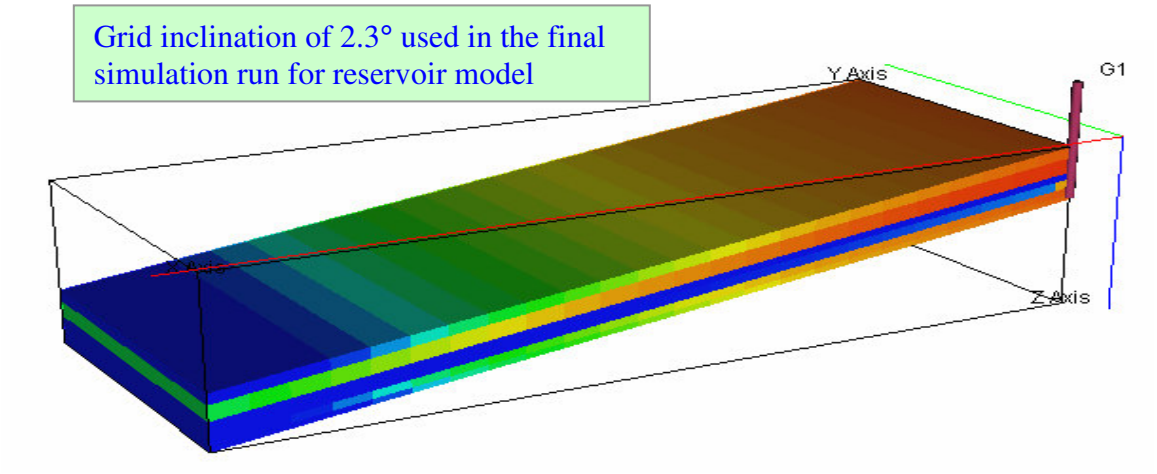

Fig. E2: Grid Configuration for Reservoir Model (2.3° dip).

Reservoir Properties	
Reservoir Fluids	Gas & Water
Maximum Depth	10000 ft
Net Pay Thickness	1000 ft
Original Reservoir Pressure	4500 psi
Formation Permeability	0.002 - 10 md
Gas Specific Gravity	0.65
Water Specific Gravity	1.15
Formation Porosity	2 - 14%
Water Compressibility	3.00E-06
Rock Compressibility	4.00E-06
Reservoir Dimensions	10000 ft x 500 ft x 1000 ft
Grid Dimensions	45x8x15
Hydraulic Fracture Length	500 ft
Fracture Conductivity	250 mDft
Minimum BHP	400 psi

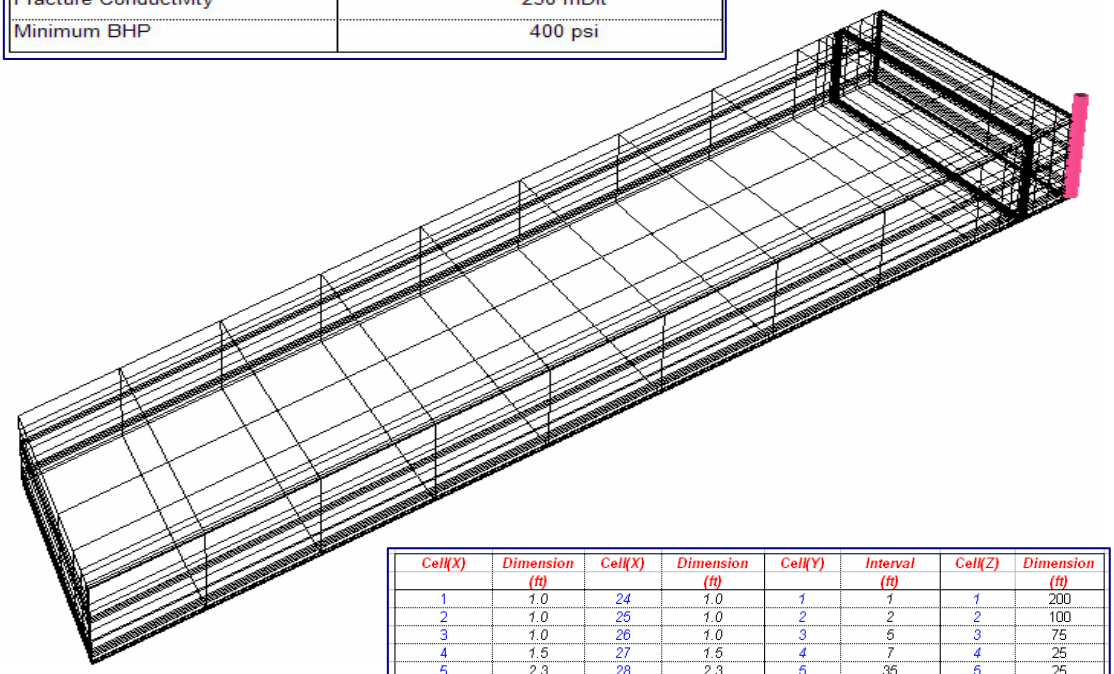

Cell(X)	Dimension (ft)	Cell(X)	Dimension (ft)	Cell(Y)	Interval (ft)	Cell(Z)	Dimension (ft)
1	1.0	24	1.0	1	1	1	200
2	1.0	25	1.0	2	2	2	100
3	1.0	26	1.0	3	5	3	75
4	1.5	27	1.5	4	7	4	25
5	2.3	28	2.3	5	35	5	25
6	3.4	29	3.4	6	50	6	25
7	5.1	30	5.1	7	100	7	100
8	7.7	31	7.7	8	300	8	150
9	11.5	32	11.5			9	100
10	17.3	33	17.3			10	25
11	48.1	34	23.1			11	25
12	150.0	35	75.0			12	25
13	150.0	36	100.0			13	25
14	65.4	37	250.0			14	60
15	11.5	38	1000.0			15	40
16	7.7	39	1100.0				
17	5.1	40	1150.0				
18	3.4	41	1150.0				
19	2.3	42	1150.0				
20	1.5	43	1150.0				
21	1.0	44	1150.0				
22	1.0	45	1150.0				
23	1.0						

Fig. E3: Reservoir and Grid Properties for Sensitivity Analysis.

Reservoir Properties	
Reservoir Fluids	Gas & Water
Maximum Depth	9500 ft
Net Pay Thickness	500 ft
Original Reservoir Pressure	4500 psi
Formation Permeability	0.002 - 2 md
Gas Specific Gravity	0.65
Water Specific Gravity	1.15
Formation Porosity	2 - 12%
Water Compressibility	3.00E-06
Rock Compressibility	4.00E-06
Reservoir Dimensions	25000 ft x 1000 ft x 500 ft
Grid Dimensions	60 x 10 x 6
Hydraulic Fracture Length	500 ft
Fracture Conductivity	250 mDft
Minimum BHP	400 psi

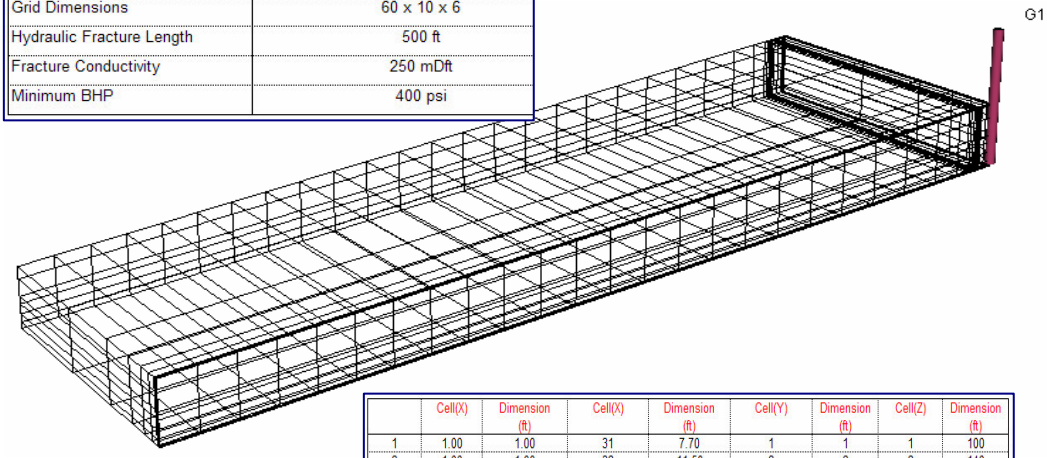

	Cell(X)	Dimension (ft)	Cell(X)	Dimension (ft)	Cell(Y)	Dimension (ft)	Cell(Z)	Dimension (ft)
1	1.00	1.00	31	7.70	1	1	1	100
2	1.00	1.00	32	11.50	2	2	2	140
3	1.00	1.00	33	17.30	3	5	3	60
4	1.50	1.50	34	23.10	4	7	4	80
5	2.30	2.30	35	75.30	5	35	5	70
6	3.40	3.40	36	100.00	6	50	6	50
7	5.10	5.10	37	400.00	7	80		
8	7.70	7.70	38	750.00	8	150		
9	11.50	11.50	39	1050.00	9	270		
10	17.30	17.30	40	1050.00	10	400		
11	48.10	48.10	41	1050.00				
12	150.00	150.00	42	1050.00				
13	150.00	150.00	43	1050.00				
14	65.40	65.40	44	1050.00				
15	11.50	11.50	45	1050.00				
16	7.70	7.70	46	1050.00				
17	5.10	5.10	47	1050.00				
18	3.40	3.40	48	1050.00				
19	2.30	2.30	49	1050.00				
20	1.50	1.50	50	1050.00				
21	1.00	1.00	51	1050.00				
22	1.00	1.00	52	1050.00				
23	1.00	1.00	53	1050.00				
24	1.00	1.00	54	1050.00				
25	1.00	1.00	55	1050.00				
26	1.00	1.00	56	1050.00				
27	1.50	1.50	57	1050.00				
28	2.30	2.30	58	1050.00				
29	3.40	3.40	59	1050.00				
30	5.10	5.10	60	1050.00				

Fig. E4: Reservoir and Grid Properties for Final Reservoir Model.

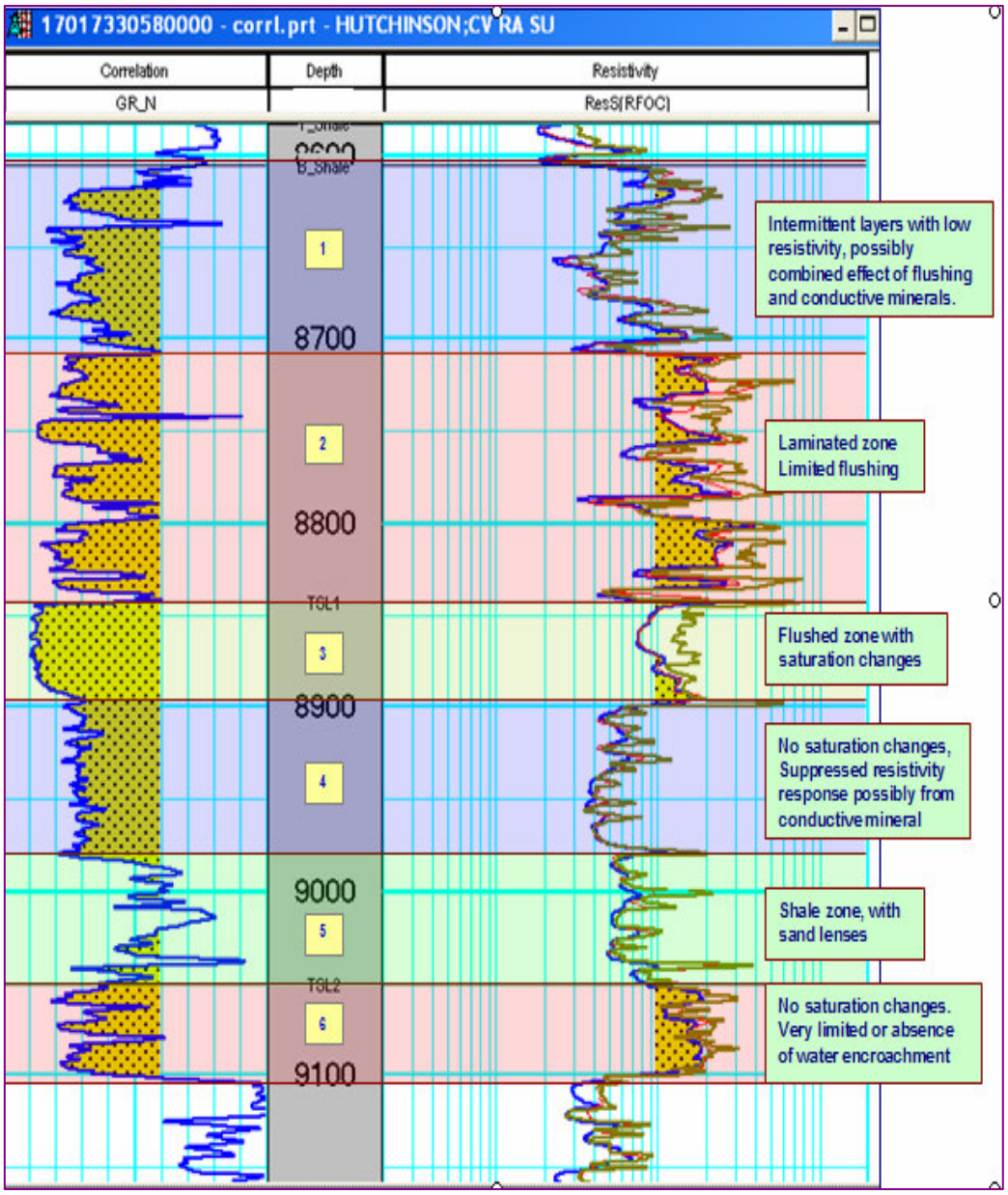

Fig. E5: Reservoir Layering with Flushed Zone for Final Reservoir Model.

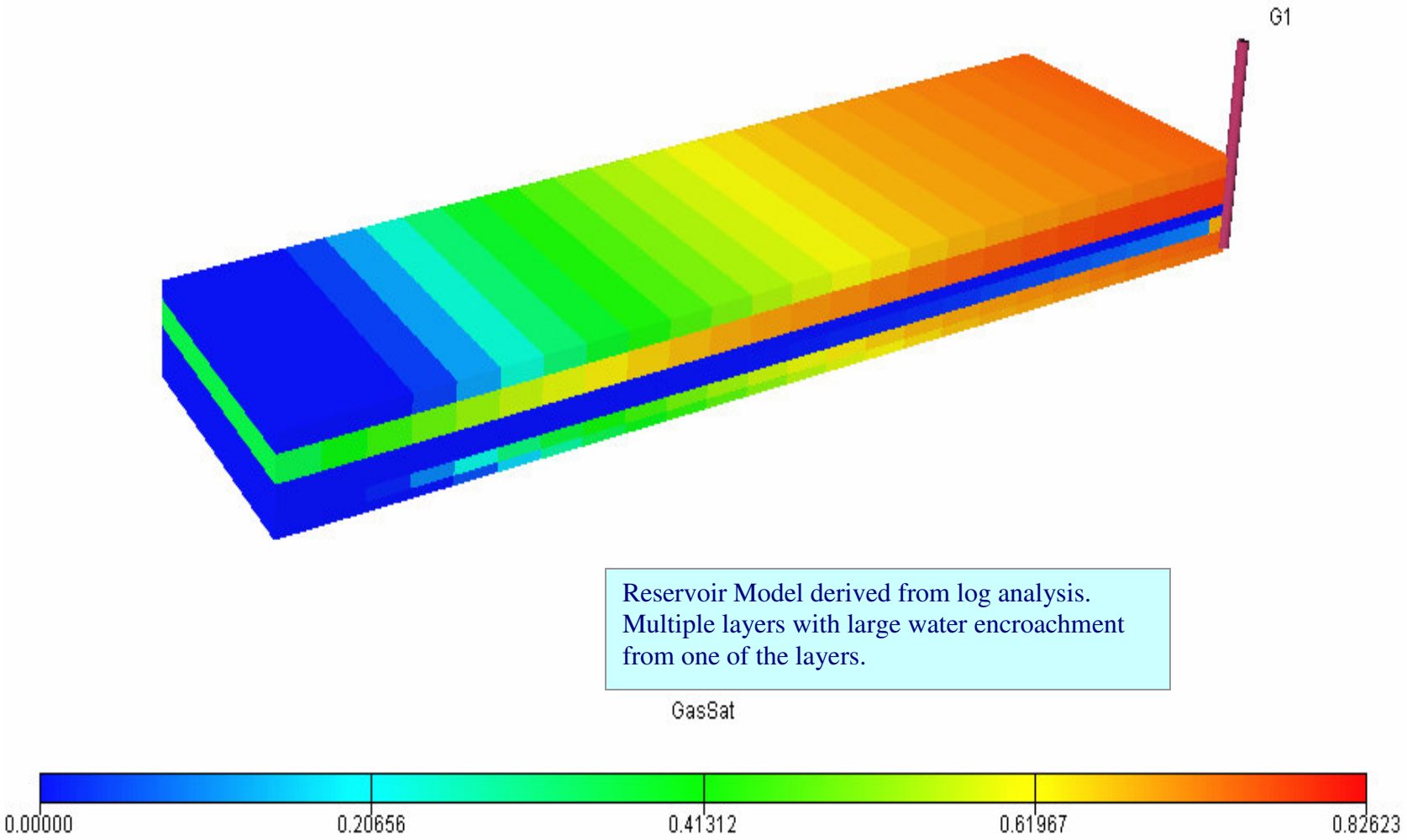

Fig. E6: 3D - Reservoir Configuration with Some Layers Flooded with Water.

Table E1: Gas Relative Permeability (Model 1-5)

Model-1		Model-2		Model-3		Model-4		Model-5	
Sg	Krg	Sg	Krg	Sg	Krg	Sg	Krg	Sg	Krg
0.000	0.000	0.000	0.000	0.000	0.000	0.000	0.000	0.000	0.000
0.011	0.000	0.010	0.000	0.011	0.000	0.010	0.000	0.001	0.000
0.048	0.000	0.020	0.000	0.048	0.000	0.020	0.000	0.002	0.000
0.088	0.000	0.030	0.000	0.088	0.000	0.030	0.000	0.005	0.000
0.140	0.000	0.100	0.000	0.140	0.000	0.100	0.000	0.006	0.000
0.213	0.000	0.160	0.000	0.213	0.000	0.160	0.000	0.018	0.000
0.270	0.076	0.210	0.009	0.270	0.013	0.210	0.013	0.110	0.000
0.330	0.140	0.270	0.066	0.330	0.070	0.270	0.070	0.211	0.000
0.369	0.183	0.390	0.183	0.369	0.185	0.390	0.185	0.314	0.000
0.412	0.223	0.500	0.254	0.412	0.306	0.500	0.306	0.409	0.000
0.480	0.306	0.530	0.289	0.480	0.350	0.530	0.350	0.554	0.008
0.528	0.351	0.590	0.374	0.528	0.427	0.590	0.427	0.602	0.018
0.588	0.418	0.630	0.431	0.588	0.480	0.630	0.480	0.677	0.050
0.680	0.549	0.650	0.480	0.680	0.510	0.650	0.510	0.727	0.140
0.775	0.766	0.723	0.620	0.775	0.631	0.723	0.673	0.782	0.220
0.805	0.883	0.815	0.997	0.805	0.840	0.815	0.997	0.877	0.471
0.821	0.994	0.913	0.000	0.821	1.000	0.913	1.000	0.920	0.726
0.841	1.000			0.841	1.000			0.930	1.000
0.863	1.000			0.863	1.000				
0.910	1.000			0.910	1.000				

Table E2: Water Relative Permeability and Capillary Pressure (Model 1-5)

Model-1			Model-2			Model-3			Model-4			Model-5		
Sw	Krw	Pcow	Sw	Krw	Pcow	Sw	Krw	Pcow	Sw	Krw	Pcow	Sw	Krw	Pcow
0.090	0.000	1647.000	0.012	0.000	6021.000	0.090	0.000	1647.000	0.012	0.000	6021.000	0.070	0.000	10000.000
0.137	0.000	700.000	0.018	0.000	5794.000	0.137	0.000	700.000	0.018	0.000	5794.000	0.080	0.000	4786.000
0.159	0.000	500.000	0.087	0.000	3696.000	0.159	0.000	500.000	0.087	0.000	3696.000	0.123	0.000	1950.000
0.179	0.011	350.000	0.185	0.011	1927.000	0.179	0.000	350.000	0.185	0.000	1927.000	0.218	0.000	741.000
0.195	0.013	250.000	0.277	0.037	1063.000	0.195	0.000	250.000	0.277	0.000	1063.000	0.273	0.000	513.000
0.225	0.025	175.000	0.350	0.064	700.000	0.225	0.000	175.000	0.350	0.000	700.000	0.323	0.000	427.000
0.320	0.059	100.000	0.370	0.067	608.000	0.320	0.000	100.000	0.370	0.000	608.000	0.398	0.000	355.000
0.412	0.084	70.000	0.410	0.084	500.000	0.412	0.000	70.000	0.410	0.000	500.000	0.446	0.000	324.000
0.472	0.109	58.000	0.470	0.109	397.000	0.472	0.000	58.000	0.470	0.000	397.000	0.591	0.000	282.000
0.520	0.134	50.000	0.500	0.120	350.000	0.520	0.000	50.000	0.500	0.000	350.000	0.686	0.007	275.000
0.588	0.176	38.000	0.610	0.176	250.000	0.588	0.000	38.000	0.610	0.000	250.000	0.789	0.078	234.000
0.631	0.209	31.000	0.730	0.243	175.000	0.631	0.040	31.000	0.730	0.040	175.000	0.890	0.200	174.000
0.670	0.255	26.000	0.790	0.283	146.000	0.670	0.096	26.000	0.790	0.096	146.000	0.936	0.300	135.000
0.730	0.330	20.000	0.840	0.330	125.000	0.730	0.166	20.000	0.840	0.166	125.000	0.982	0.480	87.000
0.787	0.400	16.000	0.900	0.417	100.000	0.787	0.274	16.000	0.900	0.274	100.000	0.994	0.632	74.000
0.860	0.527	11.000	0.970	0.603	50.000	0.860	0.497	11.000	0.970	0.497	50.000	0.995	0.673	60.000
0.912	0.669	8.000	0.980	0.669	37.000	0.912	0.535	8.000	0.980	0.535	37.000	0.998	0.751	37.000
0.952	0.807	6.000	0.990	0.807	20.000	0.952	0.605	6.000	0.990	0.605	20.000	0.999	0.907	20.000
0.989	0.980	3.000	1.000	1.000	0.000	0.989	0.750	3.000	1.000	0.750	0.000	1.000	1.000	0.000
1.000	1.000	0.000				1.000	1.000	0.000						

Table E3: Fluid Property - Formation Volume Factor and Viscosity

Pressure (Psia)	Bg (bbl/Mscf)	Visc (cP)
14.7	236.19	0.0142
214.7	16.03	0.0143
414.7	8.23	0.0144
614.7	5.5	0.0146
714.7	4.71	0.0148
814.7	4.12	0.0149
914.7	3.65	0.015
1014.7	3.28	0.0152
2014.7	1.6	0.017
3014.7	1.08	0.0194
4014.7	0.84	0.0221
5014.7	0.71	0.0248
6014.7	0.63	0.0273
6114.7	0.62	0.0276
7014.7	0.58	0.0296
8014.7	0.54	0.0319
9014.7	0.51	0.034

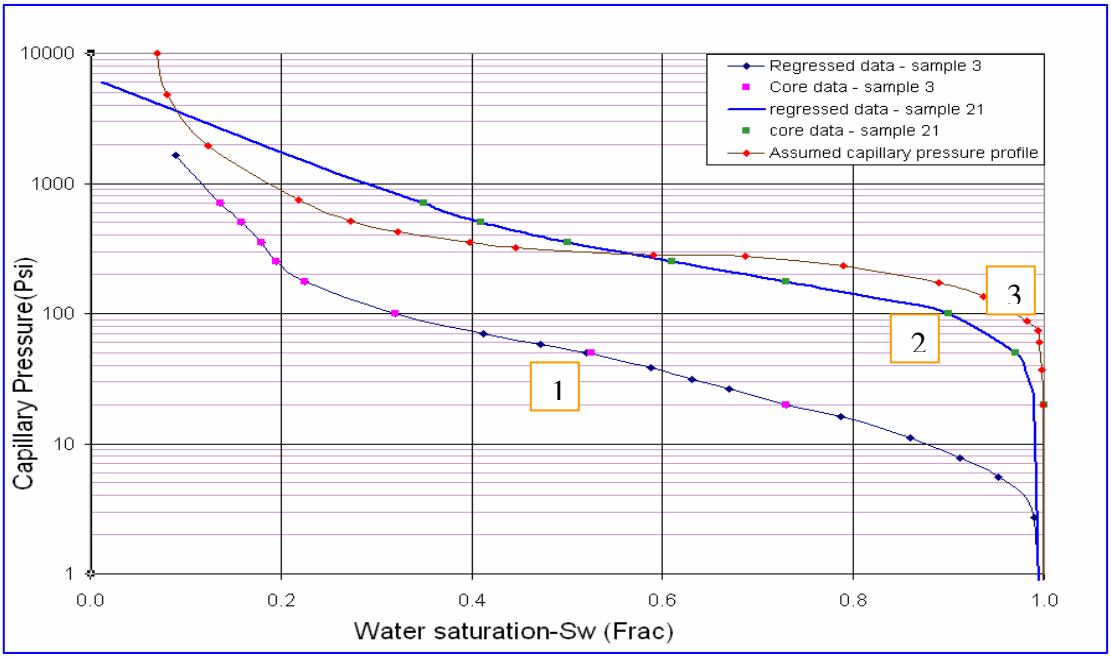

Fig. E7: Capillary Pressure Profile (Model 1-3).

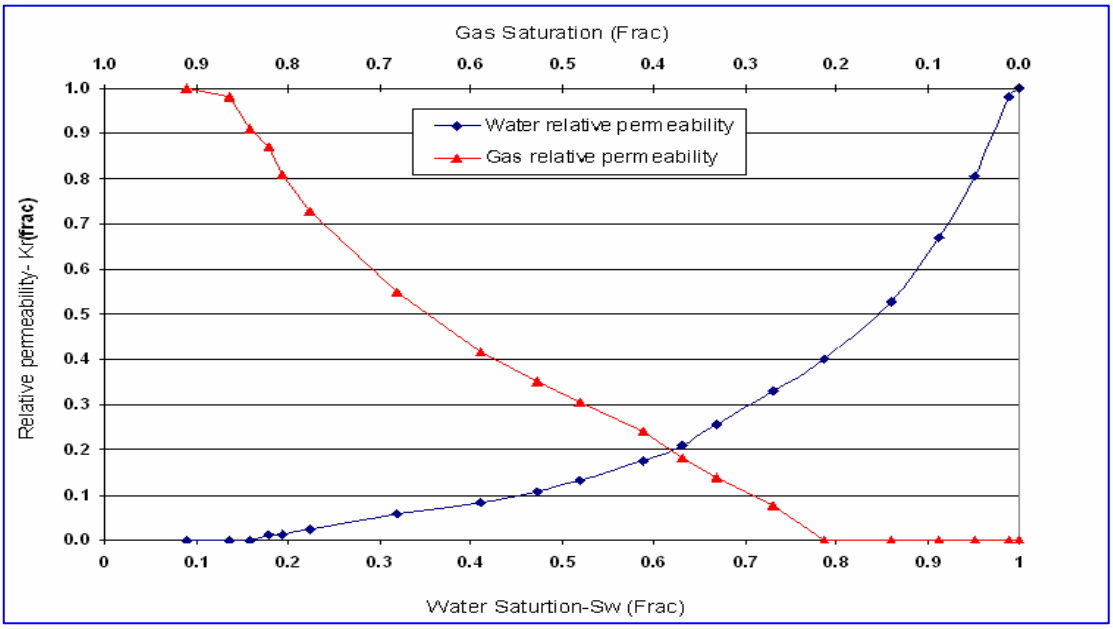

Fig. E8: Relative Permeability Profile for Model 1.

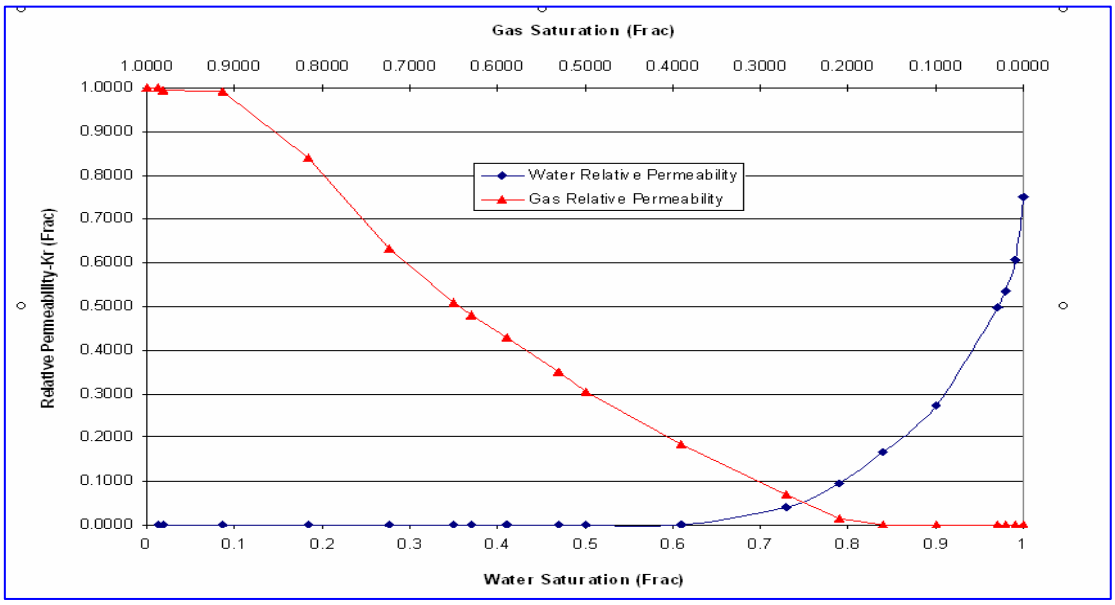

Fig. E9: Relative Permeability Profile for Model 2.

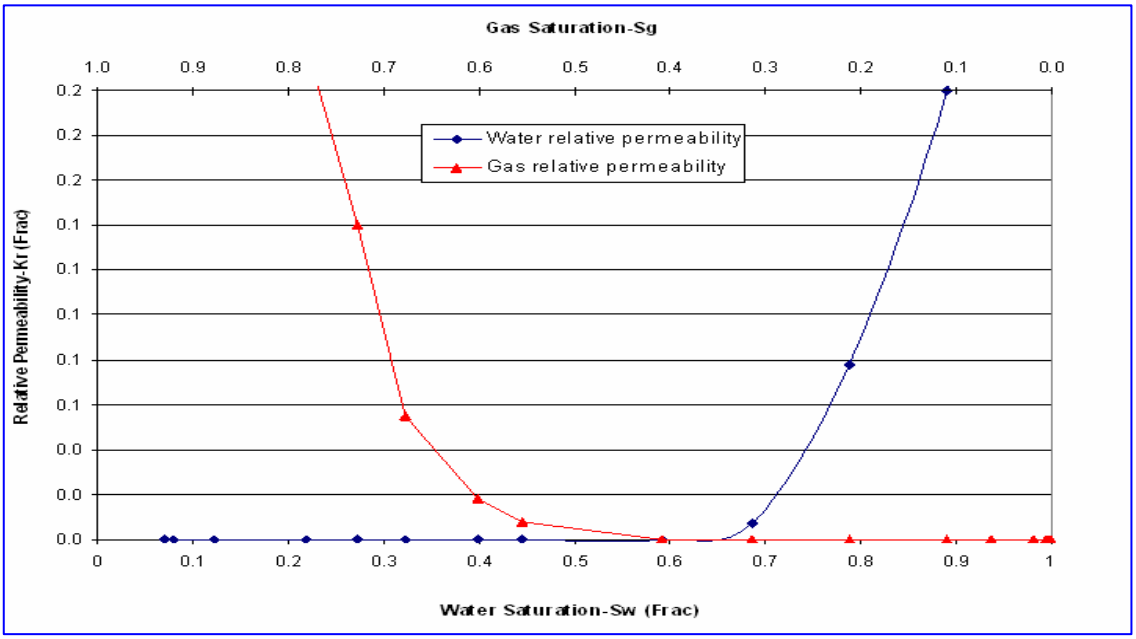

Fig. E10: Relative Permeability Profile for Model 3.

Table E4: Sensitivity Analysis on Reservoir Parameters with Different Modeling Scenarios (Case: 1-14, 18)

Layers	Absolute Permeability K (mD)	Porosity ϕ (Frac)	Simulation Cases	Transmissibility Z-direction Tz	Capillary Pressure Pc (psi)	Relative Permeability Kr (Frac)	GWC (ft)	Gas Flow rate Qg (MMcf/d)
1	0.03	0.04	2	**>0**	**Model-1**	**Model-1**	**200**	**20**
2	0.09	0.12	1	"	"	"	600	"
3	0.06	0.09	3	"	"	"	20	"
4	0.002	0.02	4	"	"	"	200	14
5	0.004	0.03	5	"	"	"	"	8
6	0.04	0.04	6	"	"	Model-2	200	20
7	0.07	0.06	7	"	"	"	20	14
8	0.1	0.14	8	**>0**	**Model-2**	**Model-1**	**2000**	**20**
9	0.08	0.07	9	"	"	"	600	"
10	0.03	0.04	10	"	"	"	200	"
11	0.1	0.08	11	"	"	"	2000	14
12	0.006	0.03	12	"	"	"	"	8
13	0.08	0.06	13	"	"	Model-2	2000	20
14	0.04	0.04	14	"	"	"	200	14
15	0.002	0.03	18	"	Model-3	Model-3	3450	20

Table E4 (Continued): Sensitivity Analysis on Reservoir Parameters with Different Modeling Scenarios (Case: 15 - 17)

Layers	Absolute Permeability K (mD)	Porosity ϕ (Frac)	Capillary Pressure Pc (psi)	Relative Permeability Kr (Frac)	Simulation Cases	Transmissibility Z-direction Tz	GWC (ft)	Gas Flow rate Qg (MMcf/d)
1	0.03	0.04	Model-1	Model-1	15	**0**	**200**	**20**
2	0.09	0.12	Model-2	Model-2	16	0	200	14
3	0.06	0.09	Model-2	Model-1	17	0	200	8
4	0.002	0.02	Model-3	Model-3				
5	0.004	0.03	Model-1	Model-2				
6	0.04	0.04	Model-2	Model-2				
7	0.07	0.06	Model-2	Model-1				
8	0.1	0.14	Model-1	Model-1				
9	0.08	0.07	Model-2	Model-1				
10	0.03	0.04	Model-1	Model-2				
11	0.1	0.08	Model-2	Model-1				
12	0.006	0.03	Model-3	Model-3				
13	0.08	0.06	Model-2	Model-1				
14	0.04	0.04	Model-1	Model-2				
15	0.002	0.03	Model-3	Model-3				

Table E4 (Continued): Sensitivity Analysis on Reservoir Parameters with Different Modeling Scenarios (Case: 19 - 24)

Layers	Absolute Permeability K (mD)	Porosity ϕ (Frac)	Capillary Pressure P_c (psi)	Relative Permeability K_r (Frac)	GWC (ft)	Simulation Cases	GWC (ft)	Transmissibility Z-direction Tz	Gas Flow rate Q_g (MMcf/d)
1	0.03	0.04	Model-1	Model-1		19	**200**	**0**	**20**
2	0.09	0.12	Model-2	Model-2		20	200	"	14
3	0.06	0.09	Model-2	Model-1		21	200	"	8
4	0.002	0.02	Model-3	Model-3	3450	22	**2000**	**"**	**20**
5	0.004	0.03	Model-1	Model-2		23	2000	"	14
6	**6**	0.04	Model-2	Model-1		24	2000	"	8
7	0.07	0.06	Model-1	Model-2					
8	0.1	0.14	Model-1	Model-1					
9	0.08	0.07	Model-2	Model-1					
10	0.03	0.04	Model-1	Model-2					
11	**10**	0.08	Model-2	Model-1					
12	0.006	0.03	Model-3	Model-3	3450				
13	0.08	0.06	Model-2	Model-1					
14	0.04	0.04	Model-1	Model-2					
15	0.002	0.03	Model-3	Model-3	3450				

APPENDIX F

COMPOSITE PLOT OF LOG DATA ANALYSIS RESULTS

LOG PRESENTATION

Track-1 (Gamma Ray) - **Color** : Blue,

Scale: **(Linear)** (0 – 150) API units

Shading: Dotted yellow - Sand Lithology

Track-2 (Resistivity Logs) - **Color**: Red (Shallow resistivity),

Blue (Deep resistivity)

Scale: (Logarithmic) (0.2 – 200) Ohm-meter

Shading: Dotted yellow - Resistivity pay

Track-3 (Density, Neutron) - **Color**: Green (Neutron), Blue (Density)

Scale: (Linear)

Neutron: (0.51 – (-0.09)) fraction

Density: (1.8 – 2.8) g/cc

Shading: Red – Sand

Dotted gray - Shale

Track-4 - **Scale: (Linear)**

(Sand, Shale, Gas and Water) Volume (0 - 1.0) fraction

Shading: Red – Gas volume

Blue – Water volume

Yellow - Sand volume

Dotted gray - Shale

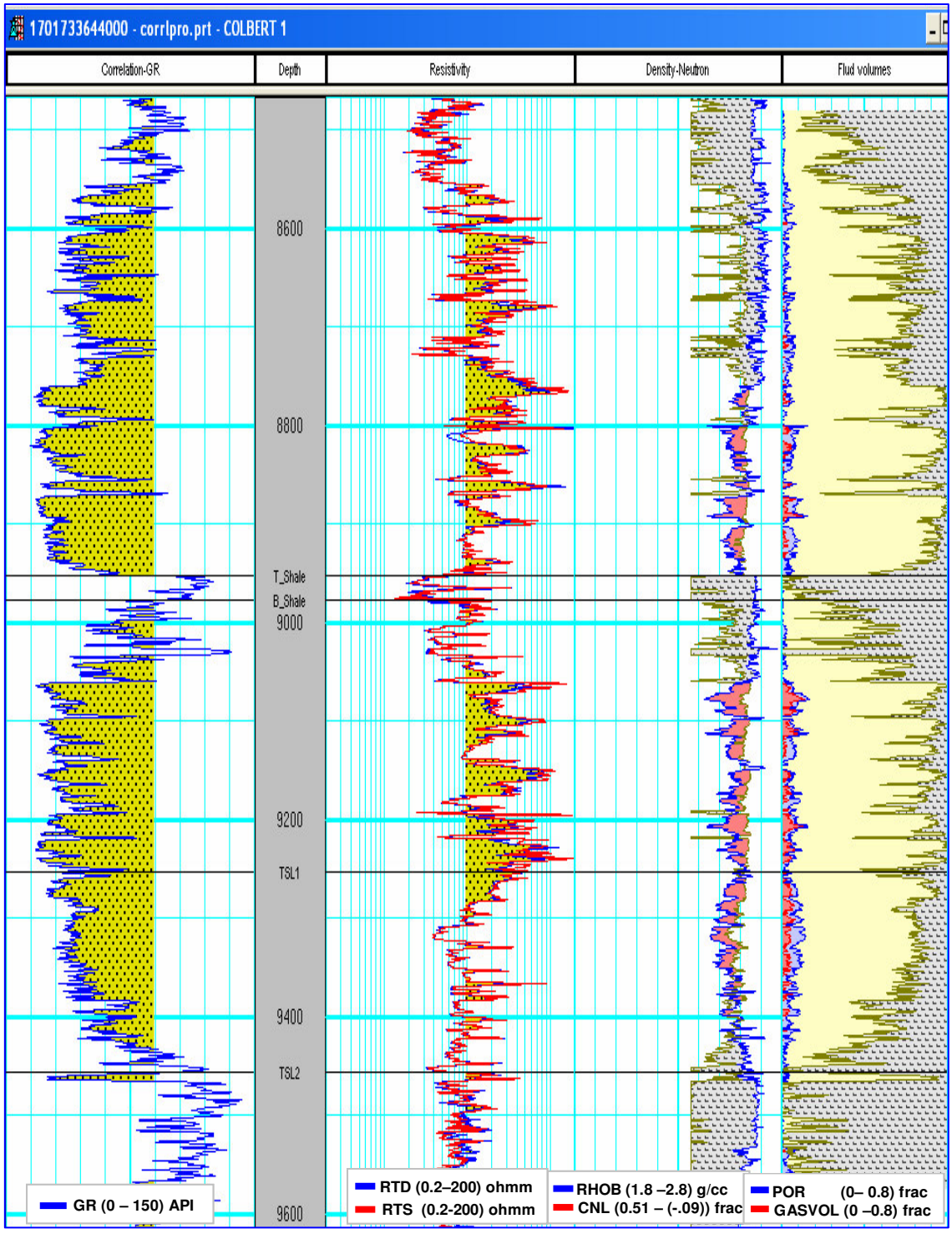

Fig. F1: Log Analysis Results (Colbert 1).

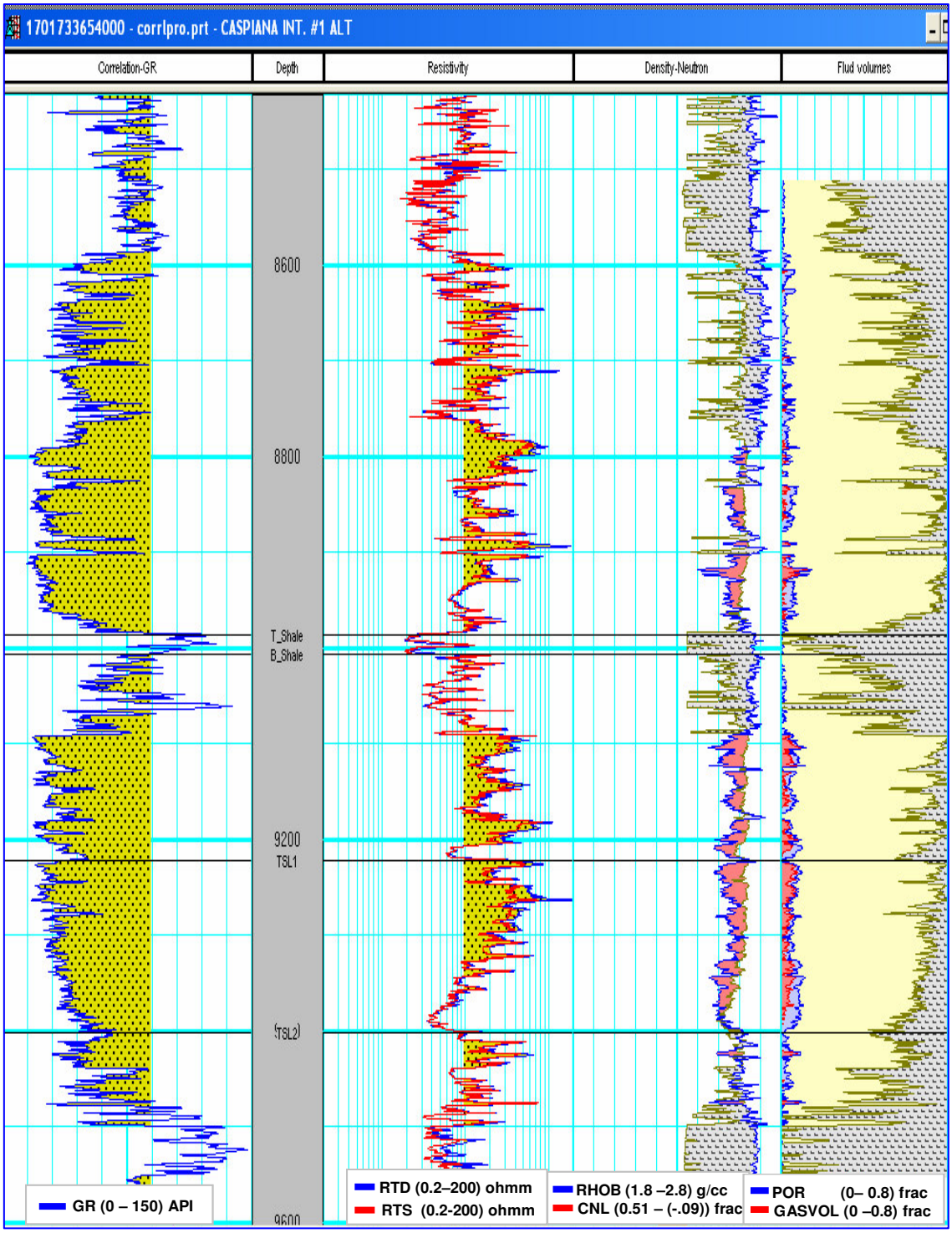

Fig. F2: Log Analysis Results (Caspiana Int. #1 Alt).

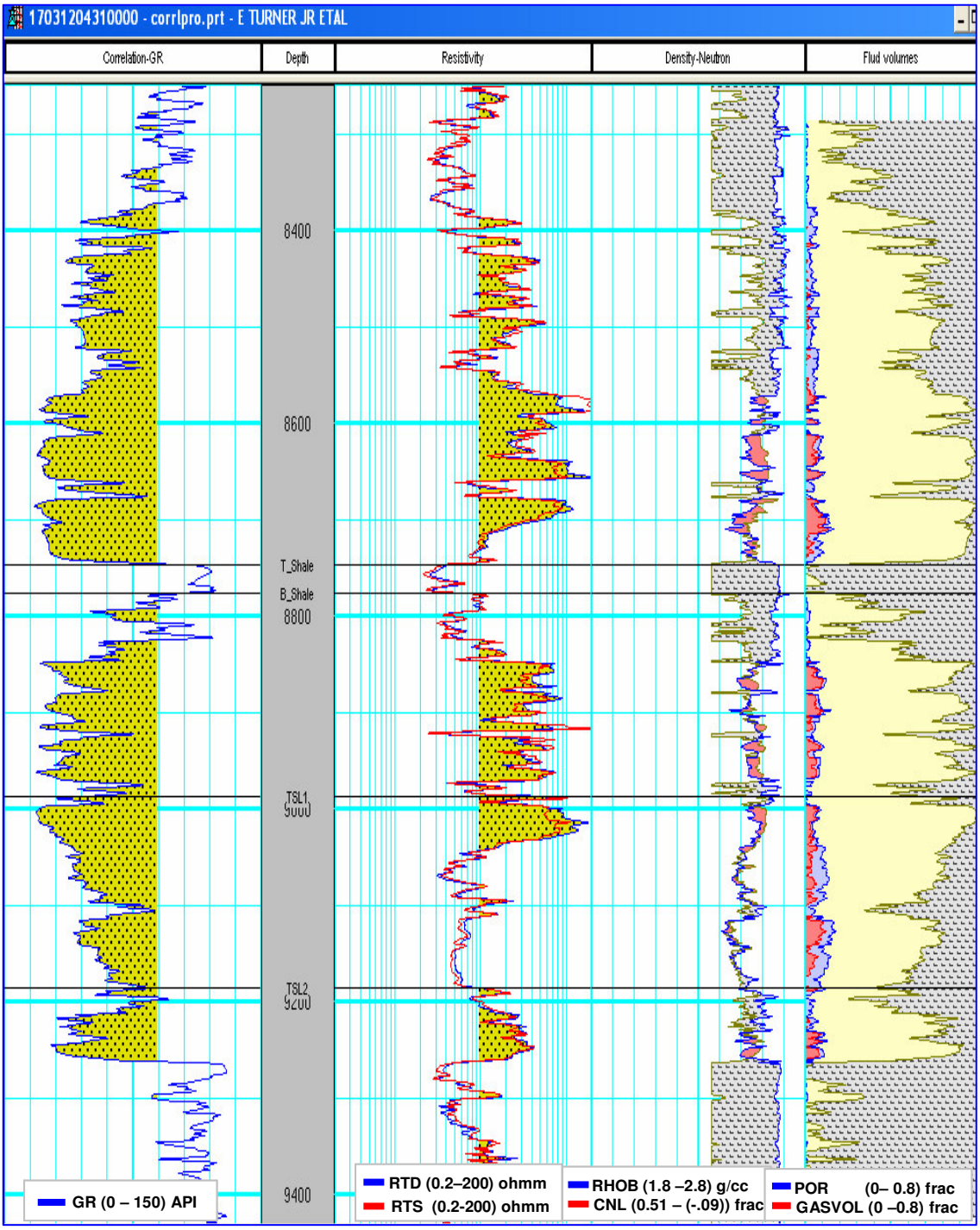

Fig. F3: Log Analysis Results (E. Turner Jr. Etal).

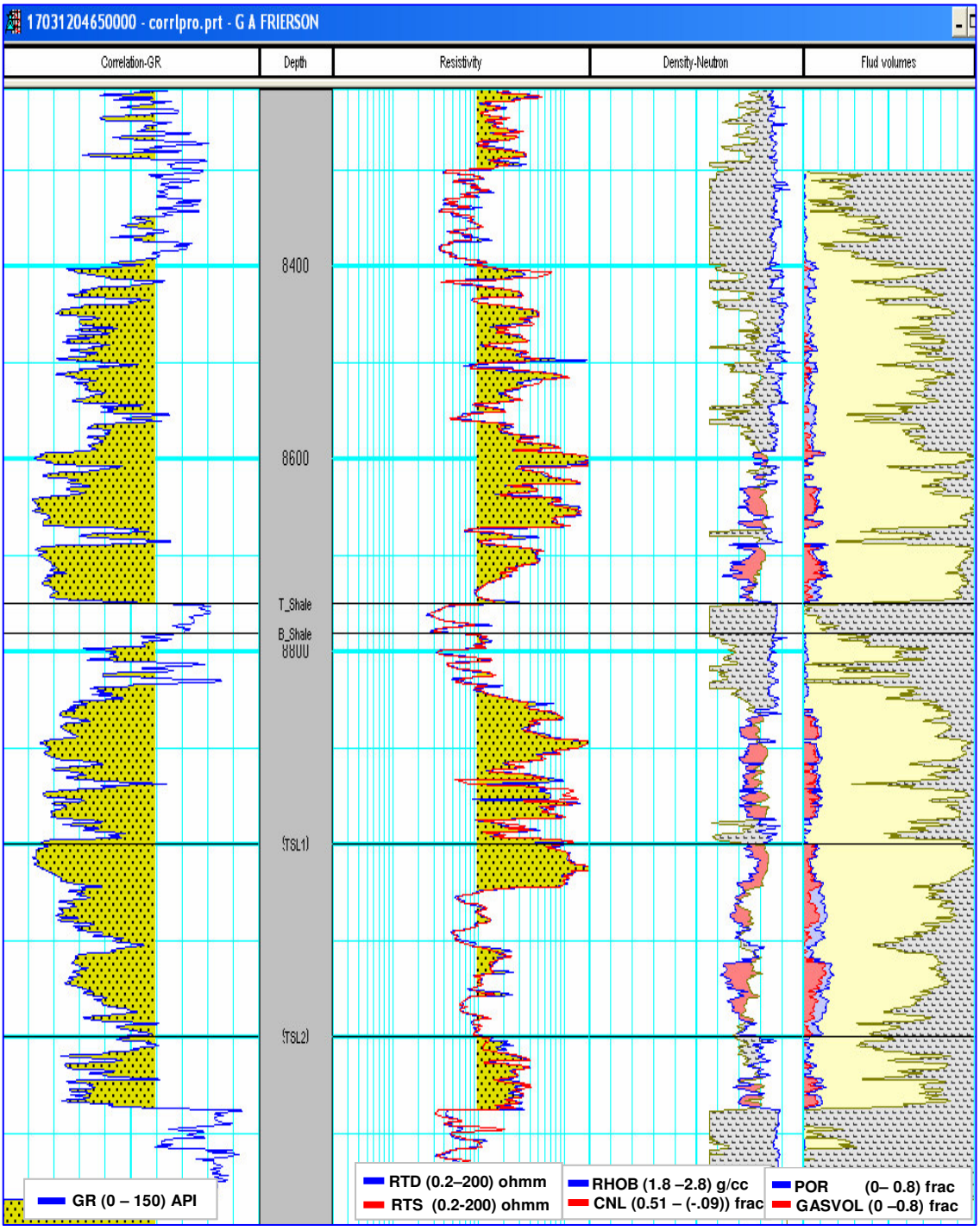

Fig. F4: Log Analysis Results (G.A. Frierson).

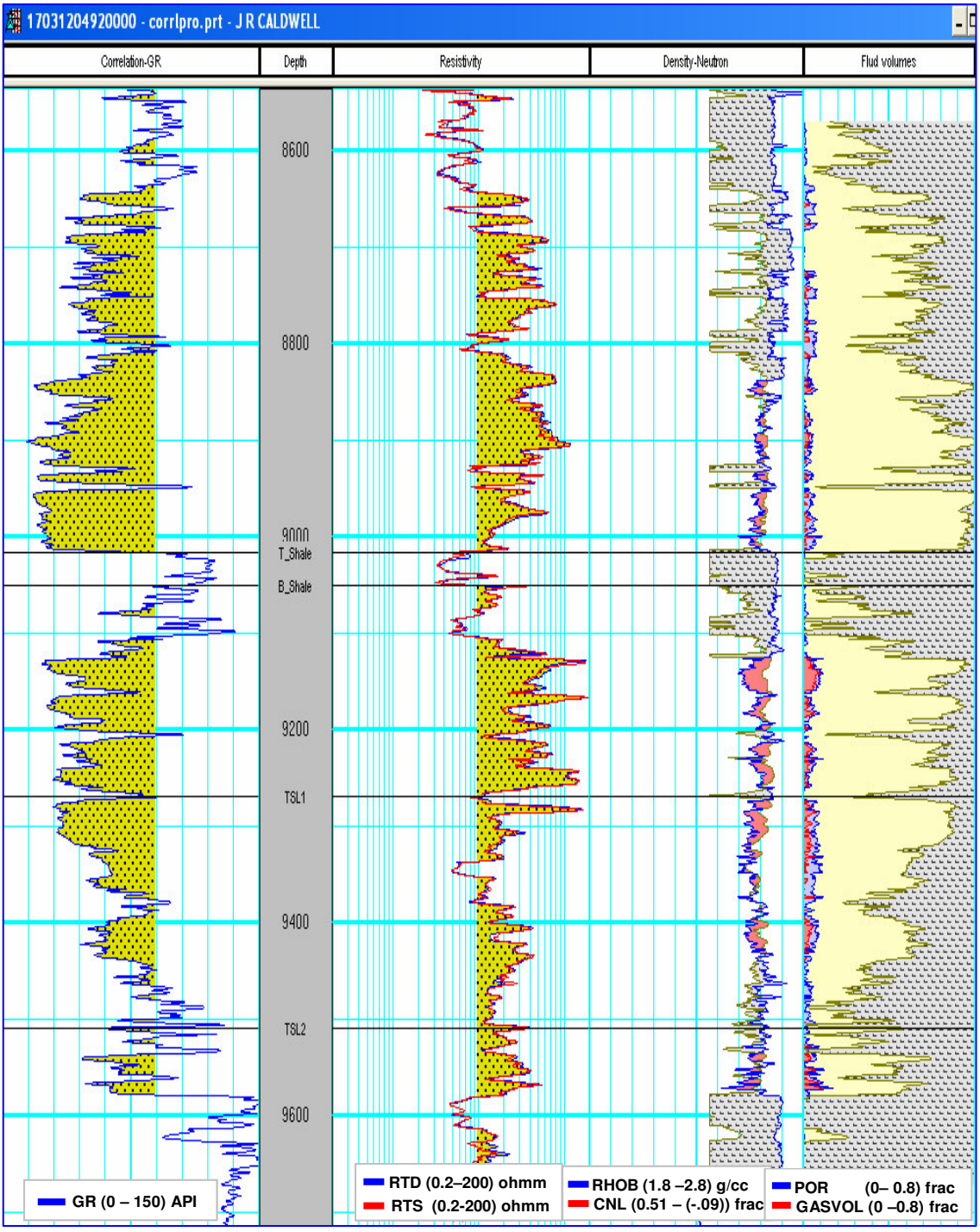

Fig. F5: Log Analysis Results (J.R. Caldwell).

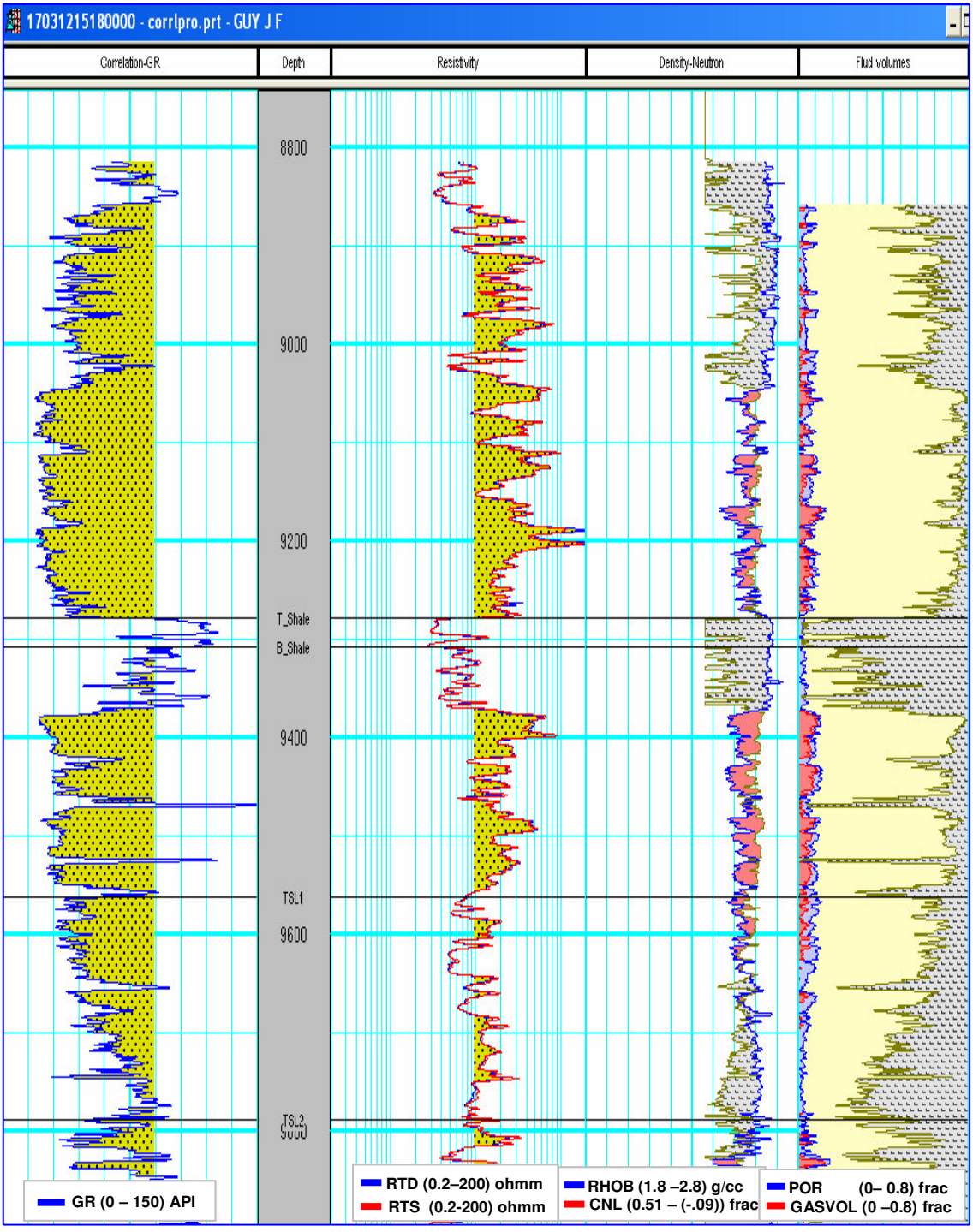

Fig. F6: Log Analysis Results (Guy J. F.).

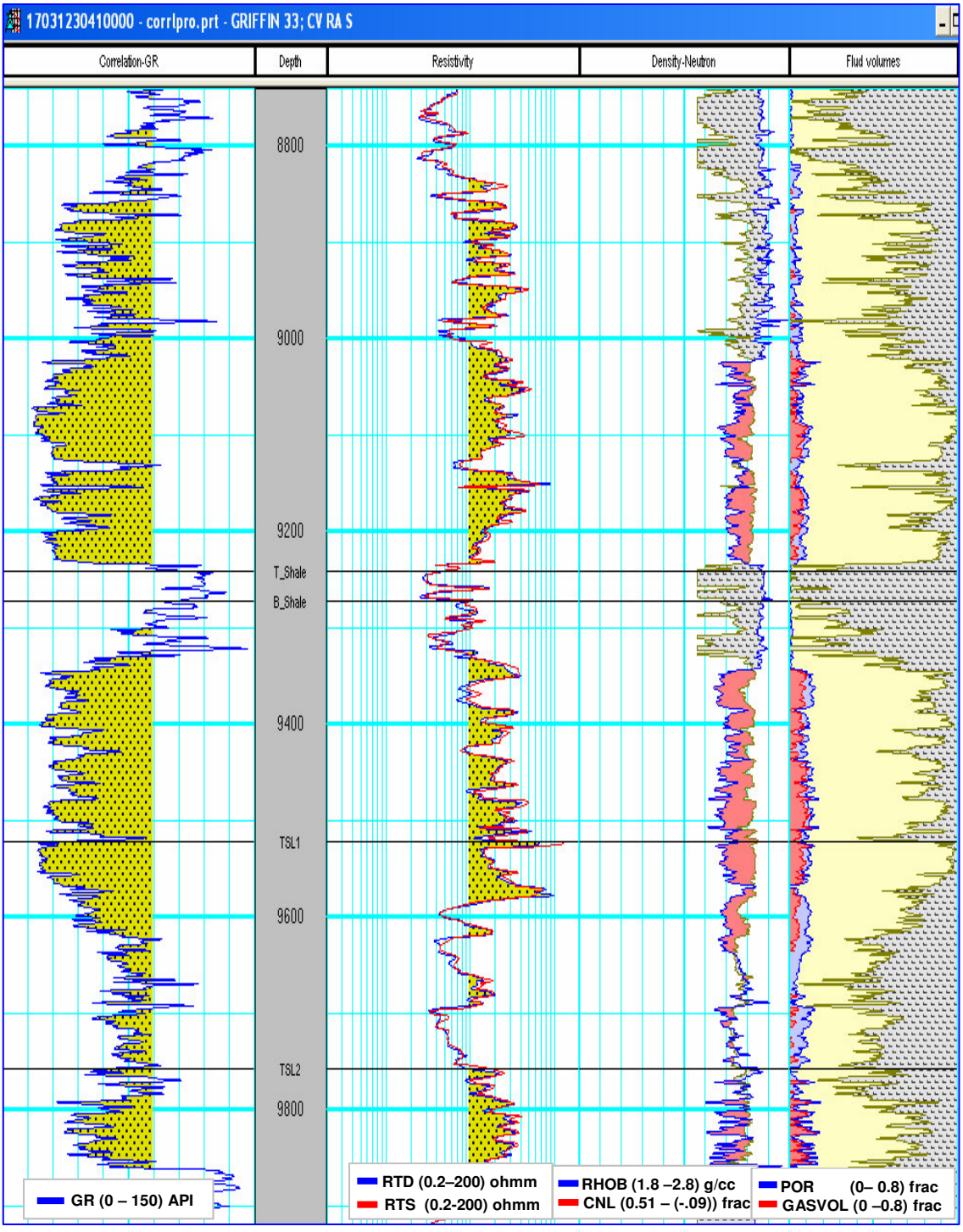

Fig. F7: Log Analysis Results (Griffin 33; CV RA S).

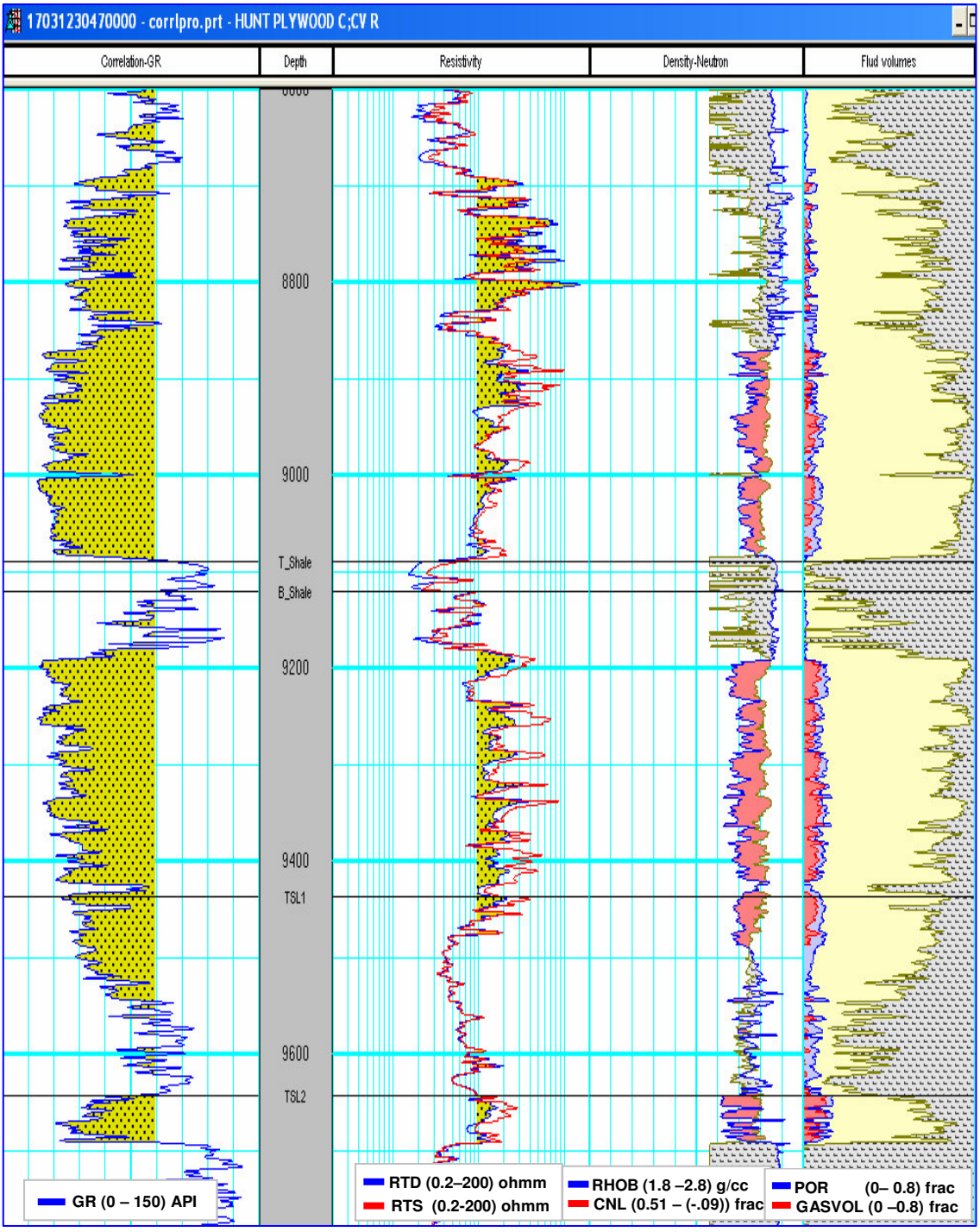

Fig. F8: Log Analysis Results (Hunt Plywood C; CV R).

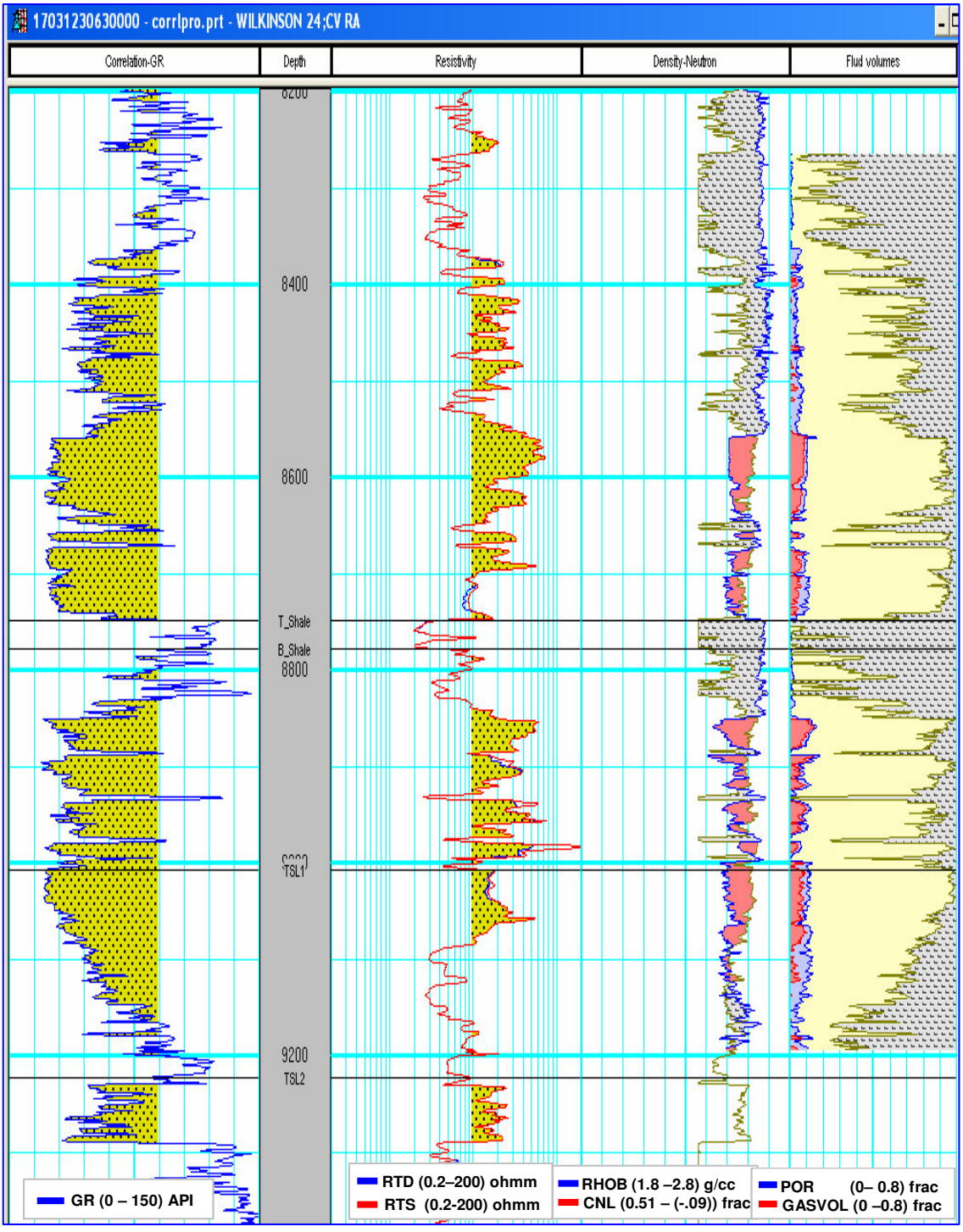

Fig. F9: Log Analysis Results (Wilkinson 24; CV RA).

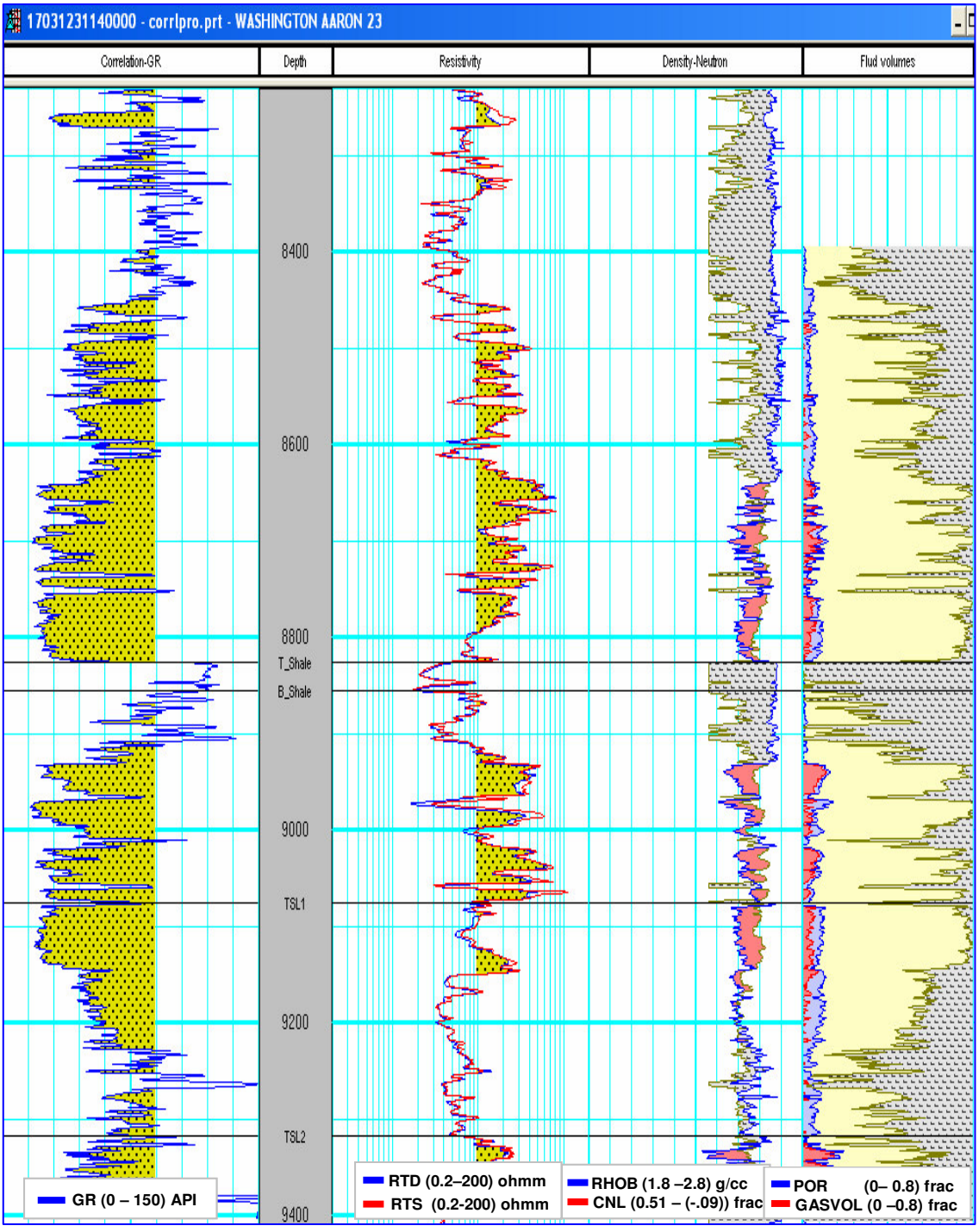

Fig. F10: Log Analysis Results (Washington Aaron 23).

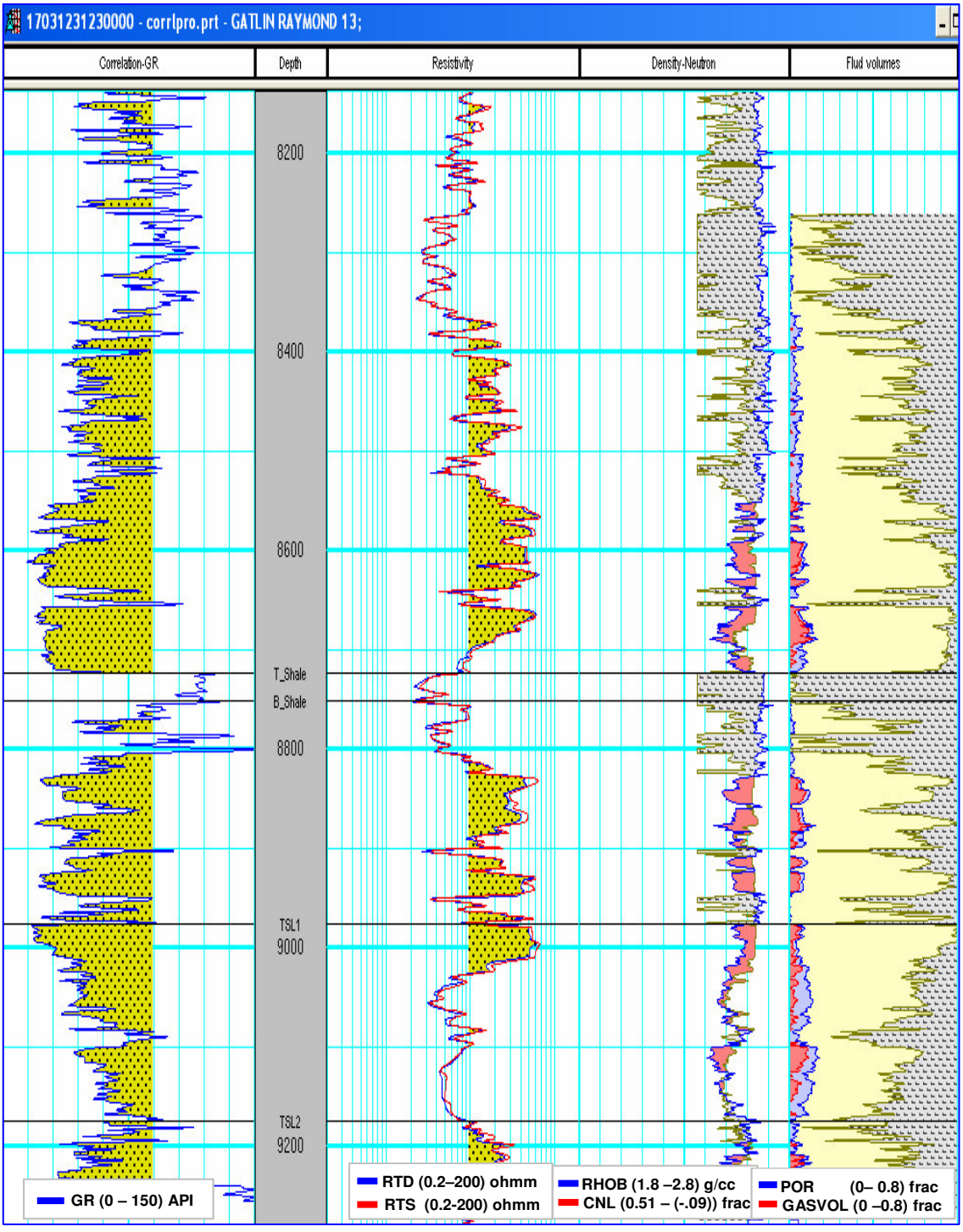

Fig. F11: Log Analysis Results (Gatlin Raymond 13).

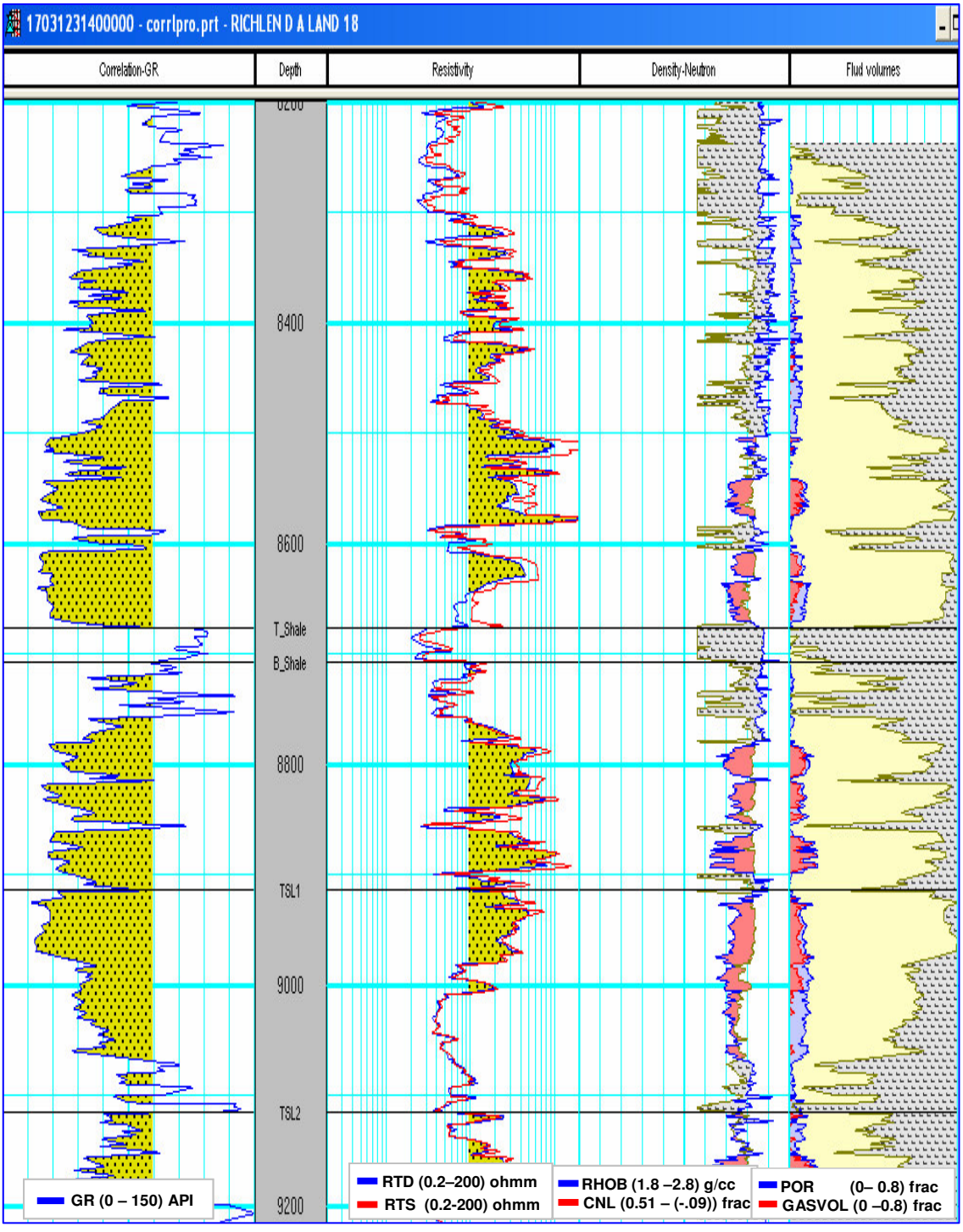

Fig. F12: Log Analysis Results (Richlend A. Land 18).

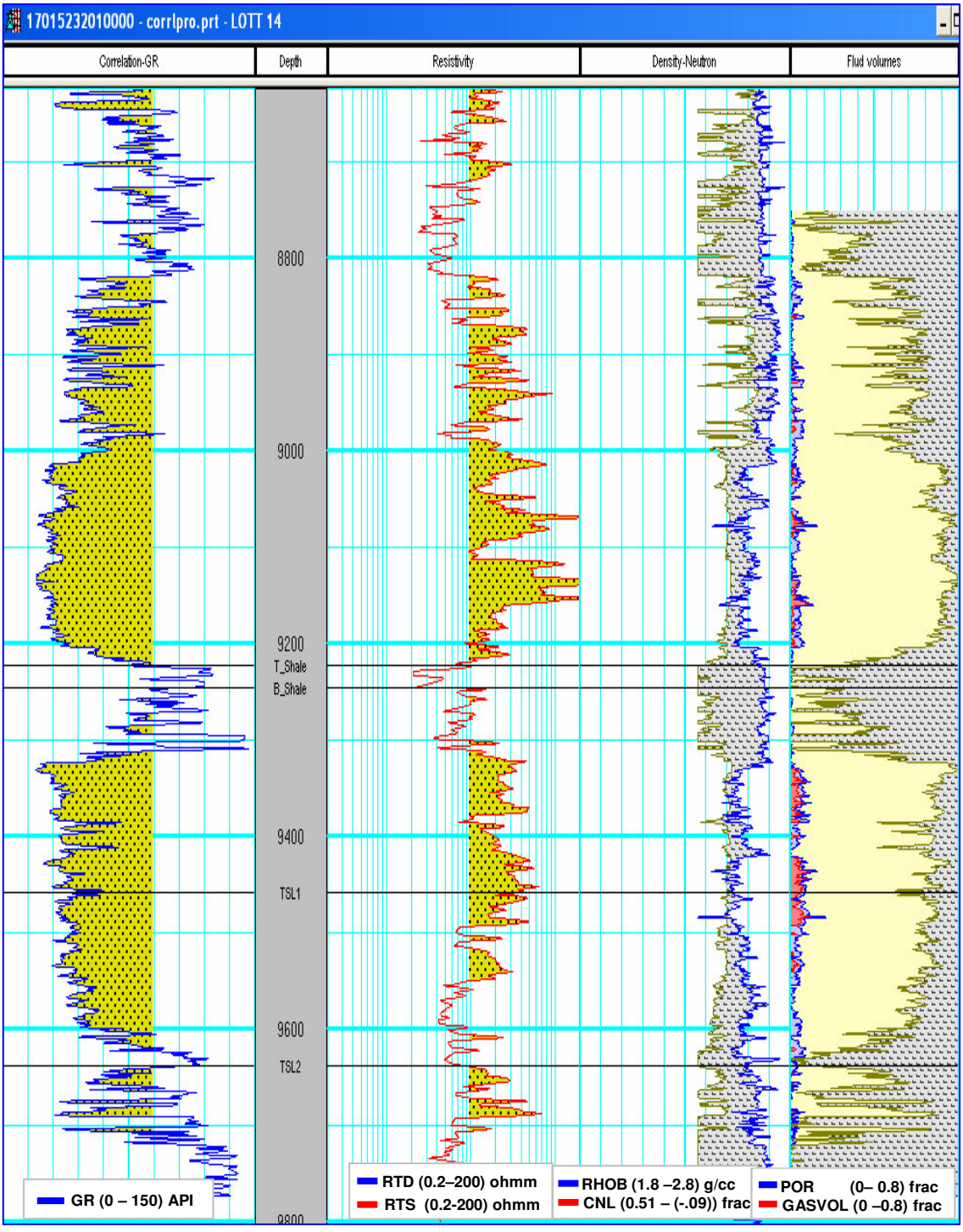

Fig. F13: Log Analysis Results (Lott 14).

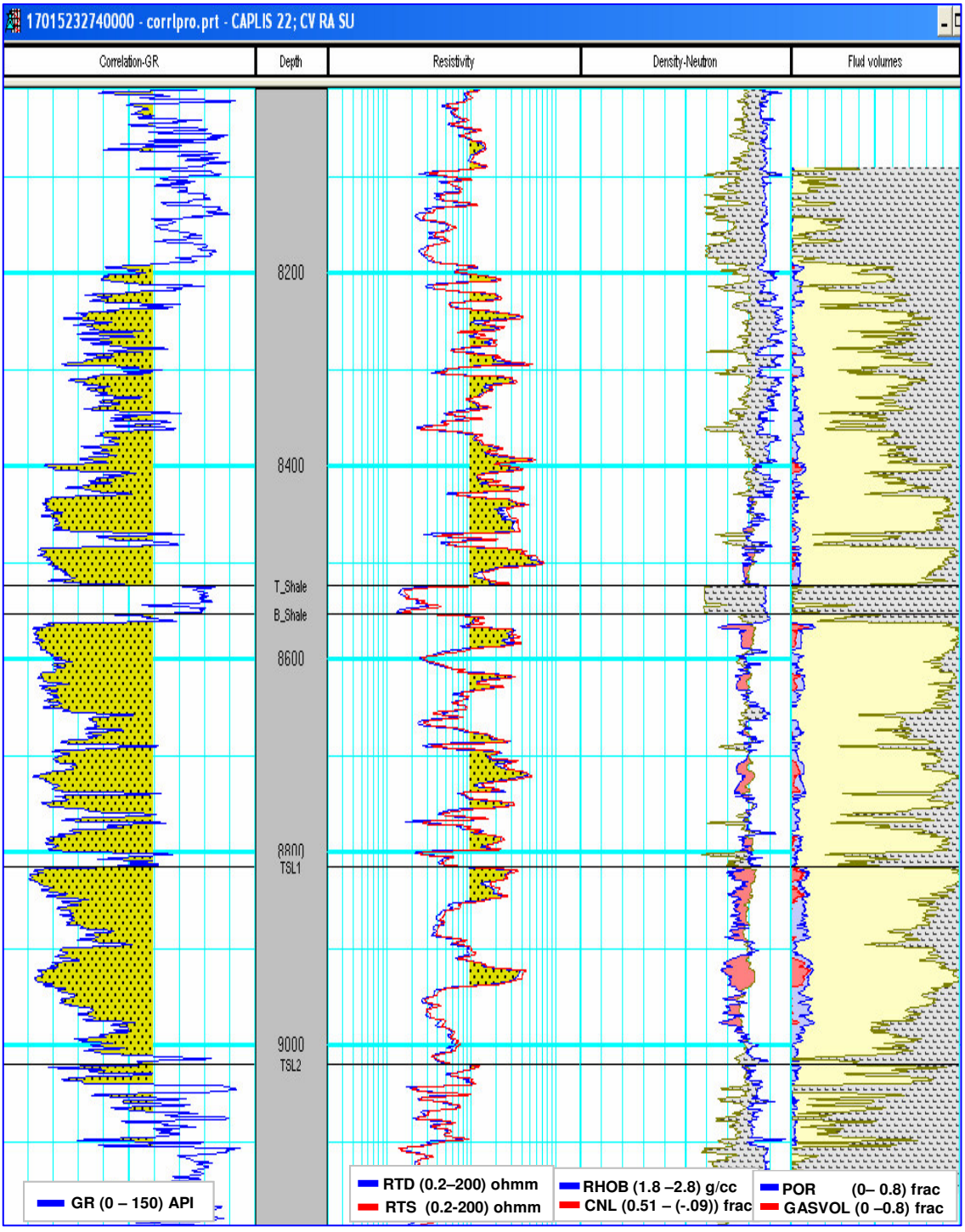

Fig. F14: Log Analysis Results (Caplis 22; CV RA SU).

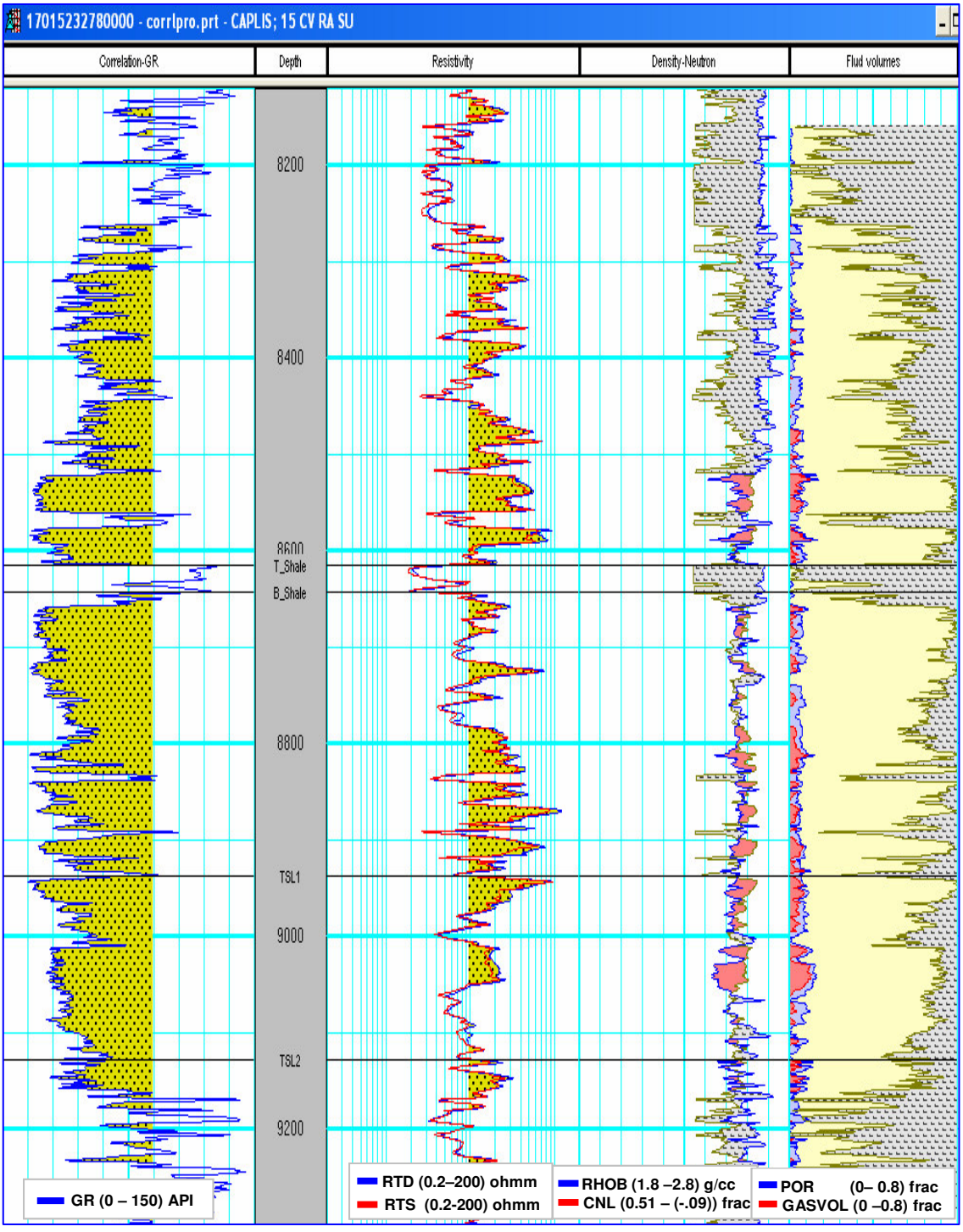

Fig. F15: Log Analysis Results (Caplis 15; CV RA SU).

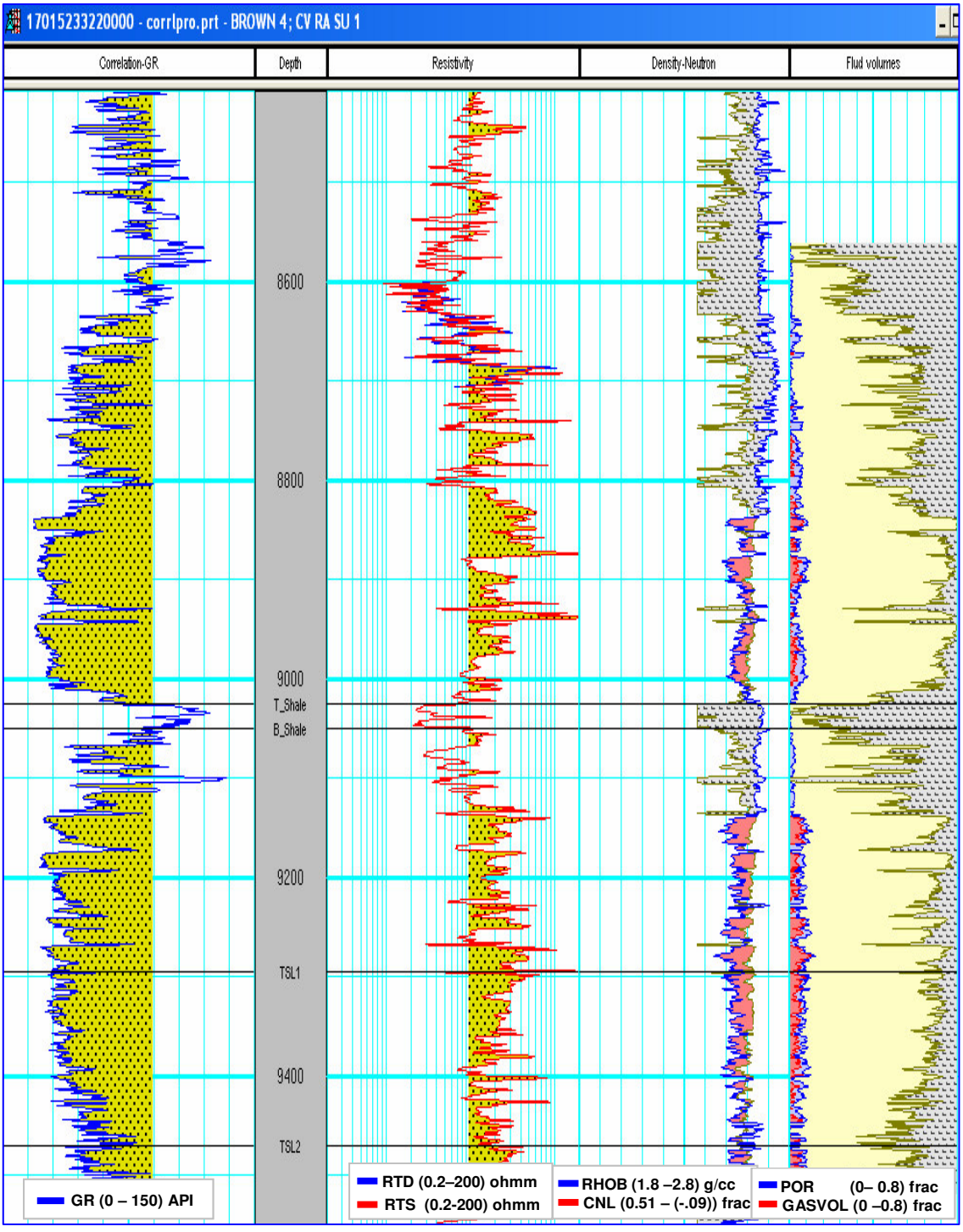

Fig. F16: Log Analysis Results (Brown 4; CV RA SU 1).

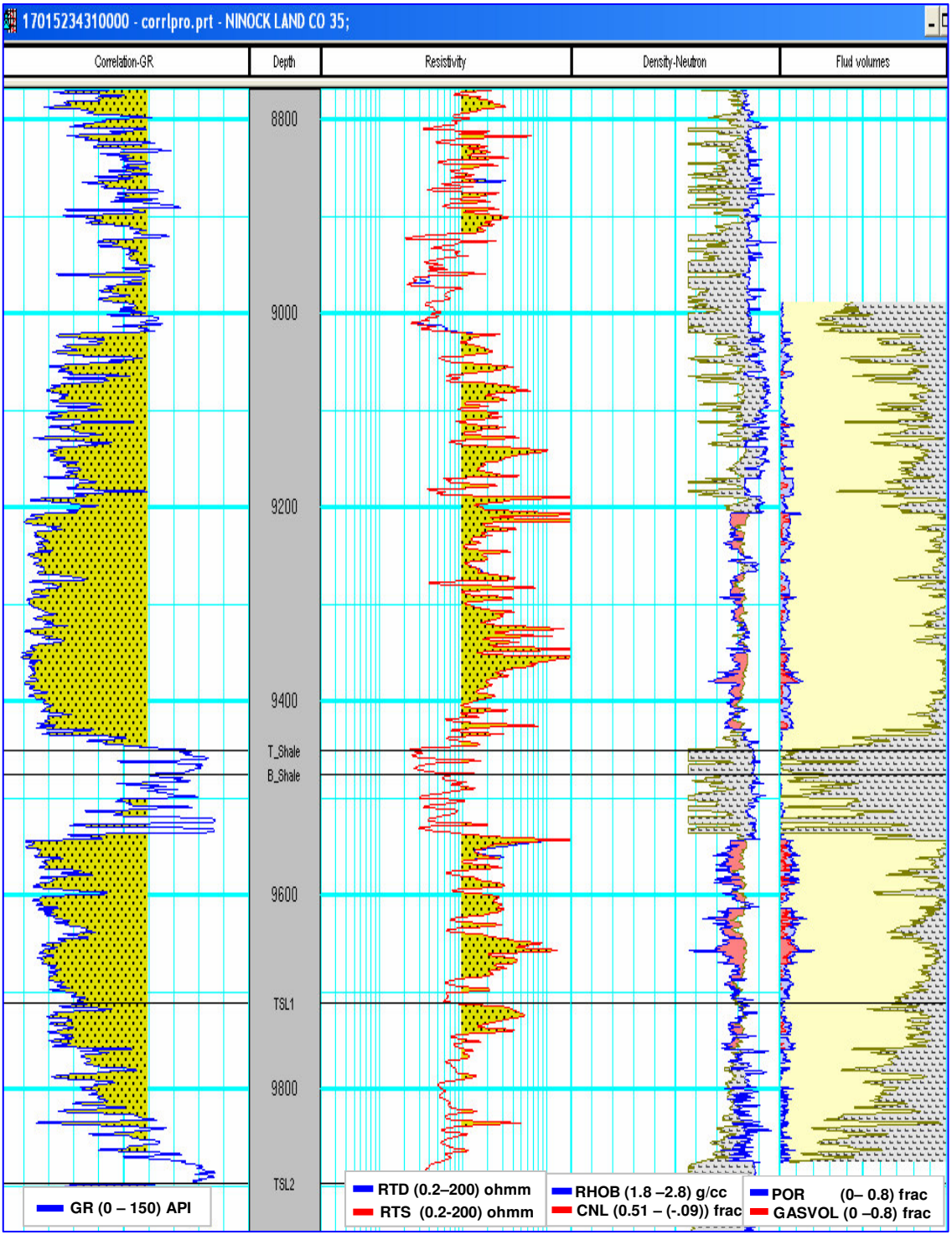

Fig. F17: Log Analysis Results (Nnock Land CO. 35).

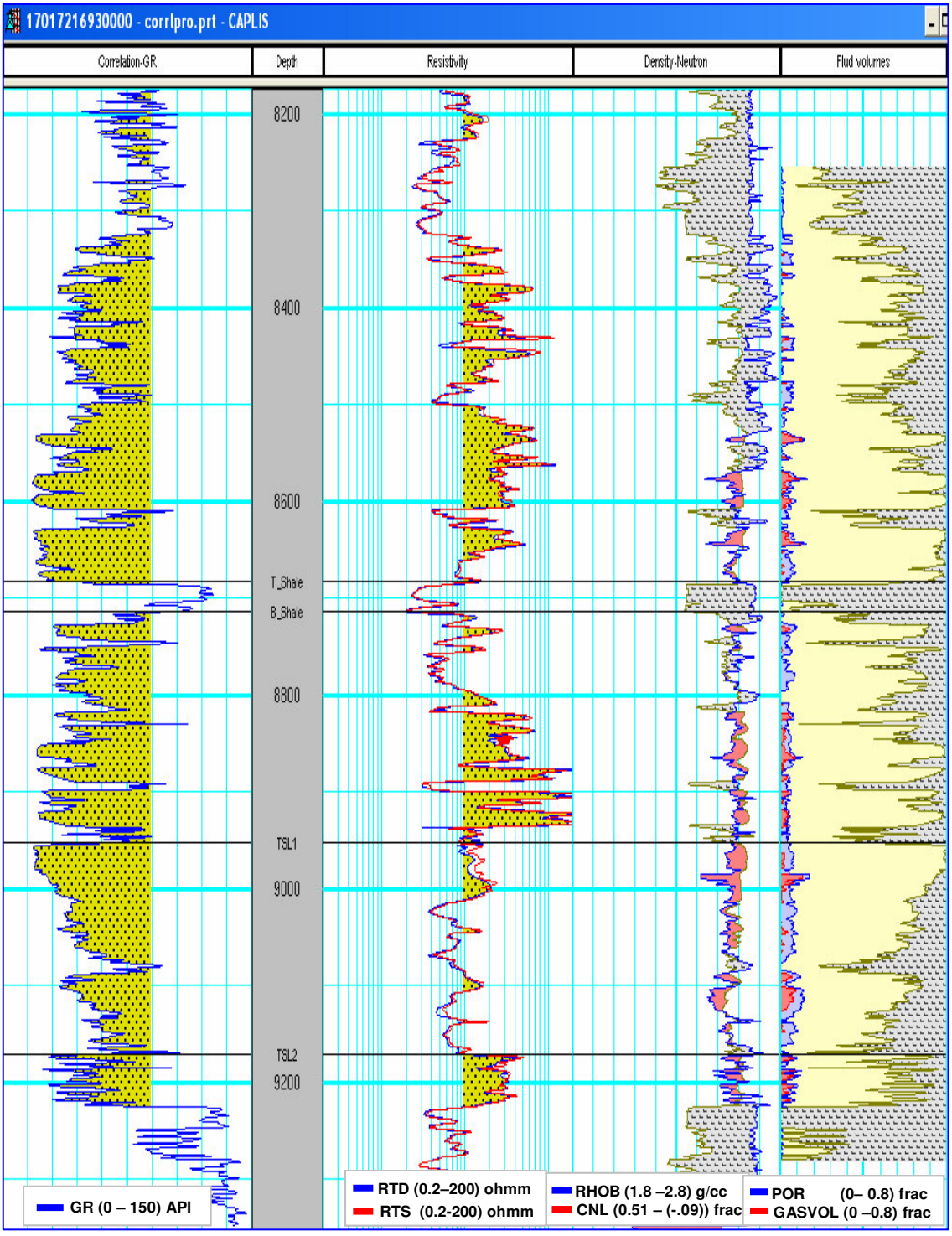

Fig. F18: Log Analysis Results (Caplis).

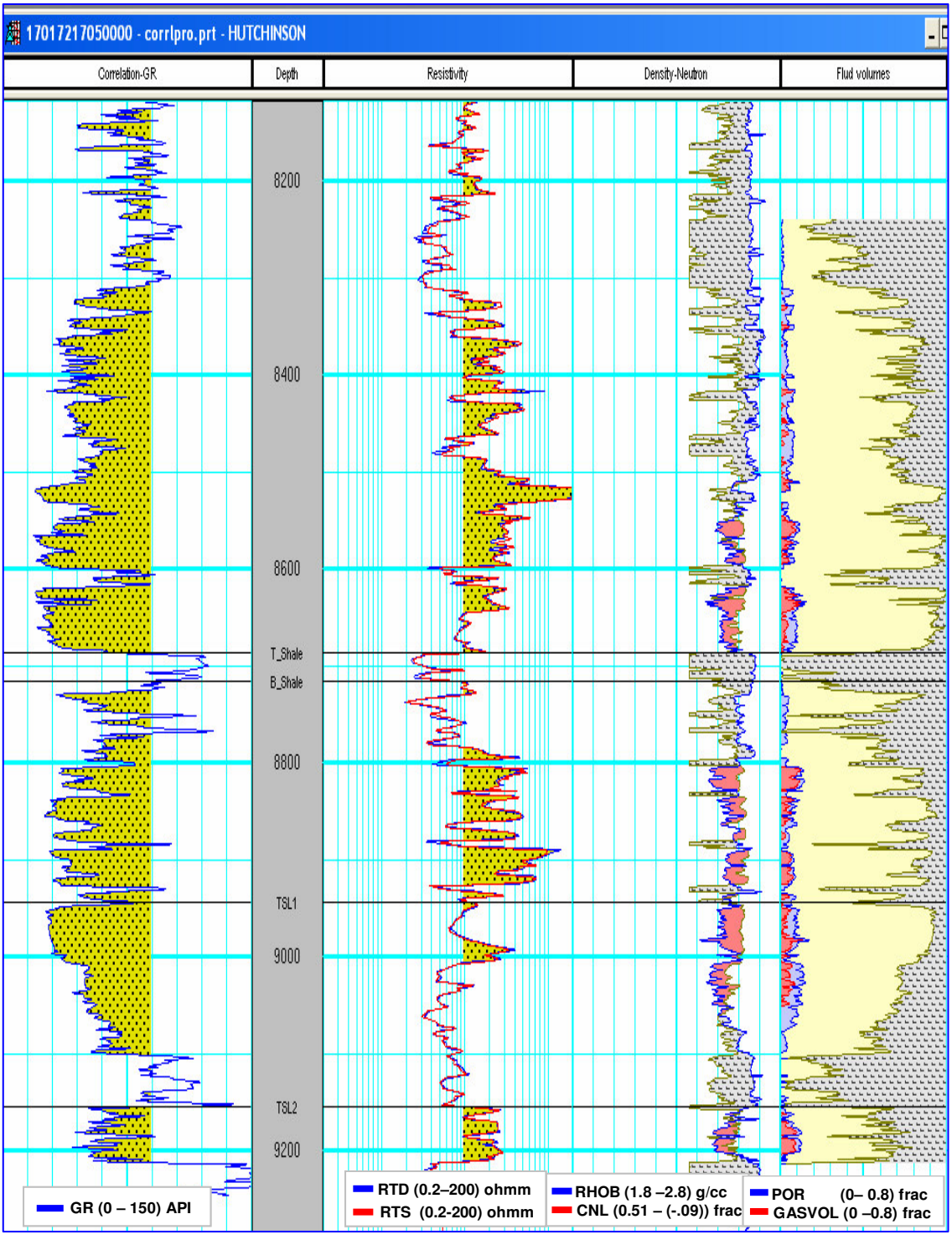

Fig. F19: Log Analysis Results (Hutchinson).

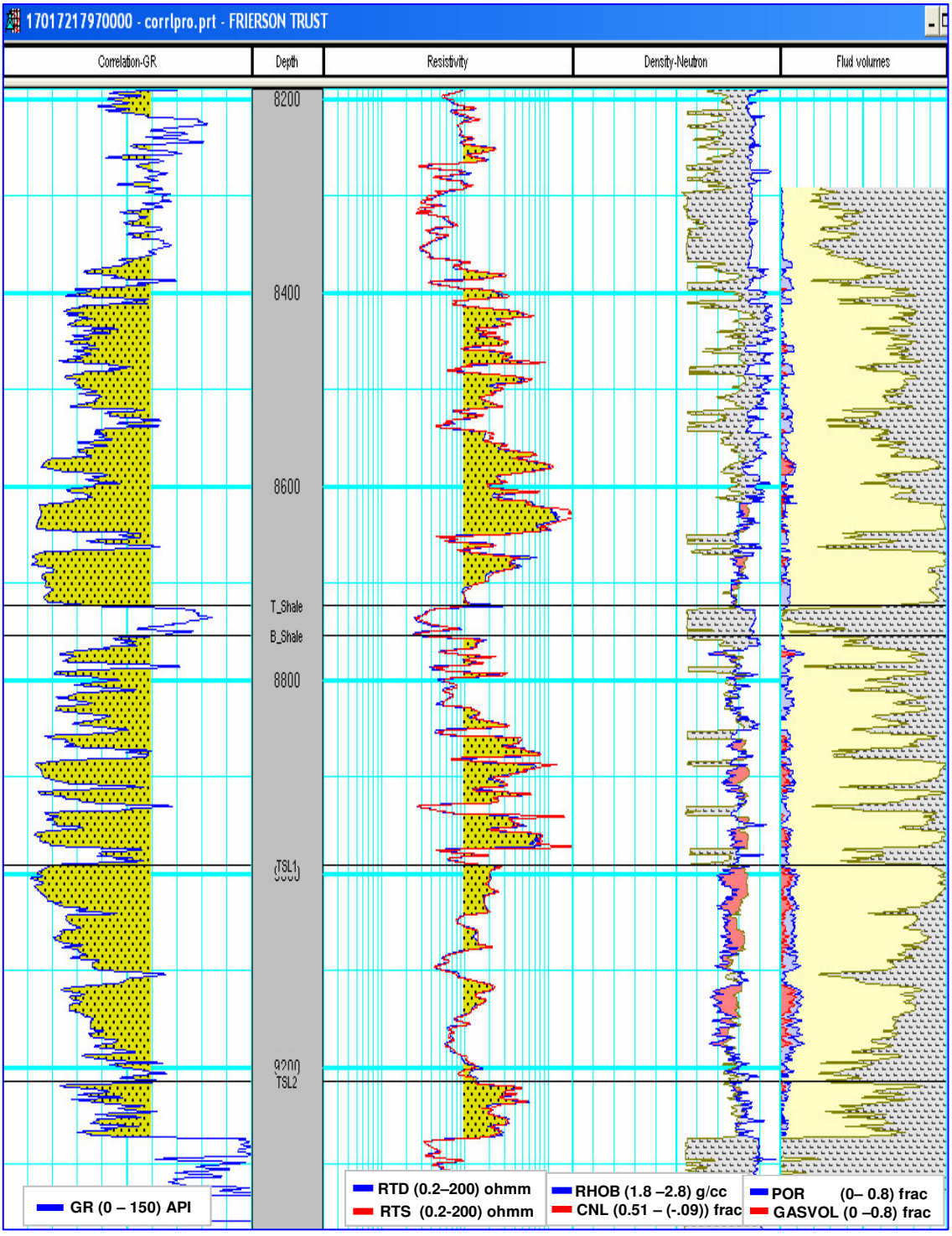

Fig. F20: Log Analysis Results (Frierson Trust).

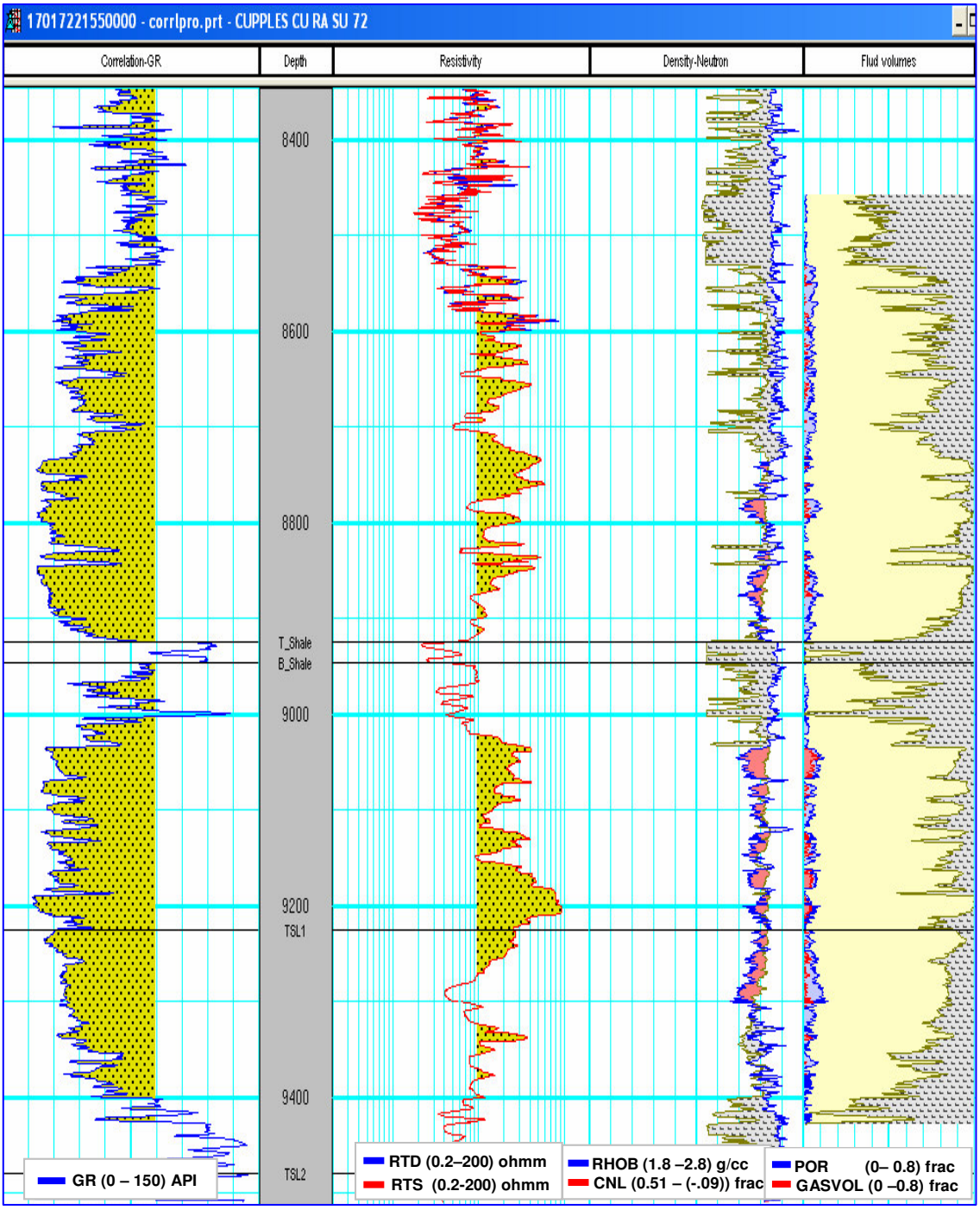

Fig. F21: Log Analysis Results (Cupples CV RA SU 72).

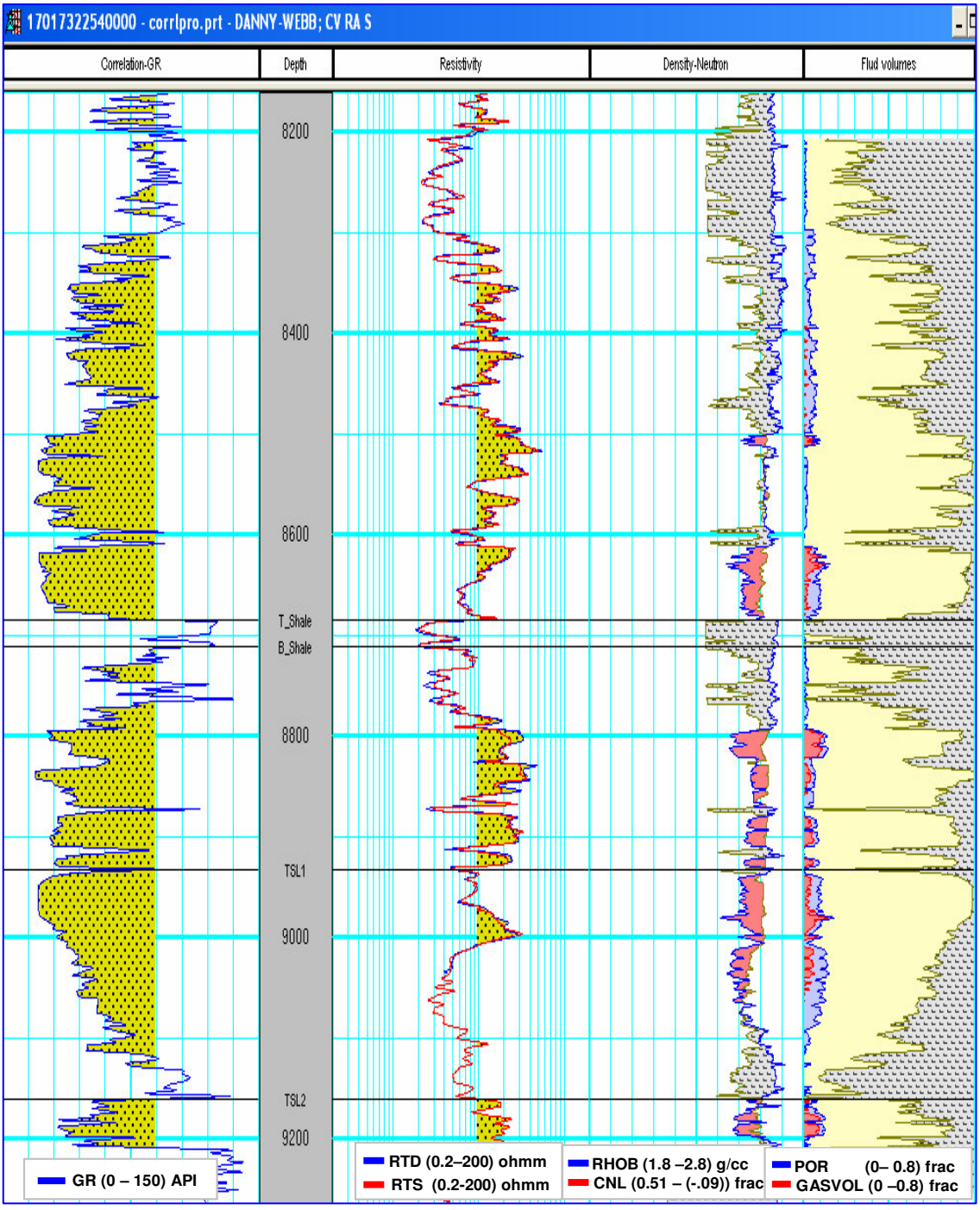

Fig. F22: Log Analysis Results (Danny-Webb; CV RA S).

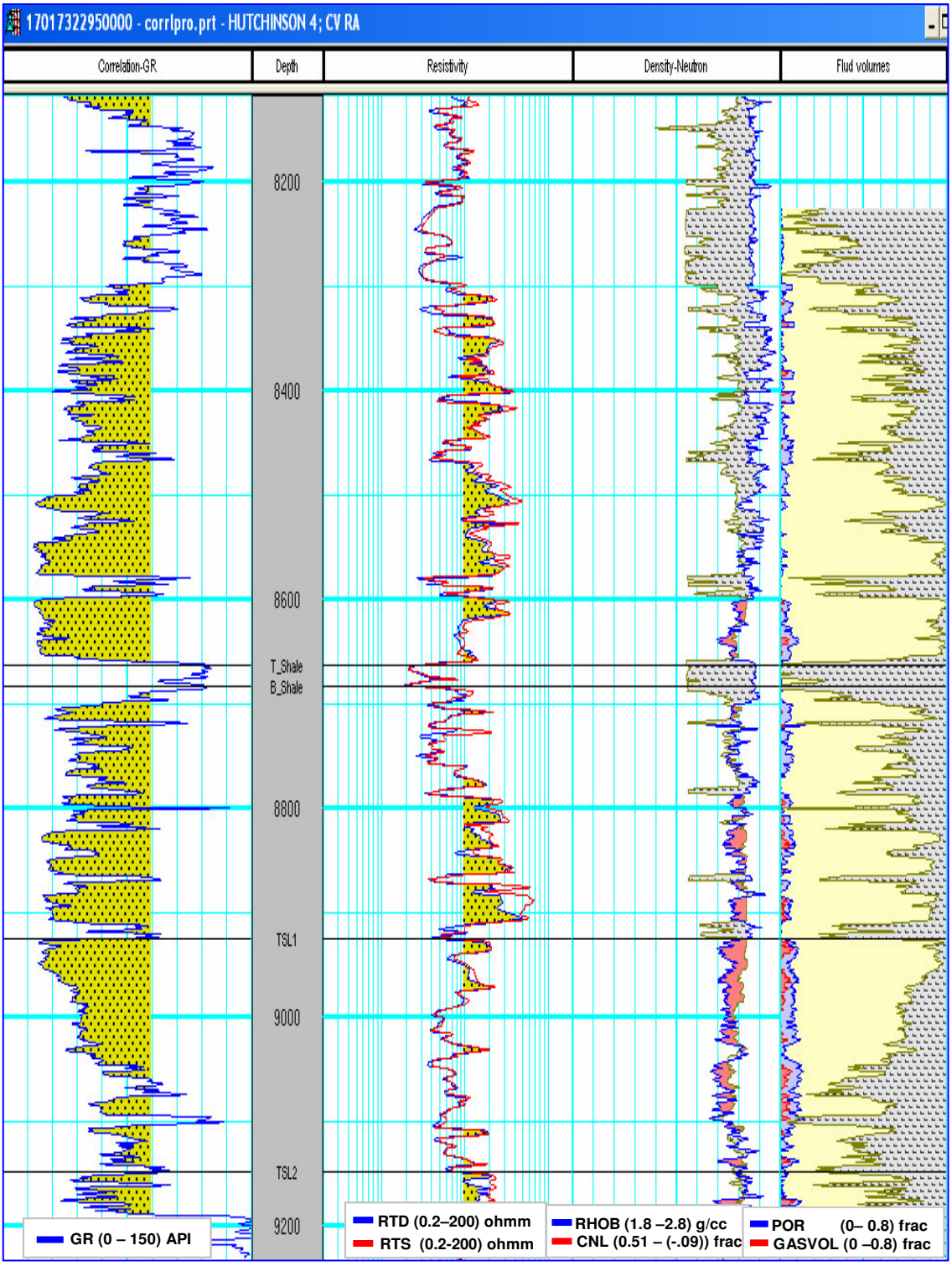

Fig. F23: Log Analysis Results (Hutchinson 4; CV RA).

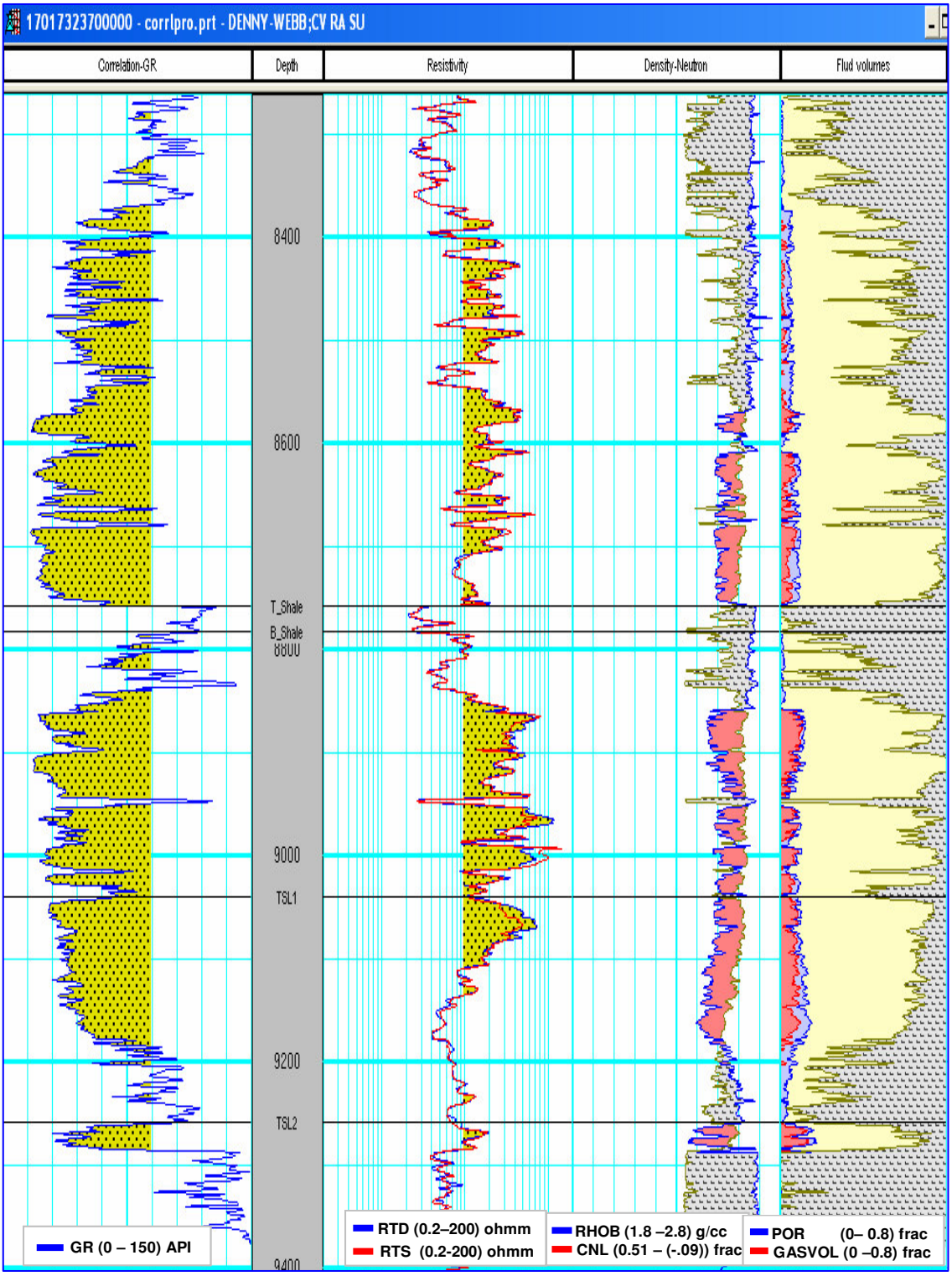

Fig. F24: Log Analysis Results (Danny-Webb; CV RA SU).

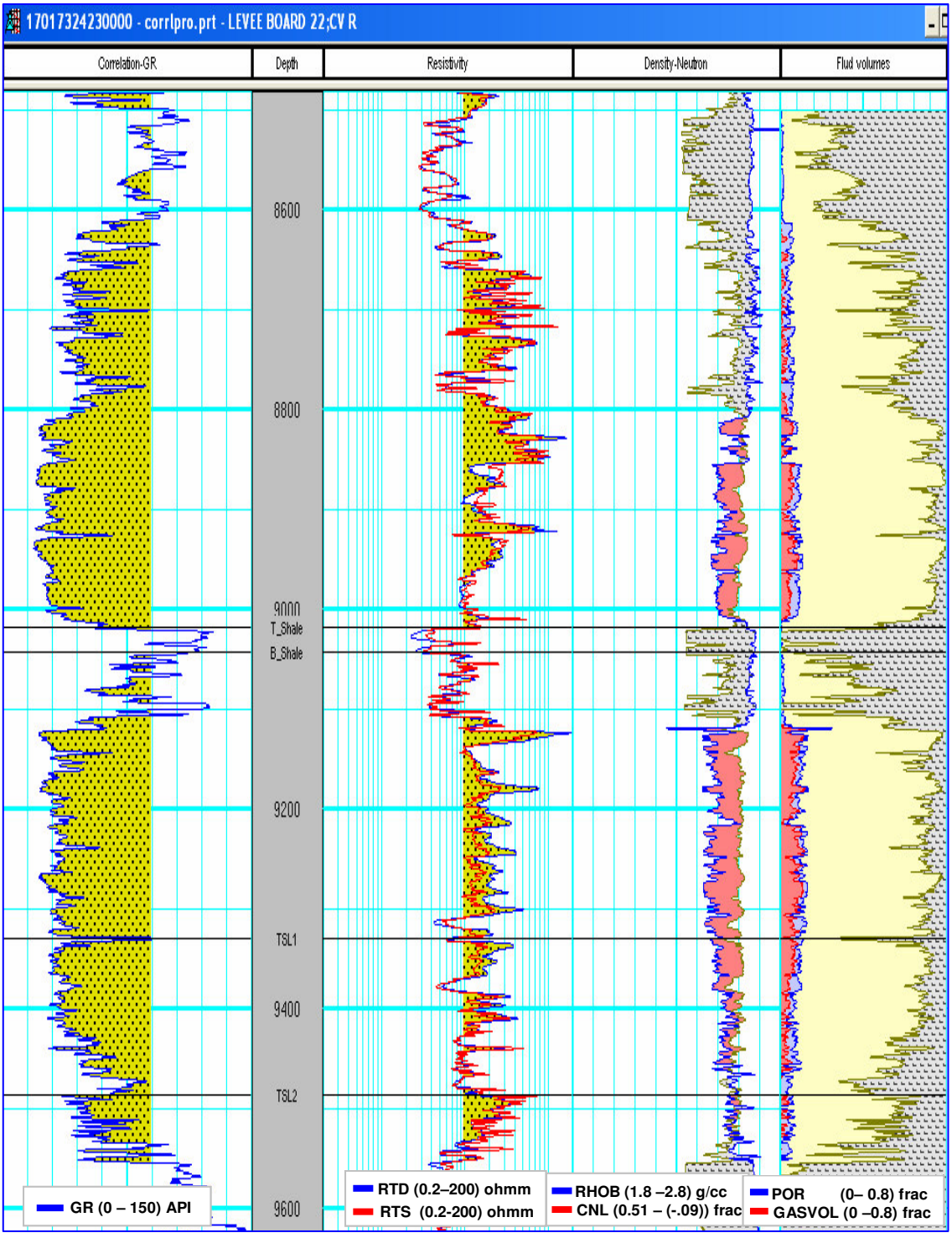

Fig. F25: Log Analysis Results (Levee Board 22; CV R).

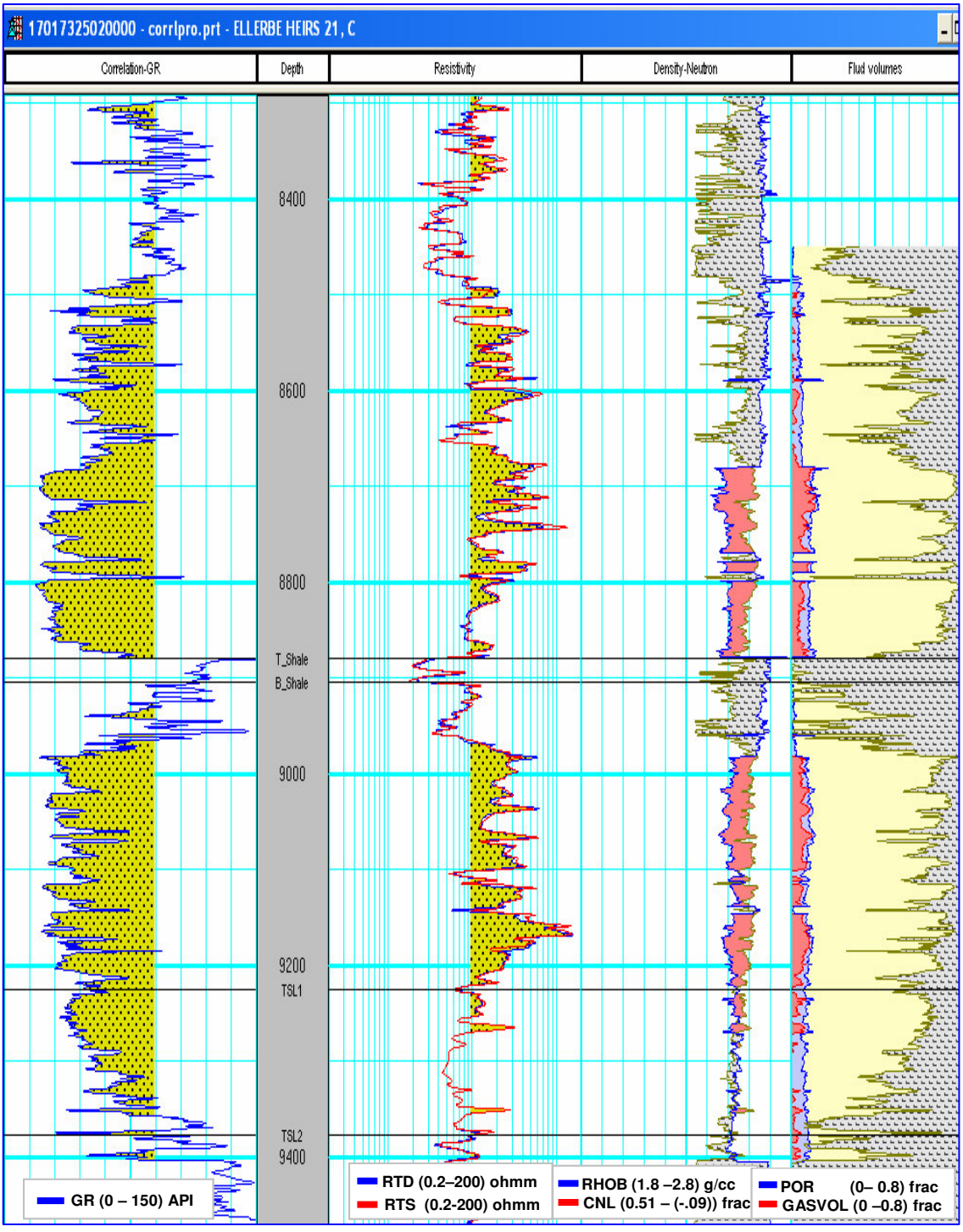

Fig. F26: Log Analysis Results (Ellerbe Heirs 21, C).

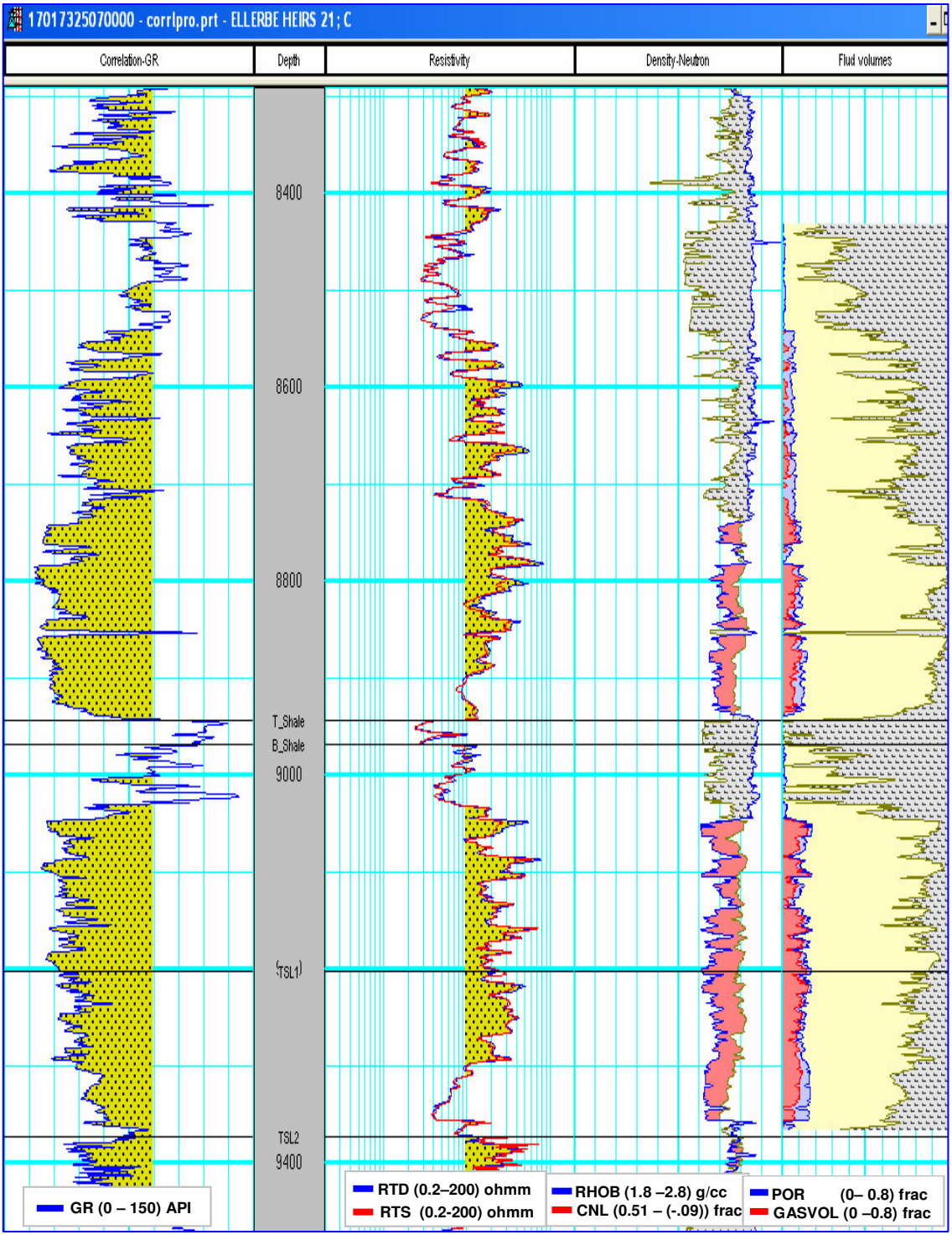

Fig. F27: Log Analysis Results (Ellerbe Heirs 21; C2).

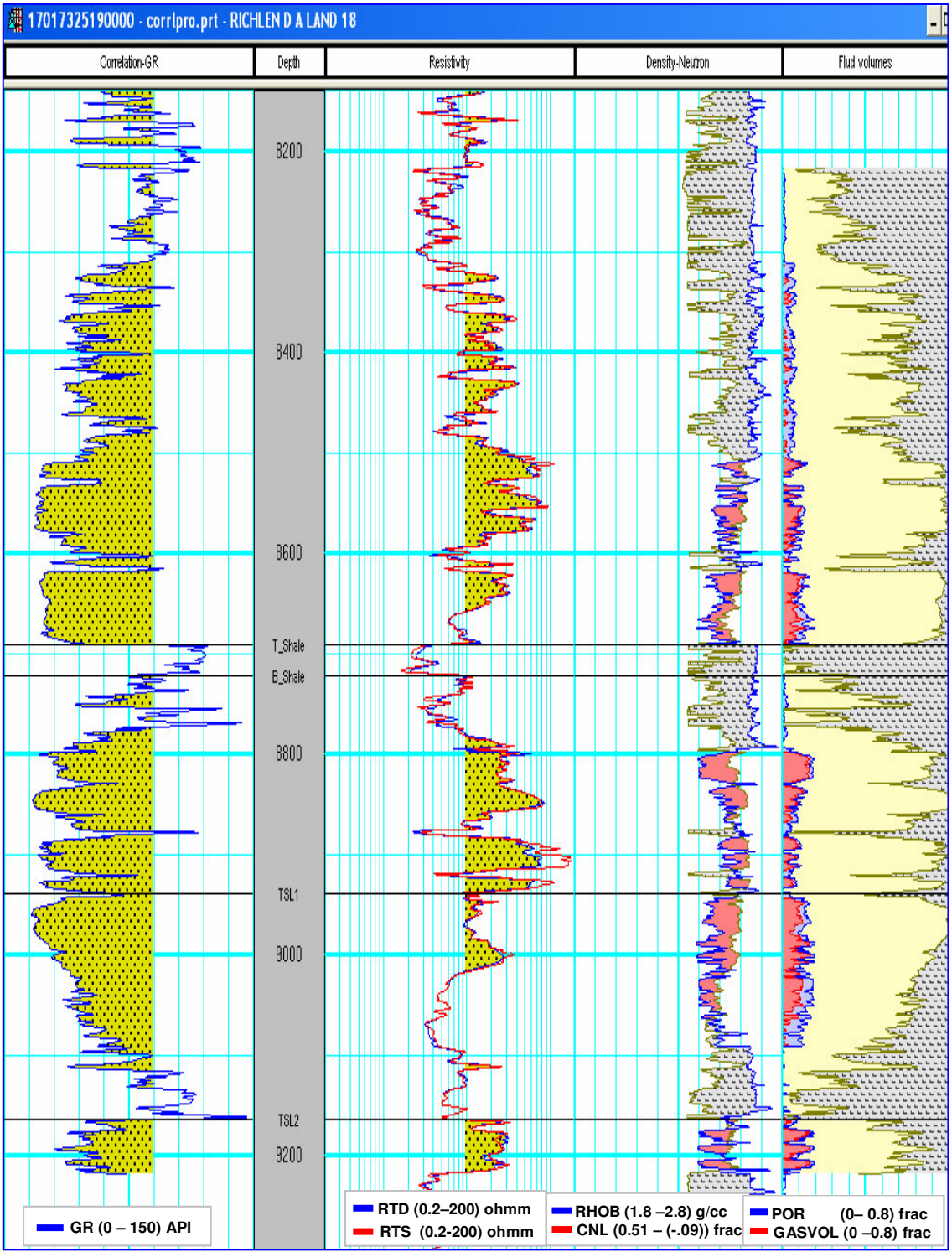

Fig. F28: Log Analysis Results (Richlend A Land 18).

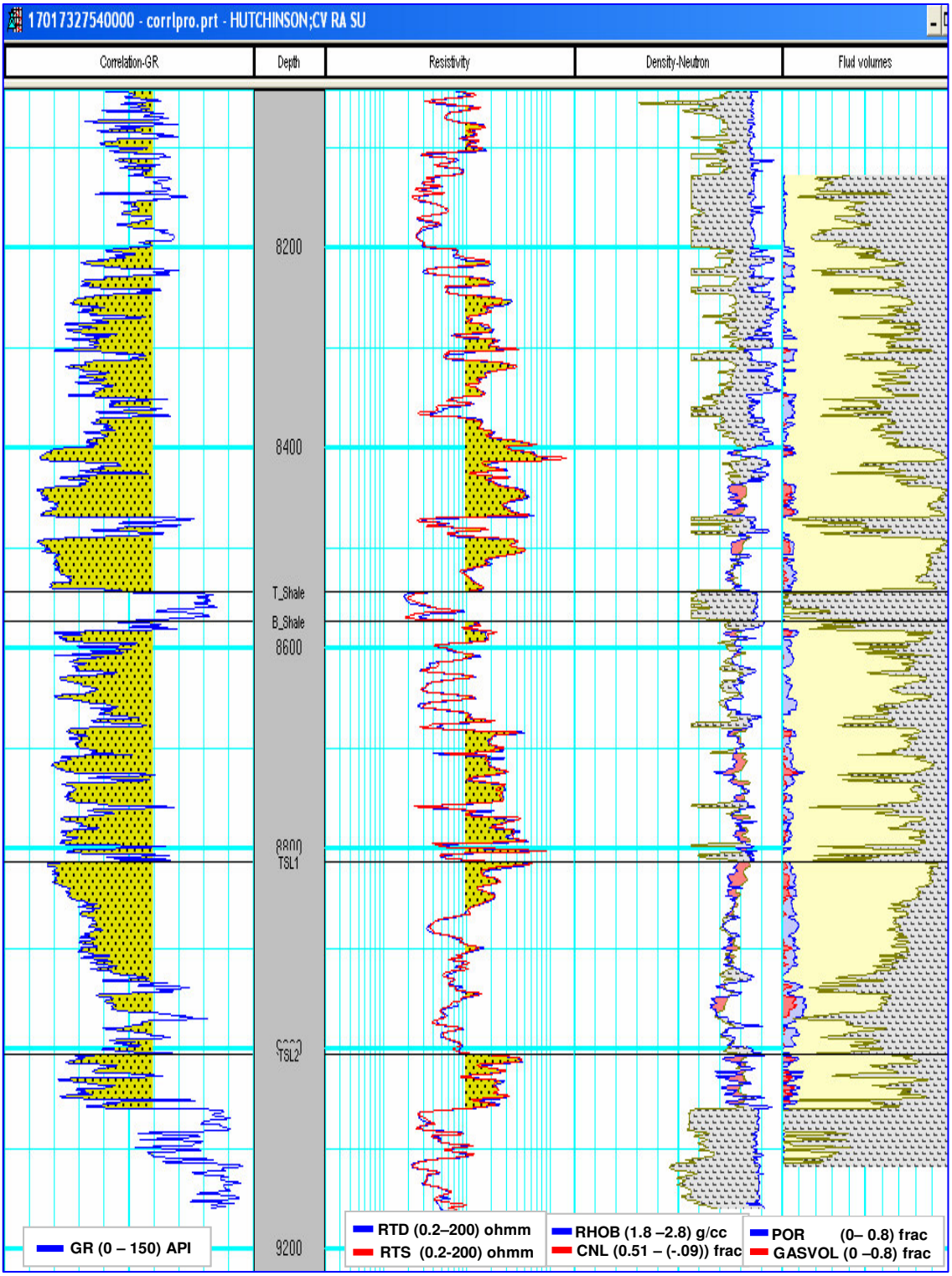

Fig. F29: Log Analysis Results (Hutchinson; CV RA SU).

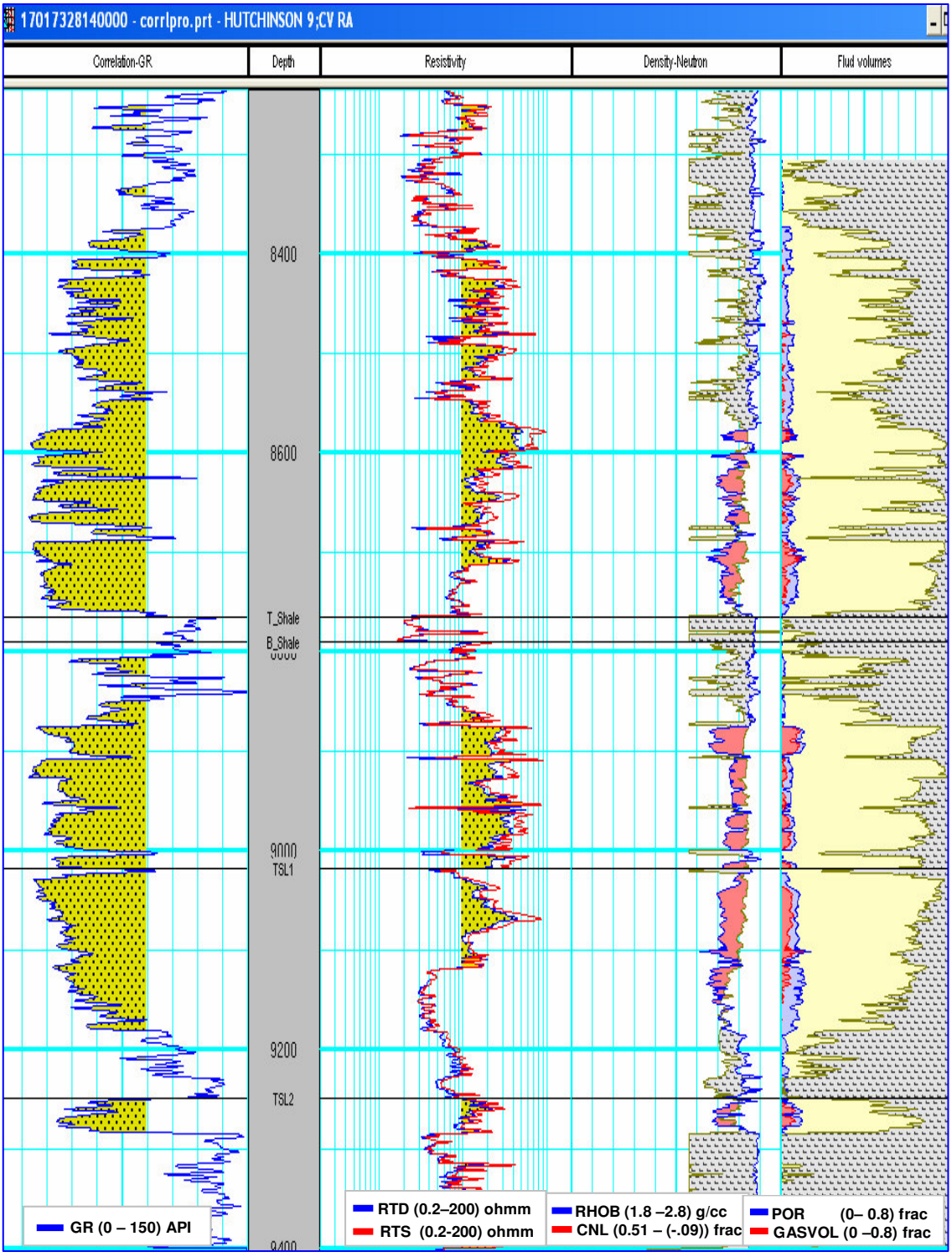

Fig. F30: Log Analysis Results (Hutchinson 9; CV RA).

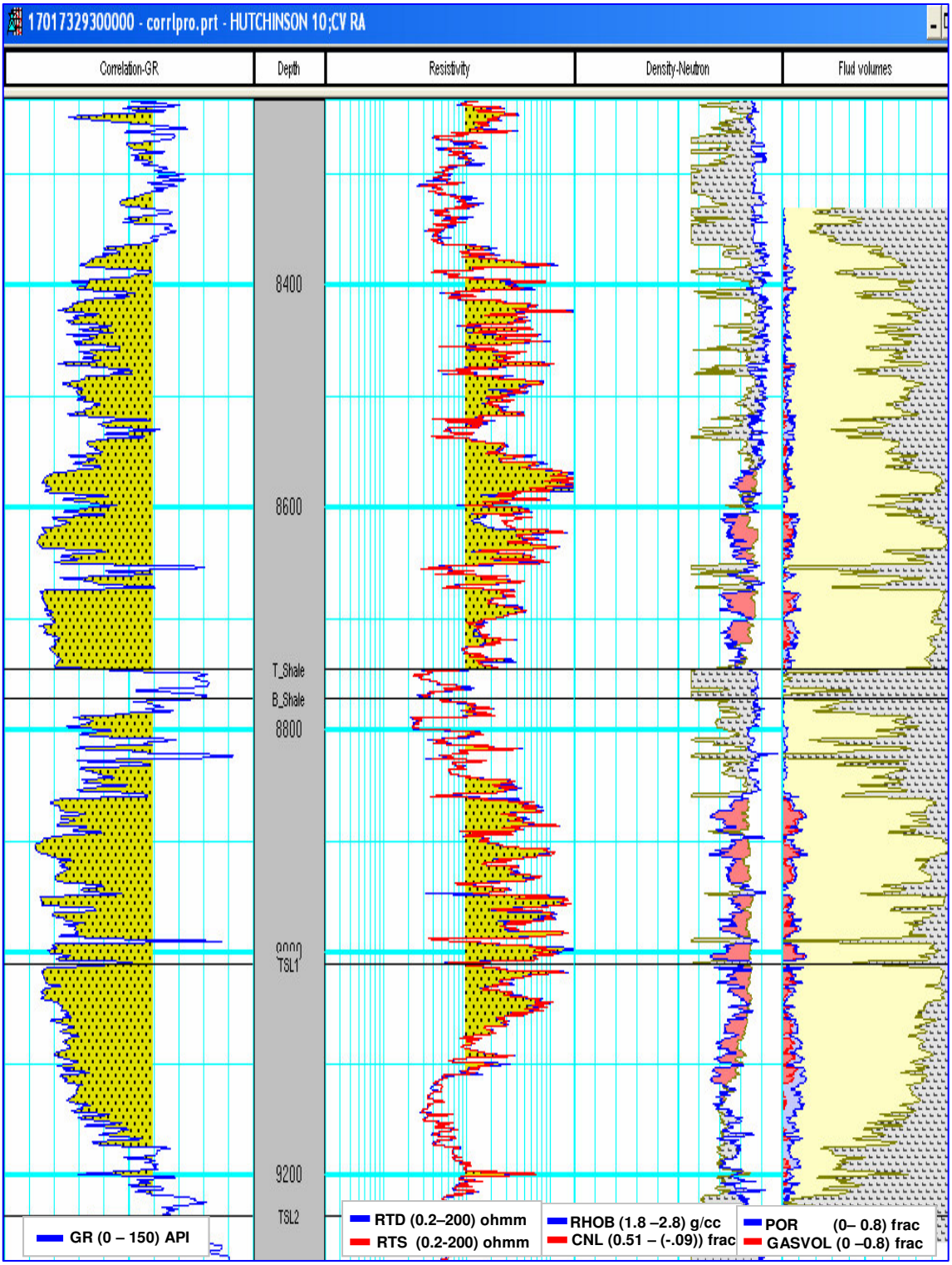

Fig. F31: Log Analysis Results (Hutchinson 10, CV RA).

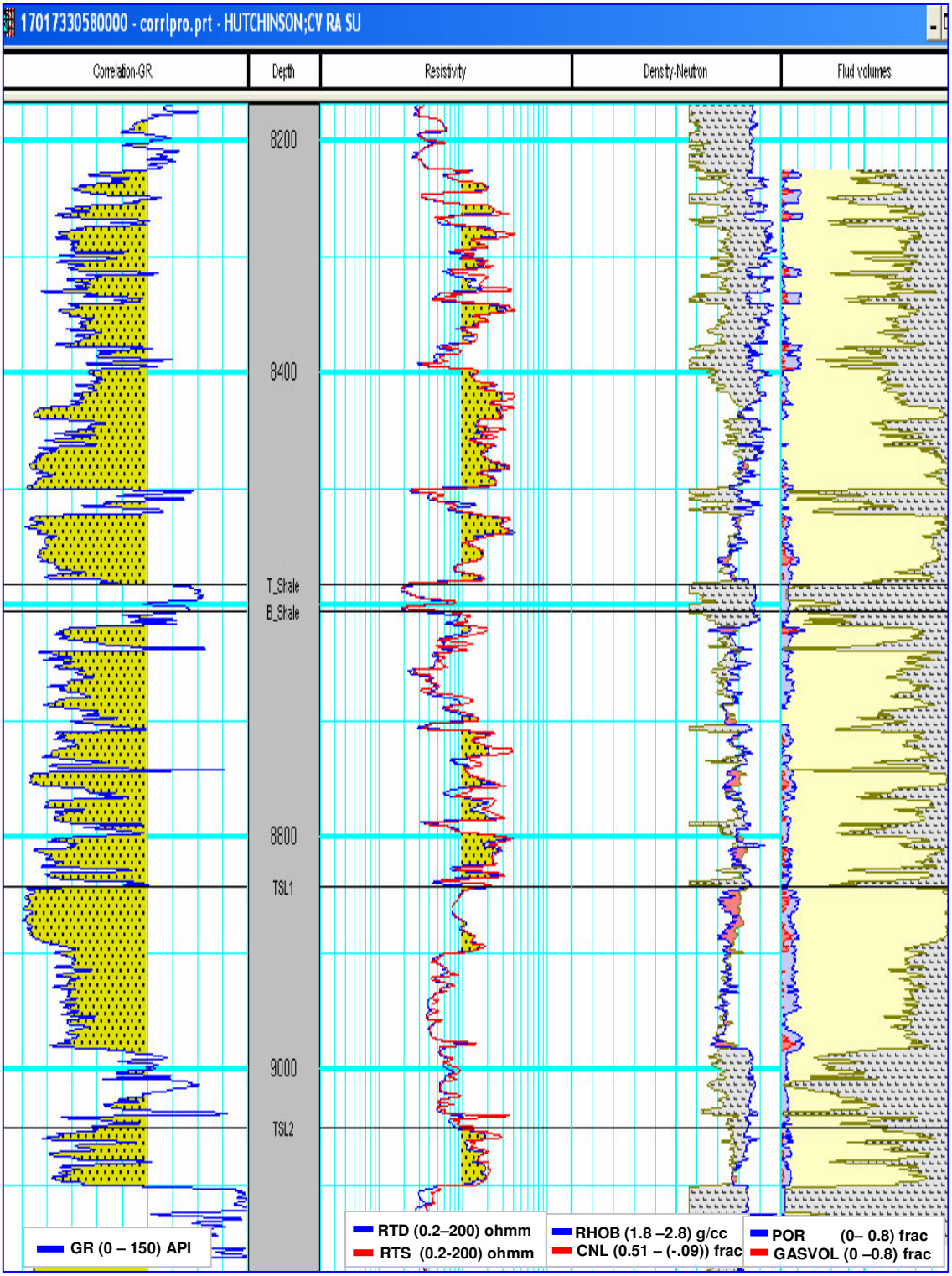

Fig. F32: Log Analysis Results (Hutchinson; CV RA SU).

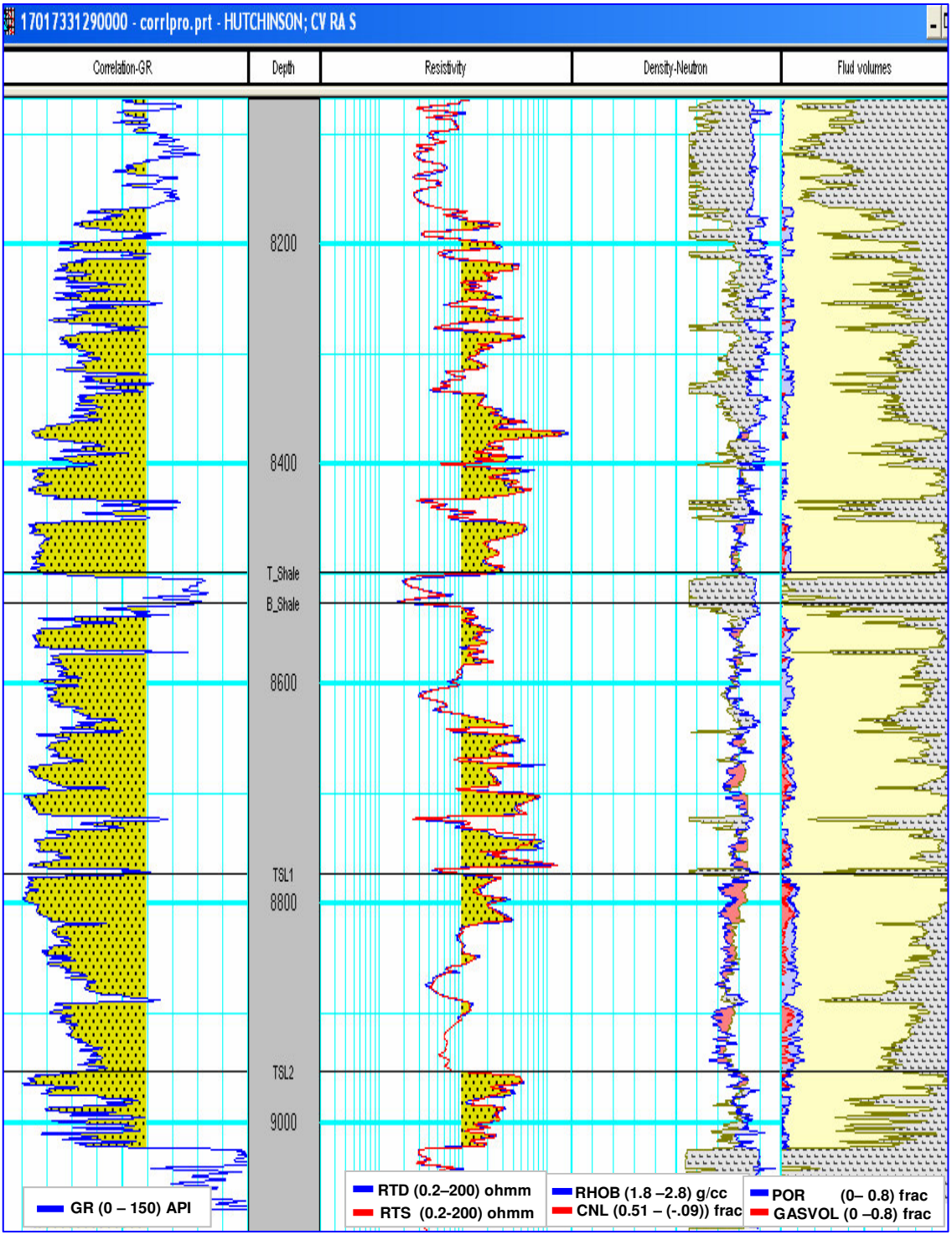

Fig. F33: Log Analysis Results (Hutchinson CV RA S).

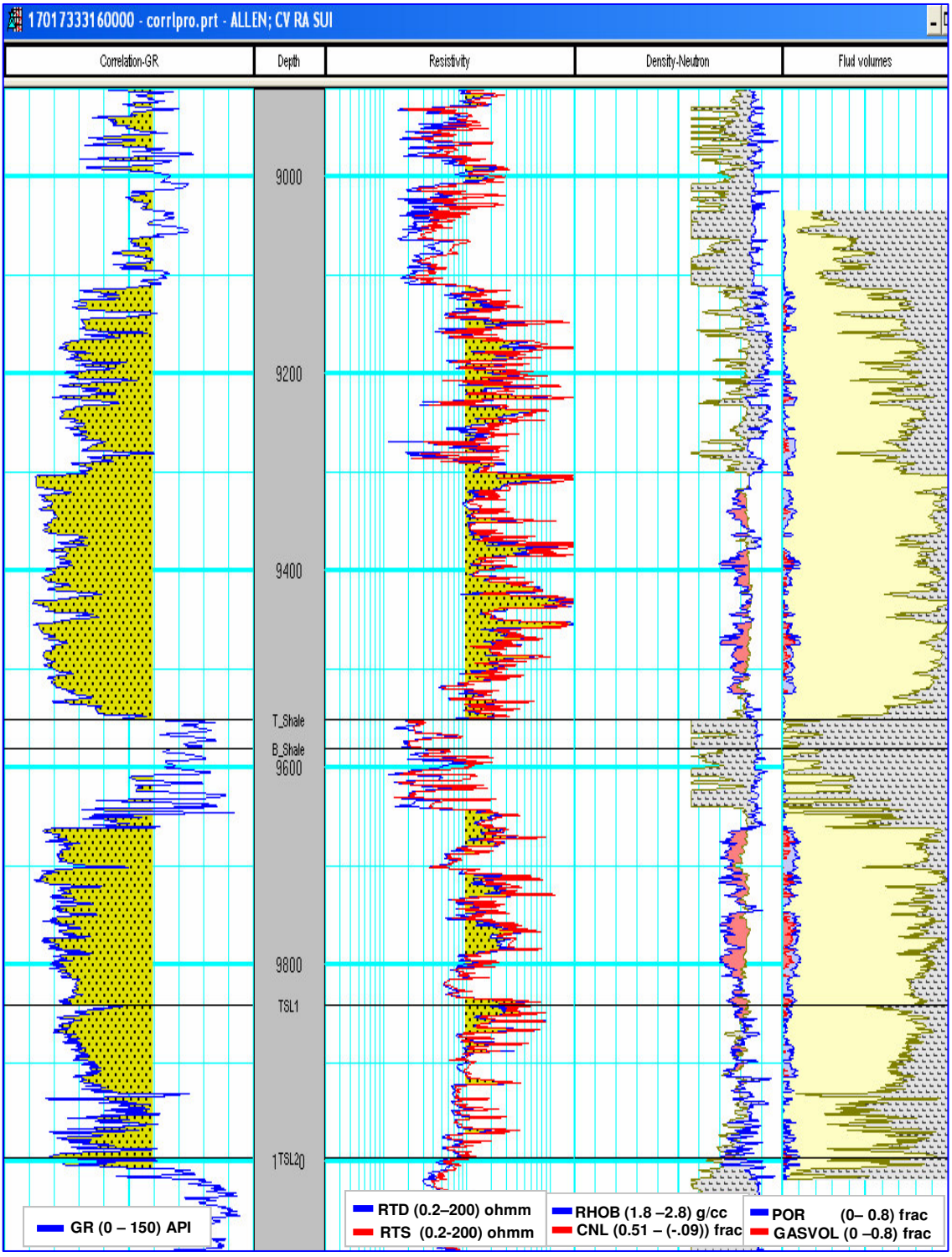

Fig. F34: Log Analysis Results (Allen; CV RA SUI).

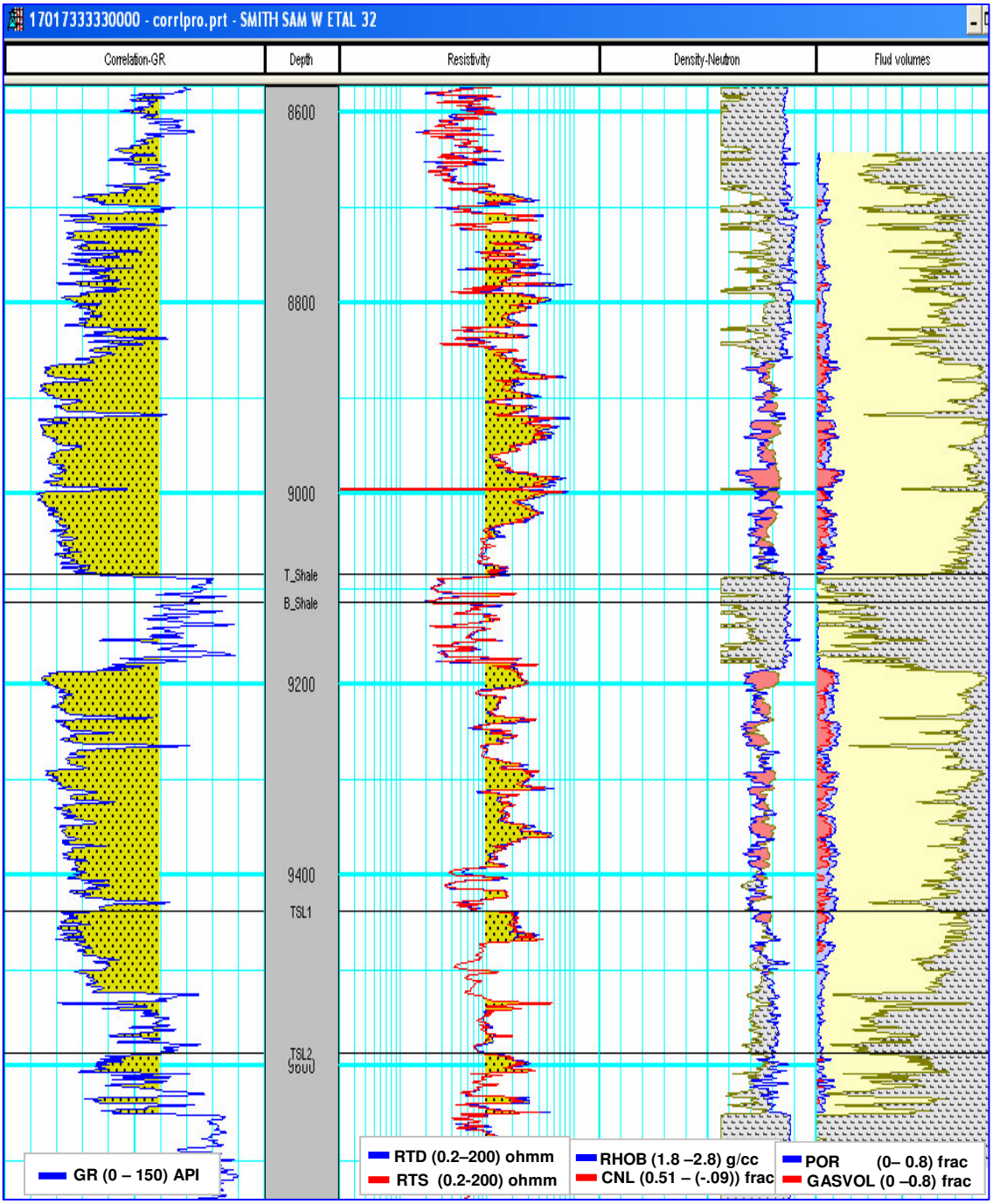

Fig. F35: Log Analysis Results (Smith Sam W. Etal 32).

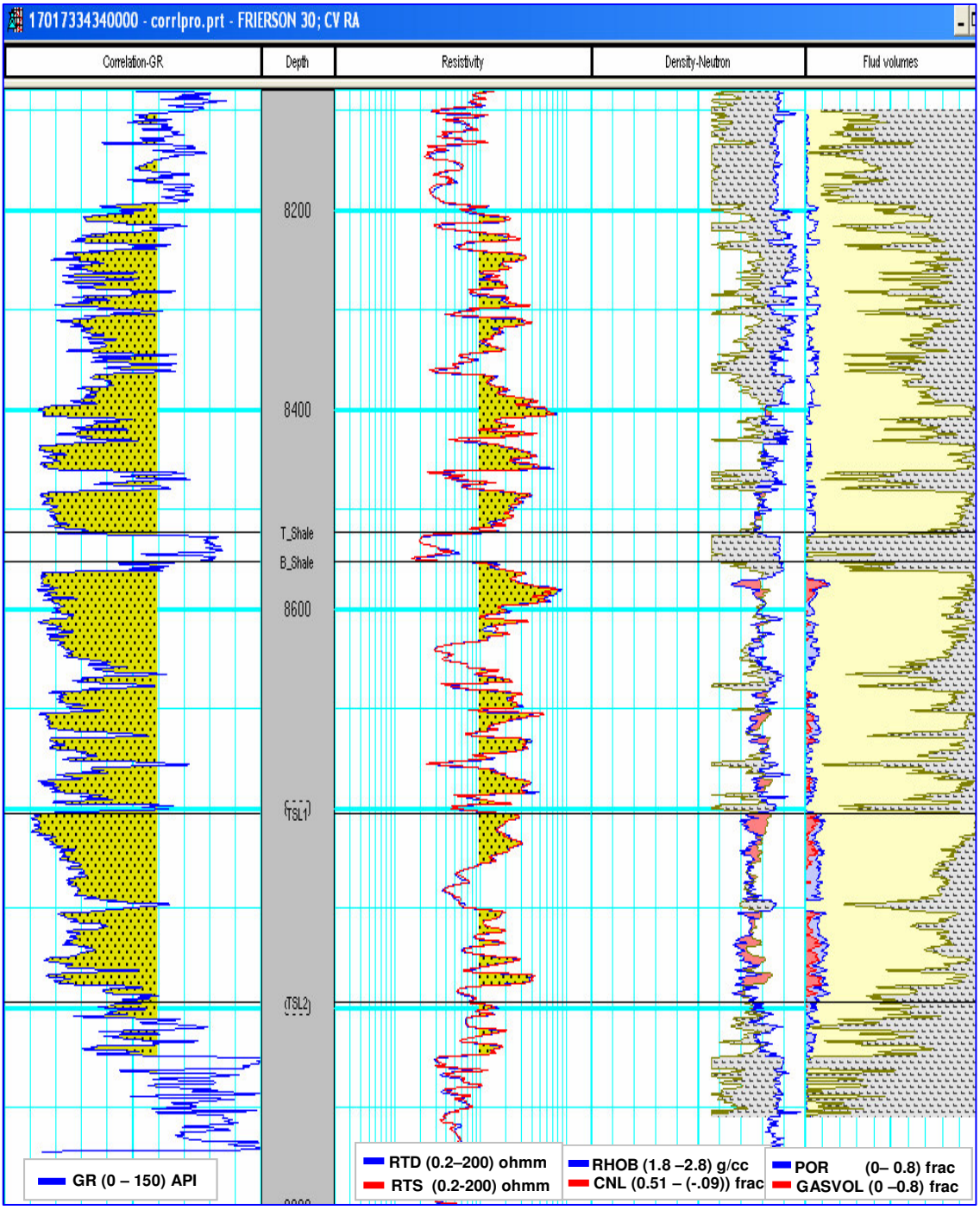

Fig. F36: Log Analysis Results (Frierson 30; CV RA).

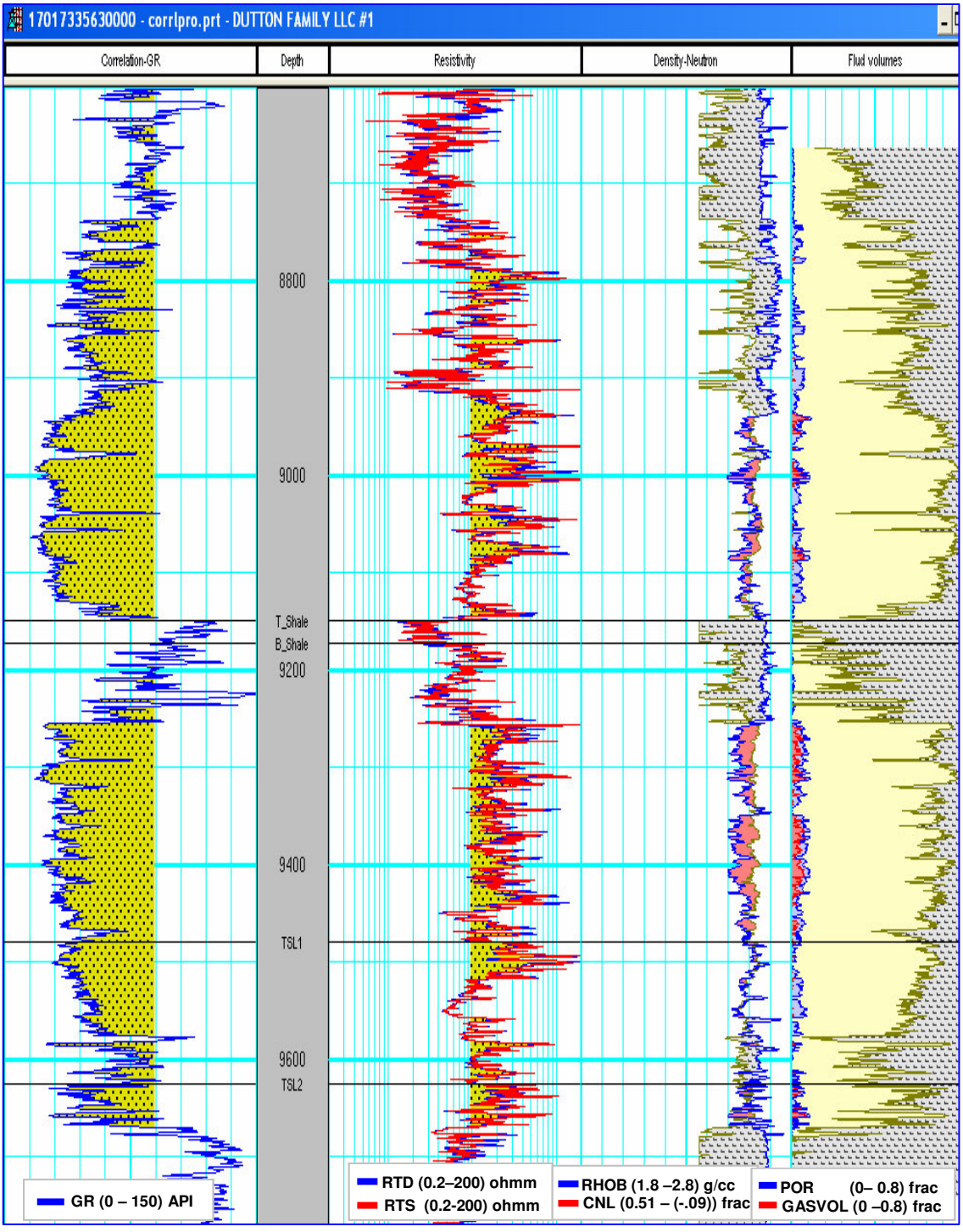

Fig. F37: Log Analysis Results (Dutton Family LLC #1).

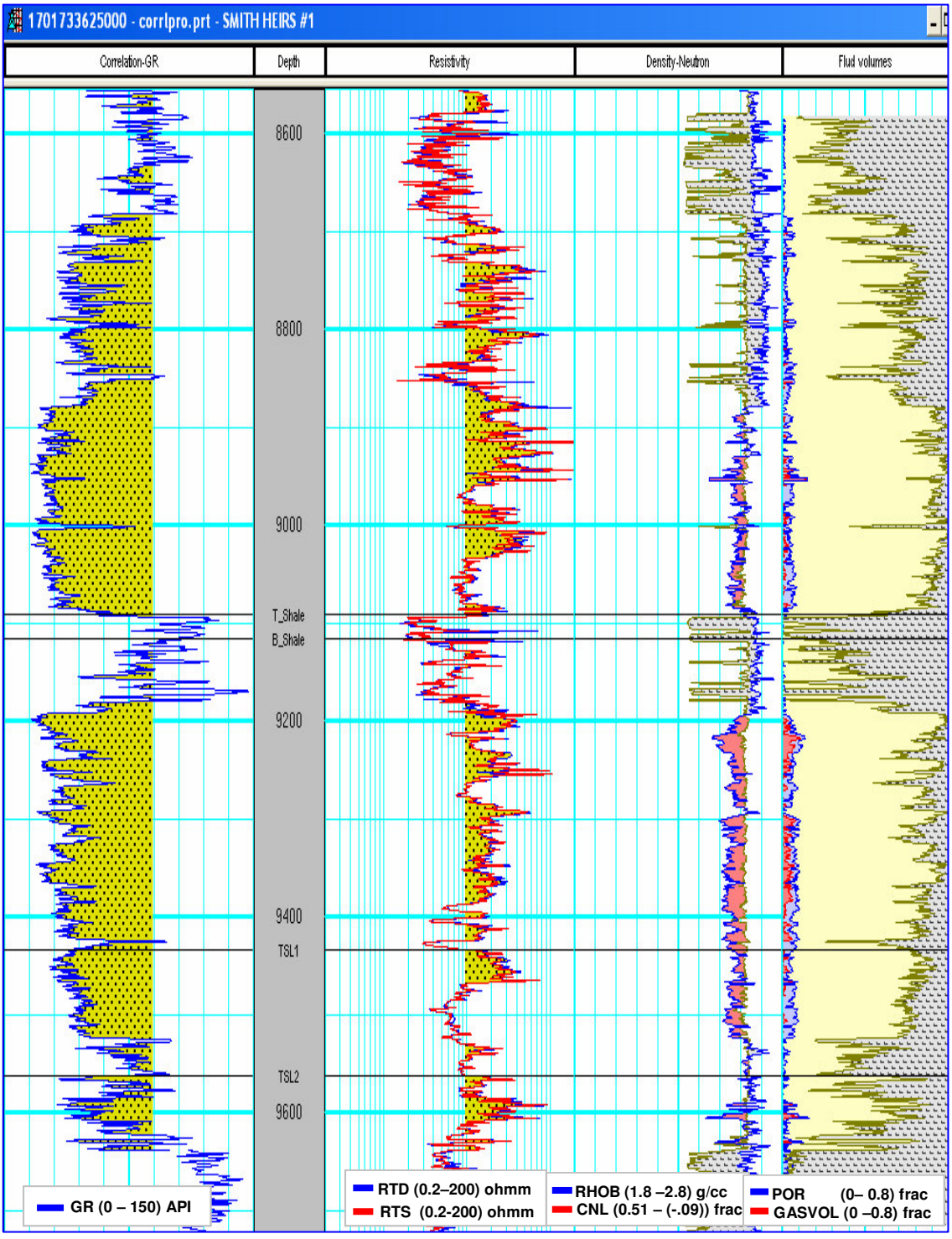

Fig. F38: Log Analysis Results (Smith Heirs #1).

APPENDIX G

RESERVOIR SIMULATION RESULTS

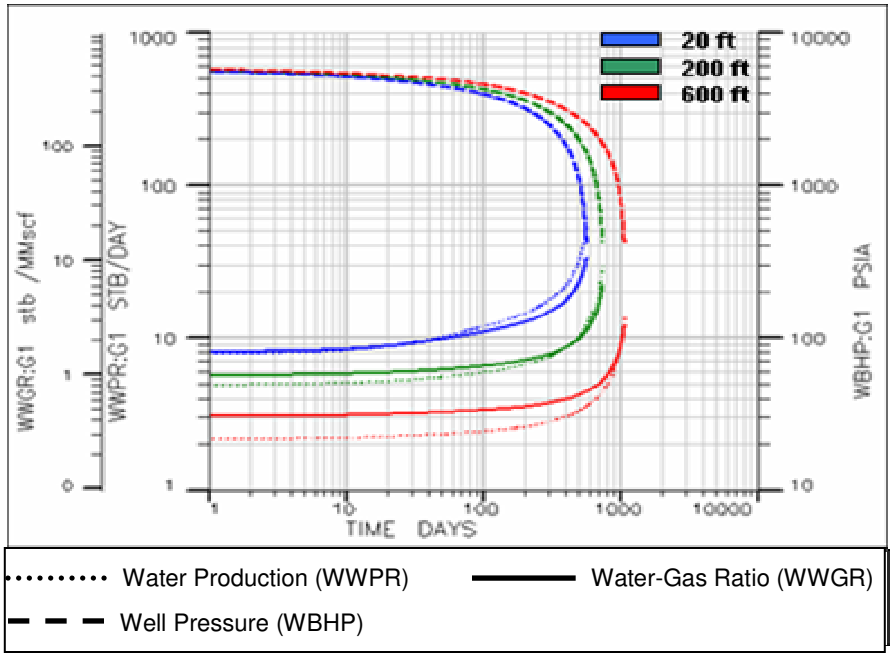

Fig. G1: Simulation Results - Case 3, 2, 1 (Effect of Variation of Water Source Distance, Limited Transition Zone).

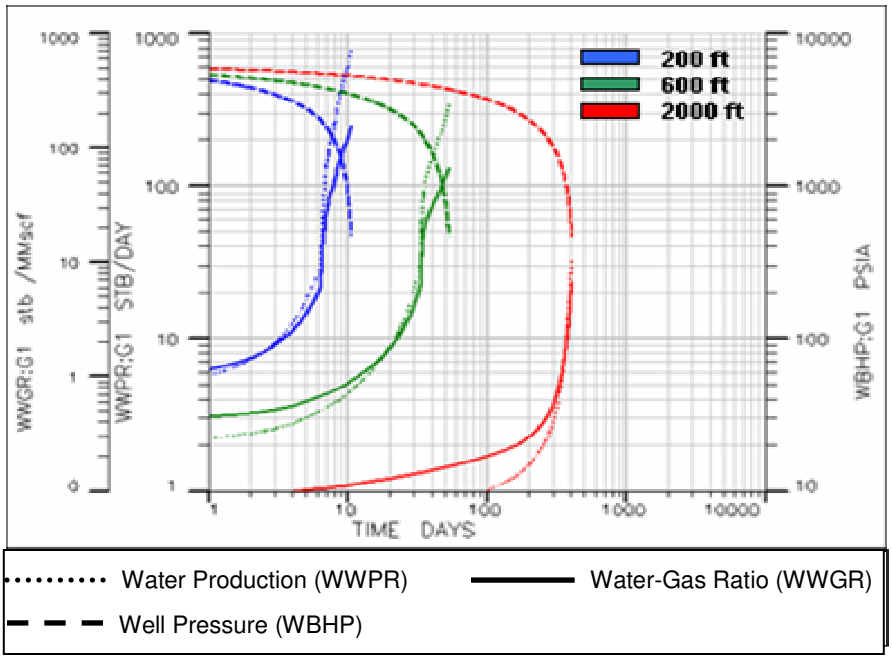

Fig. G2: Simulation Results - Case 10, 9, 8 (Effect of Variation of Water Source Distance, Large Transition Zone).

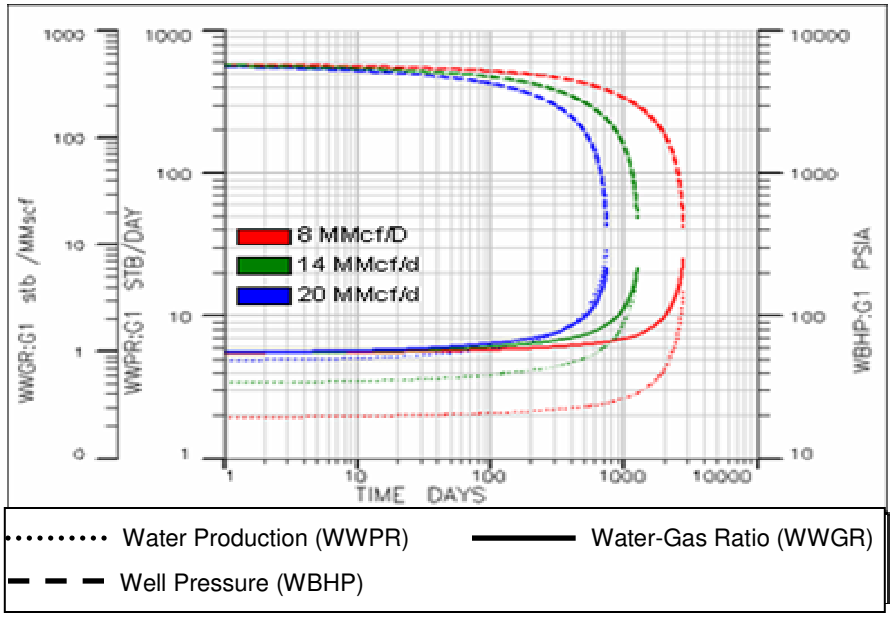

Fig. G3: Simulation Results - Case 2, 4, 5 (Effect of Gas Production Rate Variation, Limited Transition Zone).

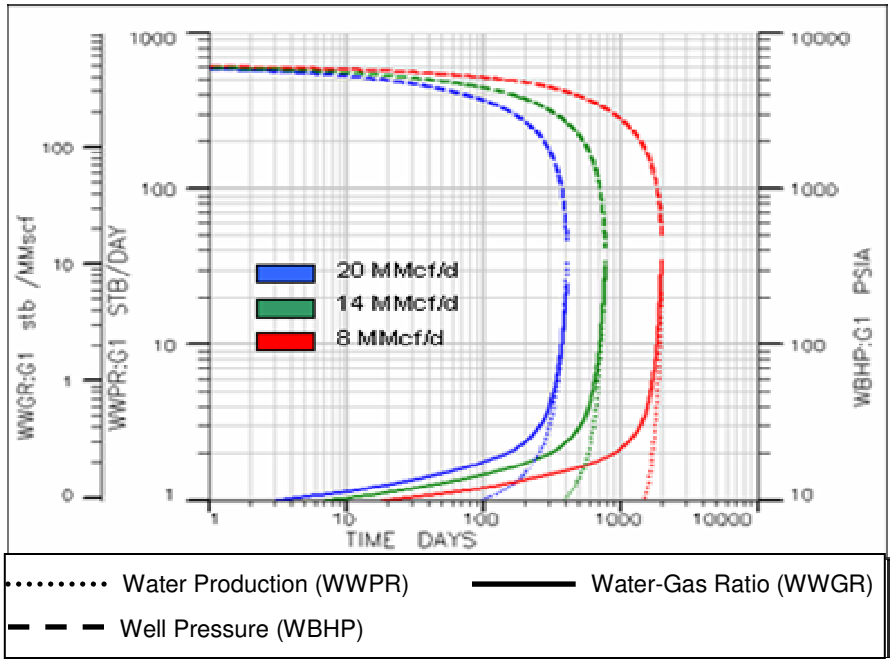

Fig. G4: Simulation Results - Case 8, 11, 12 (Effect of Gas Production Rate Variation, Large Transition Zone).

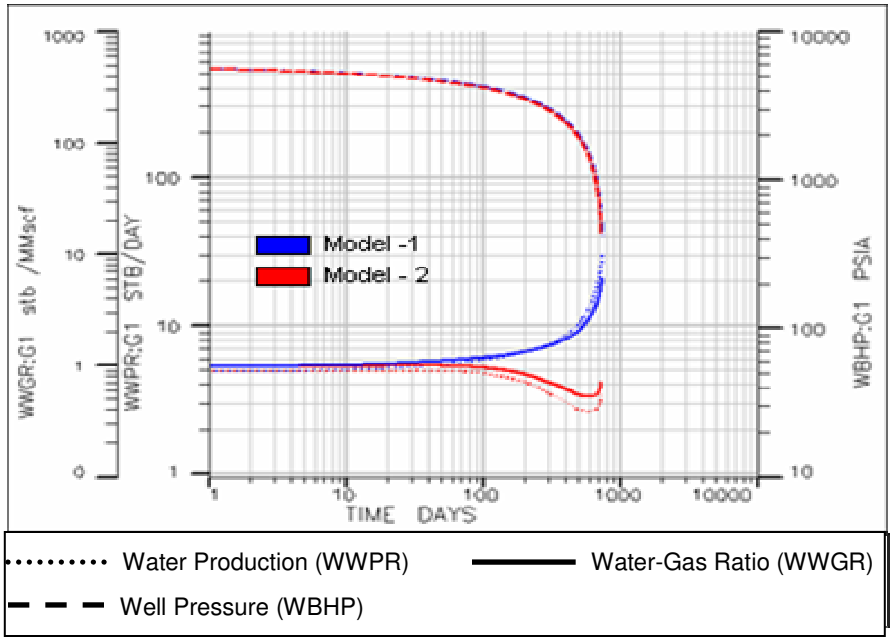

Fig. G5: Simulation Results - Case 1 and 6 (Effect of Relative Permeability Variation, Limited Transition Zone).

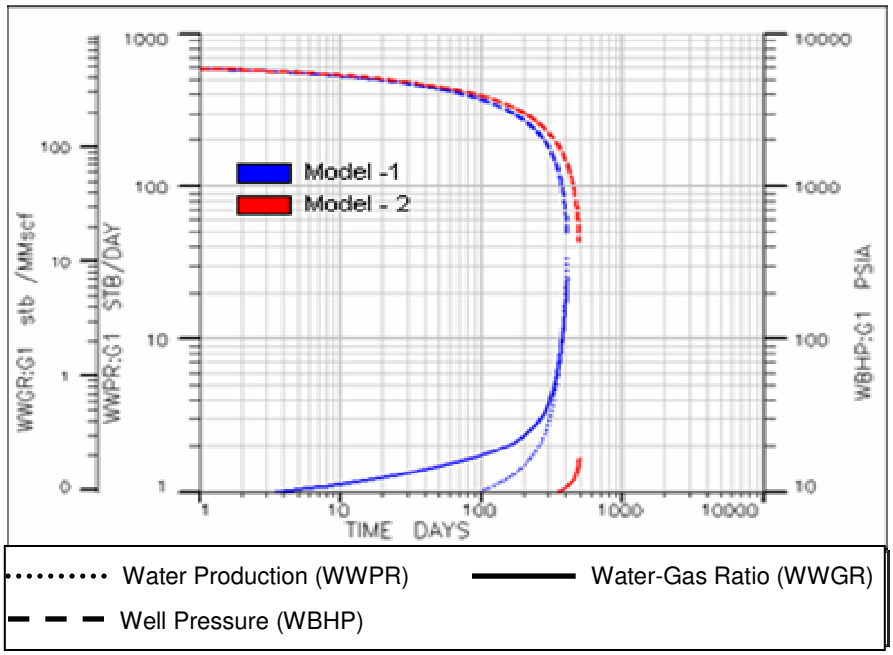

Fig. G6: Simulation Results - Case 8 and 13 (Effect of Relative Permeability Variation, Large Transition Zone).

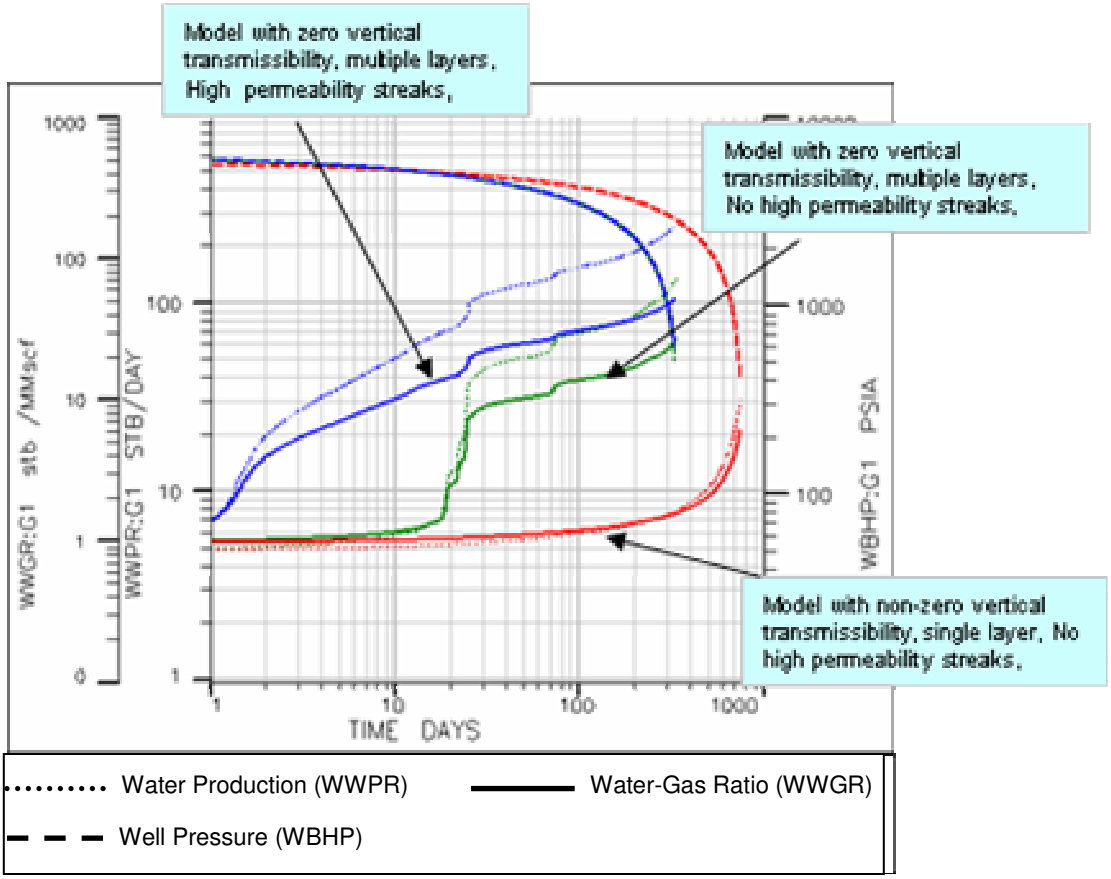

Fig. G7: Simulation Results - Case 19, 15, 1 (Effect of Layering, Vertical Transmissibility and Presence of High Permeability Zones).

APPENDIX H

WATER PRODUCTION TREND

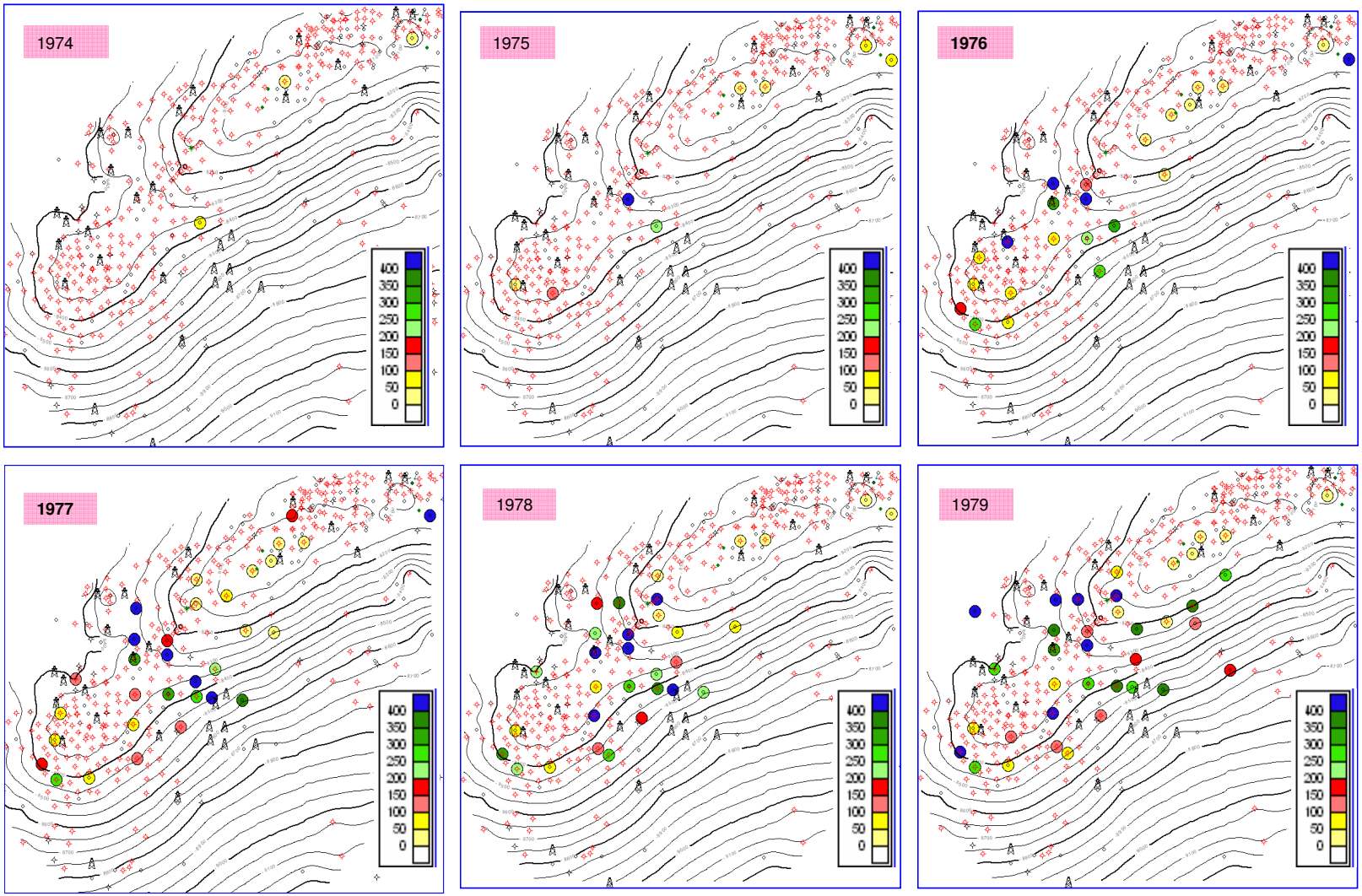

Fig. H1: Distribution of Water-Gas Ratios (1974 – 1979).

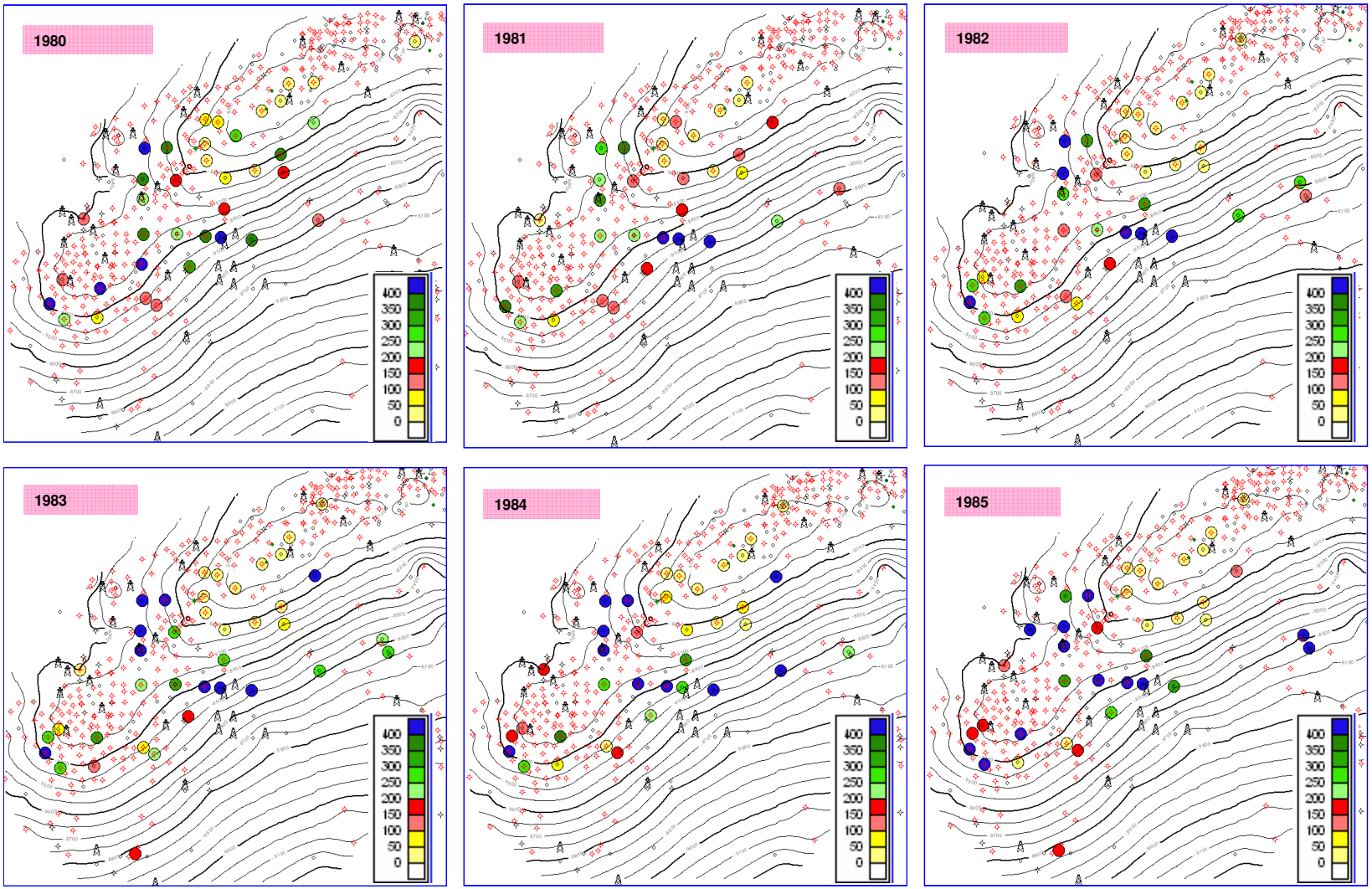

Fig. H2: Distribution of Water-Gas Ratios (1980 – 1985).

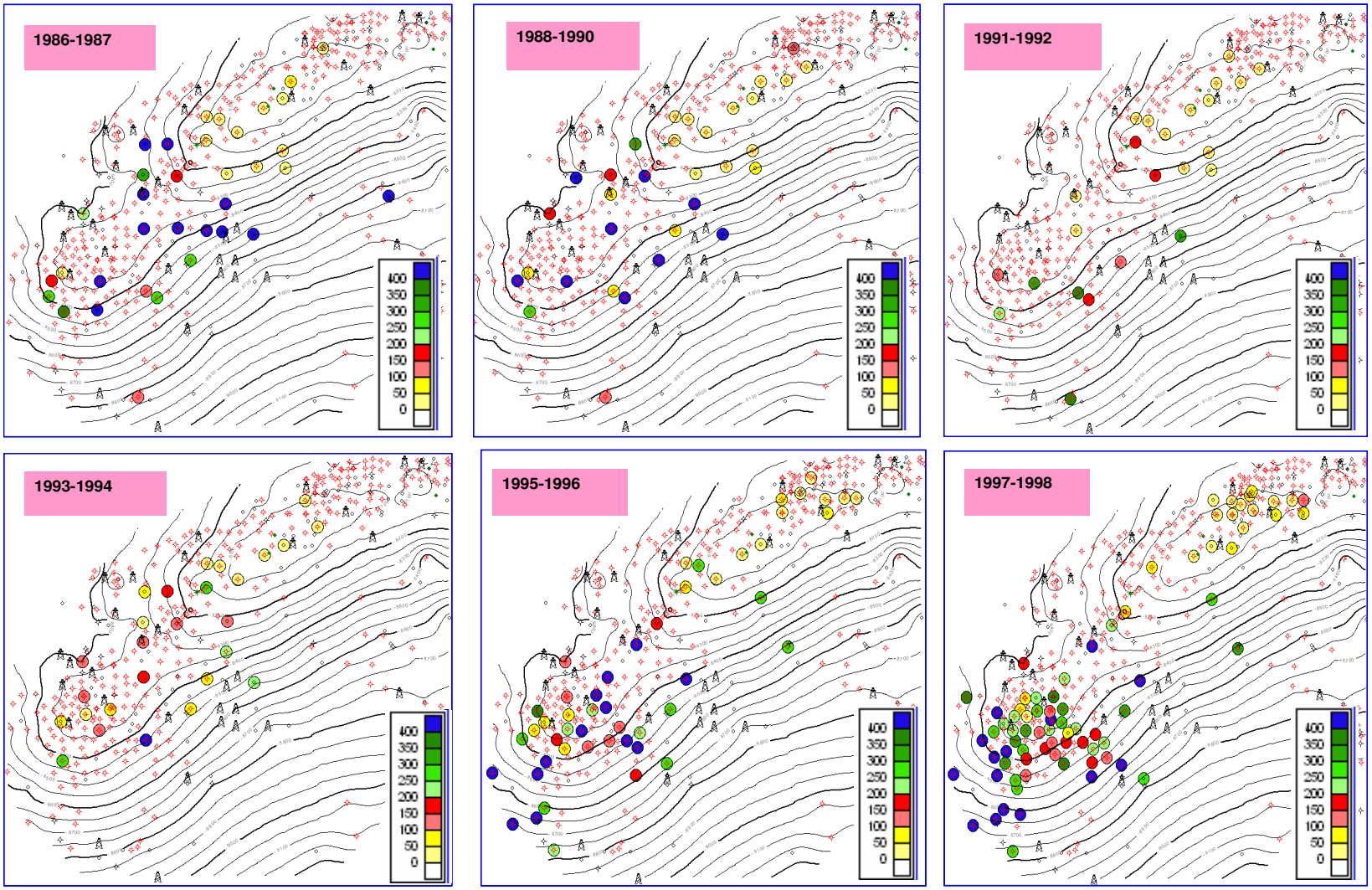

Fig. H3: Distribution of Water-Gas Ratios (1987 – 1998).

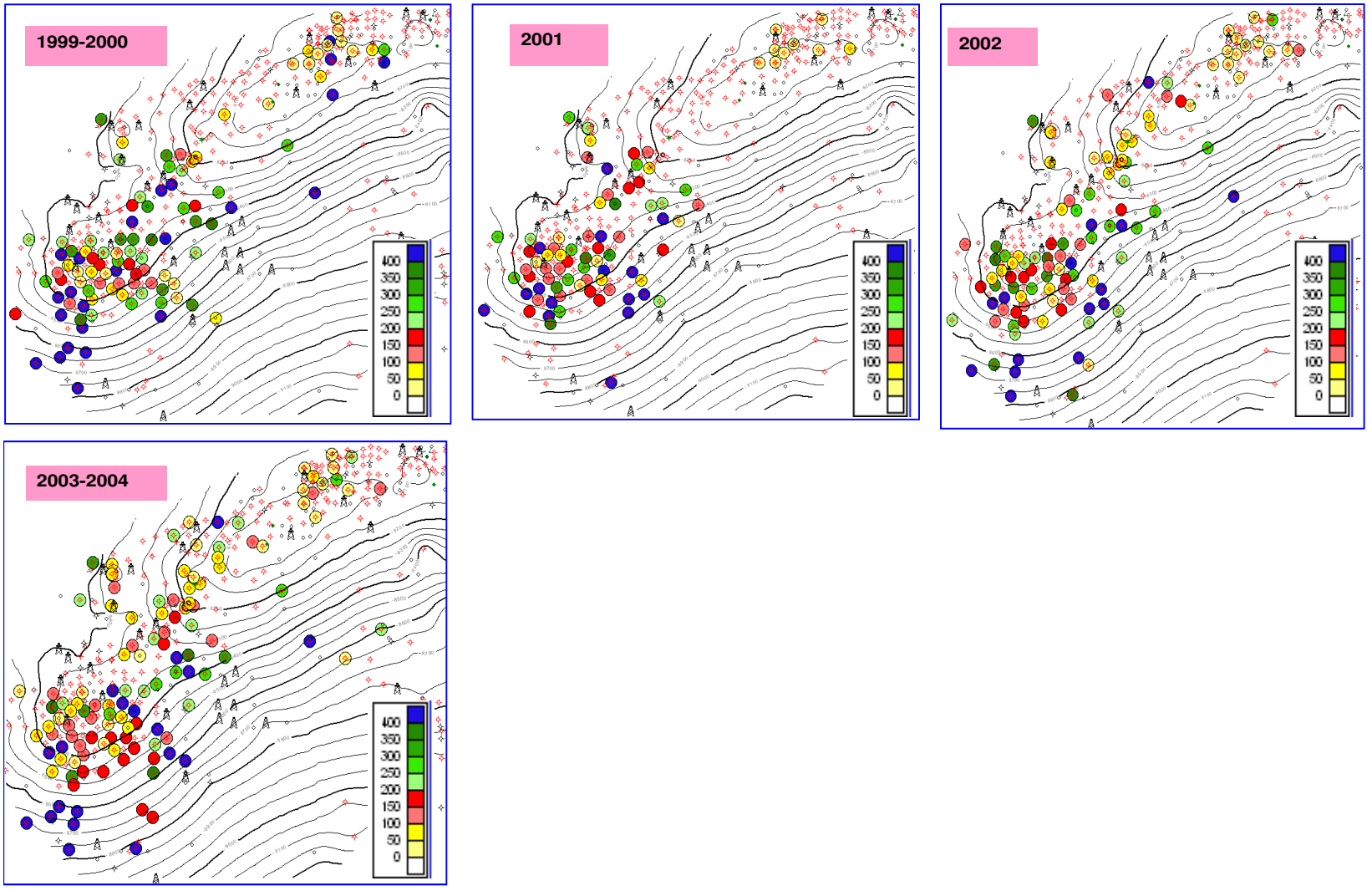

Fig. H4: Distribution of Water-Gas Ratios (1998 – 2004).

APPENDIX I

SUMS AND AVERAGES

Table I1: (Suma and Averages for Zone UCV_LS)

API	Well Name	Top (ft)	Base (ft)	GrossInt (ft)	GrossRes (ft)	NetRes (ft)	NetPay (ft)	N/G Pay (frac)	N/G Res (frac)	PhiHt (ft)	SoPhiHt (ft)	PhiPay (frac)	SwPay (frac)	VshlPay (frac)	PhiRes (frac)	VshlRes (frac)
17015232010000	LOTT 14	8814	9010	196	194	144	27	0.14	0.74	4.75	0.53	0.06	0.65	0.30	0.03	0.38
17015232740000	CAPLIS 22; CV RA SU	8193	8428	236	226	171	24	0.10	0.72	6.10	0.54	0.06	0.60	0.29	0.04	0.43
17015232780000	CAPLIS; 15 CV RA SU	8262	8518	256	253	209	50	0.19	0.81	7.88	1.22	0.06	0.57	0.29	0.04	0.38
17015233220000	BROWN 4; CV RA SU 1	8625	8838	213	213	170	52	0.24	0.80	6.37	0.87	0.05	0.66	0.27	0.04	0.35
17015234310000	NINOCK LAND CO 35;	9012	9200	188	188	141	25	0.13	0.75	4.60	0.46	0.06	0.66	0.26	0.03	0.29
17017216930000	CAPLIS	8323	8527	204	204	116	24	0.12	0.57	4.73	0.54	0.06	0.63	0.30	0.04	0.37
17017217050000	HUTCHINSON	8313	8511	198	198	197	75	0.38	1.00	8.31	1.49	0.05	0.62	0.27	0.04	0.30
17017217970000	FRIERSON TRUST	8364	8568	204	203	149	30	0.15	0.73	5.41	0.52	0.06	0.69	0.34	0.04	0.40
17017221550000	CUPPLES CU RA SU 72	8526	8731	204	204	198	61	0.30	0.97	7.94	0.89	0.05	0.69	0.25	0.04	0.31
17017322540000	DANNY-WEBB; CV RA S	8300	8496	196	196	195	27	0.14	1.00	7.81	0.32	0.05	0.78	0.29	0.04	0.36
17017322950000	HUTCHINSON 4; CV RA	8295	8499	204	201	147	22	0.11	0.72	5.29	0.51	0.06	0.62	0.30	0.04	0.37
17017323700000	DENNY-WEBB;CV RA SU	8369	8573	204	204	201	109	0.53	0.98	9.73	2.21	0.05	0.62	0.27	0.05	0.34
17017324060000	SMITH SAM W 28;CV R	8560	8764	64	62											
17017324230000	LEVEE BOARD 22;CV R	8606	8806	200	200	197	130	0.65	0.98	9.43	2.49	0.05	0.62	0.26	0.05	0.31
17017325020000	ELLERBE HEIRS 21, C	8478	8678	200	197	192	100	0.50	0.96	8.55	2.04	0.05	0.60	0.29	0.05	0.38
17017325070000	ELLERBE HEIRS 21; C	8538	8742	204	204	200	141	0.69	0.98	10.71	3.28	0.06	0.58	0.27	0.05	0.34
17017325190000	RICHLEN D A LAND 18	8306	8511	204	204	198	91	0.45	0.97	9.17	1.90	0.06	0.62	0.29	0.05	0.35
17017327540000	HUTCHINSON;CV RA SU	8199	8401	202	200	117	18	0.09	0.58	4.61	0.37	0.06	0.64	0.28	0.04	0.43
17017328140000	HUTCHINSON 9;CV RA	8377	8569	192	188	187	41	0.21	0.98	7.43	0.58	0.05	0.72	0.34	0.04	0.40
17017329300000	HUTCHINSON 10;CV RA	8361	8565	204	204	185	53	0.26	0.90	5.66	0.79	0.04	0.65	0.30	0.03	0.35
17017330580000	HUTCHINSON;CV RA SU	8223	8427	204	203	147	47	0.23	0.72	7.11	1.33	0.09	0.67	0.43	0.05	0.39
17017331290000	HUTCHINSON; CV RA S	8165	8361	196	195	141	16	0.08	0.72	5.18	0.26	0.06	0.73	0.33	0.04	0.39
17017333160000	ALLEN; CV RA SUI	9109	9301	192	192	142	28	0.15	0.74	4.84	0.67	0.06	0.60	0.30	0.03	0.33
17017333330000	SMITH SAM W ETAL 32	8681	8864	183	183	183	80	0.44	1.00	7.81	1.61	0.05	0.60	0.28	0.04	0.34
17017334340000	FRIERSON 30; CV RA	8193	8393	200	196	145	0	0.00	0.72	5.16	0.00				0.04	0.40
17017335630000	DUTTON FAMILY LLC #1	8737	8937	200	200	150	6	0.03	0.75	4.94	0.08	0.06	0.79	0.31	0.03	0.37
1701733625000	SMITH HEIRS #1	8681	8881	200	200	169	22	0.11	0.85	4.87	0.29	0.05	0.71	0.25	0.03	0.31
1701733644000	COLBERT - 1	8551	8760	208	208	187	26	0.13	0.90	5.75	0.35	0.05	0.71	0.28	0.03	0.32
1701733654000	CASPIANA INT. #1 ALT	8581	8793	213	213	167	25	0.12	0.78	5.24	0.52	0.05	0.58	0.20	0.03	0.31
17031204310000	E TURNER JR ETAL	8374	8566	192	191	190	57	0.30	0.99	7.37	0.75	0.05	0.72	0.29	0.04	0.35
17031204650000	G A FRIERSON	8391	8591	200	200	199	82	0.41	0.99	7.65	1.50	0.05	0.61	0.32	0.04	0.36
17031204920000	J R CALDWELL	8638	8834	196	195	144	44	0.23	0.74	5.32	0.86	0.05	0.63	0.38	0.04	0.41
17031215180000	GUY J F	8858	9041	183	183	183	89	0.49	1.00	8.53	1.97	0.06	0.62	0.26	0.05	0.27
17031230410000	GRIFFIN 33; CV RA S	8824	9033	208	199	189	54	0.26	0.91	7.60	1.32	0.06	0.58	0.31	0.04	0.39
17031230470000	HUNT PLYWOOD C;CV R	8676	8868	192	192	179	76	0.39	0.94	6.85	1.62	0.05	0.54	0.26	0.04	0.34
17031230630000	WILKINSON 24;CV RA	8360	8556	196	194	189	54	0.28	0.96	7.77	1.01	0.05	0.63	0.28	0.04	0.37
17031231140000	WASHINGTON AARON 23	8438	8638	200	198	195	46	0.23	0.97	7.99	0.80	0.05	0.66	0.25	0.04	0.38
17031231230000	GATLIN RAYMOND 13;	8360	8551	192	189	187	34	0.18	0.97	7.08	0.52	0.05	0.72	0.30	0.04	0.36
17031231400000	RICHLEN D A LAND 18	8300	8503	203	201	180	18	0.09	0.88	6.08	0.28	0.05	0.70	0.33	0.03	0.40

Table I2: (Sums and Averages for Zone UCV_S1)

API	Well Name	Top (ft)	Base (ft)	GrossInt (ft)	GrossRes (ft)	NetRes (ft)	NetPay (ft)	N/G Pay (frac)	N/G Res (frac)	PhiHt (ft)	SoPhiHt (ft)	PhiPay (frac)	SwPay (frac)	VshlPay (frac)	PhiRes (frac)	VshlRes (frac)
17015232010000	LOTT 14	9010	9112	102	102	82	45	0.44	0.80	3.18	1.14	0.05	0.47	0.08	0.04	0.10
17015232740000	CAPLIS 22; CV RA SU	8428	8487	58	55	42	8	0.14	0.72	1.22	0.11	0.04	0.66	0.12	0.03	0.23
17015232780000	CAPLIS; 15 CV RA SU	8518	8576	58	57	53	40	0.68	0.91	3.36	1.97	0.07	0.30	0.05	0.06	0.16
17015233220000	BROWN 4; CV RA SU 1	8838	8940	102	102	88	67	0.65	0.87	4.60	2.15	0.06	0.47	0.05	0.05	0.09
17015234310000	NINOCK LAND CO 35;	9200	9323	123	123	105	51	0.42	0.85	4.14	1.09	0.05	0.55	0.08	0.04	0.08
17017216930000	CAPLIS	8527	8627	100	99	76	53	0.53	0.76	3.92	2.02	0.06	0.37	0.05	0.05	0.15
17017217050000	HUTCHINSON	8511	8619	108	108	79	60	0.55	0.73	3.94	2.14	0.06	0.39	0.12	0.05	0.14
17017217970000	FRIERSON TRUST	8568	8666	98	98	84	46	0.47	0.86	3.02	1.21	0.04	0.40	0.15	0.04	0.23
17017221550000	CUPPLES CU RA SU 72	8731	8843	113	113	60	26	0.23	0.53	2.19	0.48	0.05	0.65	0.05	0.04	0.06
17017322540000	DANNY-WEBB; CV RA S	8496	8611	115	115	81	12	0.11	0.71	1.82	0.35	0.05	0.47	0.13	0.02	0.09
17017322950000	HUTCHINSON 4; CV RA	8499	8599	100	98	26	1	0.01	0.26	0.56	0.01	0.04	0.72	0.19	0.02	0.06
17017323700000	DENNY-WEBB;CV RA SU	8573	8682	108	108	99	80	0.74	0.92	6.82	3.65	0.08	0.41	0.11	0.07	0.16
17017324060000	SMITH SAM W 28;CV R	8764	8883	119	119											
17017324230000	LEVEE BOARD 22;CV R	8806	8927	121	121	111	104	0.86	0.92	7.75	4.67	0.07	0.38	0.08	0.07	0.08
17017325020000	ELLERBE HEIRS 21, C	8678	8795	117	116	107	103	0.88	0.92	10.60	8.06	0.10	0.24	0.12	0.10	0.12
17017325070000	ELLERBE HEIRS 21; C	8742	8855	113	112	107	94	0.84	0.95	7.82	5.13	0.08	0.32	0.08	0.07	0.10
17017325190000	RICHLEN D A LAND 18	8511	8619	108	108	95	74	0.68	0.88	6.49	4.13	0.08	0.29	0.07	0.07	0.13
17017327540000	HUTCHINSON;CV RA SU	8401	8491	90	85	45	33	0.37	0.50	2.09	1.17	0.06	0.36	0.07	0.05	0.12
17017328140000	HUTCHINSON 9;CV RA	8569	8690	121	118	104	70	0.58	0.86	5.38	2.16	0.06	0.51	0.14	0.05	0.20
17017329300000	HUTCHINSON 10;CV RA	8565	8673	108	105	74	56	0.52	0.68	3.21	1.58	0.05	0.41	0.11	0.04	0.17
17017330580000	HUTCHINSON;CV RA SU	8427	8523	96	91	34	4	0.04	0.36	0.99	0.05	0.04	0.70	0.04	0.03	0.19
17017331290000	HUTCHINSON; CV RA S	8361	8452	92	89	35	12	0.13	0.38	0.86	0.11	0.03	0.68	0.08	0.02	0.15
17017333160000	ALLEN; CV RA SUI	9301	9451	150	150	101	37	0.24	0.67	3.75	0.72	0.05	0.60	0.14	0.04	0.11
17017333330000	SMITH SAM W ETAL 32	8864	8999	135	135	128	108	0.80	0.95	8.32	5.08	0.07	0.34	0.10	0.07	0.11
17017334340000	FRIERSON 30; CV RA	8393	8480	88	85	42			0.48	1.03					0.03	0.16
17017335630000	DUTTON FAMILY LLC #1	8937	9060	116	116	92	40	0.34	0.80	3.67	1.17	0.05	0.45	0.09	0.04	0.10
1701733625000	SMITH HEIRS #1	8881	9002	121	121	91	41	0.34	0.76	3.73	1.00	0.05	0.52	0.06	0.04	0.07
1701733644000	COLBERT - 1	8760	8870	110	110	80	48	0.43	0.72	3.48	1.12	0.05	0.54	0.06	0.04	0.09
1701733654000	CASPIANA INT. #1 ALT	8793	8902	108	108	73	43	0.40	0.68	3.25	0.90	0.05	0.61	0.04	0.04	0.05
17031204310000	E TURNER JR ETAL	8566	8681	115	115	93	74	0.64	0.81	5.00	3.13	0.06	0.30	0.07	0.05	0.11
17031204650000	G A FRIERSON	8591	8687	96	96	62	58	0.60	0.65	3.66	2.83	0.06	0.21	0.09	0.06	0.09
17031204920000	J R CALDWELL	8834	8951	117	114	88	59	0.50	0.76	2.74	1.03	0.04	0.52	0.09	0.03	0.12
17031215180000	GUY J F	9041	9212	140	140	133	121	0.87	0.95	8.63	5.07	0.07	0.39	0.07	0.07	0.08
17031230410000	GRIFFIN 33; CV RA S	9033	9156	123	123	122	98	0.80	0.99	7.55	3.89	0.07	0.42	0.09	0.06	0.14
17031230470000	HUNT PLYWOOD C;CV R	8868	9004	135	135	135	103	0.76	1.00	8.43	3.83	0.07	0.48	0.11	0.06	0.13
17031230630000	WILKINSON 24;CV RA	8556	8672	117	117	101	91	0.78	0.86	7.10	4.94	0.08	0.28	0.10	0.07	0.11
17031231140000	WASHINGTON AARON 23	8638	8752	115	114	103	79	0.69	0.90	6.26	3.71	0.07	0.35	0.09	0.06	0.14
17031231230000	GATLIN RAYMOND 13;	8551	8656	104	103	79	61	0.59	0.76	4.36	2.59	0.06	0.33	0.08	0.06	0.12
17031231400000	RICHLEN D A LAND 18	8503	8607	103	103	57	44	0.42	0.55	2.88	1.73	0.06	0.35	0.08	0.05	0.13

Table I3: (Sums and Averages for Zone UCV_S2)

API	Well Name	Top (ft)	Base (ft)	GrossInt (ft)	GrossRes (ft)	NetRes (ft)	NetPay (ft)	N/G Pay (frac)	N/G Res (frac)	PhiHt (ft)	SoPhiHt (ft)	PhiPay (frac)	SwPay (frac)	VshlPay (frac)	PhiRes (frac)	VshlRes (frac)
17015232010000	LOTT 14	9112	9223	111	111	87	60	0.54	0.79	3.63	1.54	0.05	0.48	0.09	0.04	0.12
17015232740000	CAPLIS 22; CV RA SU	8487	8525	38	38	32	18	0.48	0.85	1.24	0.23	0.04	0.67	0.11	0.04	0.13
17015232780000	CAPLIS; 15 CV RA SU	8576	8615	39	39	37	30	0.78	0.96	2.21	1.17	0.07	0.43	0.09	0.06	0.10
17015233220000	BROWN 4; CV RA SU 1	8940	9026	85	85	79	53	0.62	0.92	4.15	1.28	0.06	0.61	0.08	0.05	0.14
17015234310000	NINOCK LAND CO 35;	9323	9450	127	126	101	53	0.41	0.79	4.09	1.34	0.05	0.51	0.03	0.04	0.07
17017216930000	CAPLIS	8627	8683	55	55	51	25	0.45	0.93	2.72	0.82	0.07	0.50	0.03	0.05	0.05
17017217050000	HUTCHINSON	8619	8687	68	68	68	59	0.86	1.00	4.84	2.14	0.08	0.52	0.08	0.07	0.10
17017217970000	FRIERSON TRUST	8666	8723	57	57	50	15	0.26	0.88	1.98	0.21	0.04	0.66	0.04	0.04	0.07
17017221550000	CUPPLES CU RA SU 72	8843	8923	80	80	74	22	0.27	0.92	3.03	0.38	0.06	0.69	0.06	0.04	0.12
17017322540000	DANNY-WEBB; CV RA S	8611	8685	74	74	73	61	0.82	0.99	5.22	1.90	0.08	0.59	0.08	0.07	0.10
17017322950000	HUTCHINSON 4; CV RA	8599	8663	64	60	55	16	0.24	0.87	2.47	0.31	0.06	0.69	0.05	0.05	0.06
17017323700000	DENNY-WEBB;CV RA SU	8682	8758	76	76	75	73	0.96	0.99	6.42	3.51	0.09	0.45	0.07	0.09	0.08
17017324060000	SMITH SAM W 28;CV R	8883	8973	90	90											
17017324230000	LEVEE BOARD 22;CV R	8927	9018	92	92	85	81	0.88	0.93	7.31	4.26	0.09	0.41	0.08	0.09	0.09
17017325020000	ELLERBE HEIRS 21, C	8795	8880	84	84	82	80	0.94	0.97	7.10	3.85	0.09	0.46	0.13	0.09	0.13
17017325070000	ELLERBE HEIRS 21; C	8855	8943	89	89	84	83	0.94	0.94	7.96	4.89	0.10	0.38	0.10	0.10	0.11
17017325190000	RICHLEN D A LAND 18	8619	8691	72	72	72	70	0.97	1.00	7.12	4.56	0.10	0.35	0.05	0.10	0.06
17017327540000	HUTCHINSON;CV RA SU	8491	8544	53	53	49	30	0.56	0.92	2.37	0.67	0.06	0.59	0.09	0.05	0.11
17017328140000	HUTCHINSON 9;CV RA	8690	8766	76	74	72	55	0.72	0.95	4.91	1.89	0.08	0.55	0.10	0.07	0.13
17017329300000	HUTCHINSON 10;CV RA	8673	8745	72	72	68	48	0.67	0.94	3.55	1.46	0.06	0.51	0.07	0.05	0.08
17017330580000	HUTCHINSON;CV RA SU	8523	8583	59	59	57	30	0.50	0.96	2.57	0.62	0.06	0.63	0.08	0.05	0.12
17017331290000	HUTCHINSON; CV RA S	8452	8499	47	47	42	30	0.65	0.91	1.66	0.50	0.04	0.63	0.04	0.04	0.05
17017333160000	ALLEN; CV RA SUI	9451	9551	100	100	81	47	0.47	0.81	3.44	1.19	0.05	0.51	0.08	0.04	0.11
17017333330000	SMITH SAM W ETAL 32	8999	9085	85	85	82	58	0.68	0.96	4.87	2.16	0.07	0.47	0.12	0.06	0.12
17017334340000	FRIERSON 30; CV RA	8480	8523	43	43	39			0.91	1.52					0.04	0.10
17017335630000	DUTTON FAMILY LLC #1	9060	9150	96	96	80	25	0.25	0.82	3.45	0.62	0.06	0.56	0.09	0.04	0.12
1701733625000	SMITH HEIRS #1	9002	9091	89	89	84	37	0.41	0.95	3.61	0.54	0.05	0.70	0.07	0.04	0.10
1701733644000	COLBERT - 1	8870	8953	82	82	78	43	0.52	0.94	4.20	1.06	0.07	0.64	0.06	0.05	0.11
1701733654000	CASPIANA INT. #1 ALT	8902	8986	84	83	74	44	0.52	0.88	4.22	1.41	0.07	0.53	0.06	0.06	0.10
17031204310000	E TURNER JR ETAL	8681	8746	66	66	64	53	0.80	0.97	4.77	2.87	0.08	0.33	0.05	0.08	0.07
17031204650000	G A FRIERSON	8687	8750	64	64	61	54	0.85	0.95	4.65	2.81	0.08	0.36	0.09	0.08	0.10
17031204920000	J R CALDWELL	8951	9017	67	67	62	39	0.58	0.93	2.53	0.61	0.05	0.67	0.04	0.04	0.05
17031215180000	GUY J F	9212	9279	98	98	93	79	0.81	0.95	5.44	3.12	0.07	0.39	0.10	0.06	0.11
17031230410000	GRIFFIN 33; CV RA S	9156	9241	85	82	81	72	0.84	0.95	5.64	3.06	0.07	0.43	0.15	0.07	0.17
17031230470000	HUNT PLYWOOD C;CV R	9004	9089	85	85	83	60	0.70	0.97	5.79	2.20	0.08	0.53	0.09	0.07	0.11
17031230630000	WILKINSON 24;CV RA	8672	8748	76	76	74	61	0.80	0.97	5.37	2.45	0.08	0.50	0.08	0.07	0.10
17031231140000	WASHINGTON AARON 23	8752	8826	74	74	73	61	0.82	0.98	5.19	2.34	0.08	0.51	0.06	0.07	0.08
17031231230000	GATLIN RAYMOND 13;	8656	8723	68	68	67	55	0.81	0.98	5.04	2.79	0.08	0.37	0.06	0.08	0.07
17031231400000	RICHLEN D A LAND 18	8607	8676	70	70	63	50	0.71	0.90	4.12	1.69	0.07	0.53	0.06	0.07	0.08

Table I4: (Sums and Averages for Zone UCV_BOSH)

API	Well Name	Top (ft)	Base (ft)	GrossInt (ft)	GrossRes (ft)	NetRes (ft)	NetPay (ft)	N/G Pay (frac)	N/G Res (frac)	PhiHt (ft)	SoPhiHt (ft)	PhiPay (frac)	SwPay (frac)	VshlPay (frac)	PhiRes (frac)	VshlRes (frac)
17015232010000	LOTT 14	9223	9245	23	4	1	0	0.00	0.04	0.01	0.00				0.01	0.64
17015232740000	CAPLIS 22; CV RA SU	8525	8553	29	4	1	0	0.00	0.04	0.01	0.00				0.01	0.63
17015232780000	CAPLIS; 15 CV RA SU	8615	8644	29	6	4	0	0.00	0.15	0.07	0.00				0.02	0.57
17015233220000	BROWN 4; CV RA SU 1	9026	9050	24	7	2	0	0.00	0.08	0.02	0.00				0.01	0.63
17015234310000	NINOCK LAND CO 35;	9450	9475	25	3	0	0	0.00	0.00	0.00	0.00					
17017216930000	CAPLIS	8683	8714	31	8	3	1	0.02	0.10	0.07	0.00	0.05	0.86	0.24	0.02	0.53
17017217050000	HUTCHINSON	8687	8716	29	6	1	0	0.00	0.03	0.01	0.00				0.01	0.67
17017217970000	FRIERSON TRUST	8723	8755	31	10	5	1	0.03	0.18	0.11	0.01	0.04	0.81	0.40	0.02	0.60
17017221550000	CUPPLES CU RA SU 72	8923	8946	23	5	1	0	0.00	0.04	0.01	0.00				0.01	0.65
17017322540000	DANNY-WEBB; CV RA S	8685	8712	27	4	2	0	0.00	0.08	0.02	0.00				0.01	0.65
17017322950000	HUTCHINSON 4; CV RA	8663	8684	21	3	0	0	0.00	0.00	0.00	0.00					
17017323700000	DENNY-WEBB;CV RA SU	8758	8783	25	2	0	0	0.00	0.00	0.00	0.00					
17017324060000	SMITH SAM W 28;CV R	8973	8998	25	1											
17017324230000	LEVEE BOARD 22;CV R	9018	9043	25	6	1	0	0.00	0.02	0.01	0.00				0.01	0.66
17017325020000	ELLERBE HEIRS 21, C	8880	8905	25	0	0	0	0.00	0.00	0.00	0.00					
17017325070000	ELLERBE HEIRS 21; C	8943	8968	25	1	0	0	0.00	0.00	0.00	0.00					
17017325190000	RICHLEN D A LAND 18	8691	8722	31	5	2	0	0.00	0.05	0.02	0.00				0.01	0.62
17017327540000	HUTCHINSON;CV RA SU	8544	8573	29	6	2	0	0.00	0.07	0.02	0.00				0.01	0.63
17017328140000	HUTCHINSON 9;CV RA	8766	8790	24	1	0	0	0.00	0.00	0.00	0.00					
17017329300000	HUTCHINSON 10;CV RA	8745	8772	27	7	4	0	0.00	0.15	0.06	0.00				0.02	0.55
17017330580000	HUTCHINSON;CV RA SU	8583	8606	23	3	3	0	0.00	0.14	0.14	0.00				0.05	0.72
17017331290000	HUTCHINSON; CV RA S	8499	8526	27	7	4	1	0.02	0.15	0.07	0.01	0.04	0.75	0.07	0.02	0.35
17017333160000	ALLEN; CV RA SUI	9551	9580	29	2	0	0	0.00	0.00	0.00	0.00					
17017333330000	SMITH SAM W ETAL 32	9085	9114	29	5	0	0	0.00	0.00	0.00	0.00					
17017334340000	FRIERSON 30; CV RA	8523	8552	29	6	5	0	0.00	0.16	0.12	0.00				0.03	0.42
17017335630000	DUTTON FAMILY LLC #1	9150	9172	23	6	0	0	0.00	0.00	0.00	0.00					
1701733625000	SMITH HEIRS #1	9091	9116	25	7	2	0	0.00	0.06	0.03	0.00				0.02	0.44
1701733644000	COLBERT - 1	8953	8978	25	4	1	0	0.00	0.05	0.02	0.00				0.01	0.66
1701733654000	CASPIANA INT. #1 ALT	8986	9007	21	8	4	0	0.00	0.17	0.04	0.00				0.01	0.64
17031204310000	E TURNER JR ETAL	8746	8775	29	0	0	0	0.00	0.00	0.00	0.00					
17031204650000	G A FRIERSON	8750	8782	31	1	0	0	0.00	0.00	0.00	0.00					
17031204920000	J R CALDWELL	9017	9051	33	2	0	0	0.00	0.00	0.00	0.00					
17031215180000	GUY J F	9279	9308	29	5	3	0	0.00	0.10	0.09	0.00				0.03	0.71
17031230410000	GRIFFIN 33; CV RA S	9241	9273	31	1	0	0	0.00	0.00	0.00	0.00					
17031230470000	HUNT PLYWOOD C;CV R	9089	9120	31	3	0	0	0.00	0.00	0.00	0.00					
17031230630000	WILKINSON 24;CV RA	8748	8777	29	2	1	0	0.00	0.02	0.01	0.00				0.01	0.65
17031231140000	WASHINGTON AARON 23	8826	8856	29	2	1	0	0.00	0.02	0.01	0.00				0.01	0.66
17031231230000	GATLIN RAYMOND 13;	8723	8752	29	1	1	0	0.00	0.02	0.01	0.00				0.01	0.64
17031231400000	RICHLEN D A LAND 18	8676	8708	31	3	0	0	0.00	0.00	0.00	0.00					

Table I5: (Sums and Averages for Zone LCV_LS)

API	Well Name	Top (ft)	Base (ft)	GrossInt (ft)	GrossRes (ft)	NetRes (ft)	NetPay (ft)	N/G Pay (frac)	N/G Res (frac)	PhiHt (ft)	SoPhiHt (ft)	PhiPay (frac)	SwPay (frac)	VshlPay (frac)	PhiRes (frac)	VshlRes (frac)
17015232010000	LOTT 14	9245	9323	77	51	13	0	0.00	0.17	0.20	0.00				0.02	0.53
17015232740000	CAPLIS 22; CV RA SU	8553	8672	119	118	88	41	0.34	0.75	4.05	1.13	0.06	0.54	0.04	0.05	0.10
17015232780000	CAPLIS; 15 CV RA SU	8644	8783	139	138	117	63	0.45	0.84	6.25	1.56	0.06	0.61	0.07	0.05	0.12
17015233220000	BROWN 4; CV RA SU 1	9050	9134	84	78	62	0	0.00	0.73	1.26	0.00				0.02	0.40
17015234310000	NINOCK LAND CO 35;	9475	9537	63	35	14	0	0.00	0.22	0.21	0.00				0.02	0.55
17017216930000	CAPLIS	8714	8815	101	100	76	13	0.12	0.75	3.21	0.26	0.06	0.65	0.14	0.04	0.27
17017217050000	HUTCHINSON	8716	8803	87	80	57	0	0.00	0.66	1.62	0.00				0.03	0.44
17017217970000	FRIERSON TRUST	8755	8854	99	97	73	7	0.07	0.74	3.02	0.24	0.08	0.59	0.20	0.04	0.32
17017221550000	CUPPLES CU RA SU 72	8946	9035	89	84	52	0	0.00	0.58	0.97	0.00				0.02	0.42
17017322540000	DANNY-WEBB; CV RA S	8712	8790	79	69	48	0	0.00	0.61	0.84	0.00				0.02	0.48
17017322950000	HUTCHINSON 4; CV RA	8684	8787	103	97	66	3	0.02	0.64	2.73	0.04	0.06	0.74	0.26	0.04	0.30
17017323700000	DENNY-WEBB;CV RA SU	8783	8900	80	61	48	4	0.05	0.60	1.14	0.27	0.09	0.27	0.27	0.02	0.48
17017324060000	SMITH SAM W 28;CV R	8998	9070	76	43											
17017324230000	LEVEE BOARD 22;CV R	9043	9120	77	62	51	4	0.05	0.66	1.28	0.30	0.12	0.32	0.38	0.03	0.48
17017325020000	ELLERBE HEIRS 21, C	8905	8983	78	54	44	2	0.03	0.56	0.85	0.07	0.07	0.47	0.16	0.02	0.49
17017325070000	ELLERBE HEIRS 21; C	8968	9048	80	58	45	3	0.03	0.56	0.88	0.12	0.07	0.37	0.20	0.02	0.51
17017325190000	RICHLEN D A LAND 18	8722	8796	77	66	43	1	0.02	0.55	0.90	0.06	0.07	0.30	0.11	0.02	0.46
17017327540000	HUTCHINSON;CV RA SU	8573	8678	105	104	78	9	0.09	0.74	3.35	0.25	0.07	0.57	0.24	0.04	0.30
17017328140000	HUTCHINSON 9;CV RA	8790	8873	83	56	44	0	0.00	0.52	0.74	0.00				0.02	0.49
17017329300000	HUTCHINSON 10;CV RA	8772	8859	87	78	38	0	0.00	0.44	0.74	0.00				0.02	0.45
17017330580000	HUTCHINSON;CV RA SU	8606	8707	101	95	76	5	0.05	0.76	3.24	0.27	0.09	0.42	0.21	0.04	0.29
17017331290000	HUTCHINSON; CV RA S	8526	8642	116	110	83	11	0.10	0.71	3.12	0.19	0.05	0.68	0.10	0.04	0.17
17017333160000	ALLEN; CV RA SUI	9580	9661	79	42	11	0	0.00	0.14	0.16	0.00				0.02	0.55
17017333330000	SMITH SAM W ETAL 32	9114	9189	75	48	24	6	0.08	0.32	0.67	0.26	0.07	0.39	0.30	0.03	0.52
17017334340000	FRIERSON 30; CV RA	8552	8658	105	104	82	31	0.29	0.78	3.66	1.12	0.06	0.38	0.07	0.04	0.13
17017335630000	DUTTON FAMILY LLC #1	9172	9254	81	57	16	0	0.00	0.19	0.25	0.00				0.02	0.58
1701733625000	SMITH HEIRS #1	9116	9190	74	53	10	0	0.00	0.14	0.15	0.00				0.01	0.45
1701733644000	COLBERT - 1	8978	9064	87	76	38	2	0.03	0.44	0.76	0.04	0.05	0.61	0.09	0.02	0.42
1701733654000	CASPIANA INT. #1 ALT	9007	9091	84	76	39	0	0.01	0.47	0.77	0.01	0.06	0.58	0.30	0.02	0.41
17031204310000	E TURNER JR ETAL	8775	8845	70	60	33	0	0.00	0.47	0.60	0.00				0.02	0.48
17031204650000	G A FRIERSON	8782	8851	70	59	41	0	0.00	0.58	0.73	0.00				0.02	0.46
17031204920000	J R CALDWELL	9051	9128	77	51	24	1	0.02	0.32	0.45	0.07	0.07	0.30	0.31	0.02	0.50
17031215180000	GUY J F	9308	9373	65	50	47	0	0.00	0.73	1.37	0.00				0.03	0.60
17031230410000	GRIFFIN 33; CV RA S	9273	9335	63	40	22	0	0.00	0.34	0.31	0.00				0.01	0.58
17031230470000	HUNT PLYWOOD C;CV R	9120	9183	63	46	32	0	0.00	0.51	0.45	0.00				0.01	0.59
17031230630000	WILKINSON 24;CV RA	8777	8851	74	54	33	1	0.01	0.45	0.62	0.03	0.07	0.38	0.05	0.02	0.52
17031231140000	WASHINGTON AARON 23	8856	8911	55	35	20	0	0.00	0.37	0.31	0.00				0.02	0.55
17031231230000	GATLIN RAYMOND 13;	8752	8808	55	39	22	0	0.00	0.40	0.40	0.00				0.02	0.48
17031231400000	RICHLEN D A LAND 18	8708	8780	72	55	27	0	0.00	0.37	0.49	0.00				0.02	0.48

Table I6: (Sums and Averages for Zone LCV_S2)

API	Well Name	Top (ft)	Base (ft)	GrossInt (ft)	GrossRes (ft)	NetRes (ft)	NetPay (ft)	N/G Pay (frac)	N/G Res (frac)	PhiHt (ft)	SoPhiHt (ft)	PhiPay (frac)	SwPay (frac)	VshlPay (frac)	PhiRes (frac)	VshlRes (frac)
17015232010000	LOTT 14	9323	9458	135	135	125	95	0.70	0.92	7.06	3.71	0.07	0.40	0.15	0.06	0.16
17015232740000	CAPLIS 22; CV RA SU	8672	8815	143	143	130	47	0.33	0.91	5.08	1.06	0.05	0.58	0.12	0.04	0.27
17015232780000	CAPLIS; 15 CV RA SU	8783	8938	155	154	151	122	0.78	0.97	8.53	4.29	0.06	0.42	0.17	0.06	0.22
17015233220000	BROWN 4; CV RA SU 1	9134	9267	133	133	129	95	0.71	0.97	8.02	3.85	0.07	0.42	0.13	0.06	0.17
17015234310000	NINOCK LAND CO 35;	9537	9712	175	175	162	107	0.61	0.93	8.86	3.62	0.07	0.48	0.12	0.06	0.15
17017216930000	CAPLIS	8815	8944	129	129	123	88	0.68	0.95	5.23	2.28	0.05	0.45	0.14	0.04	0.21
17017217050000	HUTCHINSON	8803	8944	142	141	134	100	0.71	0.95	8.02	4.55	0.07	0.34	0.19	0.06	0.24
17017217970000	FRIERSON TRUST	8854	8985	131	131	116	68	0.51	0.89	4.67	1.68	0.05	0.48	0.12	0.04	0.23
17017221550000	CUPPLES CU RA SU 72	9035	9185	150	150	129	83	0.55	0.86	6.27	2.61	0.06	0.47	0.12	0.05	0.14
17017322540000	DANNY-WEBB; CV RA S	8790	8934	143	142	119	93	0.65	0.84	7.21	3.83	0.07	0.39	0.14	0.06	0.16
17017322950000	HUTCHINSON 4; CV RA	8787	8923	136	135	103	54	0.39	0.76	4.19	1.09	0.05	0.61	0.15	0.04	0.21
17017323700000	DENNY-WEBB;CV RA SU	8900	9041	152	149	143	131	0.86	0.94	11.42	8.63	0.08	0.22	0.12	0.08	0.12
17017324060000	SMITH SAM W 28;CV R	9070	9220	147	147											
17017324230000	LEVEE BOARD 22;CV R	9120	9264	144	144	144	143	0.99	1.00	14.39	10.61	0.10	0.26	0.13	0.10	0.13
17017325020000	ELLERBE HEIRS 21, C	8983	9141	158	158	157	148	0.94	0.99	12.83	8.45	0.08	0.32	0.18	0.08	0.18
17017325070000	ELLERBE HEIRS 21; C	9048	9181	133	133	133	130	0.98	1.00	13.17	9.74	0.10	0.26	0.17	0.10	0.17
17017325190000	RICHLEN D A LAND 18	8796	8940	141	139	131	107	0.76	0.93	10.28	7.34	0.09	0.22	0.10	0.08	0.14
17017327540000	HUTCHINSON;CV RA SU	8678	8814	135	134	110	59	0.43	0.81	4.56	1.20	0.05	0.59	0.23	0.04	0.25
17017328140000	HUTCHINSON 9;CV RA	8873	9021	147	147	129	114	0.77	0.88	7.78	4.26	0.07	0.42	0.17	0.06	0.18
17017329300000	HUTCHINSON 10;CV RA	8859	9011	152	150	137	121	0.79	0.90	8.36	5.72	0.07	0.28	0.14	0.06	0.16
17017330580000	HUTCHINSON;CV RA SU	8707	8842	136	134	120	43	0.31	0.89	4.83	0.68	0.05	0.70	0.15	0.04	0.25
17017331290000	HUTCHINSON; CV RA S	8642	8775	133	132	103	72	0.54	0.77	4.11	1.66	0.05	0.52	0.10	0.04	0.11
17017333160000	ALLEN; CV RA SUI	9661	9838	179	179	171	98	0.55	0.95	9.54	3.13	0.07	0.52	0.14	0.06	0.16
17017333330000	SMITH SAM W ETAL 32	9189	9430	240	239	238	200	0.83	0.99	17.91	9.27	0.08	0.43	0.20	0.08	0.20
17017334340000	FRIERSON 30; CV RA	8658	8805	147	145	96	49	0.33	0.66	3.64	1.04	0.05	0.58	0.11	0.04	0.17
17017335630000	DUTTON FAMILY LLC #1	9254	9468	215	215	205	157	0.73	0.96	11.34	5.05	0.06	0.48	0.14	0.06	0.15
1701733625000	SMITH HEIRS #1	9190	9369	179	179	171	129	0.72	0.95	9.76	4.06	0.06	0.51	0.14	0.06	0.14
1701733644000	COLBERT - 1	9064	9223	158	158	150	116	0.74	0.95	9.18	4.46	0.07	0.44	0.11	0.06	0.15
1701733654000	CASPIANA INT. #1 ALT	9091	9249	158	158	144	127	0.80	0.91	8.86	4.72	0.07	0.43	0.09	0.06	0.10
17031204310000	E TURNER JR ETAL	8845	8986	140	140	127	107	0.76	0.90	7.57	4.77	0.07	0.32	0.13	0.06	0.17
17031204650000	G A FRIERSON	8851	8989	138	138	118	106	0.77	0.85	7.48	5.37	0.07	0.25	0.19	0.06	0.20
17031204920000	J R CALDWELL	9128	9272	144	142	118	105	0.73	0.82	5.36	3.19	0.05	0.37	0.19	0.05	0.20
17031215180000	GUY J F	9373	9562	190	184	183	164	0.86	0.97	13.86	8.56	0.08	0.35	0.16	0.08	0.19
17031230410000	GRIFFIN 33; CV RA S	9335	9521	186	186	181	171	0.92	0.98	16.05	10.33	0.09	0.34	0.18	0.09	0.20
17031230470000	HUNT PLYWOOD C;CV R	9183	9403	220	220	215	206	0.94	0.98	19.24	11.94	0.09	0.37	0.16	0.09	0.16
17031230630000	WILKINSON 24;CV RA	8851	9006	154	151	134	114	0.74	0.87	9.70	6.30	0.08	0.32	0.13	0.07	0.14
17031231140000	WASHINGTON AARON 23	8911	9077	166	164	151	111	0.67	0.91	10.13	5.64	0.08	0.36	0.13	0.07	0.20
17031231230000	GATLIN RAYMOND 13;	8808	8963	155	154	114	95	0.61	0.74	7.11	4.26	0.07	0.36	0.17	0.06	0.20
17031231400000	RICHLEN D A LAND 18	8780	8912	132	131	111	93	0.70	0.84	7.95	5.62	0.08	0.24	0.17	0.07	0.18

Table I7: (Sums and Averages for Zone LCV_S3)

API	Well Name	Top (ft)	Base (ft)	GrossInt (ft)	GrossRes (ft)	NetRes (ft)	NetPay (ft)	N/G Pay (frac)	N/G Res (frac)	PhiHt (ft)	SoPhiHt (ft)	PhiPay (frac)	SwPay (frac)	VshlPay (frac)	PhiRes (frac)	VshlRes (frac)
17015232010000	LOTT 14	9458	9638	100	100	97	55	0.55	0.97	5.11	1.99	0.07	0.45	0.19	0.05	0.20
17015232740000	CAPLIS 22; CV RA SU	8815	8890	74	74	74	34	0.46	1.00	4.81	1.19	0.07	0.50	0.10	0.07	0.17
17015232780000	CAPLIS; 15 CV RA SU	8938	8999	61	61	61	57	0.94	1.00	4.29	2.30	0.07	0.44	0.15	0.07	0.16
17015233220000	BROWN 4; CV RA SU 1	9267	9365	98	98	98	92	0.93	1.00	6.69	4.15	0.07	0.36	0.14	0.07	0.15
17015234310000	NINOCK LAND CO 35;	9712	9798	85	85	55	14	0.16	0.64	2.02	0.25	0.05	0.67	0.21	0.04	0.27
17017216930000	CAPLIS	8944	9022	78	78	78	44	0.57	1.00	4.63	1.34	0.07	0.57	0.08	0.06	0.14
17017217050000	HUTCHINSON	8944	9017	73	73	73	62	0.86	1.00	5.41	2.16	0.08	0.57	0.14	0.07	0.15
17017217970000	FRIERSON TRUST	8985	9052	67	67	65	51	0.77	0.98	3.92	1.61	0.07	0.53	0.11	0.06	0.14
17017221550000	CUPPLES CU RA SU 72	9185	9289	104	104	92	55	0.53	0.89	4.17	1.08	0.05	0.62	0.11	0.05	0.12
17017322540000	DANNY-WEBB; CV RA S	8934	9038	104	104	102	90	0.86	0.98	8.10	3.27	0.09	0.57	0.11	0.08	0.12
17017322950000	HUTCHINSON 4; CV RA	8923	8997	74	74	73	48	0.65	0.98	4.57	1.27	0.07	0.62	0.15	0.06	0.16
17017323700000	DENNY-WEBB;CV RA SU	9041	9115	101	101	101	95	0.94	1.00	8.83	6.20	0.09	0.28	0.19	0.09	0.21
17017324060000	SMITH SAM W 28;CV R	9220	9325	104	104											
17017324230000	LEVEE BOARD 22;CV R	9264	9375	110	110	110	110	1.00	1.00	11.27	7.74	0.10	0.31	0.15	0.10	0.15
17017325020000	ELLERBE HEIRS 21, C	9141	9231	90	90	88	80	0.89	0.98	7.02	4.74	0.08	0.29	0.21	0.08	0.22
17017325070000	ELLERBE HEIRS 21; C	9181	9274	92	92	92	92	1.00	1.00	10.14	7.98	0.11	0.21	0.20	0.11	0.20
17017325190000	RICHLEN D A LAND 18	8940	9040	100	100	100	94	0.94	1.00	11.49	7.73	0.12	0.31	0.11	0.12	0.12
17017327540000	HUTCHINSON;CV RA SU	8814	8883	69	69	69	39	0.57	1.00	3.90	0.92	0.06	0.58	0.16	0.06	0.22
17017328140000	HUTCHINSON 9;CV RA	9021	9090	69	69	68	54	0.78	0.98	4.63	2.48	0.08	0.41	0.16	0.07	0.15
17017329300000	HUTCHINSON 10;CV RA	9011	9084	73	73	68	53	0.73	0.94	3.64	1.86	0.06	0.43	0.11	0.05	0.12
17017330580000	HUTCHINSON;CV RA SU	8842	8907	64	64	62	39	0.60	0.97	3.95	0.97	0.07	0.65	0.05	0.06	0.06
17017331290000	HUTCHINSON; CV RA S	8775	8869	94	94	92	76	0.81	0.98	5.77	2.04	0.07	0.59	0.11	0.06	0.12
17017333160000	ALLEN; CV RA SUI	9838	9924	85	85	71	21	0.24	0.84	2.65	0.30	0.05	0.69	0.29	0.04	0.26
17017333330000	SMITH SAM W ETAL 32	9430	9502	72	72	68	40	0.55	0.94	3.77	1.10	0.07	0.60	0.24	0.06	0.26
17017334340000	FRIERSON 30; CV RA	8805	8879	82	82	82	55	0.67	1.00	5.23	1.74	0.07	0.52	0.09	0.06	0.13
17017335630000	DUTTON FAMILY LLC #1	9468	9550	81	81	67	15	0.18	0.83	2.39	0.17	0.04	0.73	0.23	0.04	0.26
1701733625000	SMITH HEIRS #1	9369	9477	108	108	105	74	0.69	0.97	5.75	1.66	0.06	0.63	0.18	0.06	0.21
1701733644000	COLBERT - 1	9223	9321	98	98	94	77	0.79	0.96	6.01	2.75	0.07	0.51	0.15	0.06	0.16
1701733654000	CASPIANA INT. #1 ALT	9249	9327	78	78	77	69	0.88	0.99	4.12	2.38	0.06	0.39	0.11	0.05	0.11
17031204310000	E TURNER JR ETAL	8986	9070	85	85	77	72	0.85	0.90	4.99	2.34	0.07	0.51	0.13	0.07	0.13
17031204650000	G A FRIERSON	8989	9091	102	102	93	88	0.87	0.92	6.70	3.99	0.07	0.39	0.14	0.07	0.15
17031204920000	J R CALDWELL	9272	9351	79	79	78	68	0.85	0.98	4.61	1.69	0.06	0.59	0.23	0.06	0.25
17031215180000	GUY J F	9562	9646	83	83	83	59	0.71	1.00	6.16	1.69	0.08	0.65	0.22	0.07	0.24
17031230410000	GRIFFIN 33; CV RA S	9521	9627	106	106	104	101	0.95	0.98	8.62	4.79	0.08	0.44	0.22	0.08	0.23
17031230470000	HUNT PLYWOOD C;CV R	9403	9516	113	113	111	72	0.63	0.98	7.99	3.23	0.09	0.48	0.26	0.07	0.29
17031230630000	WILKINSON 24;CV RA	9006	9102	96	96	96	89	0.93	1.00	8.29	4.49	0.09	0.43	0.11	0.09	0.12
17031231140000	WASHINGTON AARON 23	9077	9186	109	109	107	98	0.90	0.98	9.28	3.64	0.09	0.58	0.13	0.09	0.15
17031231230000	GATLIN RAYMOND 13;	8963	9060	97	97	84	80	0.82	0.86	5.90	2.35	0.07	0.59	0.17	0.07	0.18
17031231400000	RICHLEN D A LAND 18	8912	9009	97	97	92	85	0.87	0.95	6.83	4.03	0.08	0.39	0.13	0.07	0.14

Table I8: (Sums and Averages for Zone LCV_S4)

API	Well Name	Top (ft)	Base (ft)	GrossInt (ft)	GrossRes (ft)	NetRes (ft)	NetPay (ft)	N/G Pay (frac)	N/G Res (frac)	PhiHt (ft)	SoPhiHt (ft)	PhiPay (frac)	SwPay (frac)	VshlPay (frac)	PhiRes (frac)	VshlRes (frac)
17015232010000	LOTT 14	9558	9631	73	65	53	4	0.05	0.73	1.93	0.06	0.07	0.73	0.60	0.04	0.39
17015232740000	CAPLIS 22; CV RA SU	8890	9016	126	123	118	36	0.29	0.94	7.44	1.90	0.09	0.42	0.14	0.06	0.26
17015232780000	CAPLIS; 15 CV RA SU	8999	9137	138	138	123	78	0.56	0.89	8.91	4.15	0.09	0.43	0.16	0.07	0.20
17015233220000	BROWN 4; CV RA SU 1	9365	9440	75	75	75	58	0.77	1.00	4.37	1.67	0.07	0.57	0.21	0.06	0.22
17015234310000	NINOCK LAND CO 35;	9798	9885	88	71	45	2	0.02	0.51	1.41	0.04	0.05	0.64	0.22	0.03	0.46
17017216930000	CAPLIS	9022	9151	129	129	120	54	0.42	0.93	8.00	1.87	0.09	0.60	0.28	0.07	0.31
17017217050000	HUTCHINSON	9017	9151	133	114	85	30	0.22	0.63	5.48	1.17	0.10	0.60	0.31	0.07	0.39
17017217970000	FRIERSON TRUST	9052	9183	131	131	129	89	0.68	0.99	8.89	3.04	0.08	0.57	0.26	0.07	0.31
17017221550000	CUPPLES CU RA SU 72	9289	9416	127	125	96	19	0.15	0.76	3.97	0.41	0.08	0.70	0.19	0.04	0.30
17017322540000	DANNY-WEBB; CV RA S	9038	9149	110	96	74	9	0.08	0.67	4.63	0.21	0.10	0.75	0.28	0.06	0.38
17017322950000	HUTCHINSON 4; CV RA	8997	9122	125	115	112	45	0.36	0.89	7.09	1.22	0.09	0.68	0.50	0.06	0.43
17017323700000	DENNY-WEBB;CV RA SU	9115	9242	127	115	113	73	0.57	0.89	10.37	4.62	0.12	0.46	0.27	0.09	0.42
17017324060000	SMITH SAM W 28;CV R	9325	9412	88	88											
17017324230000	LEVEE BOARD 22;CV R	9375	9464	90	90	90	79	0.88	1.00	6.11	2.42	0.07	0.57	0.23	0.07	0.23
17017325020000	ELLERBE HEIRS 21, C	9231	9314	83	83	83	40	0.48	1.00	5.65	1.43	0.08	0.54	0.23	0.07	0.28
17017325070000	ELLERBE HEIRS 21; C	9274	9351	77	77	77	76	0.98	1.00	9.07	5.66	0.12	0.37	0.29	0.12	0.29
17017325190000	RICHLEN D A LAND 18	9040	9153	113	93	55	38	0.34	0.49	5.48	1.83	0.12	0.59	0.29	0.10	0.32
17017327540000	HUTCHINSON;CV RA SU	8883	8993	110	100	92	42	0.38	0.84	5.93	1.34	0.09	0.62	0.44	0.07	0.46
17017328140000	HUTCHINSON 9;CV RA	9090	9234	144	109	104	46	0.32	0.72	7.66	1.51	0.09	0.64	0.25	0.07	0.37
17017329300000	HUTCHINSON 10;CV RA	9084	9226	142	133	129	55	0.39	0.91	8.36	1.87	0.09	0.60	0.33	0.07	0.39
17017330580000	HUTCHINSON;CV RA SU	8907	9036	129	117	115	20	0.16	0.89	6.03	0.56	0.09	0.69	0.26	0.05	0.38
17017331290000	HUTCHINSON; CV RA S	8869	8946	77	77	76	42	0.55	0.98	5.48	1.47	0.09	0.61	0.28	0.07	0.32
17017333160000	ALLEN; CV RA SUI	9924	9989	65	63	35	1	0.01	0.54	1.17	0.01	0.06	0.75	0.19	0.03	0.34
17017333330000	SMITH SAM W ETAL 32	9502	9583	81	76	71	2	0.03	0.88	1.90	0.02	0.05	0.78	0.21	0.03	0.52
17017334340000	FRIERSON 30; CV RA	8879	8987	101	101	89	77	0.77	0.89	6.83	3.08	0.08	0.50	0.23	0.08	0.24
17017335630000	DUTTON FAMILY LLC #1	9550	9625	75	73	39	7	0.09	0.51	1.42	0.14	0.05	0.58	0.19	0.04	0.35
1701733625000	SMITH HEIRS #1	9477	9565	88	86	66	9	0.10	0.75	2.94	0.11	0.07	0.82	0.24	0.04	0.35
1701733644000	COLBERT - 1	9321	9456	135	127	117	54	0.40	0.87	6.35	1.46	0.08	0.65	0.24	0.05	0.35
1701733654000	CASPIANA INT. #1 ALT	9327	9446	119	119	113	65	0.55	0.95	7.32	2.54	0.09	0.54	0.20	0.07	0.26
17031204310000	E TURNER JR ETAL	9070	9185	115	115	115	86	0.75	1.00	10.29	3.87	0.10	0.56	0.33	0.09	0.36
17031204650000	G A FRIERSON	9091	9179	88	88	88	74	0.85	1.00	8.08	4.21	0.10	0.44	0.33	0.09	0.35
17031204920000	J R CALDWELL	9351	9488	138	133	116	47	0.34	0.84	4.84	1.09	0.06	0.59	0.41	0.04	0.52
17031215180000	GUY J F	9646	9777	131	131	125	18	0.14	0.95	4.18	0.38	0.07	0.67	0.28	0.03	0.47
17031230410000	GRIFFIN 33; CV RA S	9627	9754	127	122	120	41	0.32	0.95	7.75	0.94	0.09	0.75	0.54	0.07	0.54
17031230470000	HUNT PLYWOOD C;CV R	9516	9631	115	86	81	23	0.20	0.71	4.16	0.59	0.08	0.68	0.63	0.05	0.59
17031230630000	WILKINSON 24;CV RA	9102	9220	119	100	89	28	0.24	0.75	5.69	0.84	0.09	0.68	0.44	0.06	0.48
17031231140000	WASHINGTON AARON 23	9186	9315	129	115	111	22	0.17	0.86	6.97	0.41	0.09	0.80	0.43	0.06	0.50
17031231230000	GATLIN RAYMOND 13;	9060	9175	115	115	114	72	0.63	1.00	9.78	2.98	0.10	0.60	0.37	0.09	0.43
17031231400000	RICHLEN D A LAND 18	9009	9115	106	88	83	18	0.17	0.78	5.02	0.27	0.09	0.83	0.29	0.06	0.42

Table I9: (Sums and Averages for Zone LCV_S5)

API	Well Name	Top (ft)	Base (ft)	GrossInt (ft)	GrossRes (ft)	NetRes (ft)	NetPay (ft)	N/G Pay (frac)	N/G Res (frac)	PhiHt (ft)	SoPhiHt (ft)	PhiPay (frac)	SwPay (frac)	VshlPay (frac)	PhiRes (frac)	VshlRes (frac)
17015232010000	LOTT 14	9598	9719	88	54	31	8	0.09	0.35	0.98	0.15	0.05	0.63	0.43	0.03	0.52
17015232740000	CAPLIS 22; CV RA SU	9016	9104	88	61	43	0	0.00	0.49	1.08	0.00				0.03	0.55
17015232780000	CAPLIS; 15 CV RA SU		9168	102	84	68	22	0.21	0.66	3.04	0.75	0.07	0.51	0.29	0.05	0.45
17015233220000	BROWN 4; CV RA SU 1	9440	9520	79	79	57	39	0.49	0.73	3.17	1.69	0.07	0.38	0.31	0.06	0.34
17015234310000	NINOCK LAND CO 35;	9885	9962	63	11											
17017216930000	CAPLIS	9151	9224	73	72	57	32	0.43	0.78	2.92	1.22	0.06	0.40	0.25	0.05	0.31
17017217050000	HUTCHINSON	9151	9213	63	58	50	33	0.52	0.79	3.17	1.77	0.08	0.34	0.40	0.06	0.43
17017217970000	FRIERSON TRUST	9183	9273	90	89	60	16	0.17	0.67	2.02	0.20	0.04	0.71	0.36	0.03	0.45
17017221550000	CUPPLES CU RA SU 72	9416	9506	90	33	6	0	0.00	0.06	0.16	0.00				0.03	0.53
17017322540000	DANNY-WEBB; CV RA S	9149	9213	65	56	47	26	0.40	0.72	2.77	1.31	0.08	0.39	0.25	0.06	0.37
17017322950000	HUTCHINSON 4; CV RA	9122	9189	67	65	39	13	0.19	0.58	1.71	0.46	0.08	0.52	0.43	0.04	0.49
17017323700000	DENNY-WEBB;CV RA SU	9242	9286	44	27	26	22	0.50	0.59	2.98	2.03	0.13	0.29	0.27	0.12	0.32
17017324060000	SMITH SAM W 28;CV R	9412	9519	106	89											
17017324230000	LEVEE BOARD 22;CV R	9464	9554	90	88	77	29	0.32	0.86	3.51	0.70	0.06	0.57	0.30	0.05	0.42
17017325020000	ELLERBE HEIRS 21, C	9314	9402	88	64	64	41	0.46	0.73	4.61	1.10	0.08	0.65	0.52	0.07	0.51
17017325070000	ELLERBE HEIRS 21; C	9351	9449	98	96	14	8	0.08	0.14	1.10	0.36	0.11	0.58	0.42	0.08	0.45
17017325190000	RICHLEN D A LAND 18	9153	9219	67	61	54	44	0.66	0.80	5.08	3.63	0.11	0.24	0.30	0.10	0.33
17017327540000	HUTCHINSON;CV RA SU	8993	9064	71	65	50	32	0.45	0.71	2.58	1.07	0.06	0.47	0.33	0.05	0.37
17017328140000	HUTCHINSON 9;CV RA	9234	9282	48	33	30	21	0.44	0.63	2.01	0.94	0.08	0.47	0.31	0.07	0.33
17017329300000	HUTCHINSON 10;CV RA	9226	9276	50	30	13	1	0.01	0.26	0.29	0.00	0.04	0.82	0.33	0.02	0.41
17017330580000	HUTCHINSON;CV RA SU	9036	9101	65	61	55	21	0.32	0.85	2.13	0.23	0.05	0.77	0.20	0.04	0.31
17017331290000	HUTCHINSON; CV RA S	8946	9023	77	76	53	12	0.16	0.69	1.83	0.19	0.04	0.62	0.12	0.04	0.29
17017333160000	ALLEN; CV RA SUI	9989	9997	8	8	7	5	0.54	0.82	0.47	0.13	0.08	0.65	0.17	0.07	0.22
17017333330000	SMITH SAM W ETAL 32	9583	9650	67	59	51	13	0.19	0.77	1.97	0.26	0.06	0.65	0.45	0.04	0.53
17017334340000	FRIERSON 30; CV RA	8987	9052	65	55	45	5	0.07	0.69	1.78	0.05	0.07	0.83	0.61	0.04	0.53
17017335630000	DUTTON FAMILY LLC #1	9625	9677	52	47	35	18	0.34	0.68	1.62	0.66	0.06	0.41	0.19	0.05	0.31
1701733625000	SMITH HEIRS #1	9565	9638	73	68	33	13	0.18	0.46	1.43	0.60	0.07	0.34	0.25	0.04	0.36
1701733644000	COLBERT - 1	9456	9519	63	17	8	0	0.00	0.12	0.20	0.00				0.03	0.35
1701733654000	CASPIANA INT. #1 ALT	9446	9500	54	47	32	5	0.09	0.59	1.17	0.23	0.07	0.39	0.32	0.04	0.38
17031204310000	E TURNER JR ETAL	9185	9262	77	77	70	38	0.49	0.90	3.58	1.64	0.07	0.39	0.25	0.05	0.32
17031204650000	G A FRIERSON	9179	9277	98	96	90	53	0.54	0.91	4.94	2.09	0.07	0.45	0.36	0.06	0.40
17031204920000	J R CALDWELL	9488	9578	90	72	64	30	0.33	0.72	2.83	1.17	0.07	0.41	0.47	0.04	0.54
17031215180000	GUY J F	9777	9848	71	69	67	22	0.31	0.95	3.73	1.20	0.10	0.43	0.41	0.06	0.48
17031230410000	GRIFFIN 33; CV RA S	9754	9865	110	106	98	62	0.56	0.88	6.62	3.87	0.09	0.30	0.36	0.07	0.42
17031230470000	HUNT PLYWOOD C;CV R	9631	9694	63	61	58	46	0.73	0.92	5.41	3.17	0.11	0.37	0.35	0.09	0.38
17031230630000	WILKINSON 24;CV RA	9220	9291	71	70											
17031231140000	WASHINGTON AARON 23	9315	9378	63	60	55	41	0.65	0.88	5.09	3.51	0.12	0.25	0.31	0.09	0.35
17031231230000	GATLIN RAYMOND 13;	9175	9243	69	63	55	29	0.41	0.80	2.86	1.28	0.07	0.38	0.27	0.05	0.35
17031231400000	RICHLEN D A LAND 18	9115	9199	84	81	76	41	0.49	0.90	4.98	2.33	0.09	0.35	0.35	0.07	0.42

APPENDIX J

LOG SECTIONS AND CORRELATION

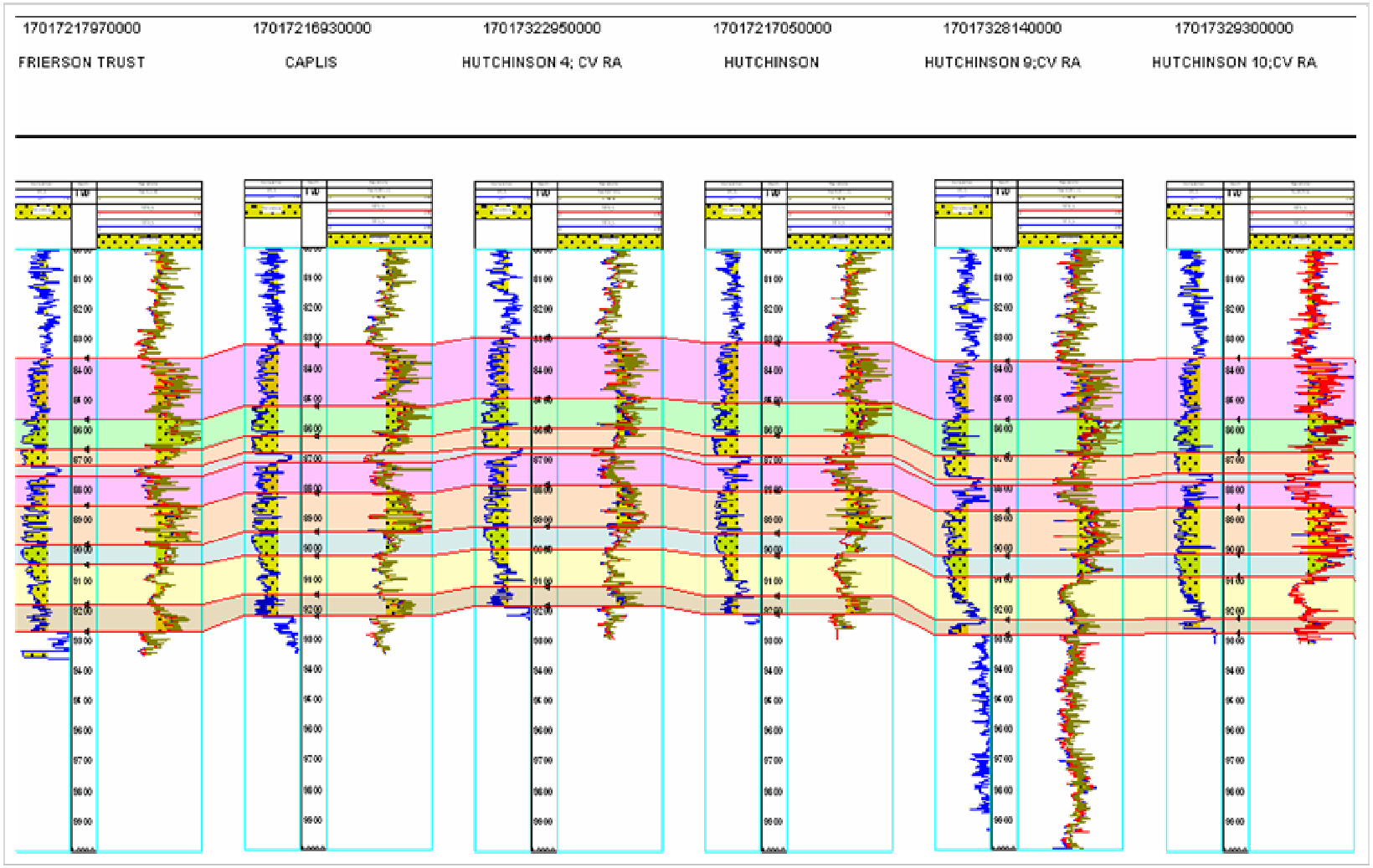

Fig. J1: Cross Section of Well Logs: North-South Direction (Saddle Region).

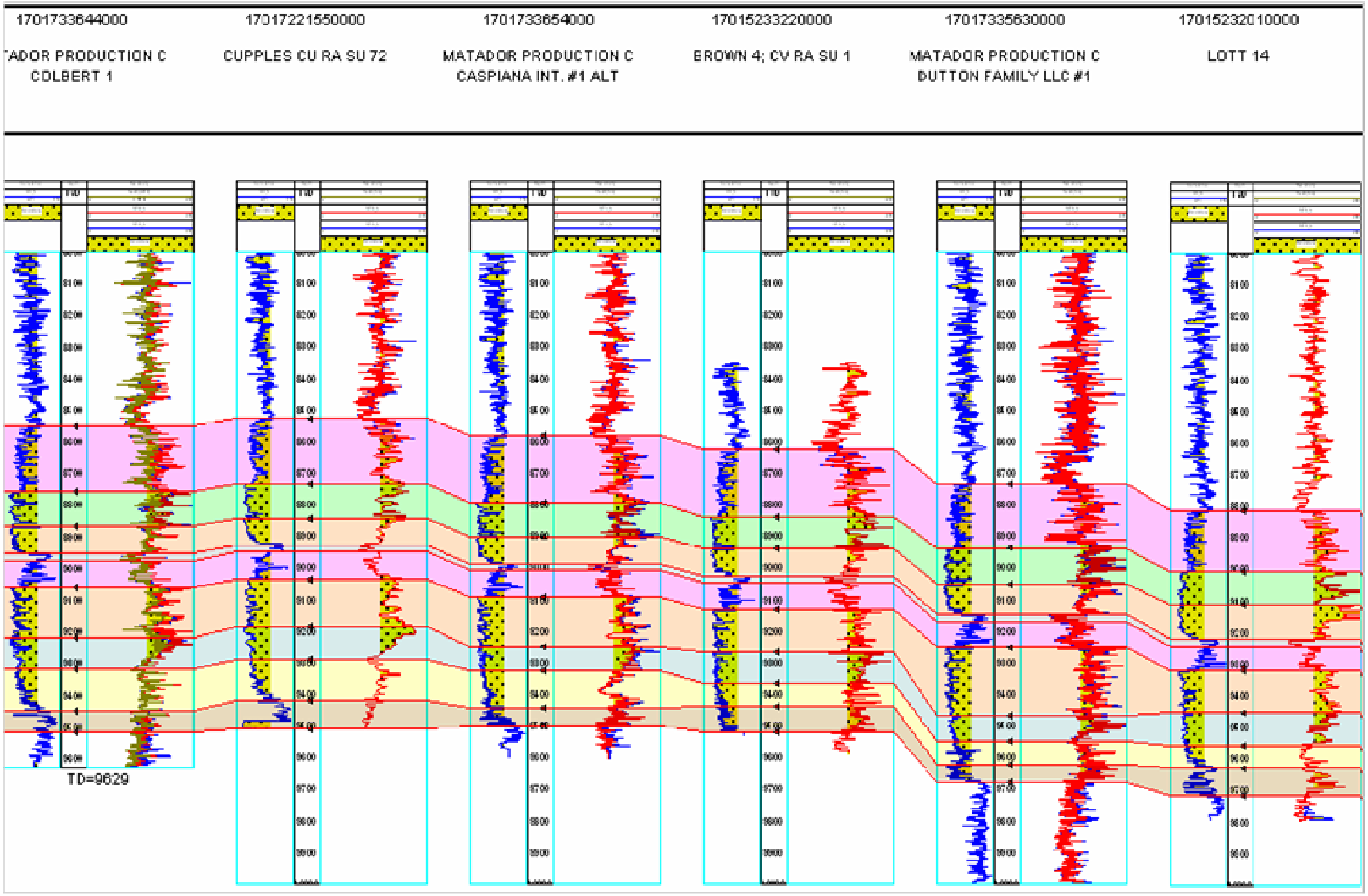

Fig. J2: Cross Section of Well Logs: North-South Direction (Southern Flank).

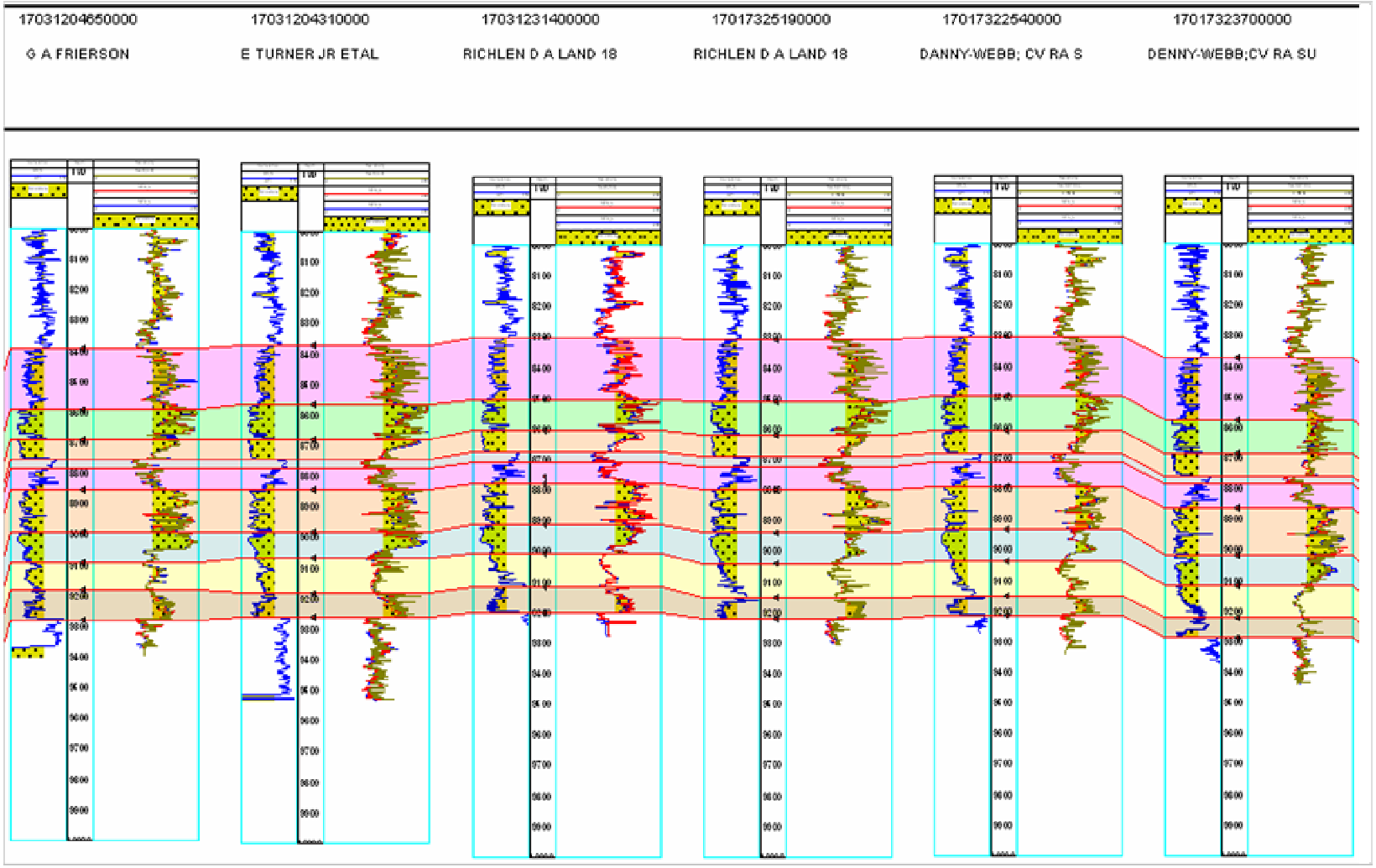

Fig. J3: Cross Section of Well Logs: North – South Direction (Saddle Region).

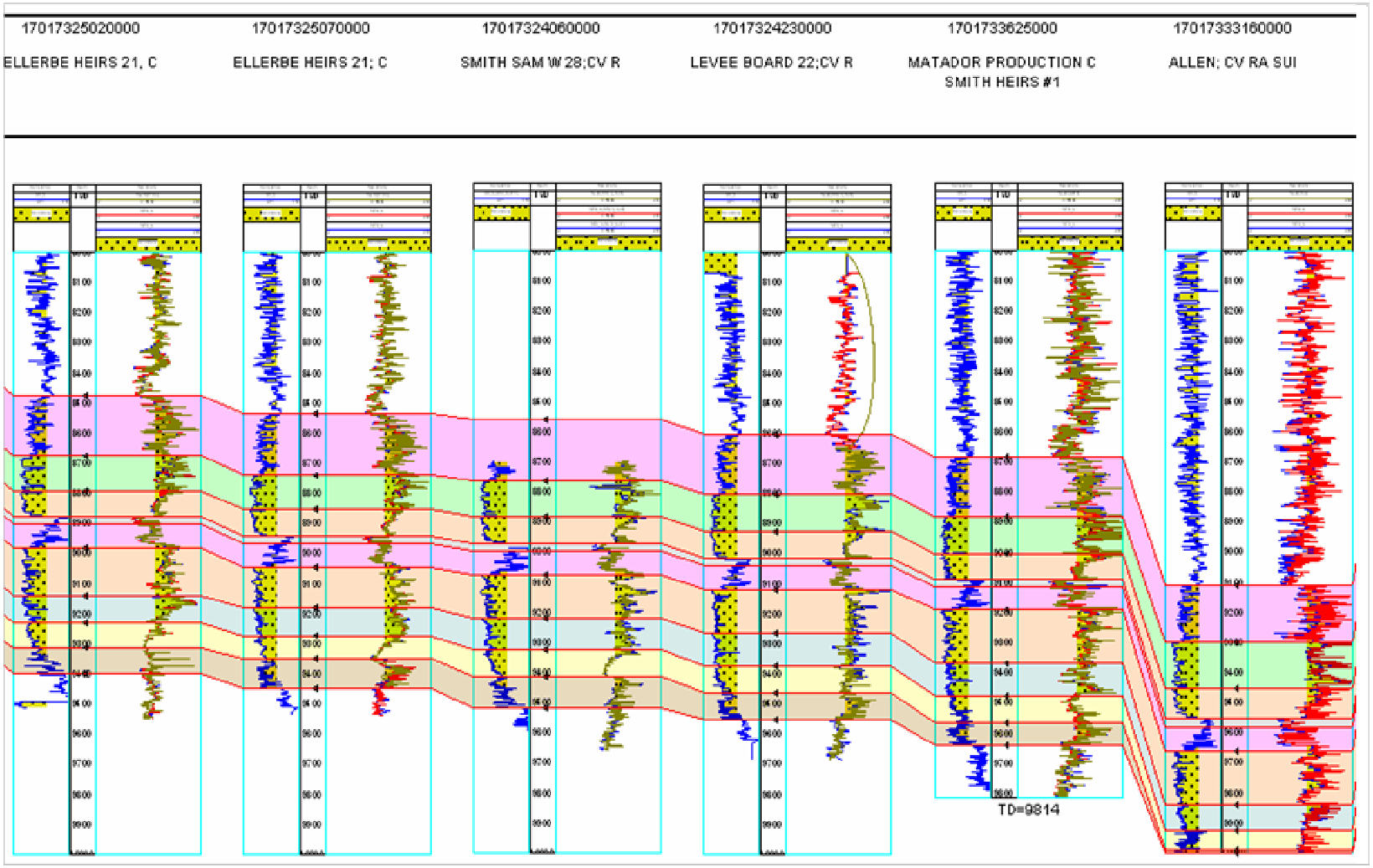

Fig. J4: Cross Section of Well Logs: North – South Direction (Southern Flank).

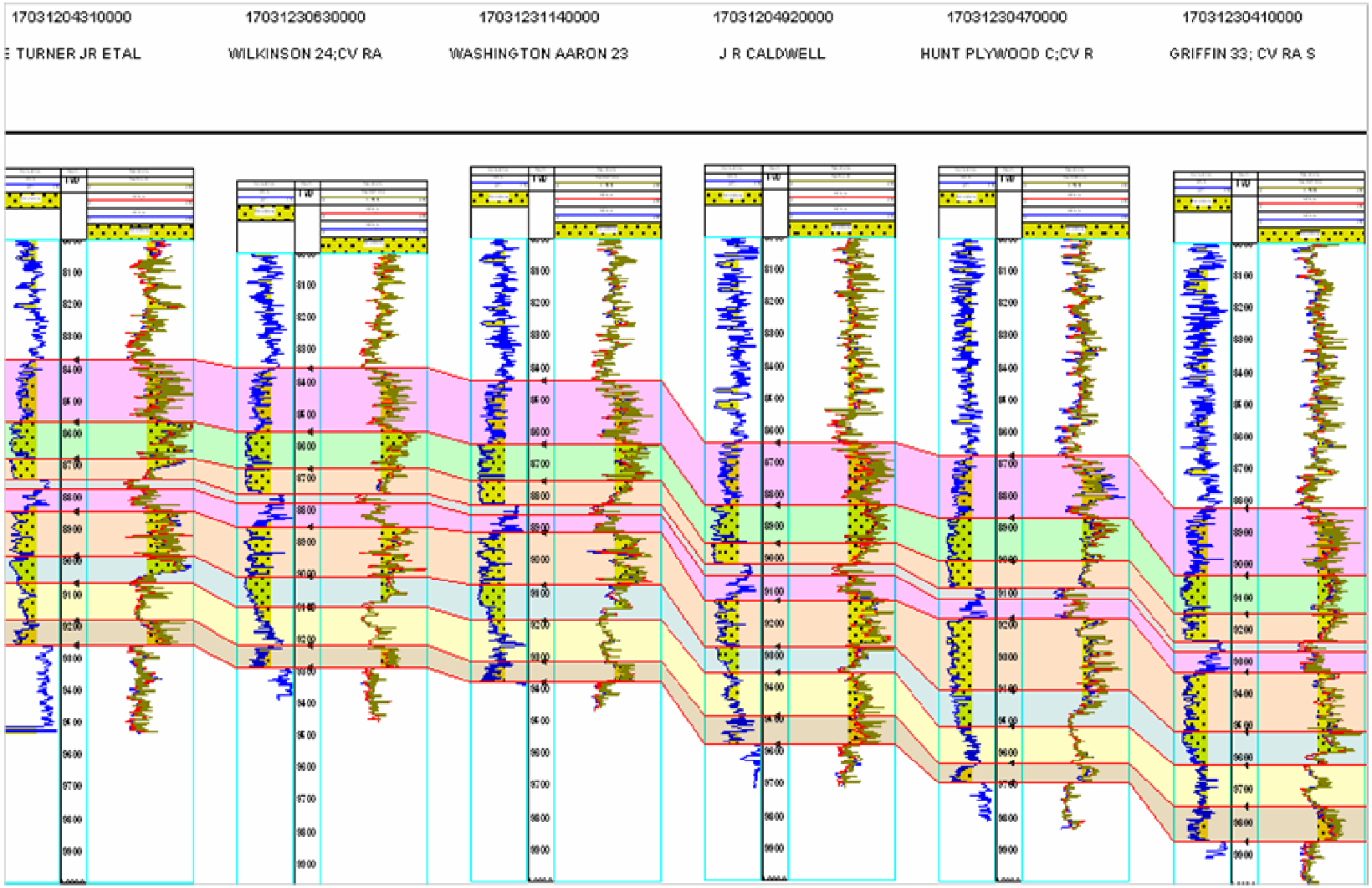

Fig. J5: Cross Section of Well Logs: East – West Direction (Saddle Region).

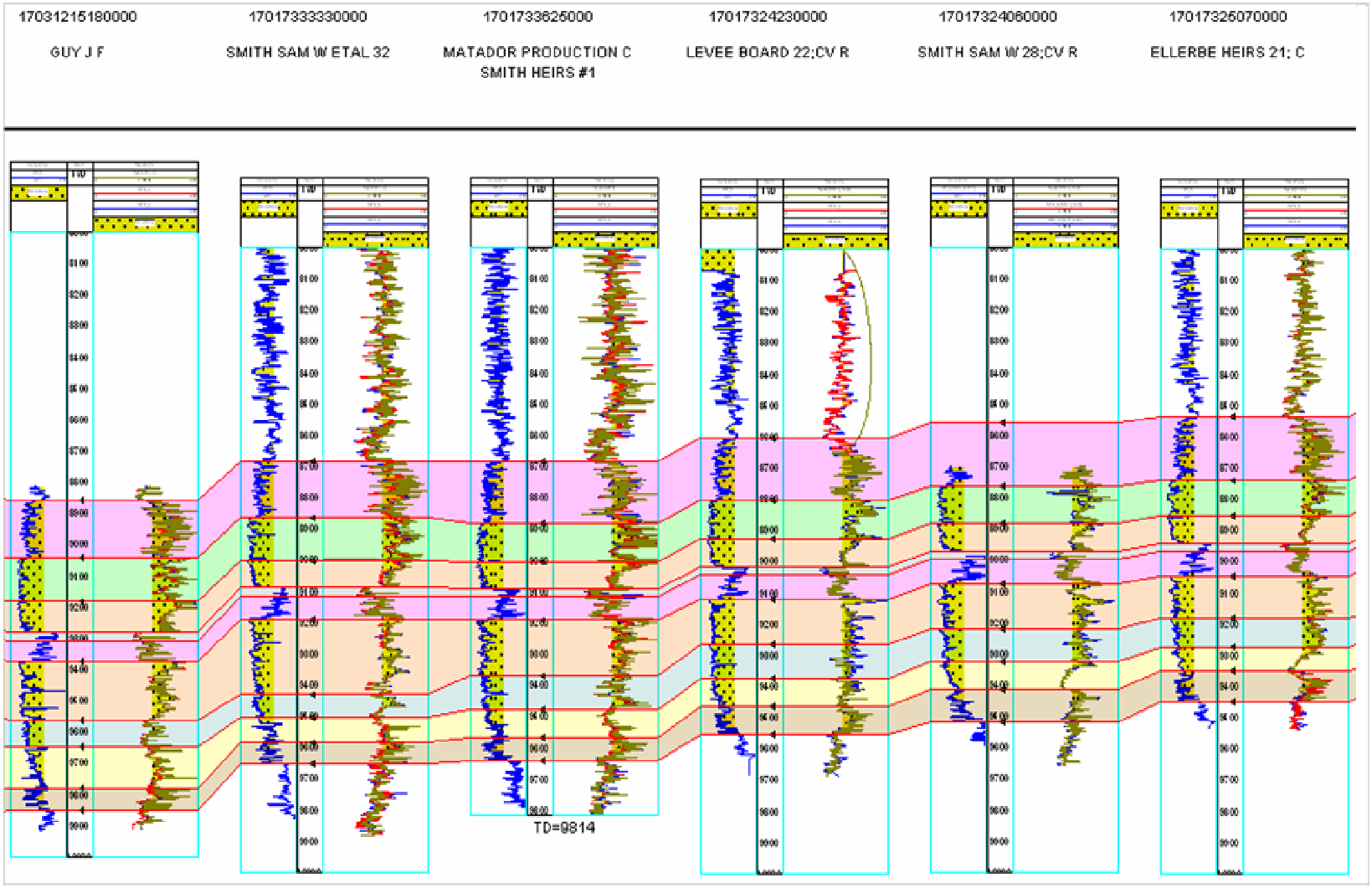

Fig. J6: Cross Section of Well Logs: Southwest – Northeast Direction (Southwest Flank).

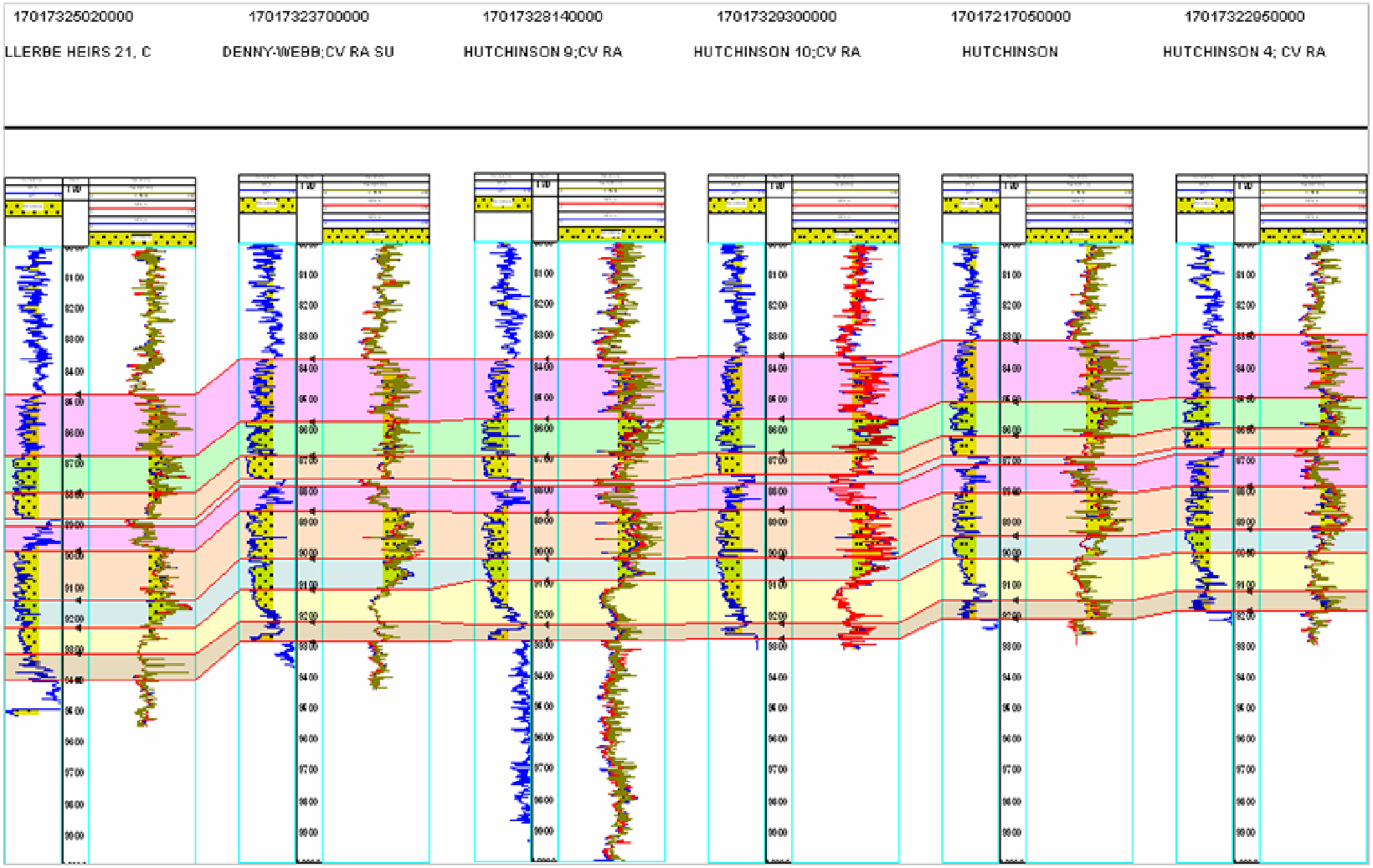

Fig. J7: Cross Section of Well Logs: Southwest – Northeast Direction (Saddle Region).

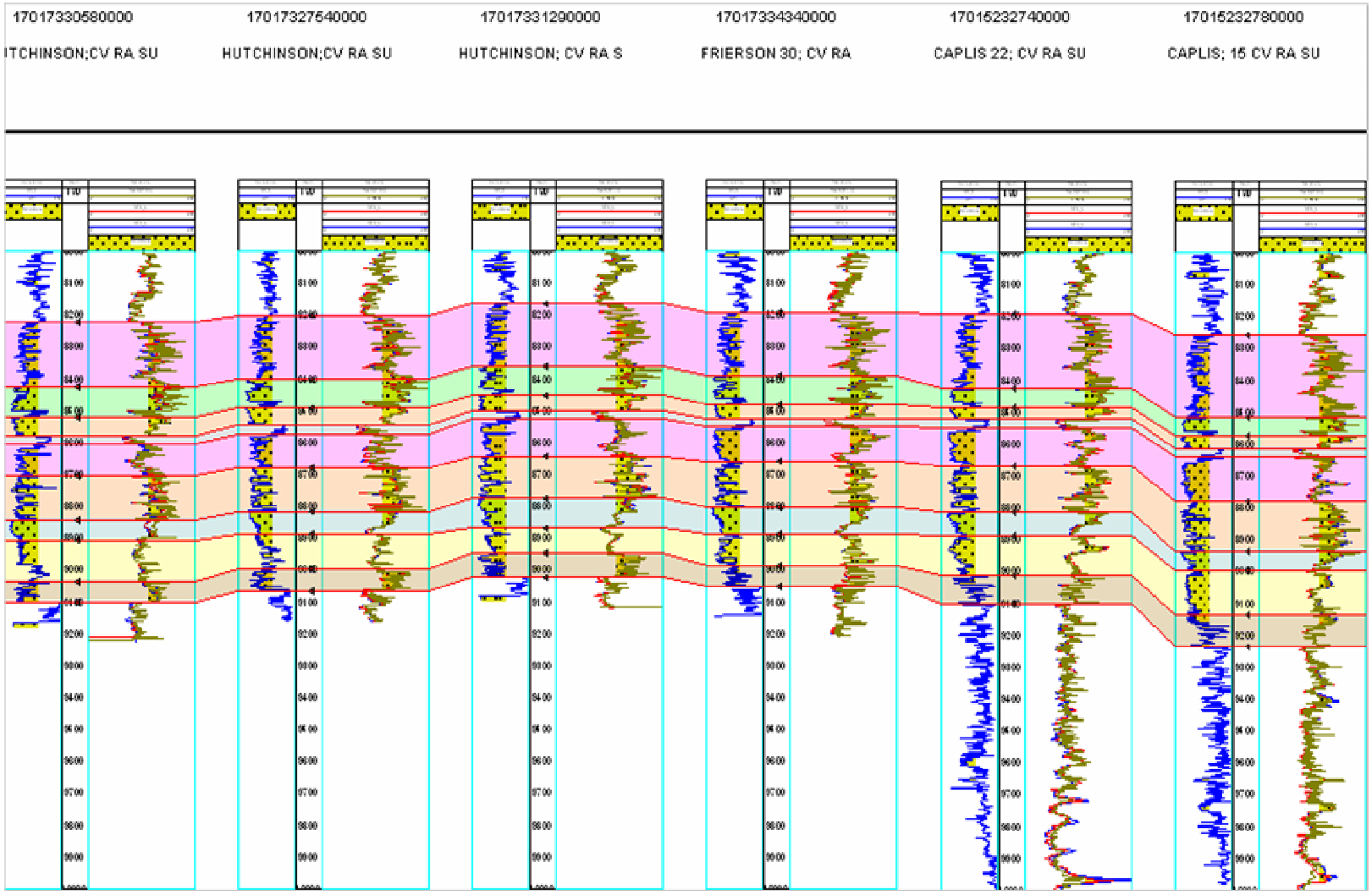

Fig. J8: Cross Section of Well Logs: Southwest – Northeast Direction (Crestal Region).

VITA

Name: Charles Chinedu Ozobeme

Permanent Address: 8A Fatai Animashaun St,
Magodo-Shangisha, Lagos, Nigeria.

Email Address: ccozobs@yahoo.com

Education: B.Engr. Mechanical Engineering
University of Nigeria Nsukka (UNN)
Lagos, Nigeria, 1991

M.S. Petroleum Engineering
Texas A&M University
College Station, USA, 2006